United States Environmental Protection Agency
Office of Transportation and Air Quality
EPA420-D-06-005
February 2006

California Heavy Heavy-Duty Diesel Truck Emissions Characterization for Program E-55/59

Draft Report

EPA420-D-06-005
February 2006

California Heavy Heavy-Duty Diesel Truck Emissions Characterization for Program E-55/59

Draft Report

Assessment & Standards Division
Office of Transportation and Air Quality
U.S. Environmental Protection Agency

Prepared for EPA by:

Coordinating Research Council (CRC)

TABLE OF CONTENTS

TABLE OF CONTENTS i
LIST OF FIGURES iii
LIST OF TABLES viii
LIST OF APPENDICES x
LIST OF APPENDICES x
EXECUTIVE SUMMARY 1
NOMENCLATURE 6
INTRODUCTION AND OBJECTIVES 7
VEHICLE PROCUREMENT 9
EQUIPMENT & METHODS – REGULATED SPECIES 15
Translab Description 15
Preparation of the Vehicle for Testing 15
Engine/Vehicle Preparation 16
Wheel-Hub Adapter Installation 17
Test Vehicle Mounting 17
Connections of Vehicle to Laboratory 17
Pre-test Vehicle Operation 17
Vehicle Driving Instructions 18
Vehicle Practice Run 18
Test Run Procedures 19
Gaseous and PM sampling system 19
Gas Analyzer Operation 22
Calibration Procedures 22
Particulate Matter Filter Conditioning and Weighing 23
Test Cycles 23
Test Weights 27
EQUIPMENT AND METHODS – NON-REGULATED SPECIES & PARTICLE SIZING 31
DRI's Residence Time Dilution Tunnel 31
Mini Dilution System 33
Particle Sizing with the SMPS 37
Particle sizing with the DMS500 40
Unregulated Emissions 42
Speciation Fleet and Approach 44
QUALITY ASSURANCE AND QUALITY CONTROL 46
RESULTS AND DISCUSSION, REGULATED SPECIES 48
HHDT Data Gathered 48
MHDT Data Discussion 60
Continuous Data 69
HHDDT Effect of Test Weight 72
MHDT Effect of Test Weight 74
COMPARISON OF DATA BETWEEN PHASES 75
RESULTS AND DISCUSSION, NONREGULATED SPECIES 78
Semi-Volatile Organic Compounds 78

Volatile Organic Compounds 82
SPECIATION AND SIZING RESULTS 87
CONCLUSIONS, NONREGULATED SPECIES 126
TAMPERING, MALMAINTENANCE AND REFLASH VEHICLES 131
T&M Criteria 131
Determination of Candidates from Vehicle Inspection 131
Determination of T&M Candidate from Emissions 132
Results: T&M by Inspection 135
Verifying the Criteria in Phase 1: NO_x Analysis 136
Verifying the Criteria in Phase 1: PM Analysis 137
Criteria ratios for all phases 142
“Before and After” Emissions 151
T&M and Reflash Discussion 167
ACKNOWLEDGEMENTS 170
REFERENCES 171

LIST OF FIGURES

Figure 1: WVU Sampling System Schematic..... 20
Figure 2: AC5080 Short Test (time not to scale)..... 26
Figure 3: The AC5080 Schedule as driven by a 1990 Kenworth road tractor with a 370 hp Cummins M11 engine and a 10-speed manual transmission, with a simulated vehicle test weight of 56,000 lbs..... 27
Figure 4: PM emissions for vehicle E55CRC-27 which was tested at four weights, before 66,000 lbs. was adopted as the highest test weight..... 28
Figure 5: NO_x emissions for vehicle E55CRC-27 which was tested at four weights, before 66,000 lbs. was adopted as the highest test weight..... 28
Figure 6: PM emissions for vehicle E55CRC-53 tested at two weights..... 29
Figure 7: NO_x emissions for vehicle E55CRC-53 tested at two weights..... 30
Figure 8: Schematic of DRI dilution tunnel sampler (Hildemann, et al.[6]) 32
Figure 9: Exhaust Coupler with Sampling Probe for mini dilution tunnel..... 33
Figure 10: West Virginia University-Mini Dilution System 34
Figure 11: Schematic Representation of the Damping System 36
Figure 12: Exhaust Pulsation Damper 36
Figure 13: Differential Mobility Analyzer..... 37
Figure 14: TSI Model 3936 SMPS System 39
Figure 15: Working principle of the DMS500[8]. 41
Figure 16: NO_x emissions for the Idle Mode, in units of g/minute..... 49
Figure 17: NO_x emissions for the Creep mode (56,000 lbs.)..... 49
Figure 18: NO_x emissions for the Transient mode (56,000 lbs.). One of the vehicles in the 1975-1976 MY bin emitted NO_x at 60 g/mile. 50
Figure 19: NO_x emissions for the Cruise mode (56,000 lbs.). One 1998 vehicle (E55CRC-10) was identified as a high NO_x emitter in Phase 1..... 51
Figure 20: NO_x emissions for HHDDT_S mode (56,000 lbs.). The high value for the 1975-1976 MY bin is due to a single truck with high NO_x emissions. 52
Figure 21: NO_x emissions for UDDS mode (56,000 lbs.). 53
Figure 22: PM emissions for Idle Mode. Truck E55CRC-45, in the 1991-1993 MY bin, was a prodigious emitter and raised the average value for that bin substantially..... 53
Figure 23: PM emissions for Creep mode (56,000 lbs.). One vehicle in the 1991-1993 MY bin was a very high emitter of both PM and HC at light load..... 54
Figure 24: PM Emissions for the Transient mode (56,000 lbs.). Truck E55CRC-16, a high emitter, caused the high average in the 1977-1979 MY bin..... 55
Figure 25: PM emissions for the Cruise mode (56,000 lbs.). E55CRC-16 contributed to the one very high MY bin average..... 55
Figure 26: PM emissions for HHDDT_S mode (56,000 lbs.). Four MY groups show data from only one vehicle. 56
Figure 27: PM emissions for UDDS mode (56,000 lbs.)..... 57
Figure 28: CO emissions for Transient mode (56,000 lbs.)..... 57
Figure 29: CO emissions for Cruise mode (56,000 lbs.). 58
Figure 30: HC emissions for Transient mode (56,000 lbs.)..... 59
Figure 31: HC emissions for Cruise mode (56,000 lbs.). 59
Figure 32: NO_x emissions for AC5080 (both laden and unladen). Gasoline-fueled vehicles are separated from diesel-fueled vehicles for comparison..... 60

Figure 33: NO_x emissions for the Lower Speed Transient mode (both laden and unladen)..... 61
Figure 34: NO_x emissions for the Higher Speed Transient mode (both laden and unladen). 62
Figure 35: NO_x emissions for the MHDT Cruise mode (both laden and unladen)..... 62
Figure 36: NO_x emissions for the HHDDT_S mode (both laden and unladen)..... 63
Figure 37: NO_x emissions for the UDDS mode (both laden and unladen)..... 63
Figure 38: PM emissions for the AC5080 mode (both laden and unladen)..... 64
Figure 39: PM emissions for the Lower Speed Transient mode (both laden and unladen). 65
Figure 40: PM emissions for the Higher Speed Transient mode (both laden and unladen). 65
Figure 41: PM emissions for the Cruise mode (both laden and unladen)..... 66
Figure 42: PM emissions for the HHDDT_S mode (both laden and unladen)..... 66
Figure 43: PM emissions for UDDS mode (both laden and unladen). 67
Figure 44: CO emissions for MHDTHI mode (both laden and unladen). 67
Figure 45: CO emissions for the MHDTCR mode (both laden and unladen). 68
Figure 46: HC emissions for MHDTHI mode (both laden and unladen). 68
Figure 47: HC emissions for MHDTCR mode (both laden and unladen). 69
Figure 48: Example of a continuous NO_x emissions plot in g/s for E55CRC-42 (56,000 lbs.) following the HHDDT Transient Mode..... 70
Figure 49: Example of a continuous HC emissions plot in g/s for E55CRC-42 (56,000 lbs.) following the HHDDT Transient Mode..... 70
Figure 50: Example of a continuous CO emissions plot in g/s for E55CRC-42 (56,000 lbs.) following the HHDDT Transient Mode..... 71
Figure 51: Example of a continuous exhaust temperature reading for E55CRC-42 (56,000 lbs.) following the Transient mode schedule..... 71
Figure 52: Transient mode NO_x weight effects 72
Figure 53: Transient mode PM weight effect 73
Figure 54: Cruise mode NO_x weight effect..... 73
Figure 55: Cruise mode PM weight effect..... 74
Figure 56: Variation of HHDDT CO_2 emissions by vehicle model year and by phase of the program for the UDDS (56,000 lbs.). 75
Figure 57: Variation of HHDDT CO emissions by vehicle model year and by phase of the program for the UDDS (56,000 lbs.). 76
Figure 58: Variation of HHDDT oxides of NO_x by vehicle model year and by phase of the program for the UDDS (56,000 lbs.). 77
Figure 59: Variation of PM emissions by vehicle model year and by phase of the program for the UDDS (56,000 lbs.)..... 77
Figure 60: PAH in fuels and oils..... 81
Figure 61: Concentrations of carbonyl compounds (in ppbv) measured during the runs. 84
Figure 62: SMPS Particle Size Distribution for E55CRC-39 Operating on an Idle Mode88
Figure 63: SMPS Particle Size Distribution for E55CRC-39 Operating on Various Steady Cycles..... 89
Figure 64: PM Mass Emissions for E55CRC-39..... 89
Figure 65: Ion Composite Results for E55CRC- 39 91

Figure 66: Elemental Carbon and Organic Carbon PM Analysis for E55CRC-39 91
Figure 67: DMS500 Total Number of Particles and Vehicle Speed vs. Time during the UDDS for E55CRC-39 tested at 56,000 lbs. 92
Figure 68: DMS500 Total Number of Particles and Engine Power vs. Time during the UDDS for E55CRC-39 tested at 56,000 lbs. 93
Figure 69: DMS500 60 nm and 20 nm Particle Number vs. Time during the UDDS for E55CRC-39 tested at 56,000 lbs. 93
Figure 70: DMS500 60 nm Particle Number vs. 20 nm Particle Number during the UDDS for E55CRC-39 tested at 56,000 lbs. 94
Figure 71: DMS500 60 nm Particle Number vs. Total Hub Power during the UDDS for E55CRC-39 tested at 56,000 lbs. 94
Figure 72: DMS500 20 nm Particle Number vs. Total Hub Power during the UDDS for E55CRC-39 tested at 56,000 lbs. 95
Figure 73: DMS500 size distribution of particles during Idle (t = 230 s) of the UDDS for E55CRC-39 tested at 56,000 lbs. 96
Figure 74: DMS500 size distribution of particles during acceleration (t = 530 s) of the UDDS for E55CRC-39 tested at 56,000 lbs. 97
Figure 75: DMS500 size distribution of particles during deceleration (t = 770 s) of the UDDS for E55CRC-39 tested at 56,000 lbs. 97
Figure 76: DMS500 size distribution of particles during HHDDT_S and Vehicle Speed vs. Time for E55CRC-39 tested at 56,000 lbs. 98
Figure 77: DMS500 size distribution of particles during Transient and Vehicle Speed vs. Time for E55CRC-39 tested at 56,000 lbs. 98
Figure 78: DMS500 size distribution of particles during Cruise3 and Vehicle Speed vs. Time for E55CRC-39 tested at 56,000 lbs. 99
Figure 79: SMPS Particle Size Distribution for E55CRC-40 Operating on an Idle Mode 100
Figure 80: SMPS Particle Size Distribution for E55CRC-40 Operating on Various Steady Cycles 101
Figure 81: PM Mass Emissions for E55CRC-40 102
Figure 82: Ion Composite Results for E55CRC-40 102
Figure 83: Elemental Carbon and Organic Carbon PM Analysis for E55CRC-40 103
Figure 84: SMPS Particle Size Distribution for E55CRC-41 Operating on an Idle Mode 104
Figure 85: Elemental Carbon and Organic Carbon PM Analysis for E55CRC-41 105
Figure 86: Total PM Mass Emissions Rate (g/hour) for E55CRC-41 106
Figure 87: SMPS Particle Size Distribution for E55CRC-41 Operating under Cruise and Steady Conditions 106
Figure 88: SMPS Particle Size Distribution for E55CRC-41 Operating on Cruise and Steady Conditions (50% GVWR) 107
Figure 89: Ion Composite Results for E55CRC-41 107
Figure 90: SMPS Single Particle Trace (82 nm) for E55CRC-41 Operating on UDDS, Low Transient and High Transient Cycles (75%GVWR) 108
Figure 91: SMPS Single Particle Trace (24 nm) for E55CRC-41 Operating on Low Transient and High Transient Cycles (75% GVWR) 109

Figure 92: SMPS Single Particle Trace (88 nm) for E55CRC-41 Operating on Low Transient and High Transient Cycles (50% GVWR) 109
Figure 93: DMS500 Total Number of Particles and Vehicle Speed vs. Time during UDDS for E55CRC-41 tested at 56,000 lbs. 110
Figure 94: DMS500 60 nm and 20 nm Particle Number vs. Time for E55CRC-41 tested at 56,000 lbs. 111
Figure 95: DMS500 Total Number of Particles and CO vs. Time for E55CRC-41 tested at 56,000 lbs. 112
Figure 96: DMS500 60 nm Particle Number vs. 20 nm Particle Number for E55CRC-41 tested at 56,000 lbs. 112
Figure 97: DMS500 20 nm Particle Number vs. Total Hub Power for E55CRC-41 tested at 56,000 lbs. 113
Figure 98: DMS500 60 nm Particle Number vs. Total Hub Power for E55CRC-41 tested at 56,000 lbs. 113
Figure 99: DMS500 size distribution of particles during acceleration and deceleration for E55CRC-41 tested at 56,000 lbs. 114
Figure 100: SMPS Particle Size Distribution for E55CRC-42 Operating on an Idle Mode 115
Figure 101: SMPS Particle Size distribution for E55CRC-42 operating on various steady cycles 115
Figure 102: PM Mass Emissions for E55CRC-42 116
Figure 103: Ion Composite Results for E55CRC-42 117
Figure 104: Elemental Carbon and Organic Carbon PM Analysis for E55CRC-42 117
Figure 105: DMS500 Total Number of Particles and Vehicle Speed vs. Time on Transient mode for E55CRC-42 tested at 56,000 lbs. 118
Figure 106: SMPS Particle Size Distribution for E55CRC-43 Operating on an Idle Mode 119
Figure 107: SMPS Particle Size Distribution for E55CRC-43 Operating on Various Steady Cycles 119
Figure 108: PM Mass Emissions for E55CRC-43 120
Figure 109: Ion Composite Results for E55CRC-43 121
Figure 110: Elemental Carbon and Organic Carbon PM Analysis for E55CRC-43 121
Figure 111: DMS500 Total Number concentration of Particles and Vehicle Speed vs. Time for E55CRC-43 tested at 56,000 lbs. 122
Figure 112: SMPS Particle Size Distribution for E55CRC-44 Operating on an Idle Mode 123
Figure 113: SMPS Particle Size Distribution for E55CRC-44 Operating on Various Steady Cycles 123
Figure 114: PM Mass Emissions for E55CRC-44 124
Figure 115: Ion Composite Results for E55CRC-44 125
Figure 116: Elemental Carbon and Organic Carbon PM Analysis for E55CRC-44 125
Figure 117: Elemental Carbon Emissions (Percentage of Total Carbon) 127
Figure 118: Inorganic Ionic Species Emissions 128
Figure 119: Lubrication Oil Emissions 129
Figure 120: Engine Wear Emissions 130

Figure 121: NO_x/CO_2 ratios for each run on the 25 vehicles, both transient and cruise. One vehicle was found to have high NO_x emissions on two runs of the cruise mode 136
Figure 122: NO_x emissions plotted against the dispersed and time aligned power for vehicle E55CRC-10. Most emissions during the Cruise mode were at an off-cycle level. The vehicle was targeted for Reflash as a result of these data. 137
Figure 123: PM/CO_2 ratios for Cruise Mode operation of average value for each vehicle. There are two runs each for E55CRC-1 to -13, and three runs each for E55CRC-14 to -25. 138
Figure 124: PM/CO_2 ratios for the Transient Mode operation of average value for each vehicle. There are 2 runs each for E55CRC-1 to -13, 3 runs each for E55CRC-14 to -25. One run for E55CRC-20 was anomalous low, but no cause was evident..... 139
Figure 125: Occurrence of criterion ratios by bin for the Laden Transient Mode (PM/CO_2). E55CRC-16 was not included in this analysis, because it was an extreme outlier. 140
Figure 126: Occurrence of criterion ratios by bin for the Laden Cruise mode (PM/CO_2). E55CRC-16 was not included in this analysis because it was an extreme outliner.141
Figure 127: Transient Mode NO_x emissions before and after reflashing E55CRC-10... 153
Figure 128: NO_x emissions versus power for E55CRC-10 after reflashing. The mass rate of NO_x emissions was reduced in many parts of the Cruise mode (compared to Figure 122). The highest mass rate emissions were also slightly lower than before the reflash. 154
Figure 129: NO_x emissions on Cruise mode (56,000 lbs.) for three vehicles before reflash. NO_x emissions and hub power were time-aligned before plotting. 158
Figure 130: NO_x emissions on the three reflash vehicles were reduced in Cruise mode after reflash. Test weight was 56,000 lbs. 158
Figure 131: As-received and retest after reflash NO_x data for E55CRC-26 (56,000 lbs.). 159
Figure 132: As-received and retest after reflash PM data for E55CRC-26 (56,000 lbs.). 159
Figure 133: PM emission for E55CRC-28 for the UDDS, Cruise and HHDDT_S Modes. 160
Figure 134: PM emissions for the Transient and Creep Modes for E55CRC-28. 161
Figure 135: NO_x emissions for E55CRC-28 at 56,000 lbs. on the UDDS and the Cruise and HHDDT_S Modes. 162
Figure 136: NO_x emissions for E55CRC-28 at 56,000 lbs. on the Transient and Creep Modes. 162
Figure 137: As-received and reflash emissions for NO_x emissions for E55CRC-31 tested at 56,000 lbs. 164
Figure 138: As-received and reflash emissions for PM emissions for E55CRC-31..... 164
Figure 139: shows the inability of E55CRC-57 to meet the target trace. 167

LIST OF TABLES

Table 1: Highest, lowest, and average emissions of NO_x and PM for all HHDDT (56,000 lbs.)..... 2
Table 2: Emissions of regulated species by MY for HHDDT tested on the UDDS (56,000 lbs.)..... 3
Table 3: Highest, lowest, and average emissions of NO_x and PM for all MHDDT tested at 75% GVWR. 3
Table 4: The effect of changing test weight on the diesel-fueled MHDT, in terms of a simple average of emissions for that fleet..... 4
Table 5: Vehicles planned for recruiting in the E-55/59 program. 10
Table 6: Federal and ARB past and present emissions standards..... 11
Table 7: Vehicle Selection Matrix: NO_x, PM, VMT population (as percentages of total). 11
Table 8: Basic Information on the 78 trucks actually recruited..... 12
Table 9: Sampling system description and media type..... 21
Table 10: Test Schedule Summary. AC5080 performance depends on truck power to weight ratio. 24
Table 11: AC5080 Methodology. 26
Table 12: Test Vehicle Details..... 44
Table 13: List of Target Analytes in the Particulate and Semi-Volatile Fractions. 78
Table 14: List of Gas-phase Compounds Quantified by GC/MS Method from Canisters. 82
Table 15: List of Target Analytes in the Gas-Phase Carbonyl Compound Fraction 83
Table 16: Nitrosoamines Targeted for Analysis in the Vehicle Exhaust..... 84
Table 17: List of Heavy Hydrocarbons for Tenax Samples 85
Table 18: Damaged Tenax Samples. 86
Table 19: Emissions level criteria used to declare a truck to be a high NO_x emitter..... 134
Table 20: Definition of criterion ratios by bin for the Laden Transient Mode: see Figure 125..... 140
Table 21: Definition of criterion by bin for the Laden Cruise Mode: See Figure 126. .. 141
Table 22: T&M Determination Data for the HHDDT Vehicles over the Cruise Mode . 143
Table 23: T&M Determination Data for the HHDDT Vehicles over the Transient Mode 147
Table 24: E55CRC-3: UDDS (g/mile)..... 151
Table 25: E55CRC-3 retest UDDS (g/mile) 151
Table 26: E55CRC-3: 1828-1 Idle, 1828-2 Creep, 1828-3 Transient, 1828-4 Cruise. (g/mile, except idle in g/cycle)..... 151
Table 27: E55CRC-3: 1829-1 Idle, 1829-2 Creep, 1829-3 Transient, 1829-4 Cruise. (g/mile, except idle in g/cycle)..... 152
Table 28: E55CRC-3 retest: 1939-1 Idle, 1939-5 Creep, 1939-3 Transient, 1939-4 Cruise (g/mile, except idle in g/cycle)..... 152
Table 29: E55CRC-3 retest: 1942-1 Idle, 1942-5 Creep, 1942-3 Transient, 1942-4 Cruise. (g/mile, except idle in g/cycle)..... 152

Table 30: E55CRC-10 baseline emissions and “reflash” emissions. T&M runs are denoted in bold. NO_x^1 and NO_x^2 show values from two similar analyzers in parallel. It should be noted that Idle and Creep Modes often return highly variable emissions due to changing auxiliary loads on the vehicle. 154
Table 31: E55CRC-16 Emissions before and after T&M procedures. T&M 1 in bold represents testing with a new fuel injection pump; T&M 2 in bold italics represents testing with a new pump and EGR totally disabled. 155
Table 32: E55CRC-21 emissions T&M results in bold. 157
Table 33: Sequence of testing for E55CRC-31 163
Table 34: E55CRC-45 as received, after first repair (R), and after second repair (RR). 166

LIST OF APPENDICES

Appendix A: Photograph and Description of Each Test Vehicle
Appendix B: WVU Test Vehicle Information Sheets
Appendix C: Description of the WVU Transportable Heavy Duty Vehicle Emissions Testing Laboratory (Translab)
Appendix D: WVU Vehicle Inspection Sheets
Appendix E: WVU Tampering and Malmaintenance (T&M) Issues Sheets
Appendix F: Engine Control Unit Downloads
Appendix G: DRI Methods
Appendix H: Graphical Representation of Each Test Schedule
Appendix I: SMPS and CPC reduction program
Appendix J: Table of Test Runs
Appendix K: WVU Short Reports for Each Test
Appendix L: WVU Summary Data Tables
Appendix M: Graphical Representation of Data Found in the WVU Short Reports
Appendix N: Chemical Speciation Results
Appendix O: List of Target Chemical Species Analyzed
Appendix P: Quality Assurance and Control

EXECUTIVE SUMMARY

Program E-55/59 had the objective of acquiring regulated emissions measurements (for the whole test fleet) and non-regulated emissions measurements (on a subset of the test fleet) from in-use trucks in southern California. The project was conducted in four Phases (denoted 1, 1.5, 2 and 3). The Phase 1 test fleet consisted of 25 Heavy Heavy-Duty Diesel Trucks (HHDDT), selected to match a model year (MY) distribution developed by the sponsors and to reflect engines in common use in California. In Phase 1.5 an additional twelve HHDDT were studied, with a thirteenth truck tested on idle alone. The Phase 2 test fleet consisted of ten HHDDT and nine Medium Heavy-Duty Trucks (MHDT), which included seven diesel - fueled MHDT (MHDDT) and two gasoline-fueled MHDT (MHDGT). Phase 3 gathered data from nine HHDDT, eight MHDDT, and two MHDGT. The Phase 2 and 3 data were valuable in adding post-2002 MY (2.5 g/bhp-hr NO_x standard) HHDDT to the E-55/59 program.

Test cycles for all HHDDT were the Urban Dynamometer Driving Schedule (UDDS) and the HHDDT schedule, and some trucks were tested using the AC50/80. The HHDDT Schedule consisted of four modes, namely Idle, Creep, Transient and Cruise, and a high speed" cruise mode (HHDDT_S) was added for phase 1.5, 2 and 3. The MHDT were all tested using a Lower Speed Transient Mode (MHDTLO), a Higher Speed Transient Mode (MHDTHI) and a Cruise Mode (MHDTCR) of a recently developed California Air Resources Board (CARB) MHDT Schedule, and three MHDT were tested using the High-speed HHDDT_S mode of the HHDDT Schedule as well.. All HHDDT were tested at 56,000 lbs weight, with subsets tested at 30,000 lbs. and 66,000 lbs. as well. MHDT were tested at 50% and 75% of Gross Vehicle Weight Rating (GVWR). The first thirteen HHDDT in Phase 1 were subjected to sampling for non-regulated emissions, and the samples from the first three of these trucks were analyzed. Non-regulated species were measured from five HHDDT and one MHDDT in the Phase 2 test fleet. The HHDDT emissions were characterized using the West Virginia University (WVU) Transportable Heavy-Duty Emissions Testing Laboratory (TransLab).

Emissions were diluted in an 18 inch diameter tunnel, with flow controlled by a critical flow venturi. Gaseous emissions were measured with research grade analyzers, and total PM was measured from dilute exhaust using 70mm filters. PM data were acquired in Phases 1.5, 2 and 3 using both conventional filters and a Tapered Element Oscillating Microbalance (TEOM). The TEOM correlated well with the filters in each phase. Two chemiluminescent analyzers were used to assure quality of NO_x measurements.

The regulated emissions data for HHDDT (56,000 lbs. test weight) were compared between phases. Carbon dioxide data agreed well between phases, suggesting that vehicle loading was consistent from phase to phase. Data for CO, NO_x and PM were compared between phases. There were too few trucks, distributed over a wide range of model years, to reach emissions conclusions based on data from a single phase. For example, the Phase 2 fleet included only one truck in the 1991-1993 model year range, and its NO_x emissions were substantially lower than the NO_x emissions from the five trucks in the 1991-1993

model year range tested in Phases 1 and 1.5. The value of using the combined emissions data from all phases to reach conclusions on age or model year effects was evident.
Table 1 provides a summary of NO_x and PM data averages and ranges for the HHDDT fleet in all Phases, and for all MY, by test cycle or mode, at 56,000 lbs. test weight. Oxides of nitrogen (NO_x) varied fourfold on the Transient Mode, but sevenfold on the Cruise Mode, reflecting both off-cycle behavior and recent stringent NO_x standards. The high-speed HHDDT_S mode also showed a sevenfold range of NO_x. Average values for NO_x, in distance specific units, declined with respect to average cycle or mode speed. PM variation (geometrically) was greater than NO_x variation, with trucks producing emissions at the laboratory lower detection limit on all modes, but with the maximum values between four and eighteen times the average value for each mode or cycle.

Table 1: Highest, lowest, and average emissions of NO_x and PM for all HHDDT (56,000 lbs.).

	Idle	**HHDDT Creep**	**HHDDT Transient**	**HHDDT Cruise**	**HHDDT HHDDT_S**	**UDDS**
	(g/min)	(g/mile)	(g/mile)	(g/mile)	(g/mile)	(g/mile)
Highest NO_x	4.43	162.94	60.22	49.43	55.75	53.35
Average NO_x	1.10	56.68	23.50	18.07	17.94	21.67
Lowest NO_x	0.00	7.77	13.65	7.03	8.05	11.98
Highest PM	0.71	67.77	17.14	17.14	3.83	12.99
Average PM	0.04	5.25	2.65	1.08	0.85	1.78
Lowest PM	0.00	0.00	0.00	0.00	0.00	0.00

Emissions were influenced by MY, as shown in Table 2, for the UDDS. Fuel consumed (by carbon balance from CO_2) was highest for the oldest MY bin. For the remaining vehicles the 1999 and later MY vehicles used more fuel than the pre-1999 MY vehicles. 2003 and later MY HHDDT used 16% more fuel on the UDDS than 1975-1998 MY trucks, on average. HHDDT for the three oldest MY bins produced about 27 g/mile NO_x on the UDDS. NO_x was lower for intermediate MY trucks, rising back to about 27 g/mile in 1998 MY trucks. For 1999-2002 MY, NO_x was reduced to 19.22 g/mile, and, for 2003 and later MY, NO_x was reduced to 13.74 g/mile on the UDDS. There was a strong trend showing that PM was reduced for the HHDDT on the UDDS as MY advanced, with the 1986 and older MY fleet at 2 to 5 g/mile, and 2003 and later MY trucks at 0.50 g/mile. The trend for CO followed the PM trend. Fleet-averaged HC emissions on the UDDS showed a substantial reduction in the mid ‘90s.

Table 2: Emissions of regulated species by MY for HHDDT tested on the UDDS (56,000 lbs.).

		CO g/mile	CO_2 g/mile	NO_x g/mile	HC g/mile	PM g/mile
Pre-1975	Average	12.21	2766	28.46	6.11	3.47
	Std Dev.	1.82	21	3.53	1.94	0.55
1975-1979	Average	33.53	2298	26.41	1.98	4.94
	Std Dev.	29.19	206	10.98	0.47	5.33
1980-1983	Average	21.31	2225	27.40	2.11	2.18
	Std Dev.	11.60	243	2.99	0.06	1.11
1984-1986	Average	16.40	2174	18.67	2.44	2.30
	Std Dev.	8.36	80	8.71	1.37	1.03
1987-1990	Average	13.50	2111	19.42	1.63	1.86
	Std Dev.	6.11	183	3.67	1.82	0.86
1991-1993	Average	8.45	2071	18.00	2.64	1.10
	Std Dev.	4.90	71	2.21	3.67	0.50
1994-1997	Average	7.59	2142	23.77	1.24	0.76
	Std Dev.	4.25	218	6.23	1.85	0.56
1998	Average	7.05	2206	26.87	0.69	0.75
	Std Dev.	2.36	100	12.36	0.48	0.22
1999-2002	Average	9.89	2419	19.22	0.88	1.04
	Std Dev.	12.74	314	5.54	0.74	1.30
2003+	Average	2.33	2529	13.74	0.54	0.50
	Std Dev.	2.44	254	1.36	0.24	0.47

Table 3 presents an overview of NO_x and PM emissions for the MHDDT. NO_x emissions from MHDDT varied less than for the HHDDT fleet. For laden operation on the all cycles and modes, the highest NO_x emitter was about twice the level of the lowest emitter. PM variation was more substantial for the MHDDT; the highest PM mass emissions were four or five times the lowest emissions. MHDDT showed little change in NO_x between tests at laden and unladen weight, as shown in Table 4. The increase of 50% in test weight produced an average NO_x increase of only 11% on the UDDS, and 16% on the MHDTLO. There was virtually no weight effect on NO_x emissions for the MHDTCR for the MHDDT. The mode with the highest weight influence on PM was the MHDTLO (40% increase). The mode with the lowest weight influence on PM was the MHDTCR (7% increase).

Table 3: Highest, lowest, and average emissions of NO_x and PM for all MHDDT tested at 75% GVWR.

	MHDT AC5080	MHDTCR	MHDTHI	MHDTLO	UDDS
	(g/mile)	(g/mile)	(g/mile)	(g/mile)	(g/mile)
Highest NO_x	16.50	14.03	20.87	33.05	18.82
Average NO_x	9.81	10.48	12.95	20.20	12.71
Lowest NO_x	6.49	8.74	8.85	12.20	8.36
Highest PM	2.52	1.72	2.95	4.38	4.13
Average PM	0.79	0.71	0.94	1.48	1.10
Lowest PM	0.16	0.19	0.20	0.25	0.19

Table 4: The effect of changing test weight on the diesel-fueled MHDT, in terms of a simple average of emissions for that fleet.

	MHDT AC5080	MHDTCR	MHDTHI	MHDTLO	UDDS
	(g/mile)	(g/mile)	(g/mile)	(g/mile)	(g/mile)
Average Laden NO_x	9.81	10.48	12.95	20.20	12.71
Average Unladen NO_x	8.85	10.13	11.20	17.40	11.44
Average Laden PM	0.79	0.71	0.94	1.48	1.10
Average Unladen PM	0.62	0.66	0.72	1.06	0.82

A Tampering and Malmaintenance (T&M) program was initiated in Phase 1 to identify the incidence of high emitters and to determine the effect of repair on high emitters. Vehicles were selected based either on an inspection, or on the measurement of PM and NO_x emissions above thresholds that took into account MY emissions standards. A 1985 MY truck showed reduction of PM and increase in NO_x after a mechanical timing fault was repaired. A 1979 truck was a prodigious PM emitter, and was found to defy effective repair. A 1990 truck with a plugged air filter showed 27% PM reduction on the UDDS with a new air filter. A 1993 truck with high HC and PM was repaired twice but emissions remained high. A defective temperature sensor in one MHDT caused emissions effects, but it was not subjected to repair. A 1998 MY HHDDT with high NO_x emissions was reflashed in Phase 1, and NO_x was reduced during cruising behavior. Reflash of three additional HHDDT in Phase 1.5 showed NO_x reductions of 13.3%, 21.5% and 30.7% on the Cruise Mode of the HHDDT schedule. One of these vehicles was also repaired by replacement of a manifold air pressure (MAP) sensor, which also affected NO_x emissions.

Size distributions of PM were characterized from six trucks that were selected for non-regulated emissions measurement. These data were acquired using a Scanning Mobility Particle Sizer (SMPS), as well as a Differential Mobility Spectrometer (DMS500), which was a newly released instrument. A raw exhaust slipstream was diluted by a factor of thirty in a mini-dilution tunnel, and this dilute stream was sampled by the SMPS. The DMS used the main dilution tunnel of the WVU TransLab, which had a fixed flow and a varying dilution ratio. The SMPS detected a bimodal distribution with a nuclei mode for Idle operation of one 2004 MY truck (E55CRC-40), and the DMS 500 detected both the nuclei mode and accumulation mode during deceleration on this truck. The nuclei mode was not evident under load for E55CRC-40. The other 2004 MY truck had only one mode, with a very low particle count on Idle. A 1989 MY truck had a bimodal Idle distribution, but the remaining HHDDT were unimodal. Comprehensive data were acquired for steady operation using the SMPS on all trucks, and the DMS500 acquired transient distributions for four of the trucks.

Sampling for chemical speciation was performed on thirteen HHDDT in Phase 1 and on five HHDDT and one MHDDT in Phase 2. In Phase 1, only three of the thirteen trucks had the samples analyzed, and the remaining samples were archived. The exhaust from the TransLab tunnel was fed to a residence time chamber of the Desert Research Institute (DRI). Data were acquired for methane and volatile organic compounds using a canister and a field gas chromatograph. Semi-volatile organic compounds were captured in

PUF/XAD media and PM soluble fractions were captured on Teflon-Impregnated Glass Fiber Filters (TIGF) filters, and these were extracted and analyzed at the DRI laboratory. Carbonyls were captured using DNPH cartridges, and nitrosamines were captured in Thermosorb cartridges. Ions and Elemental/Organic carbon (EC/OC) split were determined from quartz filters. Results from the speciation data are legion, and examples include the fact that the EC/OC split differed substantially on Idle between the two 2004 MY trucks equipped with EGR, and that the ion and metal analyses varied widely between trucks. The total carbon emissions from cruise mode were found to be the highest, while the total PM mass emissions rates were the highest from the transient mode. All pre-1999 vehicles, which were subjected to speciation analysis, were found to emit higher levels of engine wear elements, such as iron, than the newer vehicles. Likewise, oil control, as demonstrated by the lubricating oil-based ash components, was better in post-1999 vehicles.

NOMENCLATURE

CA	California
CARB	California Air Resources Board
CFR	Code of Federal Regulations
CO	Carbon Monoxide
CO_2	Carbon Dioxide
CRC	Coordinating Research Council
CSHVR	City Suburban Heavy Vehicle Route
CTA	California Trucking Association
DAS	Data Acquisition System
DRI	Desert Research Institute
ECU	Engine Control Unit
EMFAC	Emissions Inventory Model employed by CARB
GVWR	Gross Vehicle Weight Rating
HC	Hydrocarbons
HEPA	High Efficiency Particulate Air
HHDDT	Heavy Heavy-Duty Diesel Truck
HHDDT_S	HHDDT Short (referring to a shortened high-speed cruise mode)
MEMS	Mobile Emissions Measurement System
mg	Milligrams
MHDDT	Medium Heavy-Duty Diesel Truck
MHDGT	Medium Heavy-Duty Gasoline Truck
MHDT	Medium Heavy-Duty Truck
MHDTCR	MHDT Cruise Mode
MHDTHI	MHDT High-speed Transient Mode
MHDTLO	MHDT Low Speed Transient Mode
MY	Model Year
N_2O	Nitrogen Dioxide
NIST	National Institute of Standards and Technology
NO_X	Oxides of Nitrogen
PA	Power Absorber
PM	Particulate Matter
PSVOC	Particulate/Semi-Volatile Organic Compound
QA/QC	Quality Assurance & Quality Control
RH	Relative Humidity
SOP	Standard Operating Procedures
T&M	Tampering and Malmaintenance
TEOM	Tapered Element Oscillating Microbalance
TRANS3	HHDDT Transient
Translab	Transportable Heavy Duty Vehicle Emissions Testing Laboratory
UDDS	Urban Dynamometer Driving Schedule
USDOE	United States Department Of Energy
VMT	Vehicle Miles Traveled
VOC	Volatile Organic Compounds
WVU	West Virginia University

INTRODUCTION AND OBJECTIVES

Heavy-duty diesel vehicles are known to be substantial contributors to the inventory of oxides of nitrogen (NO_X) and particulate matter (PM), but the quantification of their real world emissions may be imprecise. As a result, emissions inventory predictions may err. To remedy this uncertainty, Program E-55/59 was initiated. This program, consisting of Phases 1, 1.5, 2, and Phase 3, was managed by the Coordinating Research Council (CRC), and supported by the following sponsors:

Coordinating Research Council, Inc.
California Air Resources Board
United States Environmental Protection Agency
United States Department of Energy Office of FreedomCar & Vehicle Technologies through the National Renewable Energy Laboratory
South Coast Air Quality Management District
Engine Manufacturers Association

The primary objective of the E-55/59 research program was to quantify regulated and certain unregulated gaseous and PM emissions for heavy-duty (primarily diesel) vehicles in the South Coast Air Basin to support emissions inventory development. Another objective of the E-55/59 program was to quantify the influence of T&M on heavy-duty vehicle emissions. WVU and DRI also teamed to address the measurement of emissions in a comprehensive effort that carefully considered a representative fleet and representative vehicle activity. The overall E-55/59 research program involved both the medium and the heavy-duty chassis dynamometer operated together with a dilution and sampling system to address both regulated and unregulated species.

WVU characterized exhaust emissions from a total of 25 Heavy Heavy-Duty Diesel Trucks (HHDDT) in California in Phase 1 of the E-55/59 study. A T&M study was also developed in Phase 1. The first three vehicles were so-called “overlap” vehicles and were evaluated both under the USDOE “Gasoline/Diesel PM Split Study” and the E-55/59 study. The overlap vehicles were sampled for both regulated and unregulated emissions and the unregulated emissions samples were analyzed. The next ten vehicles in Phase 1 underwent testing for regulated emissions but the extent of sampling for chemical characterization was reduced and these samples were archived for possible chemical analysis at a later stage. The remaining twelve vehicles in Phase 1 were tested only for regulated emissions and the PM_{10} fraction.

Phase 1 of the research program covered only heavy heavy-duty (gross vehicle weight rating greater than 33,000 lbs.) vehicles. Test cycles included the UDDS, and four modes of the HHDDT schedule developed for the E-55/59 program and the AC5080 cycle.

Phase 1.5 of the program had the objective of acquiring regulated emissions measurements from twelve in-use trucks in southern California, and supporting a third-party characterization of certain non-regulated species from five vehicles in the Phase 1.5

test fleet. Processing of these third-party data is not addressed in this report. In addition, three vehicles were re-flashed with a post consent decree engine map, and re-tested. One of the re-flash vehicles was also repaired and re-tested. A thirteenth vehicle was added to the Phase 1.5 study when difficulties were encountered in testing a new 2004 model year (MY) truck with intelligent traction control on the chassis dynamometer. The thirteenth vehicle was also a 2004 MY truck selected to satisfy the requirements for MY distribution of the test plan for Phase 1.5. A high speed mode was added to the HHDDT schedule in Phase 1.5.

Phase 2 had the objective of acquiring regulated emissions measurements from nineteen in-use trucks in southern California. Ten were HHDDT, seven were Medium Heavy-Duty Diesel Trucks (MHDDT) and two were Medium Heavy-Duty Gasoline Trucks (MHDGT). The Phase 2 effort supported a DRI characterization of non-regulated species from five HHDDT and one MHDDT (total of 6) in the Phase 2 test fleet. Non-regulated exhaust characterization included speciation of both particulate matter (PM) and volatile organic compounds (VOC), and determination of particle size distribution. For the MHDDT and MHDGT, the AC5080 schedule was combined with a three mode Medium Heavy-Duty Truck (MHDT) schedule consisting of a low speed transient, a high-speed transient, and a cruise cycle. A twentieth vehicle was added to the study when difficulties were encountered in testing a 2002 MY truck on the WVU medium-duty chassis dynamometer.

The final phase, Phase 3, had the objective of acquiring both regulated and unregulated species from a selected fleet of California trucks. Nine trucks were HHDDT, eight were MHDDT, and two were MHDGT. For the HHDDT, test cycles were the UDDS and the HHDDT schedule. For the MHDT, the UDDS and MHDDT schedule were used.

The overall CRC E-55/59 program was planned to include sixty three HHDDT, seventeen MHDDT, and four MHDGT for measurement of regulated emissions. Regulated emissions were collected from all vehicles. In addition, non-regulated emissions were collected and analyzed on eight HHDDT and one MHDDT.

VEHICLE PROCUREMENT

Table 5 shows the combined truck recruiting objectives for all phases. This table lists the vehicles planned for each phase of the E-55/59 program broken down by vehicle MY, weight, fuel, and whether vehicles were to be subjected to non-regulated emissions analysis.

These vehicles complied with a MY distribution determined by the Air Resources Board and Coordinating Research Council. HHDDT were considered to be vehicles with a gross vehicle weight rating (GVWR) over 33,000 lbs., as well as any "full size" single axle tractors, since these typically have a Gross Combination Weight of 52,000 lbs. to 80,000 lbs. The term "full size" was intended to exclude any medium heavy-duty "hot shot" combinations that have become more common on the highways over the last decade.

The rationale for basing recruitment on MY is discussed below. The most important variable that influences emissions was believed to be the engine certification standard. This is reflected in the engine MY and the vehicle MY corresponds closely to the engine MY. The vehicle MY may not reflect the appropriate standard in the unusual case of a vehicle re-power when an engine of a newer standard may be installed. Rebuilds will normally return the engine to its original condition, whereas a re-power will usually employ a newer technology engine. The engine MY influences the level of emissions for certification, as shown in Table 6, which presents the Federal and California standards for such engines. At time of manufacture, vehicle MY is either the same as engine MY, or one year later.

The California Air Resources Board (CARB) used the EMFAC emissions inventory program to generate data for vehicle population, VMT, NO_X production and PM production. These CARB data (each weighted 25%) were combined to arrive at a test vehicle distribution by MY.

Table 7 shows the VMT, NO_X, PM and population distributions. WVU was instructed by ARB and CRC to employ these distributions in the execution of E-55/59. The Table 7 matrix was processed further to yield an integer number in each MY group. The target MY distribution was altered in Phase 2 and 3 to allow the inclusion of 2002-2004 MY trucks.

Table 5: Vehicles planned for recruiting in the E-55/59 program.

		Phase 1			Phase 1.5			Phase 2				Phase 3	
		Reg Species Qty	Chemical analysis qty[1]	Post-Oct '02 2.5g/bhp-hr NOx2	Reg Species Qty	Chemical analysis qty[1]	Post-Oct '02 2.5g/bhp-hr NOx2	Reg Species Qty	Chemical analysis qty[1]	Post-Oct '02 2.5g/bhp-hr NOx2	2004 4.0g/bhp-hr Nox	Reg Species Qty	Subttl
HHDDT	**pre-1975**	1	0	0	0	0	0	0	0	0		1	**2**
HHDDT	**1975-76**	1	0	0	0	0	0	0	0	0		1	**2**
HHDDT	**1977-79**	1	0	0	0	0	0	0	0	0		0	**1**
HHDDT	**1980-83**	2	0	0	0	0	0	0	0	0		1	**3**
HHDDT	**1984-86**	3	0	0	0	0	0	1	0	0		0	**4**
HHDDT	**Pre-1987 (Phase 1.5 only)**	0	0	0	1	0	0	0	0	0		0	**1**
HHDDT	**1987-90**	4	0	0	0	0	0	2	1	0		3	**10**
HHDDT	**1987-92 (Phase 1.5 only)**	0	0	0	1	0	0	0	0	0		0	**1**
HHDDT	**1991-93**	3	0	0		0	0	1	0	0		0	**4**
HHDDT	**1994-97**	5	0	0		0	0	2	1	0		2	**10**
HHDDT	**1998**	2	0	0	3	0	0	1	0	0		0	**6**
HHDDT	**99-02**	3	0	0	8	0	0	1	1	0		0	**13**
HHDDT	**03+**	0	0	0	0	0	0	2	2	1		1	**6**
HHDDT	**Subttl**	**25**	**0**	**0**	**13**	**0**	**0**	**10**	**5**	**1**	**0**	**9**	**63**
MHDDT	**pre-1975**	0	0	0	0	0	0	0	0	0	0	1	**1**
MHDDT	**1975-76**	0	0	0	0	0	0	0	0	0	0	0	**0**
MHDDT	**1977-79**	0	0	0	0	0	0	0	0	0	0	0	**0**
MHDDT	**80-83**	0	0	0	0	0	0	1	0	0	0	0	**1**
MHDDT	**84-86**	0	0	0	0	0	0	0	0	0	0	1	**1**
MHDDT	**87-90**	0	0	0	0	0	0	1	0	0	0	1	**2**
MHDDT	**1988-1990**	0	0	0	0	0	0	0	0	0	0	0	**0**
MHDDT	**91-97 (Phase 3 Only)**	0	0	0	0	0	0	0	0	0	0	0	**0**
MHDDT	**91-93**	0	0	0	0	0	0	1	0	0	0	1	**2**
MHDDT	**94-97**	0	0	0	0	0	0	1	0	0	0	2	**3**
MHDDT	**98**	0	0	0	0	0	0	1	1	0	0	1	**3**
MHDDT	**99+ (Phase 2 Only)**	0	0	0	0	0	0	2	0	1	0	0	**3**
MHDDT	**99-02 (Phase 3 Only)**	0	0	0	0	0	0	0	0	0	0	1	**1**
MHDDT	**00+**	0	0	0	0	0	0	0	0	0	0	0	**0**
MHDDT	**Subttl**	**0**	**0**	**0**	**0**	**0**	**0**	**7**	**1**	**1**	**0**	**8**	**17**
MHDGT	**pre-1975**	NA	NA	NA	NA	NA	NA	0	0	0	0	0	**0**
MHDGT	**1975-76**	NA	NA	NA	NA	NA	NA	0	0	0	0	0	**0**
MHDGT	**1977-79**	NA	NA	NA	NA	NA	NA	0	0	0	0	0	**0**
MHDGT	**80-83**	NA	NA	NA	NA	NA	NA	0	0	0	0	0	**0**
MHDGT	**84-86**	NA	NA	NA	NA	NA	NA	1	0	0	0	0	**1**
MHDGT	**87-90**	NA	NA	NA	NA	NA	NA	0	0	0	0	0	**0**
MHDGT	**1988-1990**	NA	NA	NA	NA	NA	NA	0	0	0	0	1	**1**
MHDGT	**91-97 (Phase 3 Only)**	NA	NA	NA	NA	NA	NA	0	0	0	0	1	**1**
MHDGT	**00+**	NA	NA	NA	NA	NA	NA	1	0	0	0	0	**1**
MHDGT	**Subttl**	**0**	**0**	**0**	**0**	**0**	**0**	**2**	**0**	**0**	**0**	**2**	**4**
Overall Total		**25**	**0**	**0**	**13**	**0**	**0**	**19**	**6**	**2**	**0**	**19**	**84**

Table 6: Federal and ARB past and present emissions standards.

FEDERAL HEAVY-DUTY TRUCK STANDARDS						CALIFORNIA HEAVY-DUTY TRUCK STANDARDS					
MODEL YEAR	HC[1]	CO	NO_X	PM	HC+NO_X	MODEL YEAR	HC[1]	CO	NO_X	PM	HC+NO_X
	g/bhp-hr						g/bhp-hr				
						1975-76	---	30.0	---	---	10.0
1974-78	---	40.0	---	---	16.0	1977-79	1.0	25.0	7.5	---	---
1979-83	1.5	25.0	---	---	10.0	1980-83	1.0	25.0	---	---	6.0
1984-87	1.3	15.5	10.7	---	---	1984-86	1.3	15.5	5.1	---	---
1988-90	1.3	15.5	10.7	0.60	---	1987-90	1.3	15.5	6.0	0.60	---
1991-93	1.3	15.5	5.0	0.25	---	1991-93	1.3	15.5	5.0	0.25	---
1994-97	1.3	15.5	5.0	0.10	---	1994-97	1.3	15.5	5.0	0.10	---
1998-02	1.3	15.5	4.0	0.10	---	1998-02	1.3	15.5	4.0	0.10	---
2003+	0.5[2]	15.5	2.0	0.10	---	2003+	0.5[2]	15.5	2.0	0.10	---

[1] **Note:** the HC standards shown are total hydrocarbons except for model year 2003+ which is NMHC.
[2] Assumes 2.5 g/bhp-hr (NO_X+NMHC) with a 0.5 g/bhp-hr NMHC cap effective October 2002.

Table 7: Vehicle Selection Matrix: NO_x, PM, VMT population (as percentages of total).

	Pop	**VMT**	**NO_X**	**PM**	**Average**
pre-1975	5.2	1.2	2.0	3.4	2.95
1975-76	1.5	0.5	0.8	1.3	1.03
1977-79	4.8	1.9	3.1	5.3	3.78
1980-83	7.8	3.9	6.1	10.7	7.13
1984-86	12	7.7	9.1	13.7	10.63
1987-90	23.7	19.8	18.5	21.8	20.95
1991-93	13.3	14.2	13.1	14.1	13.68
1994-97	16.6	22.9	24.4	18.1	20.50
1998	4.0	7.0	8.5	4.2	5.93
1999-01	11.1	20.9	14.5	7.4	13.48
	100	100	100.1	100	100.03

The California Trucking Association (CTA), through a survey, obtained information for use in Phase 1 on the distribution of engine types by MY, and so by certification standard (MY group). The CTA matrix was then reviewed to identify preferred engine manufacturers in each MY group. The matrix did contain errors due to imprecise survey replies (with similar engine models having multiple names, truck models substituted for engines, some medium duty engines in the matrix and engines assigned to the wrong manufacturer) and an effort was made to compensate for these errors. The test matrix was selected considering engine count and in some cases the need to gather some engine models together or represent a variety of engines.

Many of the vehicles recruited in Phase 1 were procured by CTA. To identify potential

study participants, CTA first contacted the survey respondents that had the desired MY trucks and engines in their fleets and indicated on the survey that they would be willing to participate in the study. CTA also sent out several faxes soliciting participation and phoned the entire membership in the Los Angeles/Orange/San Bernardino/Riverside areas to complete the study. Since not all the members had participated in the survey, the engine makeup of many fleets was unknown and the CTA staff were "cold calling" to find the appropriate study engines. One truck, E55CRC-21, was procured from a rental company by CTA.

A few trucks in Phase 1 were procured directly by WVU. In all subsequent phases of the study, WVU recruited all of the test vehicles. These vehicles were procured from a variety of sources including owner-operators, truck fleets, and rental companies. Many of the trucks in Phase 1.5 and following were procured from used truck dealerships.

Table 8 lists the vehicles which were actually recruited under this program. The vehicles are broken down by their reference number, weight class and fuel, vehicle MY, vehicle manufacturer, horsepower, and engine manufacturer. Trucks were designated as E55CRC-XX according to the order of recruitment. Details are provided in Table 8 for 78 trucks, but three of the trucks recruited were not characterized fully for emissions. Truck E55CRC-37 was a 2004 Volvo HHDDT with traction control and the truck could not be operated on the chassis dynamometer. Idle emissions only were obtained for this truck. Truck E55CRC-67 was a 1975 Ford HHDDT procured with assistance from the Gateway Cities Program. It was not functional beyond brief periods of idle. Truck E55CRC-52 was a 2002 Isuzu MHDDT. Subsequent to testing, a detailed quality assurance review of the data found that coastdown parameters had been incorrect and, therefore, that the dynamometer loading was significantly in error. The vehicle had been sold and the new owner would not allow it to be returned for a retest. A substitute vehicle was found.

Table 8: Basic Information on the 78 trucks actually recruited.

E55CRC-(truck)	M=MHDT H=HHDT	Vehicle model year	Vehicle Manufacturer	Engine Model	Engine Power (hp)	Engine Manufacturer
E55CRC-1	H	1994	Freightliner	Series 60	470	Detroit
E55CRC-2	H	1995	Freightliner	3406B	375	Caterpillar
E55CRC-3	H	1985	International	NTCC-300	300	Cummins
E55CRC-4	H	2000	International	C-10	270	Caterpillar
E55CRC-5	H	2000	Freightliner	N14-435E1	435	Cummins
E55CRC-6	H	1995	Freightliner	M11-370	370	Cummins
E55CRC-7	H	1990	Peterbilt	Series 60	450	Detroit
E55CRC-8	H	1996	Kenworth	M11-300	370	Cummins
E55CRC-9	H	1998	Peterbilt	C12	410	Caterpillar
E55CRC-10	H	1998	Sterling	Series 60	470	Detroit
E55CRC-11	H	2000	Freightliner	ISM-11	330	Cummins
E55CRC-12	H	1986	International	300	300	Cummins
E55CRC-13	H	1978	Freightliner	350	350	Cummins
E55CRC-14	H	1986	Freightliner	LTA10	270	Cummins

E55CRC-(truck)	M=MHDT H=HHDT	Vehicle model year	Vehicle Manufacturer	Engine Model	Engine Power (hp)	Engine Manufacturer
E55CRC-15	H	1973	Kenworth	NTC-350	350	Cummins
E55CRC-16	H	1979	White	3208	200	Caterpillar
E55CRC-17	H	1993	Freightliner	L-10	330	Cummins
E55CRC-18	H	1991	Ford	L-10	300	Cummins
E55CRC-19	H	1987	International	L-10	300	Cummins
E55CRC-20	H	1992	Peterbilt	Series 60	450	Detroit
E55CRC-21	H	1990	Freightliner	3406B	400	Caterpillar
E55CRC-22	H	1993	Ford	L10-280	280	Cummins
E55CRC-23	H	1983	Peterbilt	Plate Not Available	UNK	Cummins
E55CRC-24	H	1975	Kenworth	NTCC-350	350	Cummins
E55CRC-25	H	1983	Freightliner	Plate Not Available	UNK	Cummins
E55CRC-26	H	1999	Freightliner	C-10	270	Caterpillar
E55CRC-27	H	2000	Freightliner	Series 60	500	Detroit
E55CRC-28	H	1999	Freightliner	Series 60	500	Detroit
E55CRC-29	H	2000	Volvo	1SX475ST2	450	Cummins
E55CRC-30	H	1999	Freightliner	Series 60	500	Detroit
E55CRC-31	H	1998	Kenworth	N14-460E+	460	Cummins
E55CRC-32	H	1992	Volvo	3406B	280	Caterpillar
E55CRC-33	H	1985	Freightliner	3406	310	Caterpillar
E55CRC-34	H	2004	Freightliner	Series 60	500	Detroit
E55CRC-35	H	2001	Sterling	Series 60	470	Detroit
E55CRC-36	H	2001	Peterbilt	C-15	475	Caterpillar
E55CRC-37	H	2004	Volvo	ISX	500	Cummins
E55CRC-38	H	2003	Volvo	ISX	530	Cummins
E55CRC-39	H	2004	Volvo	ISX	530	Cummins
E55CRC-40	H	2004	Freightliner	Series 60	500	Detroit
E55CRC-41	M	1998	Ford	B5.9	210	Cummins
E55CRC-42	H	2000	Freightliner	3406	435	Caterpillar
E55CRC-43	H	1995	Peterbilt	Series 60	470	Detroit
E55CRC-44	H	1989	Volvo	3406	300 (est.)	Caterpillar
E55CRC-45	H	1993	Volvo GM	L10-280	280	Cummins
E55CRC-46	H	1989	Volvo GM	3176	400 (est.)	Caterpillar
E55CRC-47	H	1986	Ford	6V92	350	Detroit
E55CRC-48	H	1998	Freightliner	N14 Plus	447	Cummins
E55CRC-49	H	1994	International	3406?	300 (est.)	Caterpillar
E55CRC-50	M	2001	International	DT466 C-195	195	International
E55CRC-51	M	1994	International	DT-408 A210F	210	International
E55CRC-52	M	2002	Isuzu	4HE1-TCS	175	Isuzu
E55CRC-53	M	2001	GMC	1GMXH08.15 12 Gas V8	270	GM

E55CRC-(truck)	M=MHDT H=HHDT	Vehicle model year	Vehicle Manufacturer	Engine Model	Engine Power (hp)	Engine Manufacturer
E55CRC-54	M	1983	Ford	370-2V Gas V8	296	Ford
E55CRC-55	M	1992	Ford	210	210	Ford
E55CRC-56	M	1988	Ford	3208	215	Caterpillar
E55CRC-57	M	2000	Freightliner	3126	330	Caterpillar
E55CRC-58	M	1982	Ford	V8-8.2 4087-7300 770	160 (est.)	Detroit
E55CRC-59	M	1990	International	LTA10	300	Cummins
E55CRC-60	H	1995	Ford	L10	300	Cummins
E55CRC-61	M	2000	1999	3126	190	Caterpillar
E55CRC-62	H	1983	Kenworth	3406	350	Caterpillar
E55CRC-63	H	2005	Freightliner	C15	500	Caterpillar
E55CRC-64	H	1994	Kenworth	N14	310	Cummins
E55CRC-65	H	1988	International	LTA10	240	Cummins
E55CRC-66	H	1989	International	LTA10	270	Cummins
E55CRC-67 (not tested)	H	1975	Ford	UNK	UNK	Cummins
E55CRC-68	M	1995	International	DT466 C-195	230	International
E55CRC-69	H	1989	Ford	C215	215	Ford
E55CRC-70	M	1998	Freightliner	LTA10	210	Cummins
E55CRC-71	M	1995	Ford	LTA10	300	Cummins
E55CRC-72	M(G)	1992	Ford	7.0 EFI	UNK	Ford
E55CRC-73	M	1974	Ford	1150	185	Caterpillar
E55CRC-74	H	1969	Kenworth	UNK	UNK	Cummins
E55CRC-75	M	1975	Ford	V8-8.2 4087-7300 C59	UNK	Detroit Diesel
E55CRC-76	M	1993	Ford	8.3L	UNK	Ford
E55CRC-77	M(G)	1987	Chevrolet	V8	UNK	Chevrolet
E55CRC-78	H	1975	Peterbilt	UNK	UNK	Cummins

Once a vehicle was recruited, a WVU driver or WVU commercial driver (when required) drove the vehicle to the WVU test site. The driver inspected the vehicle before moving the vehicle: no vehicles were rejected on the basis of this preliminary inspection. A few vehicles, not licensed at the time of testing, were towed to the test site.

Each vehicle was photographed at the laboratory site. These photographs are gathered in Appendix A of this report. Basic vehicle information was logged on the Vehicle Information Forms which are gathered in Appendix B.

EQUIPMENT & METHODS – REGULATED SPECIES

Translab Description

The characterization of the emissions took place using a WVU Transportable Heavy Duty Vehicle Emissions Testing Laboratory (Translab). The Translab incorporated a chassis dynamometer testbed, full scale dilution tunnel with a critical flow venturi and blower, 70mm PM filtration system and research grade analyzers. For all of Phases 1 and 1.5 and for the first several vehicles of Phase 2, the Translab was located at Ralphs Grocery, 1500 Eastridge Ave., Riverside, CA. The latter part of the testing was completed at 1084 Columbia Ave., Riverside, CA on property leased from the University of California, Riverside. The Translab had the same basic arrangement in all of phases of the E-55/59 CRC Study. WVU employed two different HHDDT chassis dynamometer test beds, one for Phase 1 and the other for Phases 1.5, 2, and 3. These test beds were similar in design and calibrated to provide the same inertia and road-load characteristics. Some MHDTs were tested using the second HHDDT test bed, while others were tested using WVU's medium-duty chassis dynamometer. The coastdown methodologies used to determine vehicle inertial and drag characteristics assured that loading was properly applied independent of which chassis dynamometer was utilized.

The laboratory equipment, including the gaseous emissions analyzer bench, PM system and dilution system used, remained the same throughout the program. Procedures with respect to PM filter processing, analyzer calibration and background correction were the same for all four phases. For completeness of this report, a description of the WVU Translab has been included in Appendix C.

Beginning with E55CRC-26, the laboratory used a Tapered Element Oscillating Microbalance (TEOM) analyzer to quantify continuous PM mass. The TEOM sampled at a rate of 2 liters/minute from the primary (full scale) dilution tunnel using the same port as the PM filter.

In Phase 1.5, Phase 2, and Phase 3 research, exhaust temperature was measured in the first section of test exhaust after the tailpipe using a J-type thermocouple. Exhaust temperature was not measured in Phase 1 research.

Preparation of the Vehicle for Testing

Vehicle Inspection

Each truck, when received at the test site, was inspected for safety, tampering or malmaintenance and engine control unit (ECU) status. The safety inspection was conducted by the truck's test driver (who in most instances also drove the vehicle from its source). The vehicle was inspected for:

- Exhaust leaks

- Air leaks in the brake system
- Other visible brake problems (including frayed lines, damaged slack adjusters)
- Damaged drive tires
- Drivetrain damage (including worn universal joints)
- Loose fan bearing or worn engine drive belts
- Damaged vehicle controls

Vehicle information was collected on the WVU Test Vehicle Information Sheets and they are included in Appendix B. The vehicle safety inspection was verified by the completion of WVU Vehicle Inspection Report. These sheets appear in Appendix D.

Each vehicle was also visually inspected for T&M. This inspection procedure was developed in Phase 1 of this program. Items for inspection appeared in the WVU T&M Issues sheet for each vehicle. Copies of the WVU T&M Issues Sheets appear in Appendix E of this report.

The engine control unit (ECU), in vehicles so equipped, was interrogated where possible. An interface and software for this interrogation, developed for use by the WVU Mobile Emissions Measurement System (MEMS) and used in other related programs for on-board vehicle emissions measurement[1] was used to log ECU data continuously for vehicles equipped with a compatible ECU. These data were transmitted to WVU-Morgantown electronically as soon as they were available. In several cases, relating both to the system used to read the data and to the vehicle ECU, interrogation was not possible. All available ECU downloads are presented in Appendix F. In cases where the same vehicle ECU download was performed on two occasions (and was identical), only the first download is shown in Appendix F.

Engine/Vehicle Preparation

Prior to being placed on the dynamometer, each vehicle was inspected and the following inspections and checks were performed and recorded as the T&M report for that vehicle:

- Engine oil, power steering fluid, and coolant levels confirmed to be in operating range.
- Fuel tanks filled to provide sufficient fuel for the entire testing procedure (typically ¾ tank for multiple weights with repeated runs or ½ tank for testing at one or two weights with single runs).
- Inspection for signs of fuel, oil, and coolant leaks from the vehicle.
- Exhaust after-treatment devices, when installed, inspected and model/type recorded and compared to specifications provided on engine and vehicle data plates.
- Condition of the air filter checked air cleaner service indicator checked and, if the air filter was severely blocked, project supervisors and sponsors contacted prior to fitting with a new filter.
- Fuel sample (32 oz.) and oil sample (4 oz.) take for post testing analysis.
- Exhaust system inspected for leaks.
- Engine checked for excessive/irregular noise and malfunctions in the cooling system.

Wheel-Hub Adapter Installation

In order to connect the drivetrain of the vehicle to the dynamometer components, the outer wheels of the dual wheel set were removed on the forward-most drive axle and replaced with rims designed to accept specially designed adapters. The inside tires were checked for any cuts and bulges and tire pressure was verified/adjusted to be within $\pm$5 psi of the manufacturer's maximum tire pressure specifications.

For vehicles equipped with a power divider, the power divider was locked in.

Using the information stamped on the vehicle tires, the rolling diameter was determined and recorded into the vehicles database to allow for the proper dynamometer flywheel selection.

Certain MHDT were characterized using a medium-duty chassis dynamometer test bed. In these cases the installation on the dynamometer was conventional. Power was taken from the vehicle's wheels by the rollers, and no hub connection was employed.

Test Vehicle Mounting

In order to mount the vehicle onto the dynamometer, ramps were installed and the vehicle was backed on to the test bed with the driven wheels (forward wheel set in the case of dual axle vehicles) centered over the front set of rollers. The vehicle axles were then attached to the dynamometer bed using chains to prevent both forward-aft and side-to-side motion. The hub adapters were then connected to the dynamometer drivetrain and the front of the vehicle was raised to level the vehicle.

If excess tire side wall deflection was observed (or later if tire heating became an issue) on vehicles with single rear axles, the rear of the vehicle was supported partly using jacks. Up to 50% of the normal weight was removed from the single wheel (which normally would share the weight with another wheel). Scales were used beneath the jacks to verify the amount of weight reduced.

Connections of Vehicle to Laboratory

A monitor, used by the driver to observe the target and actual vehicle speed, was placed in the vehicle. The exhaust of the vehicle was routed to the dilution tunnel using insulated, flexible exhaust tubing.

Pre-test Vehicle Operation

Prior to operating the vehicle, the test engineer estimated the dilution tunnel flow rate that would provide the optimum balance between providing sufficient flow to maintain the particulate filter face temperature below 125^{O}F while not over diluting the exhaust such that emissions concentrations could be accurately measured by the laboratory analyzers. After starting the dilution tunnel blower, the vehicle engine was started and operated

throughout its range while the safety officer inspected the exhaust system (including both the vehicle exhaust and the exhaust transfer tube) for leaks.

In cases where the vehicle would not start after 10 seconds of cranking, technicians investigated to determine the cause for the failure and attempted to affect repairs.

At all times, the vehicle was operated a manner representative of in-use operation, and where appropriate and available, according to the manufacturer's recommendation. For vehicles equipped with automatic transmissions, idle modes less than one minute in duration were run with the transmission in "Drive" and the brakes applied. In the case of vehicles equipped with manual transmissions, the vehicles were run in gear with the clutch disengaged.

Vehicle Driving Instructions

During high acceleration portions of the trace, the vehicle was driven at maximum power while in gear with the clutch engaged, but the gears were changed in the same manner that they would be changed while driving on the road. The gears were not "crashed" aggressively to keep up with the trace. Conversely, the vehicle was not driven with casually slow shifting. The objective during acceleration was not solely to match the trace as closely as possible, but also to mimic the way in which the subject vehicle would actually accelerate on the road.

During braking events, where that portion of the trace ended at zero velocity (idle), the driver would downshift during braking at speeds above 15 to 20 miles per hour. Below 15 to 20 miles per hour, brakes alone were used. In many 9 and 10 speed transmissions with typical over-the-road gear ratios, this would typically mean that downshifting would continue until the highest gear in low range (5th gear in a 10 speed, 4th gear in a "L plus 8" 9 speed configuration) was attained. When the deceleration did not reach zero, but blended into another acceleration ramp, or a cruise section, gears were used throughout to maintain normal on-road driving practice.

The driver selected gears based upon judgment of the gears that would be used on the road. For example, the driver did not take off in the lowest gear if a higher gear would be the norm in use. In driving 13 and 18 speed (ranged and split) transmissions, it was not considered necessary to use all gears and typically splitting was not performed in this case. However, 10 speed splitter transmissions were not driven as 5 speed units at high inertial loads.

Vehicle Practice Run

For each vehicle, a practice test was performed. This served to help the driver familiarize himself with the driving/shifting/braking characteristics of the vehicle while the ranges of the gaseous emissions analyzers were set. The practice run also allowed the test engineer to ensure that the dynamometer was loading the vehicle properly.

If the driver did not follow the trace properly, variances were recorded in the comments section of the test report and an explanation was offered. If any abnormality was observed during this practice run, the supervising engineer was informed.

Test Run Procedures

Overall Vehicle Test Procedure

Background PM samples were taken at the beginning and end of each test day, unless otherwise designated by program requirements.

To execute a hot test, the truck was warmed through operation on or off the dynamometer until it had reached an operating temperature that caused the radiator to engage in cooling. This may be judged by the heat of the radiator or opening of the thermostat. Alternately, it was considered sufficient that the truck was operated for a cycle with a minimum duration of 10 minutes with a minimum energy intensity of 7.5×10^{-6} cycle energy per mile per mass of vehicle (axle hp-hr/lb.-mile). Cycles meeting this criterion include the WVU 5mile route, the CSHVR, the UDDS, and the Transient and Cruise modes of the California Heavy Heavy-Duty Diesel Vehicle Test (HHDDT) cycle. It is acknowledged that when cold weather testing is performed, these cycles may not warm the vehicle to the point that the radiator is in use but the vehicle was deemed to be at operating temperature under those ambient conditions. No cold conditions were encountered during the testing in Riverside. The truck was keyed off 30-60 seconds after the end of this warm-up.

The test schedule commenced no later than 20 minutes after the warm-up but not before 10 minutes after the warm-up. If the20 minute period was exceeded, another warm-up was required. These criteria were based on a prior study that evaluated HHDDT schedule repeatability. Based upon measurements of emissions during the warm-up, analyzers were re-ranged during this 10 to 20 minute period as required. The vehicle was started and allowed to idle between 30 and 60 seconds prior to the beginning of the test and, after the completion of the test, the vehicle was idled for 30 seconds and then keyed off.

During the 10 to 20 minute period between tests, integrated and background bags were analyzed, particulate filters were changed out and analyzers were checked for drift by checking their response to samples containing 0% and 100% of the respective analysis gas.

Gaseous and PM sampling system

WVU's Total-Exhaust Double-Dilution Tunnel

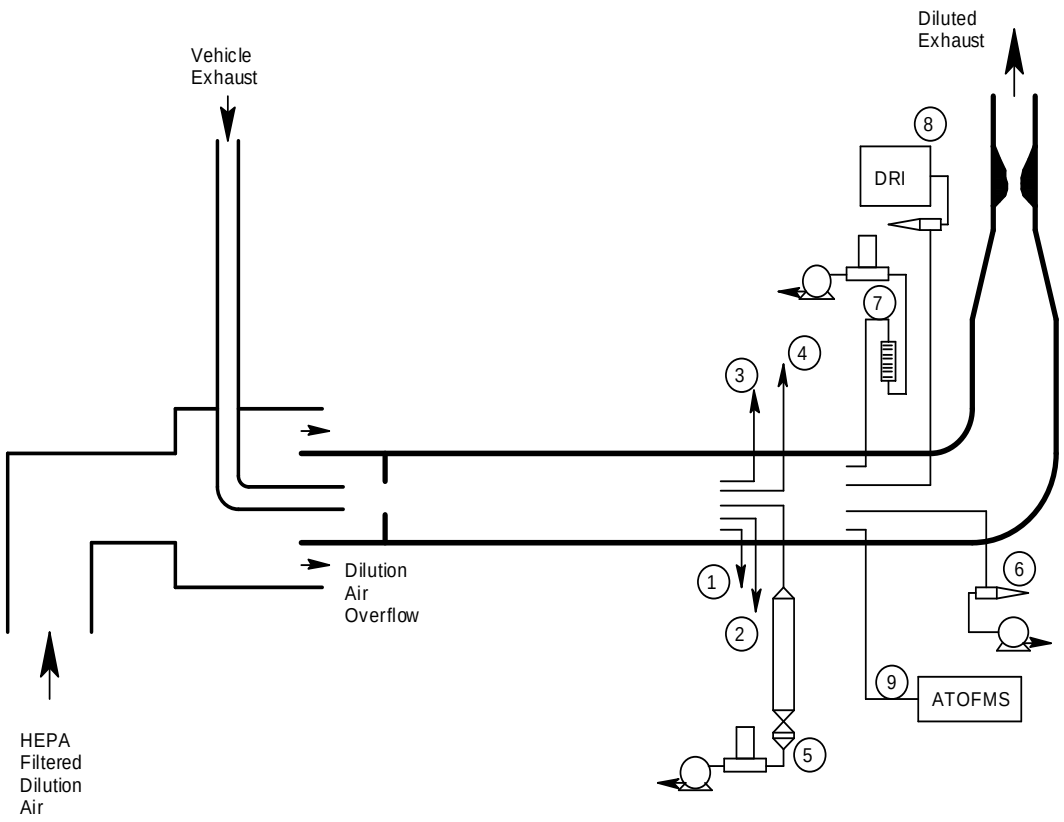

Figure 1: WVU Sampling System Schematic.

Figure 1 shows the WVU double dilution tunnel. A description of the various components on WVU's sampling system is given in Table 9. This table includes details of the DRI residence chamber and the sampling for non-regulated species from the chamber.

Table 9: Sampling system description and media type.

ID	Sample Description	Media Type	
		Phase 1	**Phase 2**
1	HC	Heated FID Analyzer	Heated FID Analyzer
2	CO/CO2	NDIR Analyzers	NDIR Analyzers
3	NOx	Chemiluminescent Analyzer	Chemiluminescent Analyzer
4	TEOM	TEOM Filter	TEOM Filter
5	TPM	70 mm T60A20	70 mm T60A20
6	PM_{10} Fraction for Gravimetric Analysis	URG Model 2000-30 EA Cyclone @ 28.3 lpm ; 47 mm TX40HI20WW Filters	URG Model 2000-30 EA Cyclone @ 28.3 lpm ; 47 mm TX40HI20WW Filters
7	MOUDI	Greased Aluminum Substrates; TX40HI20WW Afterfilter	Not Applicable
8	DRI Dilution Chamber. The chamber diluted exhaust from WVU's tunnel through two $PM_{2.5}$ cyclones.	Model Bendix-Unico 240 Cyclones@113 lpm	Model Bendix-Unico 240 Cyclones@113 lpm
	Volatile Organic Compounds (VOC)	Canister, Field GC	Canister, Field GC
	Methane	Canister	Canister
	Semi-volatile Organic Compounds (VOC)	PUF/XAD and TIGF Filters	PUF/XAD and TIGF Filters
	SVOC – Low Molecular weight	TENAX Tubes	TENAX Tubes
	Nitro-PAH	PUF/XAD and TIGF Filters	PUF/XAD and TIGF Filters
	Carbonyls	DNPH Cartridges	DNPH Cartridges
	Nitrosamines	Thermosorb Cartridges	Thermosorb Cartridges
	PM, SOF, Organic Compounds	TIGF Filters	TIGF Filters
	Elemental Analysis and Gravimetric Analysis ($PM_{2.5}$)	TIGF Filters	TIGF Filters
	Ammonium and Ions (Nitrate, Nitrite, Chloride, Sulfate)	Quartz Filters	Quartz Filters
	EC/OC	Quartz Filters	Quartz Filters
9	Particle Analysis by Mass Spectroscopy	ATOMFS	ATOMFS
10	Real-time PM Size Distribution		DMS 500

Total Particulate Matter

Total Particulate Matter (TPM), as defined by the US EPA, is sampled by filtering diluted diesel exhaust at filter face temperatures of less than 52ºC (125º F). TPM has been reported as a regulated emission species. A 70mm filter holder was connected that contained two 70mm T60A20 fiberglass filters, the primary and secondary filters to capture the regulated TPM.

Gas Analyzer Operation

Pre-Test Procedure

Prior to initiating each test, the background and integrated/dilute bags were evacuated to ensure that no sample was left in them from the previous test. Since the HC and NO_X analyzers were sensitive to temperature changes, their sample pumps were started at least 1 hour prior to starting an emissions test. The particulate filter holder was loaded with conditioned and weighed primary and secondary filters and connected to the secondary dilution tunnel. With the sample pumps and analyzers operating and sampling from the dilution tunnel, sample flow rates were adjusted to meet specifications and maintain test-to-test consistency.

In-Test Procedure

At the onset of the data collection phase of each test, the gas operator ensured that the fill rates for the dilute and background bags were sufficient to provide enough sample for two analyses if required. The flow rate through the particulate filter was checked against the setting for the test (typically 2-4 scfm depending on PM loading and outside temperature). During a test, the engineer and gas operators monitored the responses of the dynamometer controls and emissions analyzers to ensure that they were operating properly. A safety operator, stationed at the dynamometer, watched for inconsistencies in vehicle or dynamometer operation. The most common vehicle problem involved tire degradation during the test due to overheating which was compensated for by the safety operator applying a water spray to the tires. The test engineer also reviewed the data collected during the previous test to ensure that the various lab analyzers and sensors had operated correctly.

Post-Test Procedure

At the conclusion of the test, the particulate filter holder was disconnected from the secondary dilution tunnel and the loaded particulate filters were placed stored in an environmental chamber for conditioning. The integrated and background bags were analyzed for HC, NO_X, CO, CO_2 concentration and the levels were recorded. The CO and CO_2 concentrations from integrated and continuous measurements were compared to ensure that they agreed to within 5%.

Calibration Procedures

Sensors and analyzers were calibrated per the manufacturer's recommendation and per Title 40, Part 86 of the CFR. Calibration procedures for the entire laboratory were followed for each analyzer when the calibration gas source was changed or after analyzer repair.

Particulate Matter Filter Conditioning and Weighing

The relative humidity and temperature of the environmental chamber, used to condition particulate filters before weighing, were maintained at 50% (+/-10%) and 70 ^{o}F (+/- 10 ^{o}F). Filters were stored in petri dishes that were cleaned using alcohol and lint free cloth prior to use. Filters were conditioned in the environmental chamber for a minimum of 5 hours before weighing. A set of two particulate filters were kept in the chamber and weighed each time filters were weighed to check for possible problems with either the weighing instrument or the environmental chamber. Filter weight was determined using a CAHN-32 microbalance which was calibrated using a NIST traceable 200 mg calibration weight.

Speciated analysis of filters, performed by DRI, is discussed in Appendix G.

Forms

A set of forms, shown in the Quality Assurance Program section were filled out by the field engineers/technicians during vehicle emissions evaluation tests:

Quality Assurance/Quality Control and Emissions Data Report
Field Custody Log
Analyzer Check-off Sheet
Analyzer Calibration Record
Test Vehicle Information Sheet
Vehicle Test Sequence
Vehicle Inspection Form
T&M Issues Form

The "Test Sequence" form was designed to enable WVU field engineers keep track of the tests that have been completed. The "Test Sequence" depicts tests in the correct chronological order.

Test sequence numbers are employed by WVU to keep track of all tests in its database. This is WVU's primary means of accessing test results for any vehicle evaluated in the past 12 years. Each test sequence number has several run numbers associated with it.

Test Cycles

Each vehicle was tested using a suite of test schedules which varied between phases, and between HHDDT and MHDT. The target cycles and modes are shown graphically in Appendix H of this report. The UDDS was used for all classes of vehicles. For the HHDDT, the HHDDT Schedule[2], consisting of four modes (Idle, Creep, Transient and Cruise), was also used. The trucks were tested at 56,000 lbs. simulated weight on the UDDS and the HHDDT Schedule, plus a high-speed cruise mode created for Phase 1.5. The high-speed cruise mode caused high dilution tunnel and tire temperatures during testing and was shortened in duration at the beginning of Phase 1.5, after which it was

termed the "HHDDT Short" (HHDDT_S). In Phase 1.5, the five modes of the HHDDT schedule were also used to characterize emissions at 30,000 lbs. and 66,000 lbs. test weights, after preliminary work suggested that the original 75,000 lbs. maximum target weight placed too much stress on both truck brakes and the dynamometer. This mode was intended for use in testing all HHDDT. HHDDT_S has a maximum speed of 67 mph and an average speed of slightly over 50 mph. In some cases trucks were governed at a sufficiently low road speed so that the HHDDT_S mode could not be executed reasonably. In these cases, as judged by the WVU field engineer, no HHDDT_S mode was attempted.

Table 10 shows the time duration, average speed, and distance covered for each cycle or mode, and the computer code used to describe that cycle or mode.

Table 10: Test Schedule Summary. AC5080 performance depends on truck power to weight ratio.

Code	Schedule	Time(sec)	Ave Speed	Distance (miles)
TEST_D	UDDS	1060	18.8	5.5
IDLE32	HHDDT idle	1800	0	0
CREEP34	HHDDT creep	1032	1.7	0.5
TRANS3	HHDDT Transient	688	14.9	2.9
CRUISE3	HHDDT cruise	2083	39.9	23.1
HHDDT_S	HHDDT short	760	49.9	10.5
MHDTLO	MHDT low speed transient	370	9.4	1.0
MHDTHI	MHDT high-speed transient	1190	21.6	7.1
MHDTCR	MHDT cruise	1910	40.1	21.3
AC5080	AC5080	idle 10 sec 50kph 60 sec 80kph 80 sec	N/A	N/A

For those HHDDT subject to further chemical analysis, the Idle, Creep, Transient, and Cruise and higher speed modes were each repeated. In order to collect sufficient mass for speciation, it was necessary to increase the length of some of the modes. For example, the mode denoted creep34 consisted of four HHDDT creep (creep3) modes in a sequence sampled as a single cycle. Similarly idle32 consisted of two idle runs together (i.e. the idle time was doubled).

For the MHDT not subject to speciation, the AC5080 and the MHDT Schedule were added to the UDDS. The MHDT schedule consisted of three modes: lower speed transient (MHDTLO), higher speed transient (MHDTHI), and cruise (MHDTCR)[3,4] In Phase 2, for three of these vehicles, the HHDDT_S mode was included in the MHDT schedule. In Phase 3, all MHDT judged capable of adequately maintaining the necessary speed ran the HHDDT_S. For the one medium-heavy-duty vehicle subject to further chemical analysis in Phase 2, idle (not included on the other MHDT vehicles), lower speed transient, higher speed transient, and cruise modes were each repeated to create paired data sets at the laden weight.

The AC5080 is a short test proposed as an Inspection and Maintenance (I/M) cycle[5]. It is a mixed-mode test having two full-load accelerations and two steady-state cruises at 50 km/hr (31.1 mph) and 80 km/hr (49.7 mph). It is less aggressive than the DT80, but according to its creators it may be more representative of on-road driving. It requires the use of an inertia-simulating dynamometer. WVU developed a specific protocol for implementing the AC5080 Short Test because the previous descriptions of the cycle were ambiguous in the cycle execution.

The AC5080 test has two full-power accelerations and two steady-state cruises as shown in Table 11 and Figure 2. Since the time of occurrence of points "C" and "E" are vehicle and load dependent, the scheduled speed trace (the speed-time line that the driver is expected to follow) was generated in real time. When the program had finished initializing, the instruction "Start the Engine" appeared on the screen accompanied by three horn blasts. The driver then started the engine immediately and allowed it to idle. After sixty seconds, data capture commenced. This corresponds to point "A" on the Test Schematic. Ten seconds later, a ramp was drawn on the driver's display. This ramp was generated to reach point "C" in around six seconds. The driver was expected to treat this as a "free" acceleration (maximum acceleration, while driving in a normal style), and to reach the steady state speed of 50 Km/hr (31.1 mph) as quickly as possible. Once the vehicle reached 48 Km/hr (30 mph), point "D" is defined, at exactly sixty seconds in the future. When this time had elapsed, the second rapid acceleration ramp was generated. This ramp was drawn to reach point "E" in about 4.5 seconds. When the vehicle speed reached 78.5 Km/hr (49 mph), point "F" was defined to be 80 seconds later than this time. Upon reaching point "F," the data acquisition was stopped and the driver was free to slow the vehicle speed in the safest manner. The 49 mph value was determined to be a lower bound of approximation to reaching 50 mph. An actual test is shown in Figure 3.

Table 11: AC5080 Methodology.

Path	Description	Duration
A – B	Idle. Select low gear.	10 seconds
B – C	Rapidly accelerate to 50 km/hr (31.1 mph)	Vehicle Dependant
C – D	Maintain 50 km/hr. (31.1 mph)	60 seconds
D – E	Rapidly accelerate to 80 km/hr (49.7 mph)	Vehicle Dependant
E – F	Maintain 80 km/hr. (49.7 mph)	80 seconds
F - G	Return vehicle to stop with engine at idle.	Vehicle Dependant

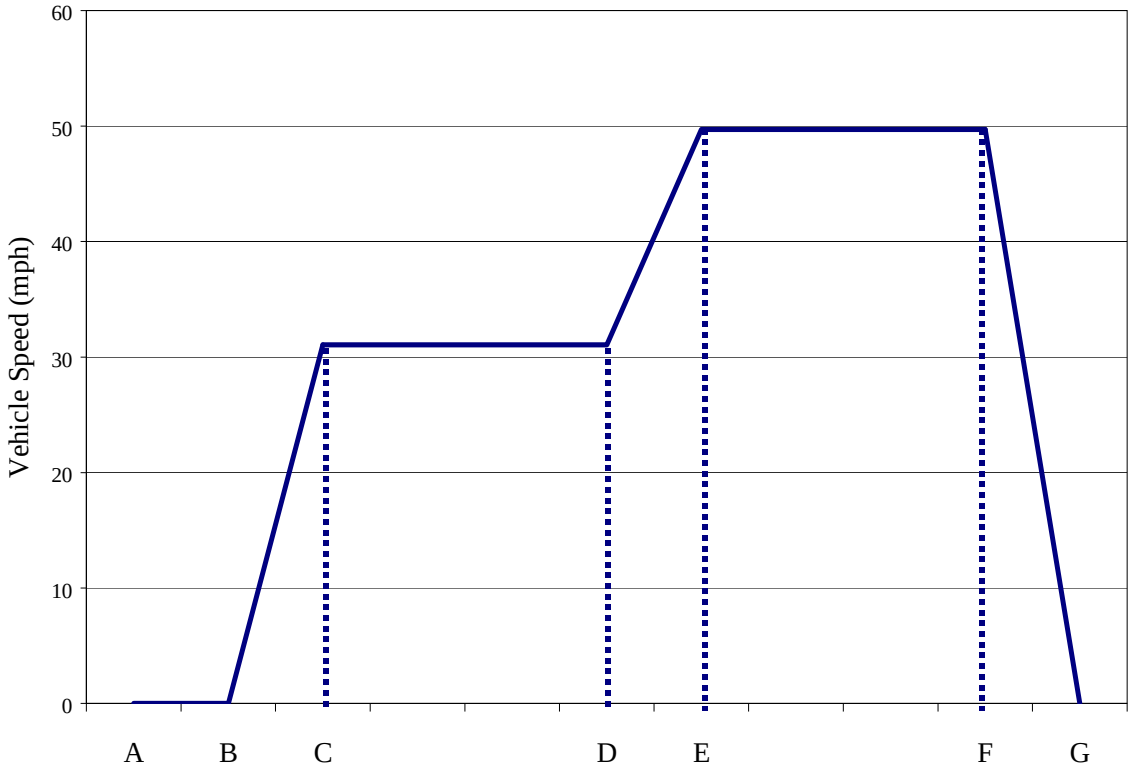

Figure 2: AC5080 Short Test (time not to scale).

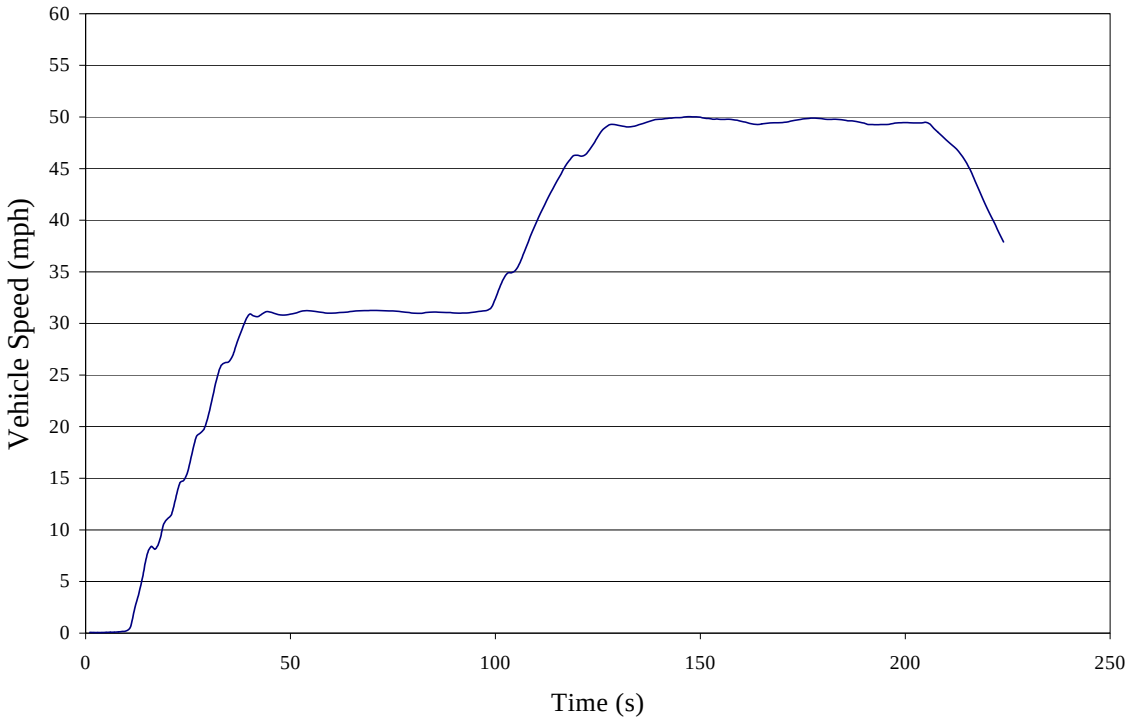

Figure 3: The AC5080 Schedule as driven by a 1990 Kenworth road tractor with a 370 hp Cummins M11 engine and a 10-speed manual transmission, with a simulated vehicle test weight of 56,000 lbs.

Test Weights

All of the HHDDT tested in this study were deemed to have gross vehicle weights of 80,000 pounds, in that they were all typical over-the-road tractors. The GVWR displayed in the cab of such tractors may vary from 30,000 lbs. (for single axle trailers) to over 52,000 lbs. (for tandem axle trailers), but trailer weight is not considered in these GVWR values. For tractor-trailers, it is the combination weight that is of interest, rather than the tractor weight. The test weight used for all vehicles was planned to be 56,000 lbs., representative of laden use. The test weights for Phase 1.5 were planned to be 30,000 lbs., 56,000 lbs. and 75,000 lbs. However, it was evident that the 75,000 lbs. operation proved stressful to the truck brakes because only one or two axles were being used to slow an inertia that would be slowed with five axles in normal on-road use. Also, the accelerations and decelerations at 75,000 lbs. showed potential to cause dynamometer damage. Some preliminary test runs, presented in Figure 4 and Figure 5, showed that a difference still existed in emissions between 56,000 lbs. and 66,000 lbs. operating weight, and so the 66,000 lbs. weight was used as a maximum weight test weight instead of the 75,000 lbs. weight for the remainder of the program. PM increased monotonically with test weight for the Transient Mode, but did not change appreciably between the 56,000, 66,000, and 75,000 lbs. runs on the HHDDT_S, where wind drag becomes more important. For the case of NO_x (see Figure 5), the Transient mode NO_x emissions at 66,000 lbs. were substantially higher than at 75,000 lbs.

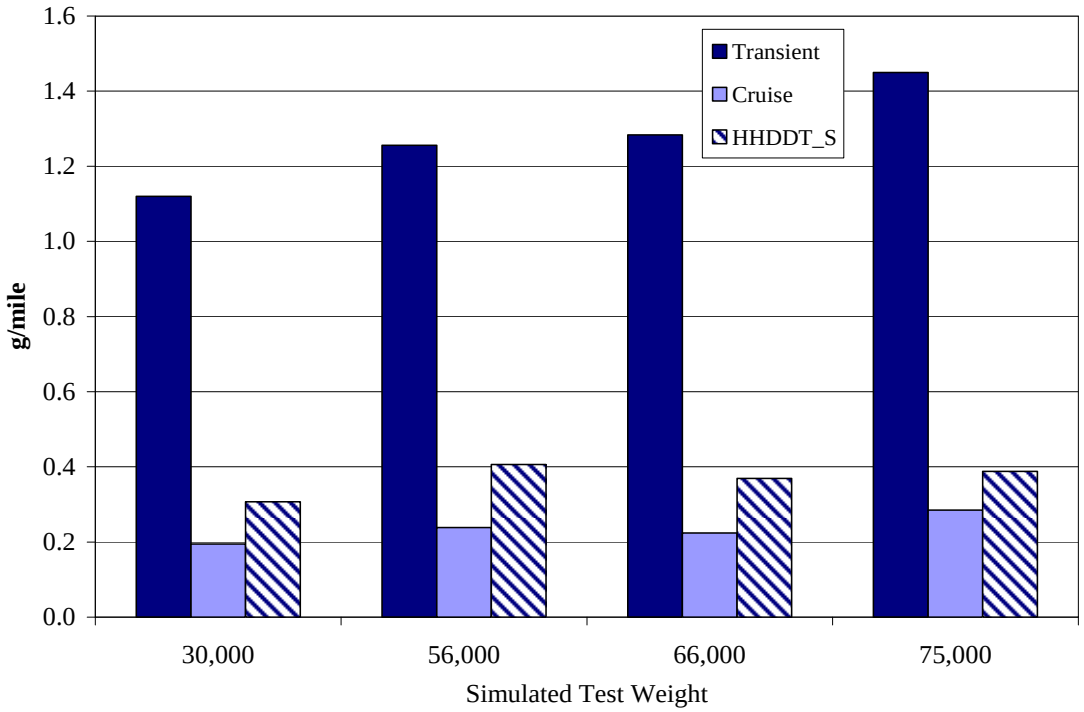

Figure 4: PM emissions for vehicle E55CRC-27 which was tested at four weights, before 66,000 lbs. was adopted as the highest test weight.

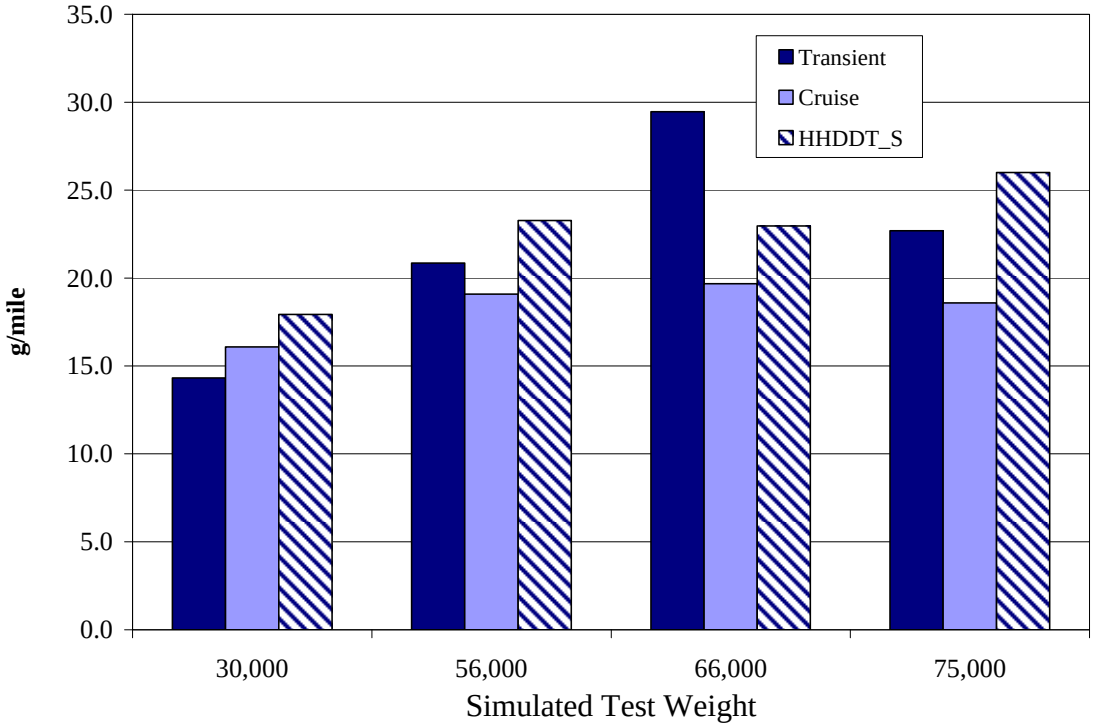

Figure 5: NO_x emissions for vehicle E55CRC-27 which was tested at four weights, before 66,000 lbs. was adopted as the highest test weight.

The MHDT were tested at both laden and unladen weights. Laden weight was set to be 75% of the gross vehicle weight rating (GVWR). The unladen weight was set at 50% of the GVWR.

Figure 6 shows an example of the monotonic increase in distance-specific emissions of PM as test weight increases. Figure 7 shows that, with the exception of the AC5080 driving schedule, NOx emissions increased with test weight as well. These emissions differences vindicated the effort associated with testing at two weights.

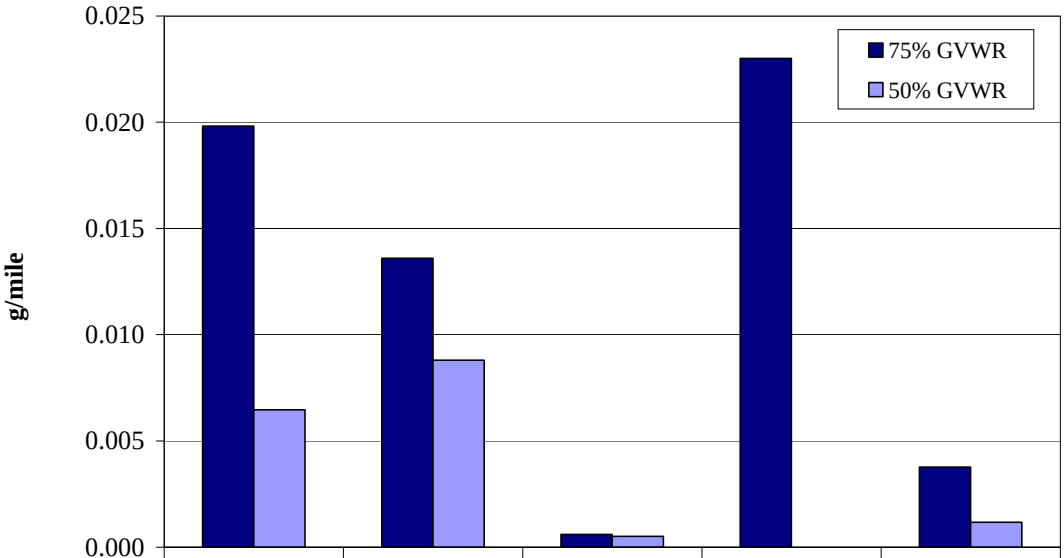

	AC5080	MHDTCR	MHDTHI	MHDTLO	TEST_D
75% GVWR	0.020	0.014	0.001	0.023	0.004
50% GVWR	0.006	0.009	0.001	0.000	0.001

Figure 6: PM emissions for vehicle E55CRC-53 tested at two weights

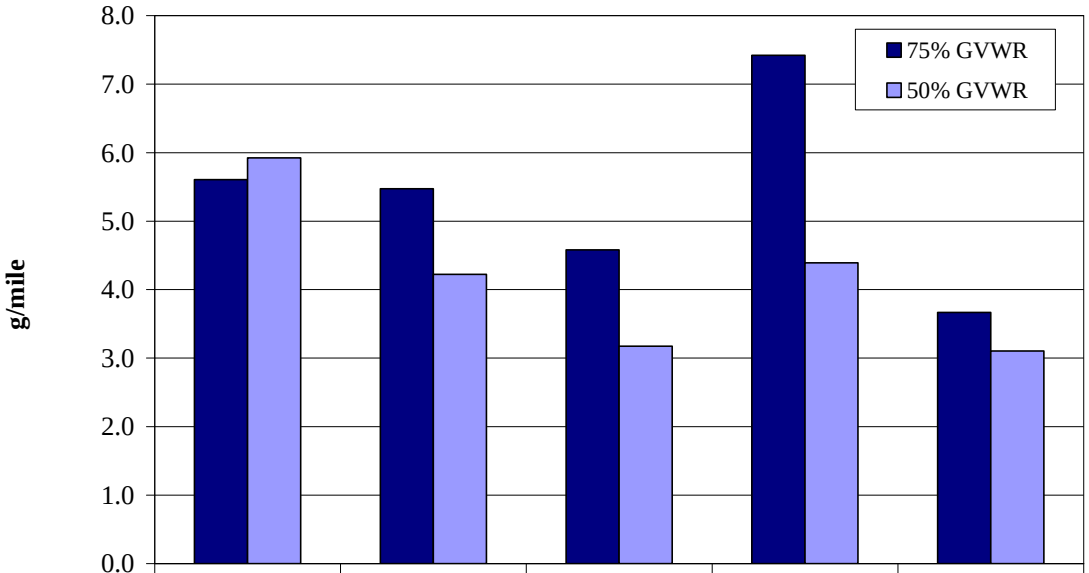

	AC5080	MHDTCR	MHDTHI	MHDTLO	TEST_D
75% GVWR	5.60	5.47	4.58	7.42	3.67
50% GVWR	5.92	4.22	3.17	4.39	3.10

Figure 7: NO_x emissions for vehicle E55CRC-53 tested at two weights.

EQUIPMENT AND METHODS – NON-REGULATED SPECIES & PARTICLE SIZING

DRI's Residence Time Dilution Tunnel

DRI provided a "residence time dilution sampling system" for sample collection during Phase 1 and Phase 2 of this study. The dilution tunnel was identical to those used during the Northern Front Range Air Quality Study and it was based on a dilution stack sampler designed and tested by a group led by Dr. G.R. Cass[6]. Figure 8 shows a schematic of the DRI sampler. Because of the short sampling time and generally low PM emission rates expected for certain cycles (particularly the Idle mode), the sampler was used without dilution as a residence time chamber only. The dilution sampler was interfaced with the WVU dynamometer dilution system. The samples were drawn through cyclone separators with a cut-off diameter of 2.5 mm, operating at 113 lpm and collected using the DRI Sequential Filter Sampler (for inorganic species) and the DRI Sequential Fine Particulate/Semi-Volatile Organic Compound (PSVOC) Samplers for organic species. In addition, a separate sampling line (without cyclone) was used for collecting canisters, DNPH cartridges and Tenax samples. The details of sample collection techniques are described in the appropriate standard operating procedures (SOPs) and are available upon request from the Organic Analytical Laboratory (OAL) of DRI.

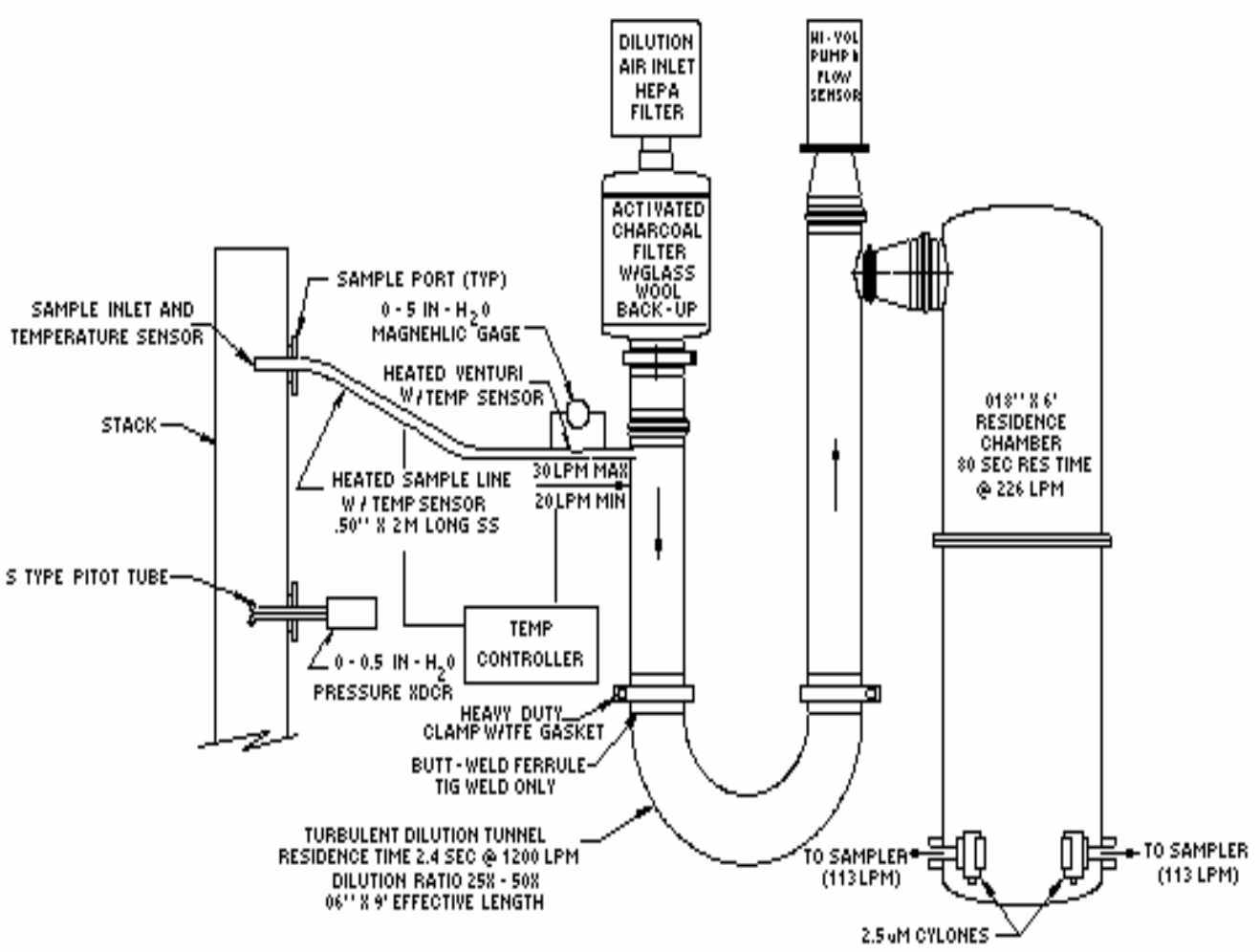

Figure 8: Schematic of DRI dilution tunnel sampler (Hildemann, et al.[6])

Mini Dilution System

The Scanning Mobility Particle Sizer (SMPS) employed a mini dilution tunnel to dilute the raw exhaust for sampling. The DMS 500 did not employ this mini dilution tunnel, but was used to sample directly from the main CVS tunnel.

The mini dilution system shown in Figure 10 incorporated a tunnel with its length maintained at ten times its diameter to facilitate good mixing and uniform distribution at the sampling zone. An orifice plate was provided at the inlet of the dilution system to ensure proper turbulence. The tunnel was wrapped with heating tape and insulation to maintain a temperature of 46º C (115º F) to prevent water condensation. A dilution ratio of 1:30 was maintained throughout this study. A 12 cm (5 inch) exhaust coupling with a 2 cm (¾ inch) probe welded on its body was used to draw a partial sample from the raw exhausts shown in Figure 9. One end of the probe had a quick disconnect fitting for ease of coupling the probe to the mini dilution tunnel. The sampling was not isokinetic. The sample line from the probe to the mini dilution tunnel was kept as short as possible and well insulated. Dilution air was supplied immediately before the mixing orifice by a separate pump. The dilution air was passed through a refrigerated dryer and a HEPA filter to provide particle and moisture free air. A separate vacuum pump was used to draw in the exhaust sample.

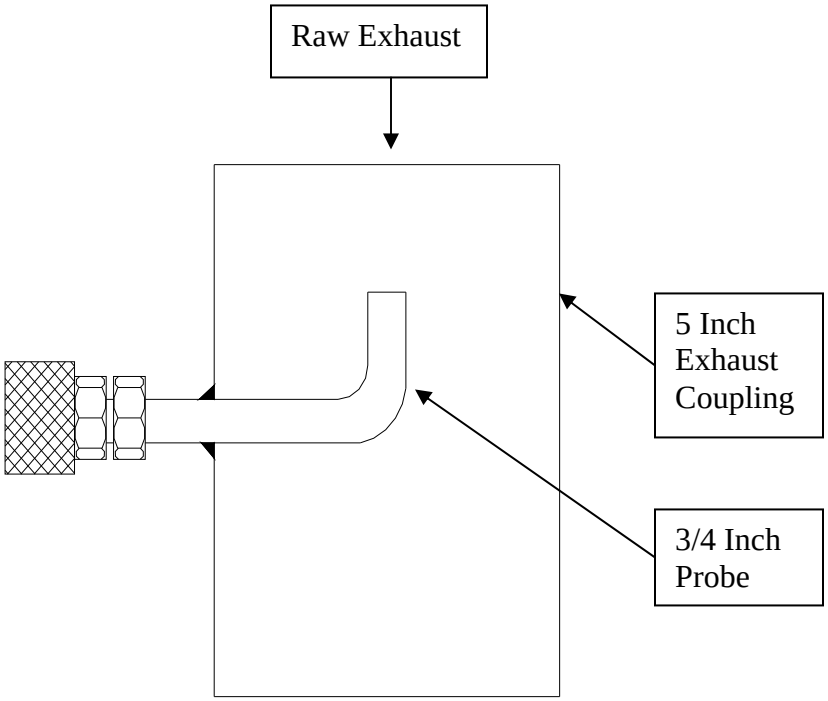

Figure 9: Exhaust Coupler with Sampling Probe for mini dilution tunnel

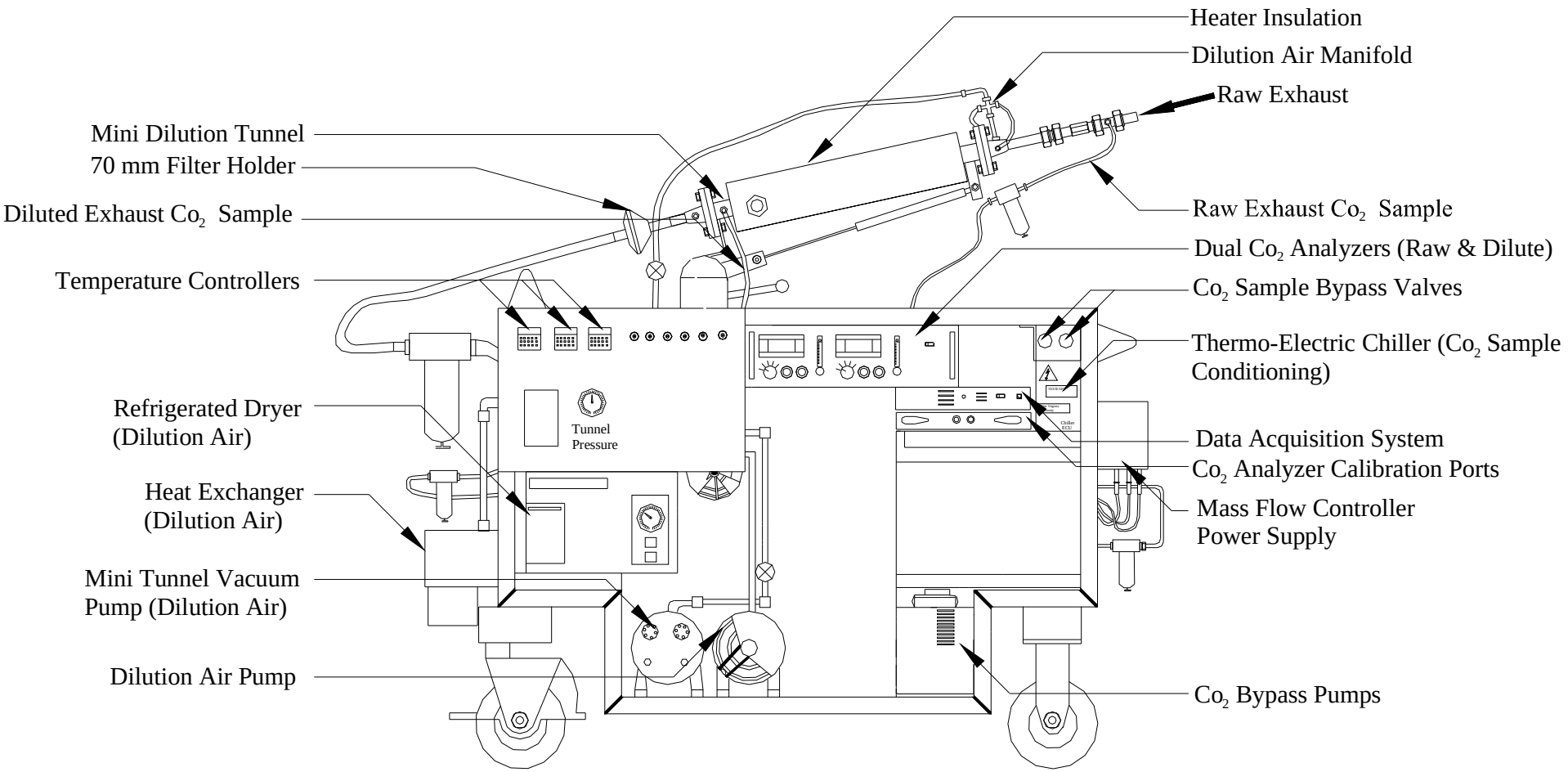

Figure 10: West Virginia University-Mini Dilution System

Both the dilution air and total air flow rates were controlled by two Sierra mass flow controllers calibrated from 0 to 200 slpm (0 to 7 scfm). Sampling probes were installed ten diameters downstream of the mixing orifice to ensure uniform concentration. A dual range CO_2 analyzer was used to measure the raw and dilute CO_2 concentrations. A 10-point analyzer calibration was employed using 15% and 1% CO_2 bottles. The analyzer was checked everyday for a zero and span using nitrogen as zero gas and 15% and 1% CO_2 bottles as span gas for the analyzers. The raw and dilute exhaust gases were filtered by inline filters and chilled by thermoelectric chillers for removal of particulates and moisture, respectively. The filters were checked every day and replaced if necessary. A purge air supply for the CO_2 analyzers was provided by an external oil free compressor through a HEPA filter. This purge air was useful in flushing the analyzer of any residual gas present, which may provide erroneous readings.

The mass flow controllers and the CO_2 analyzers were connected to a data acquisition system (National Instruments DAS 6020-E BNC). A program in Visual Basic was developed by WVU to control the data acquisition system (DAS) pad and to save continuous data from the analyzer and the mass flow controller. Other parameters such as tunnel pressure, and temperature were also recorded on a continuous basis. The DAS pad also maintained the user defined dilution ratio. The desired dilution ratios were achieved in two ways, first a flow-based system and the other is a CO2 based system. With the flow based system, the dilution ratio was calculated using the following equation:

$$DR = total / (total – dilute)$$

The dilution ratio was maintained by adjusting both the total and dilute flow rates. The total and dilute flow rates were measured and set by the mass flow controllers. The CO_2-based system measured the raw and dilute CO_2 concentrations and the dilution ratio was the simple ratio of raw to dilute concentrations. The dilution ratio was maintained by controlling the mass flow controllers based on the CO_2 readings. Through experience it had been determined by WVU that the flow based system was more accurate in controlling the dilution ratio and the CO_2 readings were used to verify the set dilution ratio. It may be argued that the dilution ratios may be better controlled using CO_2 concentrations than using mass flow controllers. WVU has both systems on the mini-dilution tunnel that is used for PM sizing work. Problems associated with deskew times, gas dispersion in the tunnel, and chillers complicate the CO_2-based control method, especially during transient tests. Over steady state tests, the CO_2-based dilution ratio control can be very accurate. One probe was installed next to the dilute CO_2 probe for particle size distribution measurements using the SMPS. Carbon impregnated electrically conductive Tygon tubing was used to transfer the sample from the tunnel to the instrument. This tubing was used to prevent any particle losses due to electrostatic deposition on the walls of the sampling tube.

Exhaust pulsations from the engine were encountered during this study and an exhaust pulsation damper was devised, as shown in Figure 12. The damper consisted of a 5 gallon tank with one end cut off and sealed with a rubber diaphragm. The rubber diaphragm was

helpful in reducing the exhaust pulsations. The top of the tank had a tee connection which incorporated a straight probe as seen in Figure 11, to minimize particle losses into the damper. This system provided a pulsation free stream of sample with minimal particle loss. The damper was flushed with particle free air and evacuated after every test to remove any remaining particles or even volatile compounds, which may have found their way into the damper. This was done because the volatile compounds may adhere to the walls of the damper and subsequently form particles and create sampling artifacts.

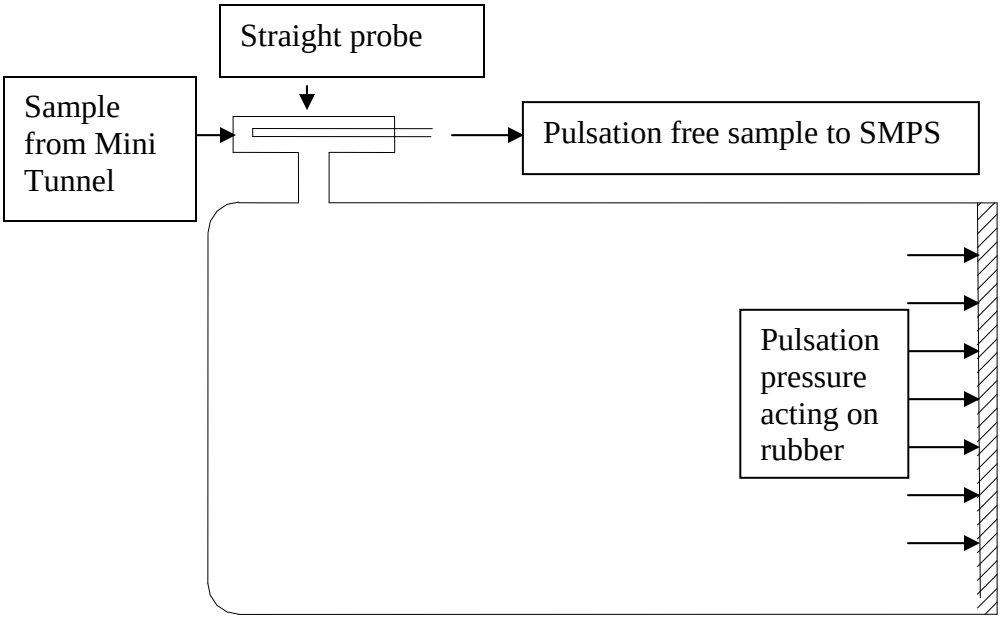

Figure 11: Schematic Representation of the Damping System

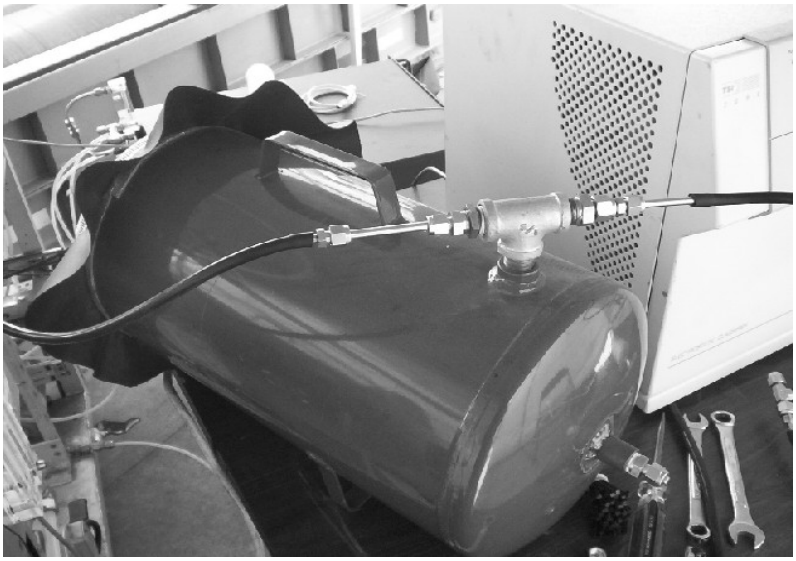

Figure 12: Exhaust Pulsation Damper

Particle Sizing with the SMPS

The SMPS consists of two basic components, the Electrostatic Classifier or the Mobility Analyzer and a Condensation Particle Counter. The use of the classifier to produce monodisperse aerosols is illustrated in Figure 13. The classifier or mobility analyzer separates particles based upon their electrical mobility and the resulting particles are transported to the particle counter to obtain number concentrations. In mobility analyzers particles are first charged, and then the aerosol is classified in a high electric field according to the electrical mobility of the particles. The particle size distribution is obtained on the basis of the relationship between mobility and sizes. The ultimate size parameter determined from electrical mobility measurements is the equivalent mobility diameter.

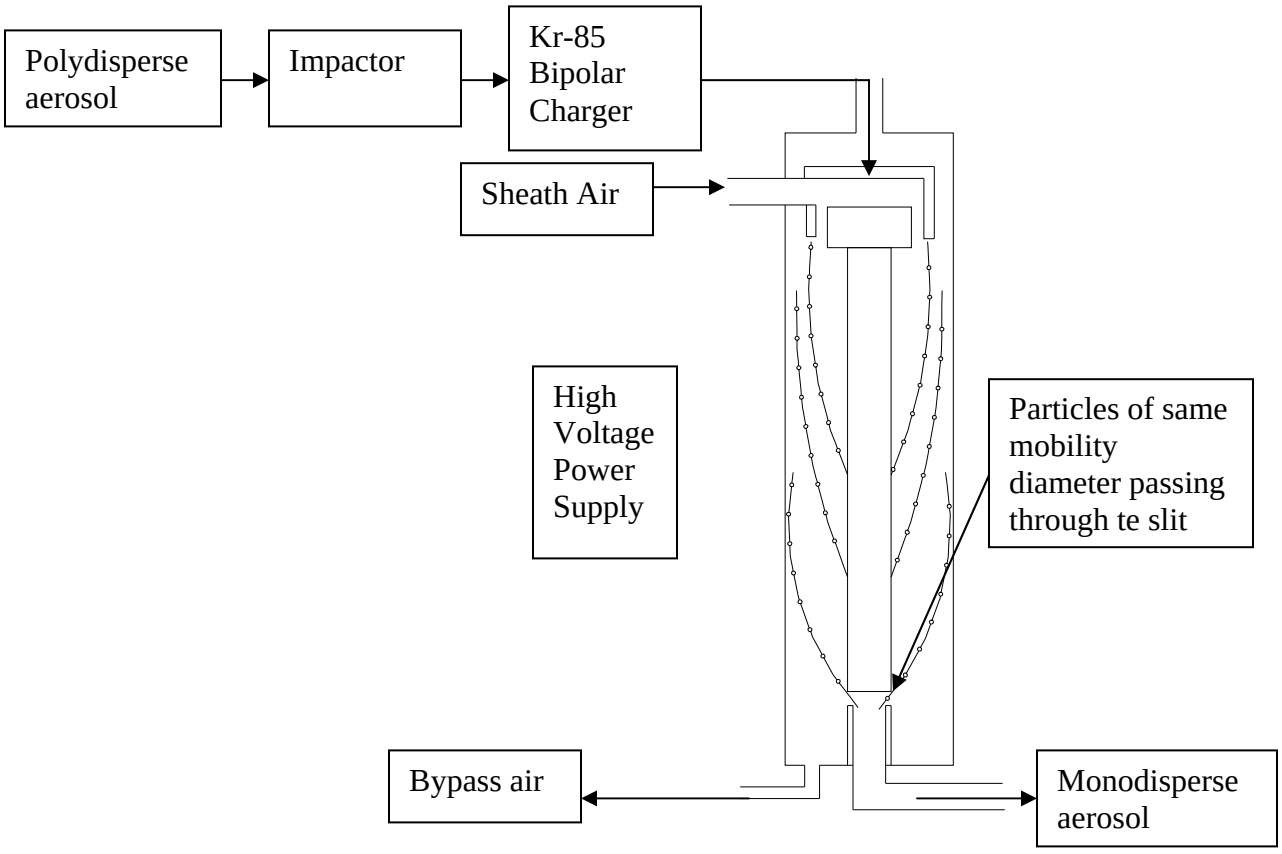

Figure 13: Differential Mobility Analyzer

The inlet of the classifier has an impactor which removes all particles above 1µm since large particles tend to have multiple charges and stripping these charges is very difficult. The impactor has a nozzle and an impactor plate and different size orifices (0.071 and 0.0475 cm) are used depending on the flow rate. The polydisperse aerosol passes through

the bipolar charger containing a radioactive source (Krypton), which exposes the aerosol particles to high concentrations of bipolar ions. The particles and ions undergo frequent collisions due to random thermal motion of the ions. After reaching a state of equilibrium, the particles carry a bipolar charge distribution. The polydisperse aerosol passes into the DMA between the sheath flow, which creates an air curtain, and the outer cylinder. The central rod is charged with a high negative voltage and the positive particles are attracted to the rod. Particles with high mobility precipitate at the top end of the rod and particles with low mobility exit the DMA along with the bypass air. Only particles with a narrow mobility range exit the DMA through the slit as monodisperse aerosol, which pass on to the Condensation Particle Counter for concentration measurements.

To obtain a full scan of the particle sizes, the voltage in the central rod of the classifier is increased exponentially with respect to time which is termed the up-scan of the DMA and the voltage is dropped to zero which is termed as the down-scan. The up-scan and down-scan times are typically 120 and 15 seconds, respectively. These times can be increased by the user to obtain a better resolution if the particle concentrations are steady.

The Condensation Particle Counter (CPC), also called the condensation nucleus counter (CNC), is the most common instrument used to determine number concentrations of diesel particles. Upon entering the CPC the aerosol stream is saturated with alcohol (typically butanol) vapor. As the mixture is cooled in the condenser tube, the vapor becomes supersaturated and condenses on particles. As a result, the particles grow to a diameter of about 10 μm, allowing for optical detection. Particle size detection limit in the CPC is related to the increasing saturation ratio which is required with decreasing particle diameters. Modern CPCs have detection limits of around 3-10 nm.

CPCs can be operated in two modes: (1) the counting mode and (2) the opacity mode. In the counting mode, pulses of scattered light from individual particles are counted. This mode provides the most accurate measurements, but can be used only at low particle concentrations. In the opacity mode, used for concentrations above $10^4/cm^3$, number concentrations are determined from the total scattering intensity. This mode, generally subject to a larger error, requires that all particles grow to the same diameter and that the optical system be frequently calibrated. The CPC instrument is very sensitive to the ambient temperature, which affects the degree of supersaturation, as well as to positioning and vibrations. For these reasons, it is suitable primarily for laboratory measurements and its use for in-field measurements is more challenging. The CPC is used for particle detection in many aerosol size distribution measurement instruments.

Both the CPC and the Electrostatic Classifier make up the SMPS system. The CPC and the classifier are interfaced with an analog BNC connector cable. A personal computer with custom software provided by TSI was used to record data and control the classifier. A TSI model 3936 SMPS system was used for this study (Figure 14). DMA models 3081 (Long DMA) and 3085 (Nano DMA) were used interchangeably to obtain a full particle size distribution down to 4 nm and up to 800 nm. A Model 3025A CPC was used for

particle counting since it could detect particles with diameters as low as 3 nm and had a response time of one second.

The SMPS is basically designed for steady state operations, where the exhaust characteristics are invariant with time; that is, the engine is at a constant load and RPM or when the vehicle is operated at a constant speed. During these steady states, concentrations of all particles are almost constant, but the concentrations vary whenever the load or speed of the engine/vehicle varies. For transient measurements of the engine/vehicle, the engine/vehicle was first operated on a steady state mode and a full size scan was obtained. Particle sizes were chosen from the full scan and the number of particles chosen was dependent upon the number of times the vehicle was operated through the transient cycle. For transient tests, the classifier operated in manual mode, which allowed the user to enter a particular particle size and track the concentration of that particular size for the entire test.

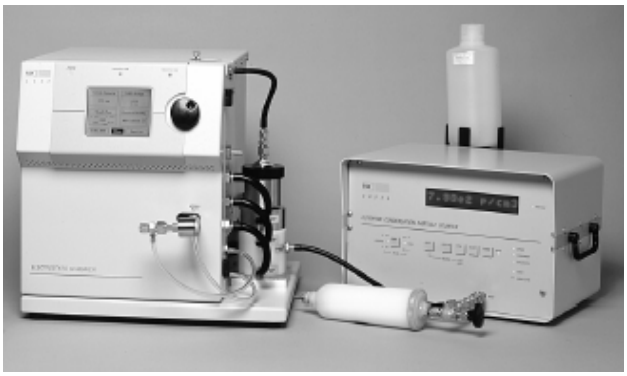

Figure 14: TSI Model 3936 SMPS System

To assure accurate measurements, the SMPS was flow calibrated before the start of the project. An electrospray aerosol generator was used to calibrate the SMPS. The generator was capable of producing 15, 30 and 70 nm sucrose particles. Leak checks were performed every day to ensure that the SMPS had no leaks. Two types of leak checks were performed, a HEPA filter check and a zero voltage check. Since HEPA filters have high filtration efficiencies, a HEPA filter was connected to the inlet of the SMPS and a full size scan was performed. If any particles were detected above the noise level of the instrument, which was typically $1x10^3$ particles/cm^3, then a thorough leak check was performed according to the instrument instruction manual. The second method required the voltage on the collector rod to be set at zero and checked for any particles being measured by the CPC. Since the voltage on the collector rod determines the particle size that exits the classifier, a zero voltage on the rod should ensure no particles exit the classifier. Both these methods were used everyday to make sure the SMPS had no leaks. If any leak was detected in the system, the manufacturer's leak check procedure was used to track and solve the problem. The inlet nozzle on the classifier was cleaned everyday with alcohol to remove any particle deposits, which may block the flow. The impactor plate was also cleaned with alcohol and a thin layer of vacuum grease was applied to prevent particle bounce.

Particles are classified in the DMA by increasing the voltage exponentially and the particles leaving the classifier are increasing in size. The particles are then counted by the CPC and the values for concentrations for each particle size are stored in the PC as raw counts. The particle size obtained from the raw data assumes that each particle has a single charge on it after passing through a bipolar charger, which is not actually true. Multiple charges on a particle increase its mobility and can be incorrectly binned into the smaller diameter range. TSI uses an inbuilt algorithm in its SMPS software (Aerosol Instrument Manager-SMPS) to correct for multiple charges based on Fuchs-Gunn aerosol charging theory and a truncated triangular transfer function based on Knutson and Whitby[7].

The software provided by TSI to record only CPC concentrations (Aerosol Instrument Manager-CPC) does not provide any algorithm for the reduction of data. The single particle charge correction, transfer function and efficiencies of the CPC and impactor have to be applied to the raw data. Two programs were developed in MathCAD, one to reduce the CPC data and the other to correct the SMPS data for the dilution ratio (Appendix I). The final data for the SMPS were presented as particle size based concentration variations with concentrations in normalized units of particles/cm^3 (dN/dlogDp). A log normal distribution was found to fit the data from the SMPS very well. The final data from the CPC were presented as time-based concentration variations of a selected particle size with concentrations in normalized particles/ cm3 (dN/dlogDp).

Particle sizing with the DMS500

A second instrument used in Phase 2 to measure the size and number distributions of PM was a differential mobility spectrometer, DMS500 (Figure 15). The DMS500 was directly connected to the secondary dilution tunnel and was used to sample at a point close to the standard 70mm filter of the laboratory. Only primary dilution in the full-scale CVS tunnel was employed. Secondary dilution was not needed in the tests because the filter face temperature remained below 52^{o}C with just primary dilution. The working principle of the DMS500 is that it draws sample flow from the dilution tunnel containing aerosols/ particles. It is capable of measuring 41 particle size bins (3.16 nm – 1000 nm) as a continuous number count at a maximum frequency of 10Hz. The size bins start at a diameter of 3.16 nm and increase in the geometric ratio of 1.15 for each next size bin up to the end limit of 1000 nm. The impactor at the inlet removes particles greater than 1000 nm and then the particles are charged by a corona charger. The charging of the particles is argued to depend only on size and not on material composition. The dilute exhaust then flows as a uniform laminar sheath through an annular geometry between the inner and outer electrodes, as shown in Figure 15, and the charged particles are carried in this dilute exhaust flow. The particles are then deflected towards grounded electrometer rings by their repulsion from a central high voltage rod. Their landing position on the electrometer rings is a function of the particle's charge and momentum. The particles give up their charge to the electrometer amplifiers through the rings and the resulting currents are output as particle number and size distribution through the user interface. There are

studies showing the good accuracy of the DMS500 when compared with the SMPS and ELPI[7].

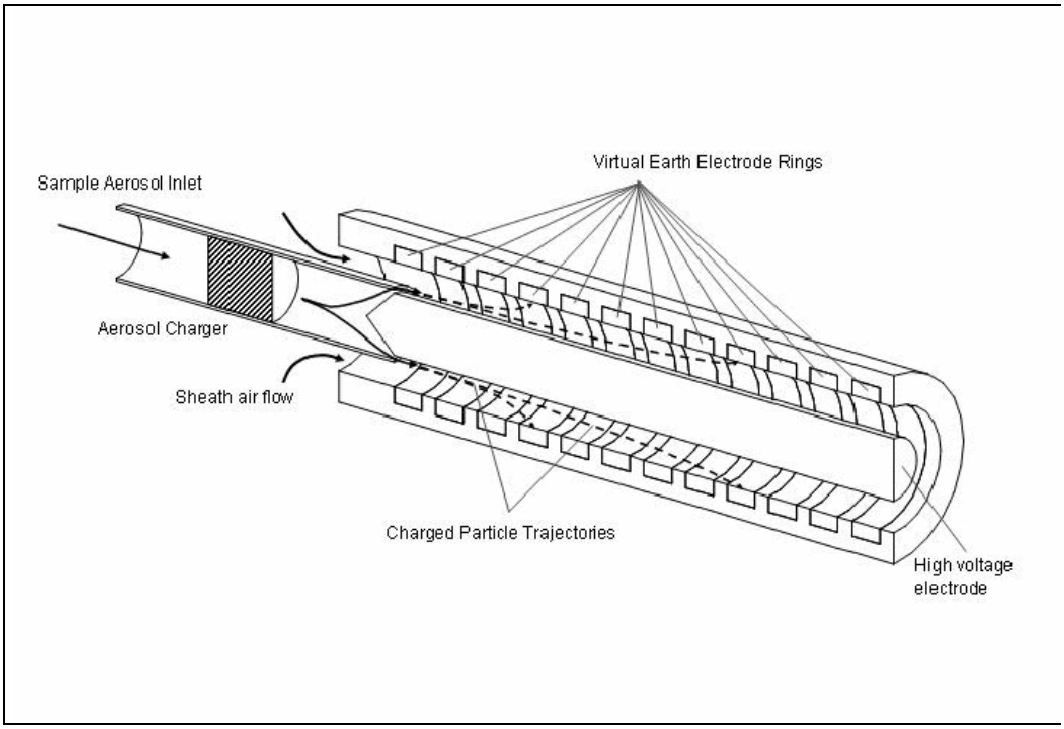

Figure 15: Working principle of the DMS500[8].

Micro-Orifice Uniform Deposit Impactor (MOUDI)

WVU used the Micro-Orifice Uniform Deposit Impactor (MOUDI) for gravimetric analysis of size-segregated $PM_{0.1}$ emissions from 10 vehicles (E55CRC-2 – E55CRC-11) in Phase 1. The MOUDI, MSP Model 110 is a cascade impactor that classifies particles by their aerodynamic diameter in the range of 18 μm to 0.056 μm. Model 110 has ten stages with nominal 50% efficiency curve aerodynamic diameters of 0.056, 0.100, 0.180, 0.320, 0.560, 1.0, 1.8, 3.2, 5.6, 10 and 18.0 μm. The MOUDI moderates the pressure drop needed to size submicron aerosols by using nozzles of very small diameter (2000 nozzles of 52 μm in diameter in the final stage). It operates at a rate of 30 lpm. The flow rate is monitored by measuring the pressure drop between the first and the fifth stage with a differential pressure gage. The differential pressure was adjusted by a needle valve to a pre-calibrated pressure drop corresponding to a flow rate of 30 lpm. The advantage that the MOUDI has over other cascade type impactors is its ability to collect ultra fine particles with a moderate pressure drop and a uniform deposit.

Samples from the MOUDI were collected on greased aluminum substrates and one 37 mm Gelman Sciences TX40 after filter (for PM size fraction less than 0.056 μm).

Gelman Sciences 47 mm Analyslides were used for transport and storage of the substrates. Several researchers have espoused the necessity of applying a thin layer of grease to the substrate surface in order to minimize particle bounce (Baron and Willeke, 1993; Marple et al., 1991). According to the majority of researchers, particle bounce is not an important issue in diesel particulate matter sampling. This claim was found to be in error by the Principal Investigators in an NREL-funded study (Gautam et al., 2002). Particle bounce is a major problem in diesel particulate matter sampling. Upon impact, some of the particles may bounce off the substrates and get re-entrained in the sample stream where they will pass to successive stages. This will distort the size distribution toward the smaller diameter regions, with no definitive method to predict or correct for this phenomenon. Substrates, used in this study were greased by Ms. Sue Stine, who had formerly worked for the US Bureau of Mines with Dr. Bruce Cantrell, and later for MSP, Inc. (manufacturer of the MOUDI).

Cyclones

Size-selective cyclone samplers (URG Model 2000-30 EA, 28.3 lpm, $_{50}d_{ae}$=10μm) were used to collect samples of PM_{10} of exhaust PM. The PM_{10} cyclone is an inertial particle separator that uses centrifugal force to remove heavier particles from a gas stream (>10 μm and >2.5 μm, respectively). The diluted exhaust sample enters the cyclone tangentially, and is drawn through the cyclone body and the in-line filter by a vacuum pump. Maintenance of this exact flow rate can be difficult if the conditions at which the sample is being collected are not near standard. Cyclone use in a dilution tunnel requires a feedback control system to adjust the flow to account for variations in temperature and pressure. This signal is used to control a mass flow rate controller that will be responsible for maintaining the required constant actual flow rate.

DRI used a Model Bendix-Unico 240 $PM_{2.5}$ cyclone to draw dilute exhaust samples from WVU's dilution tunnel into the DRI's residence time dilution chamber. The cyclones were an integral part of the residence time chamber. The cyclone in the DRI residence time chamber operated at a volumetric flow rate of 113 liters/minute.

Unregulated Emissions

WVU and DRI (subcontractor to WVU) were jointly responsible for unregulated emissions measurement, and WVU also provided support for Dr. Kim Prather's Aerosol Time-of-Flight Mass Spectrometer (ATOFMS) data collection. ATOFMS data are not discussed in this final report. Listed below are the specific tasks/activities conducted by WVU and DRI.

In addition to the gaseous sampling probes and a secondary dilution tunnel, WVU installed the following on the primary dilution tunnel:

1. PM_{10} cyclone with TX40 filters for gravimetric analysis ($PM_{2.5}$ sampling was conducted by DRI using the DRI residence time chamber).
2. Micro-Orifice Uniform Deposit Impactor (MOUDI) probe for gravimetric analysis of size-selective $PM_{0.1}$ samples. Greased aluminum substrates were employed for the purpose (for E55CRC-2 to E55CRC-11).
3. Probe for DRI's residence time dilution chamber.
4. Probe for Dr. Kim Prather's ATOFMS sampling in Phase 1.

Samples were collected by WVU using DRI's residence time dilution chamber (with dilution) for the first two runs (1773-2 and 1773-3) of E55CRC-01. These runs are not considered for the study since the filters and other media did not collect sufficient quantity of samples. For all subsequent runs in Phase 1, and for the rest of the study (6 vehicles in Phase 2), the DRI's residence time dilution chamber was used without any secondary dilution to increase the captured mass.

Tunnel blanks and tunnel backgrounds were also collected, as listed in the Test Sequence, for the three overlap vehicles.

1. Volatile organic compounds (VOC) – Canisters; field GC
2. Methane - Canisters
3. Semi-volatile organic compounds (SVOC) – PUF/XAD and TIGF filters
4. SVOC, low molecular weight compounds – Tenax tubes
5. Nitro-PAHs – PUF/XAD and TIGF filters
6. Carbonyls – DNPH cartridges
7. Nitrosamines - Thermosorb cartridges
8. PM soluble organic fraction (SOF): organic compounds – TIGF filters
9. Elemental analysis and gravimetric analysis ($PM_{2.5}$) – TIGF filters
10. Ammonium and Ions (Nitrate, Nitrite, Chloride, Sulfate) – Quartz filters
11. Elemental Carbon/Organic Carbon (EC/OC) – Quartz filters
12. $PM_{2.5}$ fraction for gravimetric analysis

WVU collected the PM_{10} fraction using a cyclone for all 25 vehicles in Phase 1, and 6 'speciation vehicles' in Phase 2. The $PM_{0.1}$ fraction was sampled in Phase 1 using the MOUDI for E55CRC-2 to E55CRC-11 only.

Chemical speciation samples were collected by DRI, using the residence time dilution chamber. DRI used a Model Bendix-Unico 240 $PM_{2.5}$ cyclone to draw dilute exhaust samples from WVU's dilution tunnel into the DRI's residence time dilution chamber. The cyclones were an integral part of the residence time chamber. The cyclone in the DRI residence time chamber operated at a volumetric flow rate of 113 lpm (4 cfm). However, there was no additional dilution performed within the DRI chamber. The list of chemical compounds analyzed and the media used to collect them are given below:

Details of the sample collection and the analytical procedures followed by DRI are provided in Appendix G.

Speciation Fleet and Approach

The sampling of non-regulated species occurred at the same time that regulated species were sampled. Five HHDDT with a Gross Vehicle Weight Rating (GVWR) of 80,000 lbs. were selected specifically for non-regulated sampling. These were E55CRC-39, E55CRC-40, E55CRC-42, E55CRC-43 and E55CRC-44. A sixth vehicle, E55CRC-41 was a MHDT and hence cannot be used for comparison purposes directly with the HHDDT in this study. The details of the test vehicles, engines, model years and the test fuel used is given below in Table 12.

Table 12: Test Vehicle Details

Vehicle ID	Vehicle Manufacturer	Vehicle Model Year	Engine Manufacturer	Engine Model	Engine Model Year	Primary Fuel
E55CRC- 39	Volvo	2004	Cummins	ISX 530	2004	CARB
E55CRC- 40	Freightliner	2004	Detroit Diesel	Series 60	2003	CARB
E55CRC- 41	Ford	1998	Cummins	B5.9	1997	CARB
E55CRC- 42	Freightliner	2000	Caterpillar	3406	1999	CARB
E55CRC- 43	Peterbilt	1995	Detroit Diesel	Series 60	1994	CARB
E55CRC- 44	Volvo	1989	Caterpillar	3406	1989	CARB

No aftertreatment devices were used on any vehicle. The vehicles were tested in an “as received tank fuel” condition in the same way as for regulated emissions characterization. Fuel samples for every vehicle were collected at the end of the test period and were sent for chemical analysis to Core Laboratories for analysis of cetane number, total sulfur content, aromatic content and viscosity. Another sample of the fuel was sent to DRI for analysis of inorganic and organic compounds. Oil samples were collected for every vehicle and were sent to oil sciences laboratory for 27-point analysis and sulfur content. Another sample of the oil was sent to DRI for organic and inorganic analysis.

This non-regulated emissions study employed the same test schedules that were used for the regulated emissions measurement.

The Idle mode was extended to run three times longer than the normal Idle mode to facilitate sufficient sample collection on the speciation media. No speciation or particle sizing data were recorded for the Creep mode. The Transient was run normally for 688 seconds. The Cruise mode was run normally for 2083 seconds. Chemical speciation and particle sizing data were recorded for the Idle, Transient, Cruise and High-speed Cruise Modes.

Each mode was repeated twice for every vehicle. Similar multiple modes were composited by DRI on the same media to ensure sufficient sample collection. The SMPS operated in a full-scan mode during the HHDDT schedule. For the Transient Mode, the SMPS was locked onto a particle size of interest and concentration variation for that

mode was measured. Particle sizes were selected based on the steady state size distribution. A steady state run at 40 kph (25 mph) mode, not required for regulated emissions testing, was executed prior to any other tests for the sole purpose of obtaining a full particle size distribution by the SMPS. The steady state speed of 40 kph (25 mph) was selected based on the average speed of the transient cycle. The DMS500 was operated during the modes because it was not restricted to steady-state measurements.

QUALITY ASSURANCE AND QUALITY CONTROL

The WVU Transportable Laboratory (TransLab) evaluated the emissions from vehicles operating in Southern California fueled with diesel or gasoline between August 2001 and May 2005. Testing was conducted in Riverside, CA. The independent Quality Assurance Quality Control (QA/QC) review of the regulated emissions is summarized below.

The procedure used in reviewing the data involved four levels of checks. First, the field engineer would make an assessment of the quality of the data as it was generated. If a test was deemed to be invalid, the field engineer would mark that test as being invalid, and provide the reason(s) why the test was invalid, and a new test would be run in its place. Additionally, if a test was performed with an atypical result, but there were no known problems, the field engineer would annotate the dataset in which this occurred and would list potential reasons for the result. For example, if the vehicle was underpowered and could not meet the desired target distance then this comment would be added to the test record. At the end of the test day, the field engineer electronically transferred the data to the project engineer at WVU in Morgantown, WV.

The second level of assessment of the data quality was performed at WVU by the project engineer assigned to maintain the data. The project engineer received the data collected the previous day and reviewed the dataset to insure that the correct vehicle/engine model, test weights, and test cycles were performed. In instances when there were problems or when atypical results were obtained, the field engineer would interact with the project engineer during testing via email and/or phone conservations to make an assessment of the actions, if any, to take. Additionally, the project engineer would review the integrated mass emissions data and the pertinent analog and digital signals required to calculate the emissions for potential problems. The project engineer maintained a database of the results in tabular and graphical format to be able to identify tampered and or mal-maintained (T/M) engines and or vehicles based on criterion developed during this project. If a potential T/M vehicle was identified, this information was passed on to the Principal Investigators, and this information was then communicated to the sponsors. If a problem was identified with the data by the project engineer, then the project engineer would interact with the field engineer to rectify the problem.

The third level of assessment was done by the Principal Investigators. The Principal Investigators examined the data and provided feedback to the project engineer of potential problems, who was separated from the data gathering process.

The fourth level of data quality assessment was performed by the QA/QC officer. The QA/QC officer received the integrated mass emissions data in the form of single page short reports from the project engineer in hardcopy or electronic (Microsoft Word) format. Short reports are presented in Appendix K. The QA/QC officer would, at times, examine raw and processed data with the project engineer as a spot check throughout this test program. The test, vehicle, and emissions data summarized in each short report were reviewed on a per test basis and per vehicle basis for inconsistencies in the information

and emissions data. Inconsistencies in the information were brought to the project engineer's attention and corrected. These corrections included misspellings, incorrect vehicle description, incorrect engine description, lack of comments, and other minor corrections. These corrections are not summarized in the table below. Questions, concerns, and inconsistencies in the emissions data that were directed to the project engineer are summarized in the table below. The corrective action taken is also listed.

The majority of the inconsistencies in the emissions data can be attributed to trying to measure very low emissions levels (such as low engine power Idle and Creep modes) and higher level emissions (high engine power transient and cruise modes) with one set of emissions analyzers and one calibration range. There was a two order of magnitude difference in the emissions concentration levels between the low and high engine power modes, so that low power modes to have a much greater variability in this data.

There were difficulties in comparing the results from two different NO_x analyzers during the first half of the test program. The difference in the two NO_x analyzers was addressed throughout this test program by improving the test procedure to adjust the second NO_x analyzer flow and the changing of NO_x analyzers to newer technology.

RESULTS AND DISCUSSION, REGULATED SPECIES

HHDT Data Gathered

Test Runs

Each execution of a cycle or mode was assigned a sequence number and a run number. Appendix J presents a listing of sequence and run numbers, with the corresponding name of the cycle, vehicle number and test weight. Some sequence and run numbers are omitted in Table 3 because they are associated with background tests or with rejected runs. In Table 3 the test modes or cycles are designated by the actual file names used. "Test D" corresponds to the UDDS, trans3 and cruise3 refer to the three point smoothed versions of the Transient and Cruise Modes that are customarily used. Some modes were lengthened by being repeated to collect sufficient PM mass during the mode. Idle32 refers to a double length idle (1,800 seconds instead of 900 seconds), and creep34 refers to four repeats of a creep run as a single mode. Table 3 corresponds to the sequence and run numbers in the short reports appearing in Appendix K. MHDT are shown with 50% and 75% test weights. The actual weights used appear in Appendix J.

Data Gathered

The cycle or mode-averaged data, in units of g/mile (except for idle, which is in time-specific units) are all presented in Appendix K in the form of "short reports." These data have also been translated into graphical representations in Appendix H**.** Data have been gathered into summary tables in Appendix L**.** The full database containing continuous vehicle operating data and gaseous emissions rates has been made available to the sponsors separately in electronic form.

Discussion of individual truck emissions within the body of this report emphasizes two species, NO_x and PM, since NO_x and PM data are assumed to be of greatest interest for truck operation. However, CO and HC have also been presented with respect to select cycles below and for all cycles in the appendices. The ARB cycles (Idle, Creep, Trans, Cruise, and HHDDT_S) demonstrate a variety of driving conditions. Additional, more comprehensive plots of the data appear in Appendix M. Some vehicles were "speed limited" to the point where they were unable to follow the schedule trace and were not tested for the HHDDT_S. HHDDT in Phase 1 were not exercised through the HHDDT_S.

Figure 16 presents the NO_x emissions for all of the HHDDT on the Idle mode of the HHDDT schedule. The range of years appearing in Figure 16 corresponds to the CRC grouping of the years of engine certification. The number below indicates the number of vehicles tested in that MY range for which data are included in the chart. The 1998 vehicles show the highest NO_x emissions of all MY bins. Later MY trucks produce higher NO_x than early MY trucks because the injection timing may be advanced on later model trucks to reduce white smoking. The reader is cautioned that small number counts of vehicles in some MY bins may cause the program data in some represent the whole

California fleet faithful. This is especially true if one of the vehicles in the group is an outlier, or high emitter.

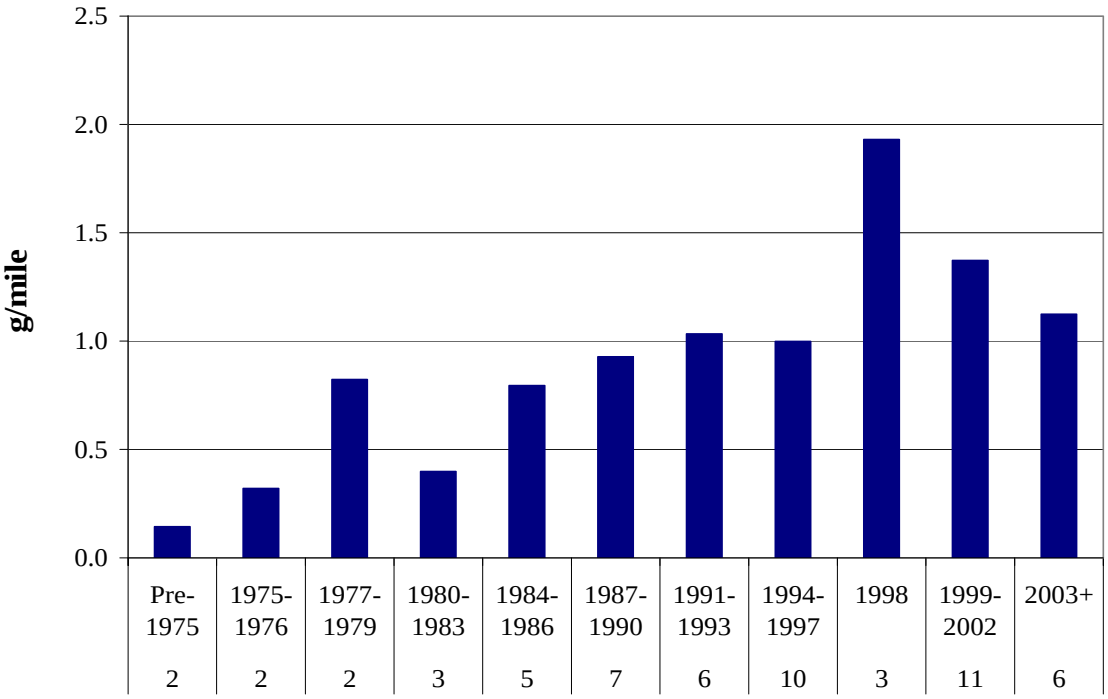

Figure 16: NO_x emissions for the Idle Mode, in units of g/minute.

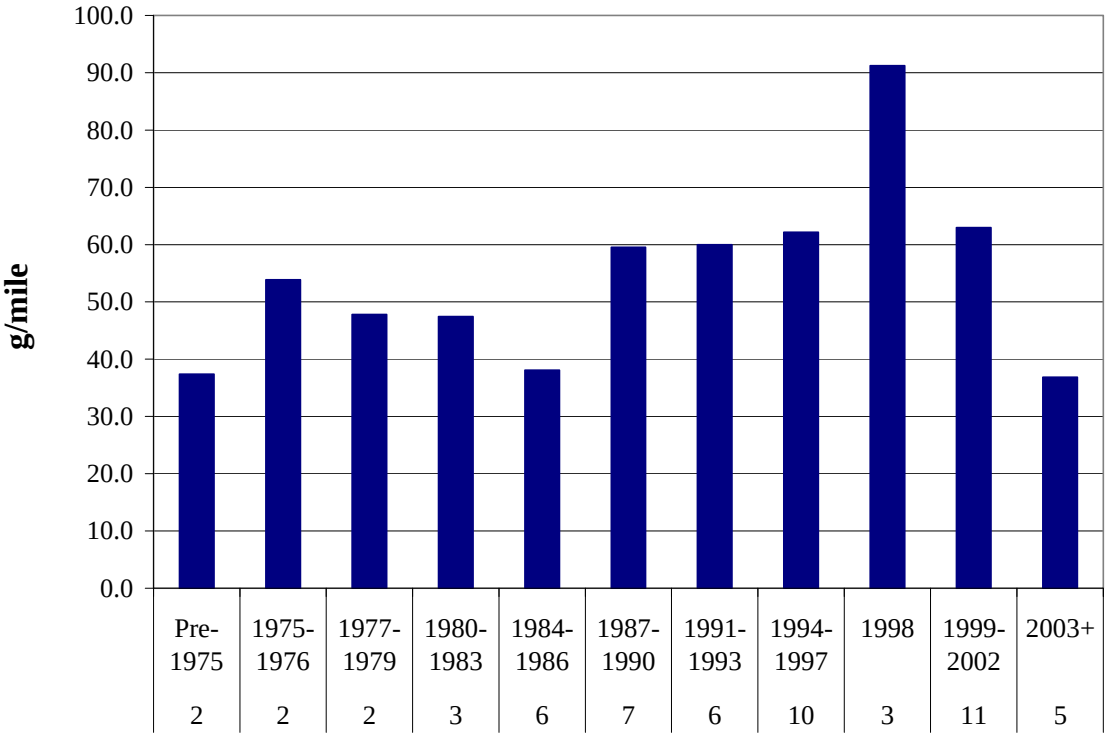

Figure 17: NO_x emissions for the Creep mode (56,000 lbs.).

Figure 17 shows NO_x emissions for all HHDDT trucks operated through the Creep mode at 56,000 lbs. test weight. This mode is primarily low speed with repeated upward and downward speed ramps. The small distance traveled and high idle content lead to high distance-specific emissions values. Results are less variable over the MY bins than for idle, but idle and low load injection timing advance is also the most likely cause for the high NO_x emissions over the 1987 to 2002 period.

Figure 18 shows NO_x emissions for all HHDDT trucks operated through the Transient mode at 56,000 lbs. test weight. The Transient mode represents typical urban driving activity. Figure 18 shows that the NO_x emissions for 1998 were higher than for neighboring MY bins, but the highest NO_x arose from the oldest vehicles. The 1975 to 1976 MY bin was the highest at 47 g/mile. This was primarily due to their being only two sample vehicles, one of which emitted 60 g/mile while the other was 34 g/mile. The 1980 to 1983 MY bin contained vehicles consistently emitting high NO_x. The emissions of NO_x prior to 2002 were all higher than 20 g/mile. The NO_x emissions of the five 2003 and newer MY vehicles (equipped with exhaust gas recirculation for Cummins and Detroit Diesel, or bridging/ACERT technology for Caterpillar) differ in that they averaged less than 17 g/mile.

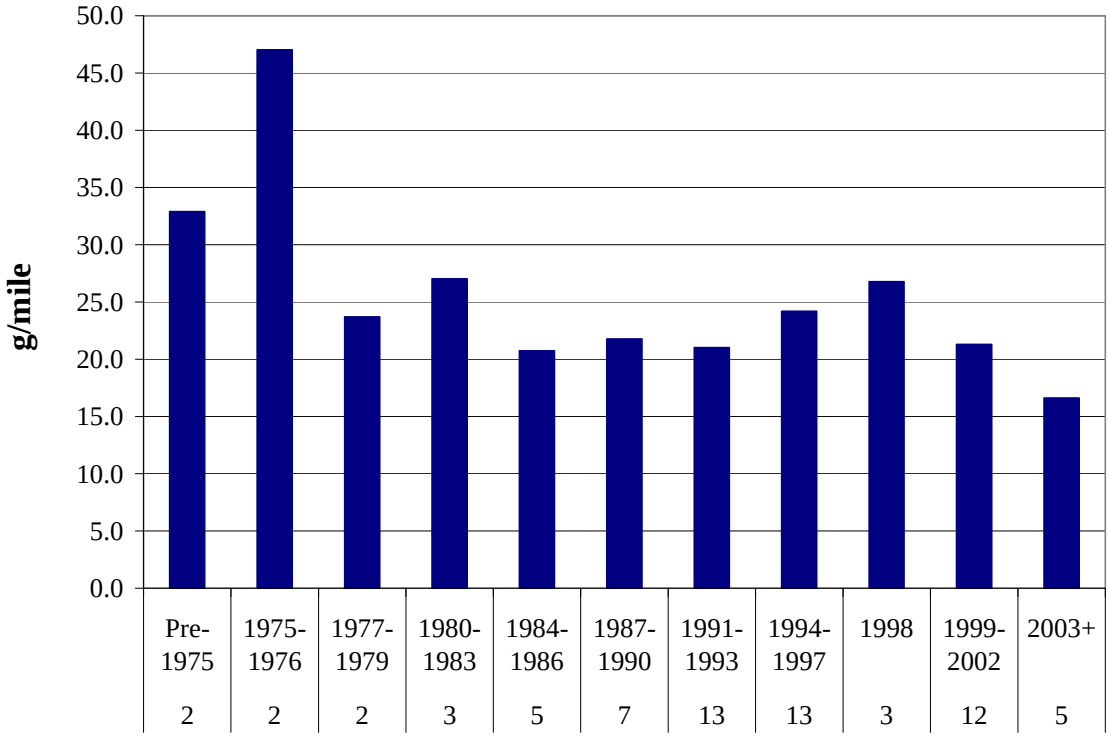

Figure 18: NO_x emissions for the Transient mode (56,000 lbs.). One of the vehicles in the 1975-1976 MY bin emitted NO_x at 60 g/mile.

Figure 19 shows NO_x emissions for all HHDDT trucks operated through the Cruise mode at 56,000 lbs. test weight. Figure 19 shows that the NO_x emissions for 1998 were higher than all but the 1975-1976 group of trucks. The 1998 trucks were also relatively higher than they were for the Transient mode. This suggests that off-cycle injection timing was enacted more on the Cruise mode than the Transient mode, which would be expected. This issue is discussed in more detail in the section on T&M and reflash. The NO_x emissions of the five 2003 and newer MY engines (equipped with exhaust gas recirculation or bridging/ACERT technology) differ in that they averaged to about 9 g/mile.

Prior studies with fewer HHDDT[1,10,11,12] and earlier reports in the E-55/59 program have suggested that NO_x did not decline with MY. Figure 19 shows a pattern of high NO_x on the oldest trucks, as well as trucks in the 90's that have off-cycle injection timing advance, with a decline in NO_x for the latest MY trucks. However, there is no clear trend in NO_x with respect to MY from 1977 to 1997 for trucks exercised through the Cruise mode at 56,000 lbs. test weight.

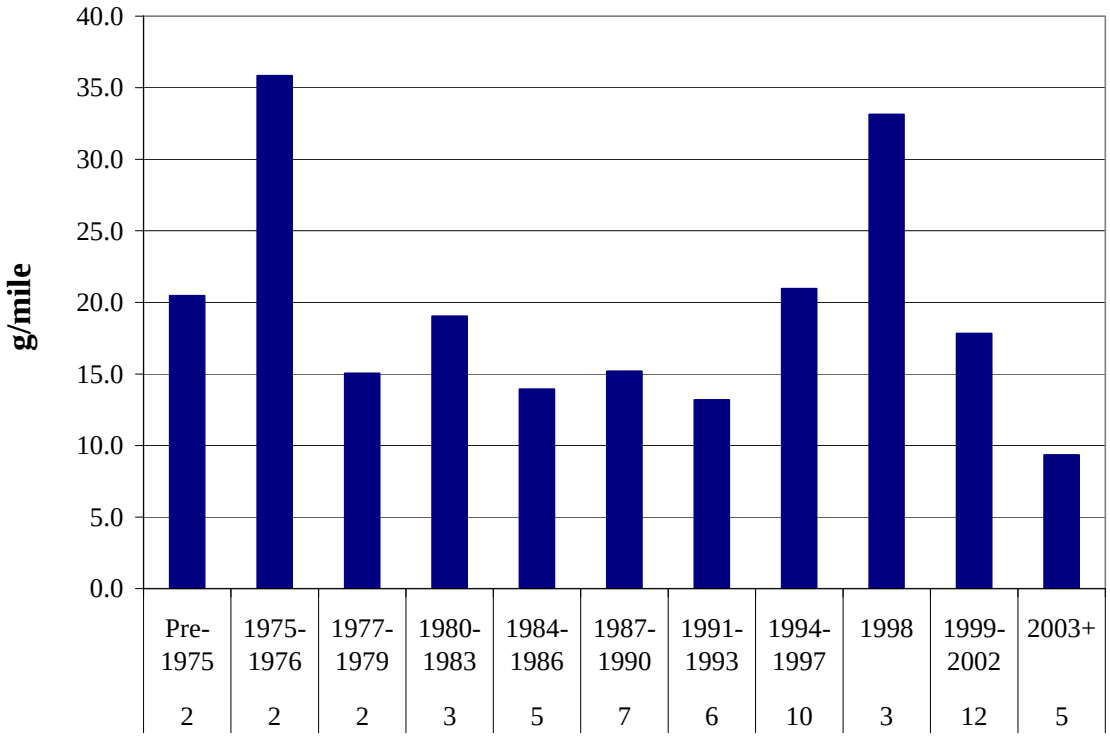

Figure 19: NO_x emissions for the Cruise mode (56,000 lbs.). One 1998 vehicle (E55CRC-10) was identified as a high NO_x emitter in Phase 1.

Figure 20 shows NO_x emissions for the HHDDT_S mode at 56,000 lbs. test weight. This sample of trucks excludes the Phase 1 HHDDT because they were not tested on the

HHDDT_S. This mode has a high content of near-steady high-speed freeway operation. A 2003 MY truck exhibited lowest NO_x, at 8.05 g/mile. The 1969, 1975 and 1998 engine years exhibited the highest NO_x at approximately 29, 56, and 22 g/mile respectively. A 1975 Cummins-powered truck had the highest with 56 g/mile, as the lone truck in the 1975-1976 category that completed the HHDDT_S mode.

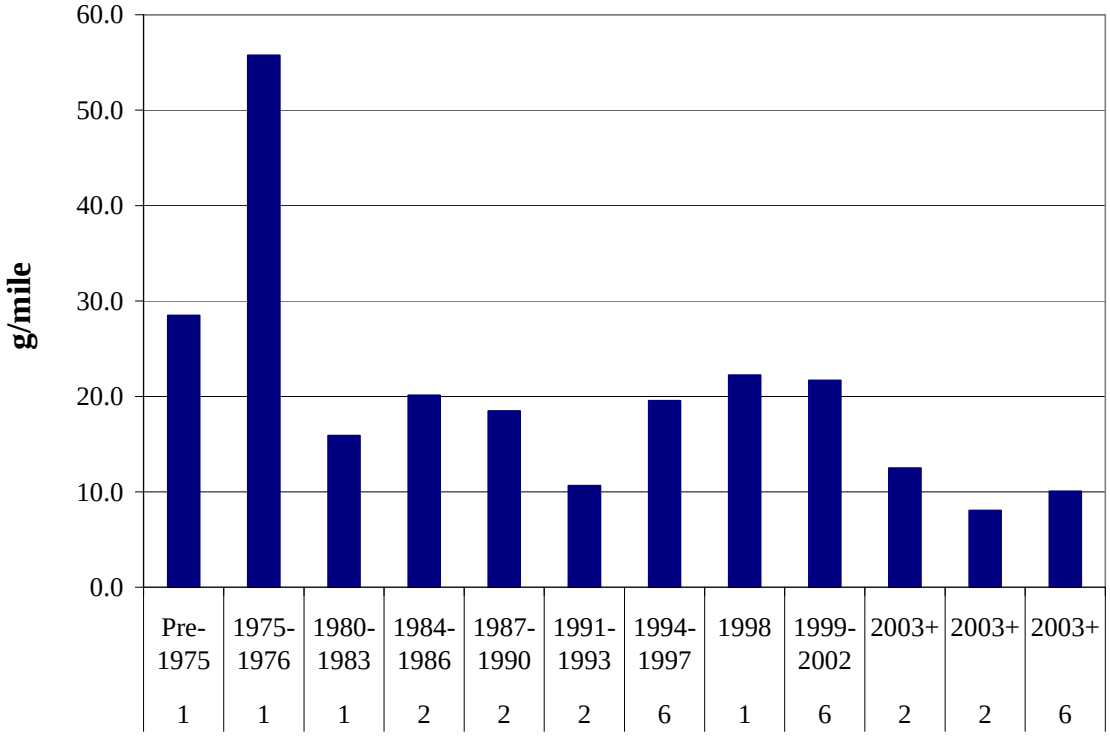

Figure 20: NO_x emissions for HHDDT_S mode (56,000 lbs.). The high value for the 1975-1976 MY bin is due to a single truck with high NO_x emissions.

Figure 21 shows the NO_x emissions for the UDDS. The distribution of emission levels of this urban driving cycle is similar to that found in the Transient mode of Figure 18 above.

Figure 22 shows the PM emissions for the Idle mode. E55CRC-37 was tested in this mode only since it could not operate on the dynamometer due to traction control technology. For this reason there is an additional 2003+ data point on the Idle graph (Figure 22) relative to the active modes. Some MY bins were high due to outlying performance by individual vehicles. For example, E55CRC-45, discussed in the T&M section, was a prodigious emitter of both PM and HC and biased the data for the 1991-1993 MY group. PM was lowest in the 2003 and later MY group.

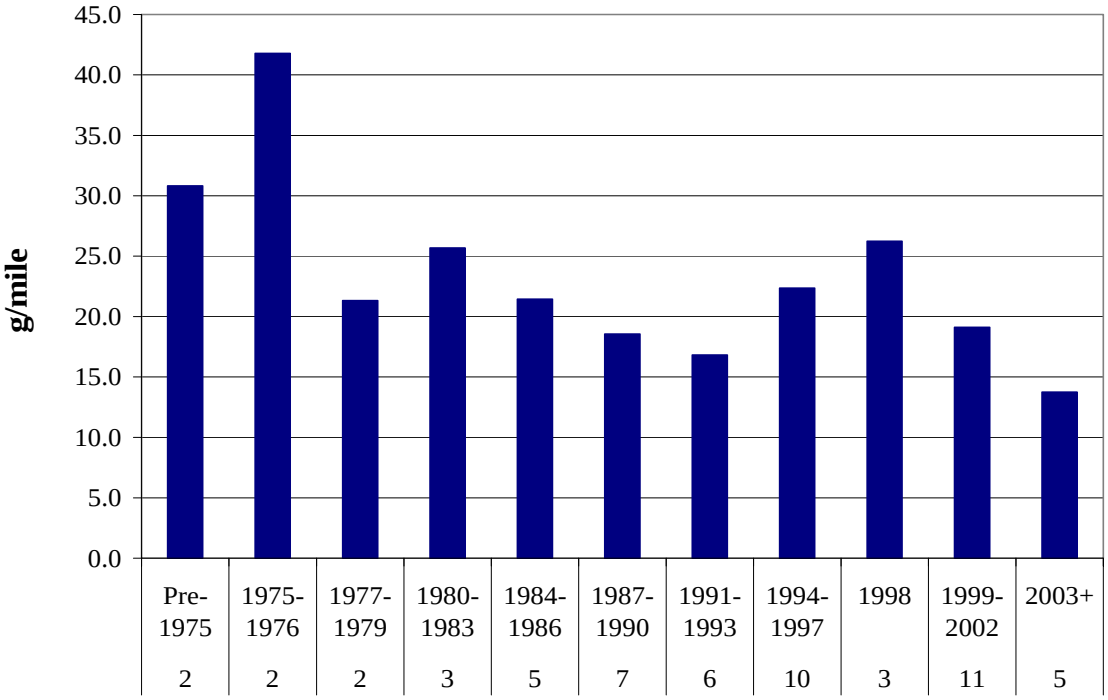

Figure 21: NO_x emissions for UDDS mode (56,000 lbs.).

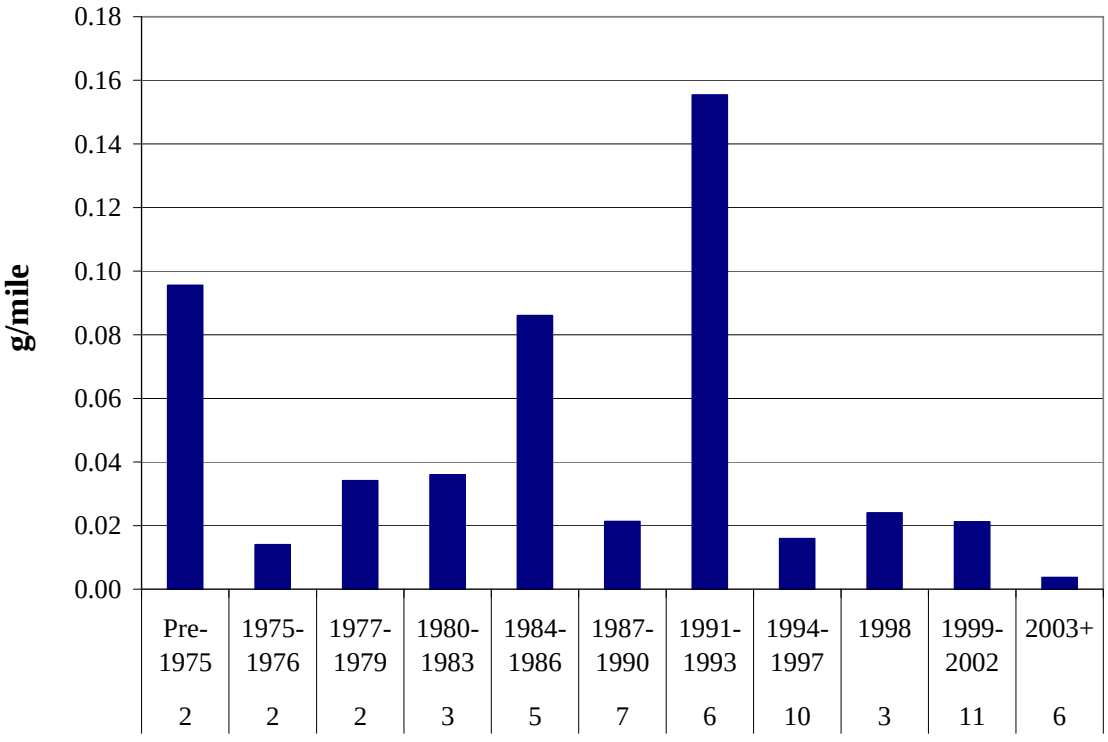

Figure 22: PM emissions for Idle Mode. Truck E55CRC-45, in the 1991-1993 MY bin, was a prodigious emitter and raised the average value for that bin substantially.

Figure 23 shows PM emissions for HHDDT for the Creep mode. The two highest bins for the Creep mode are the same as for the Idle mode. The 2003+ group has a significantly lower output than even the second lowest group (1998).

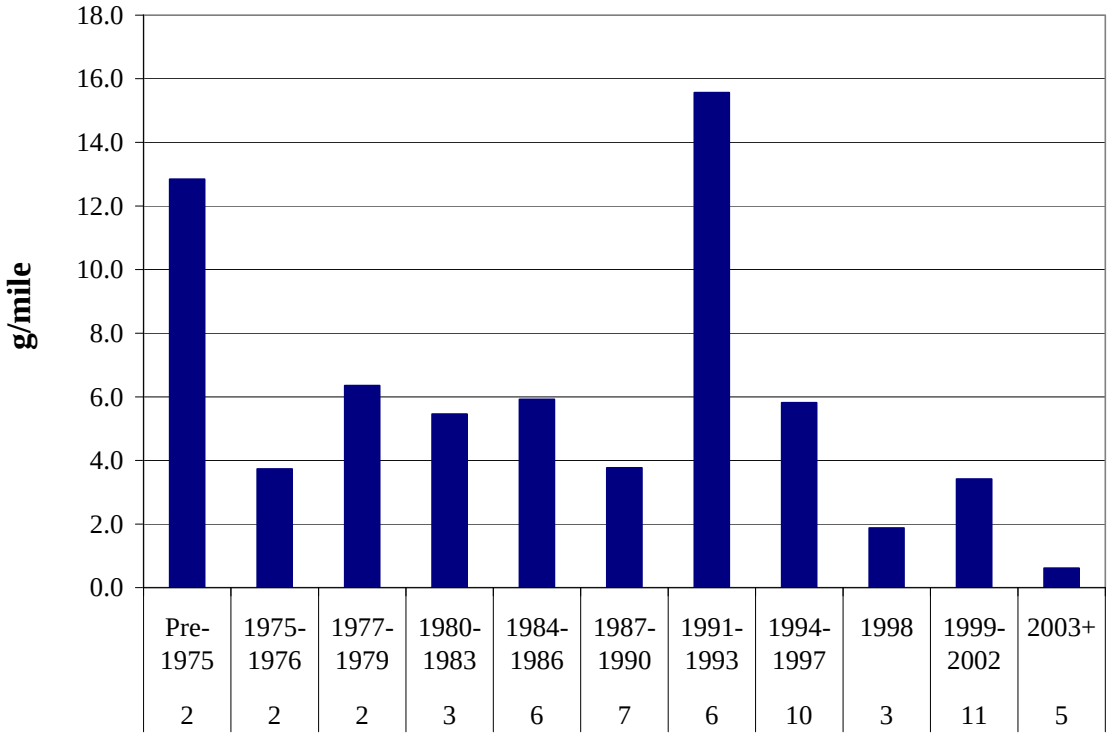

Figure 23: PM emissions for Creep mode (56,000 lbs.). One vehicle in the 1991-1993 MY bin was a very high emitter of both PM and HC at light load.

Figure 24 shows PM emissions for all HHDDT trucks operated through the Transient mode at 56,000 lbs. test weight. E55CRC-45, a 1993 Cummins-powered tractor demonstrated significantly higher PM emissions than the other test vehicles at low load, but E55CRC-45 biased the data far less in the Transient mode. In the highest emitting group, E55CRC-16 emitted 15 grams per mile of PM and the other vehicle in the 1977-1979 group emitted 2 grams per mile. E55CRC-16 is discussed in detail in the T & M section. There is a general downward trend in PM emissions on the Transient mode with respect to MY.

Figure 25 shows the PM emissions for the Cruise mode. Unlike in most other modes, the 2003+ group does not have the lowest emissions. E55CRC-16, a 1979 Caterpillar-powered HHDDT, had the highest PM emissions with 16 g/mile, and led to the high value for the 1977 to 1979 MY group. Even without this MY group, it is evident that PM has declined over three decades for cruising operation. PM emissions after the introduction of electronic engines in the 1991-1993 period are lower than the emissions from earlier mechanically controlled engines. This can be ascribed to improved fuel and boost management, and higher injection pressures for later MY regulations.

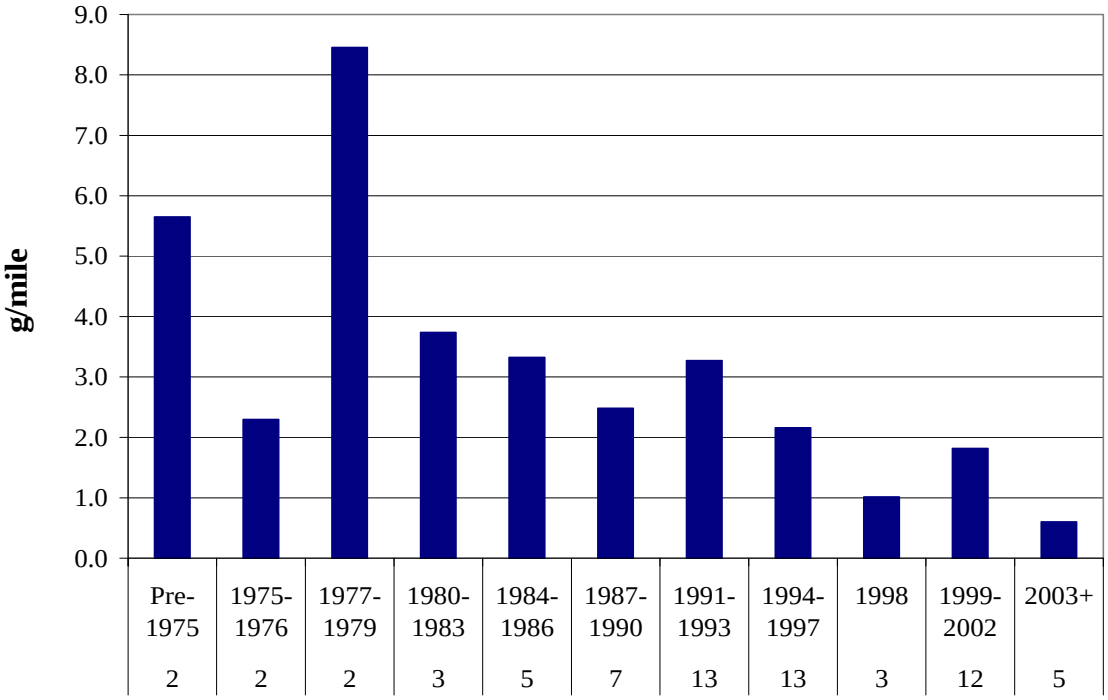

Figure 24: PM Emissions for the Transient mode (56,000 lbs.). Truck E55CRC-16, a high emitter, caused the high average in the 1977-1979 MY bin

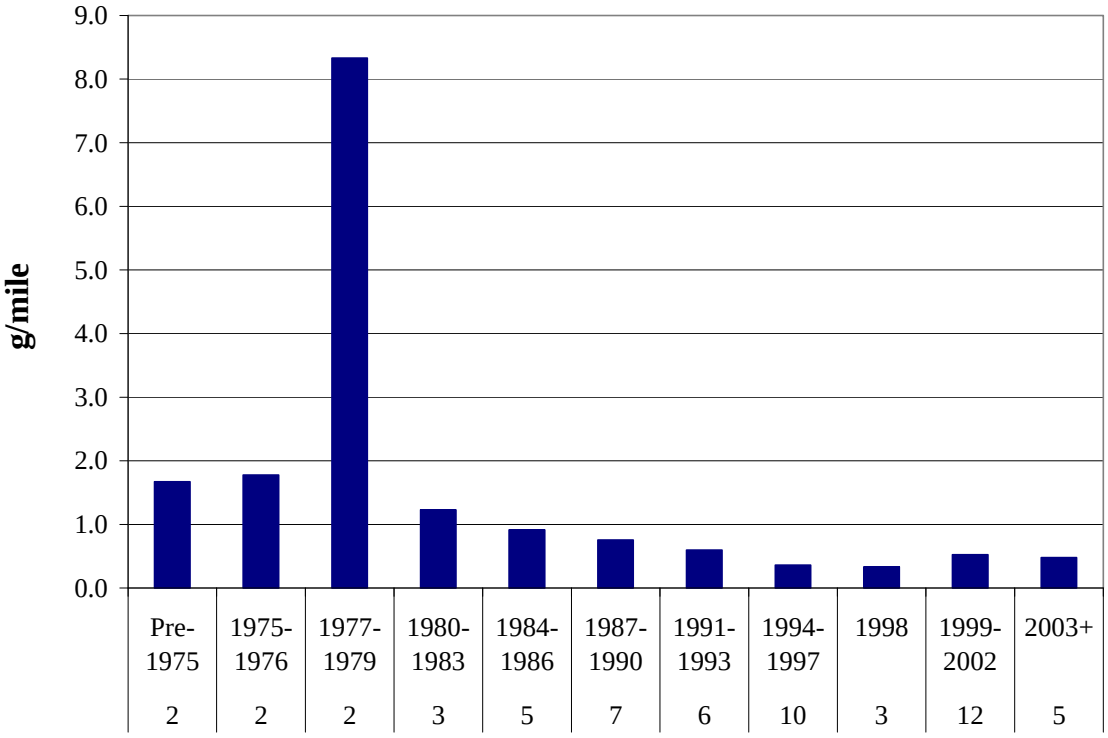

Figure 25: PM emissions for the Cruise mode (56,000 lbs.). E55CRC-16 contributed to the one very high MY bin average.

Figure 26 shows PM emissions for all HHDDT trucks operated through the HHDDT_S mode at 56,000 lbs. test weight. E55CRC-27 was the first vehicle tested using the HHDDT_S Mode. E55CRC-69 was unable to attain sufficient speed to provide meaningful data in the HHDDT_S mode. It was governed to 55 mph maximum speed.

The first three groups in Figure 26 had only one vehicle in each group, each of which had significantly higher emissions than the newer vehicles. There appears to have been a step change in PM emissions beginning with the 1991-1993 group. E55CRC-29, a 1999 Cummins, escalated the average for the 1999-2002 group by emitting 2.52 g/mile of PM, a value more than twice as high as for any other vehicle in the group.

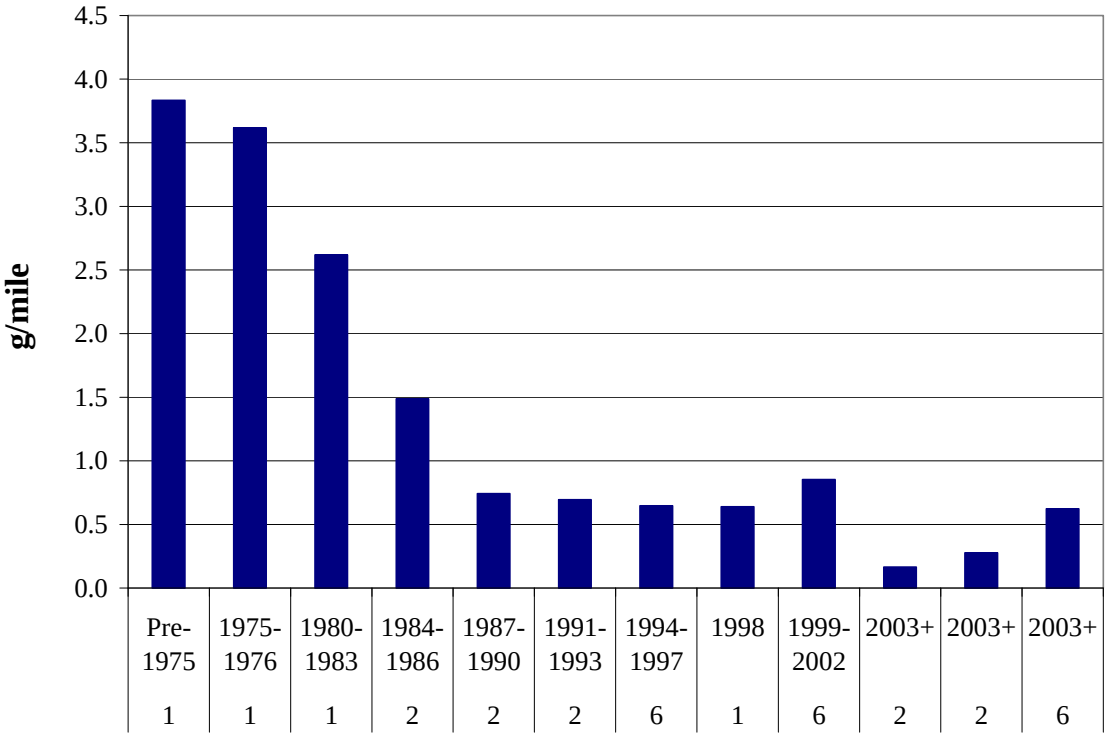

Figure 26: PM emissions for HHDDT_S mode (56,000 lbs.). Four MY groups show data from only one vehicle.

Figure 27 shows the PM emissions for the UDDS. As was the case with the NO_x emissions, the UDDS and Transient modes show a similar distribution pattern.

Figure 28 shows the CO emissions for the Trans3 Mode. While there were a handful of vehicles with emissions higher than other trucks in the MY bin, the highest was E55CRC-23 (1983 Cummins) with 40 g/mile. Also, the 2003 Detroit Diesel engine of E55CRC-44 was significantly (two to four times) higher in both CO and PM than the other four vehicles in the 2003+ group.

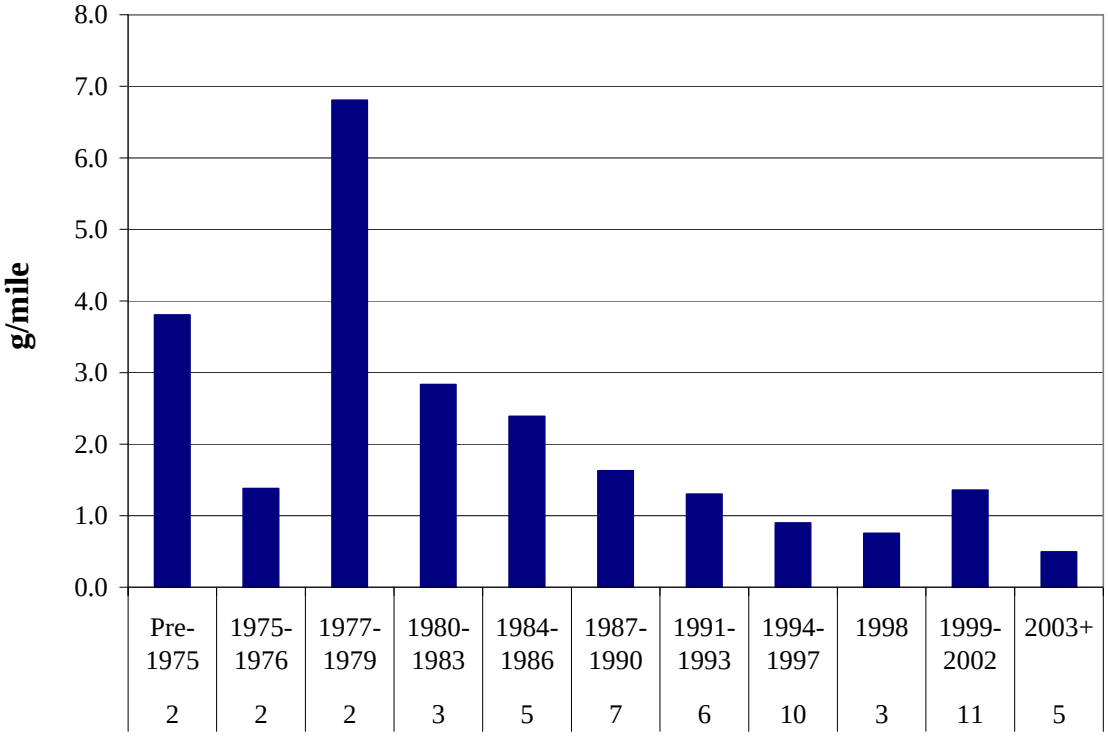

Figure 27: PM emissions for UDDS mode (56,000 lbs.).

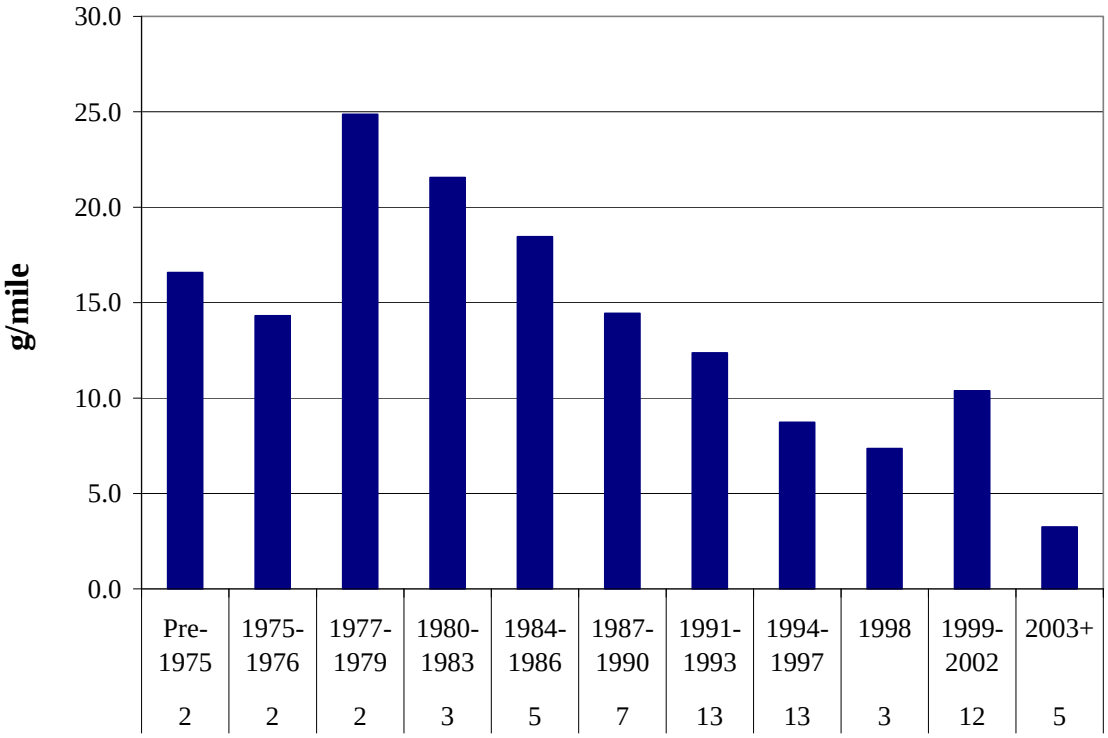

Figure 28: CO emissions for Transient mode (56,000 lbs.).

Figure 29 shows the CO emissions for the Cruise mode. In sympathy with the data for the Transient mode, E55CRC-23 with its 1983 Cummins was nearly the highest emitter. E55CRC-20 with a 1992 Detroit Diesel engine also had about 14 g/mile of CO emissions. If it were not for the 2003 Detroit Diesel engine of E55CRC-34, the 2003+ group would have represented an even more dramatic drop from previous model years.

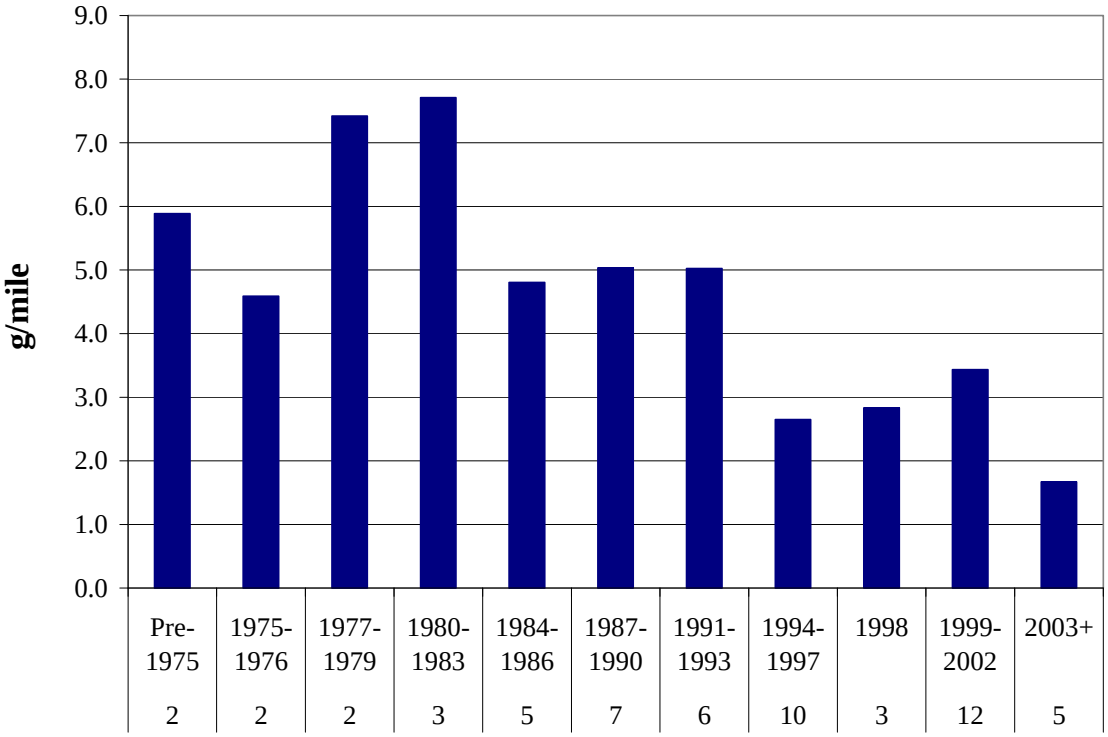

Figure 29: CO emissions for Cruise mode (56,000 lbs.).

HC emissions from vehicles built over the last decade are lower than from older vehicles in the older vehicles in the test fleet. Figure 30 shows the HC emissions for the Transient mode. E55CRC-45 had a 1993 Cummins engine. It emitted the highest level of HC at 5.43 g/mile. E55CRC-45 was a high emitter of both PM and HC at light loads, and has been discussed in the T & M section. The 1994 Cummins of E55CRC-60 emitted 4.18 g/mile. Both of these trucks showed far higher emissions than were measured from the other vehicles in each of their respective MY bins.

Figure 31 shows the HC emissions for the Cruise mode. E55CRC-45 (1993 Cummins) again ranked as one of the top HC emitting vehicles, and biased the 1991-1993 MY bin. The five most recent MY bins show lower emissions, on average than earlier MY bins, but there is no clear, monotonic, pattern to HC reduction with respect to MY.

Additional plots showing the HHDDT emissions at test weights of 30,000 and 66,000 lbs. are available in Appendix M.

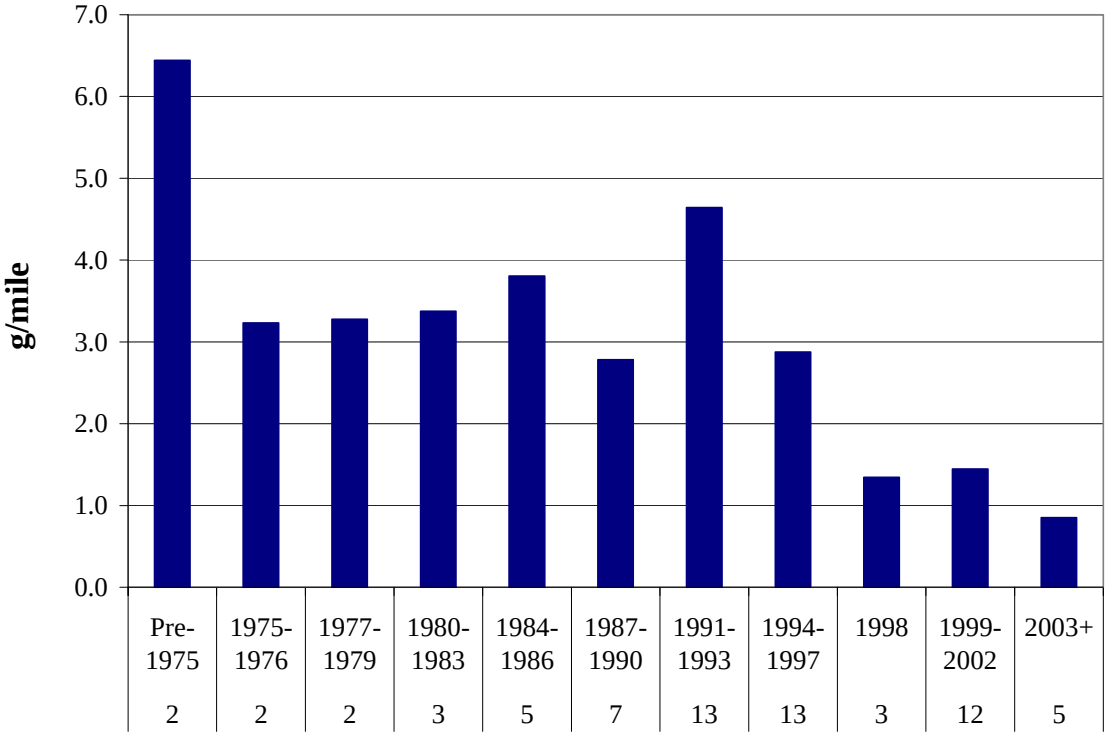

Figure 30: HC emissions for Transient mode (56,000 lbs.).

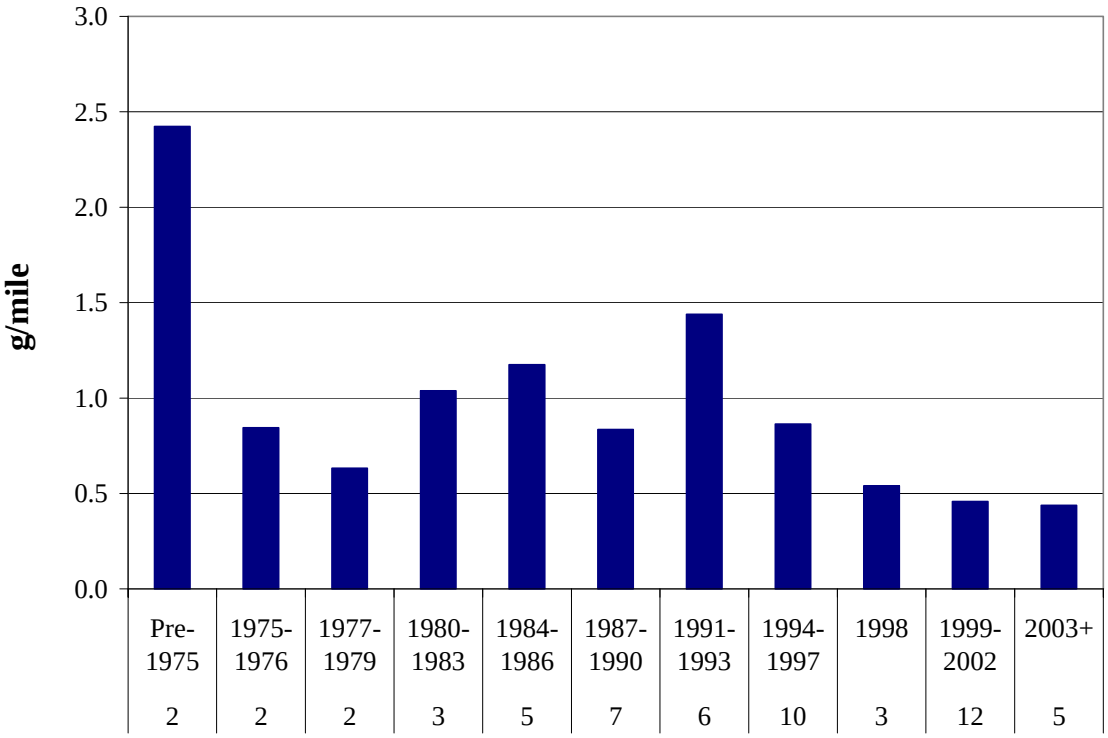

Figure 31: HC emissions for Cruise mode (56,000 lbs.).

MHDT Data Discussion

This section discusses results of the testing of the MHDT. The MHDT Schedule includes a lower speed transient mode (MHDTLO), a higher speed transient mode (MHDTHI), a cruise mode (MHDTCR), and the HHDDT_S. Figure 32 shows emissions from the AC5080, which was also used. Figure 33 presents NO_x emissions for the Lower Speed Transient mode from the MHDT. In these, and all other figures in this section, 'laden' refers to 75% of the gross vehicle weight rating (GVWR) and 'unladen' refers to 50% of the GVWR. NO_x emissions from these MHDT are similar to those of the HHDDT transient mode.

E55CRC-57, in the 1999-2002 group, showed an unusually high unladen NO_x emissions value. This was ascribed to a failed temperature sensor, which caused a limp-home mode. E55CRC-57 has been discussed in detail in the T & M section.

The three early model gasoline engines yielded NO_x emissions on the Lower Speed Transient mode that were similar in emissions from the diesel vehicles, but the one newer gasoline vehicle, E55CRC-53, produced the lowest NO_x relative to other categories of truck.

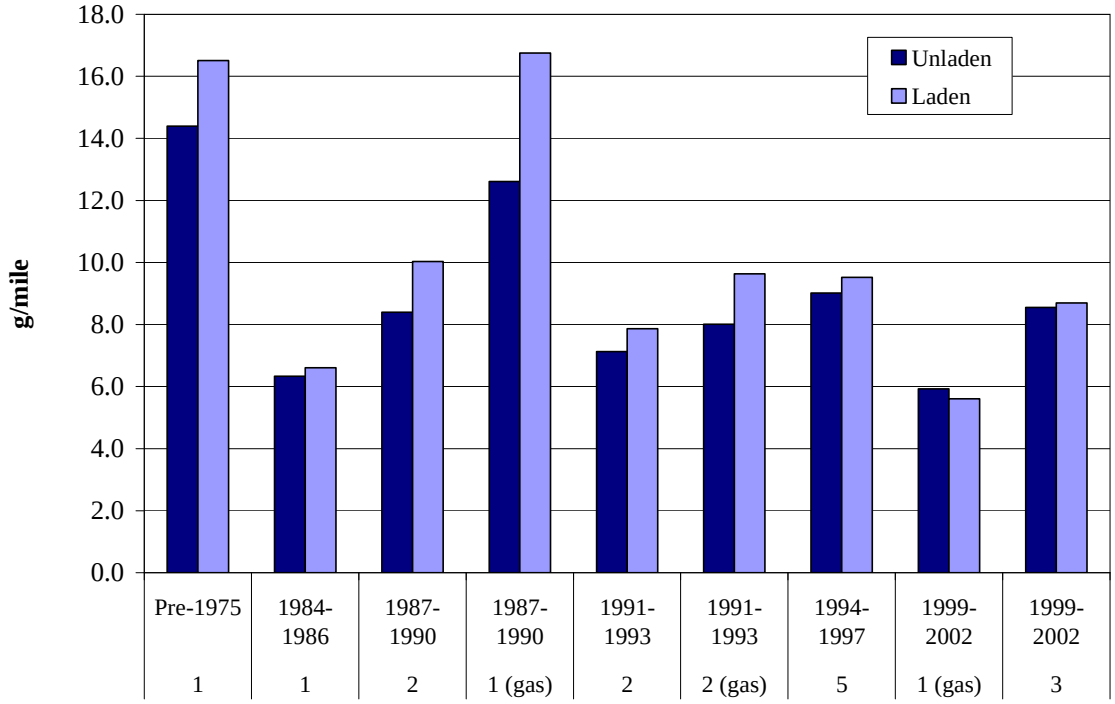

Figure 32: NO_x emissions for AC5080 (both laden and unladen). Gasoline-fueled vehicles are separated from diesel-fueled vehicles for comparison.

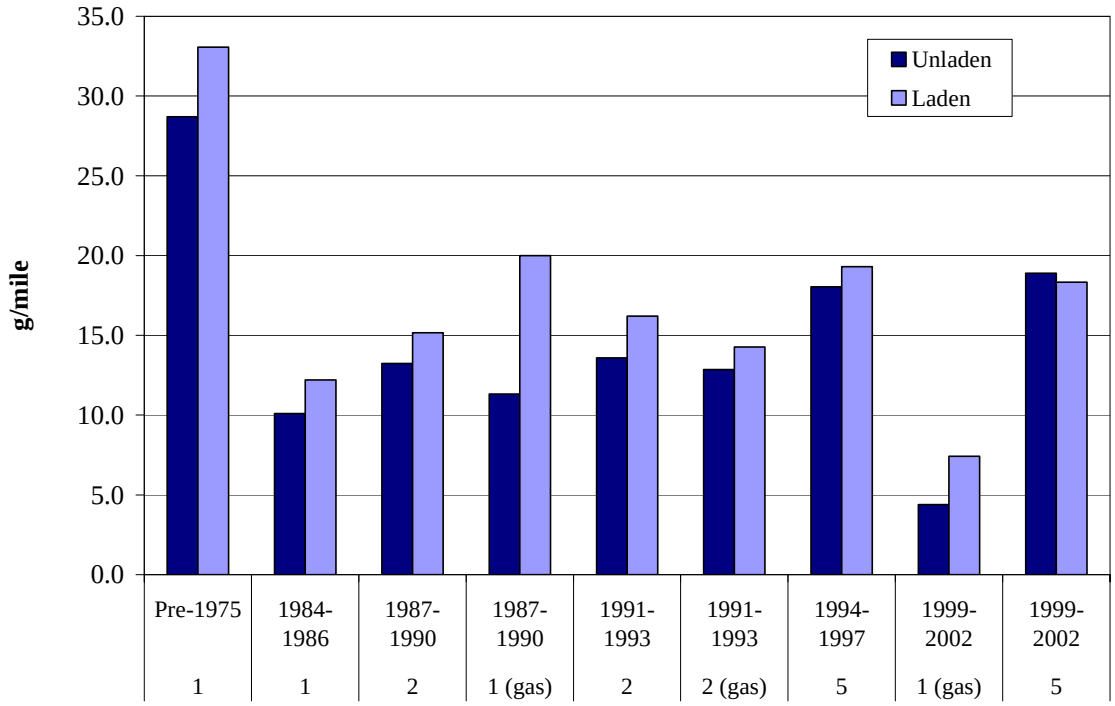

Figure 33: NO_x emissions for the Lower Speed Transient mode (both laden and unladen).

Figure 34 shows that the NO_x emissions for the Higher Speed Transient mode were consistently lower than for the Lower Speed Transient Mode. As in the previous mode, E55CRC-53, with a gasoline engine, produced the lowest NO_x emissions at fewer than 4 g/mile. The older gasoline vehicle, E55CRC-54, emitted NO_x at a level characteristic of the diesel trucks. From Figure 32 to Figure 47 it is important to realize that varying test weights from truck to truck influences distance-specific emission levels.

As seen in Figure 35, NO_x emissions during the MHDT Cruise mode were slightly lower than for either of the Transient modes and were close to those of the high-speed cruise (HHDDT_S) shown in Figure 36. The older gasoline fueled trucks on average emitted NO_x at a higher rate than the diesel fleet. Note that Figure 36 is for a small subset of vehicles. Figure 37 shows NO_x on the UDDS for MHDT.

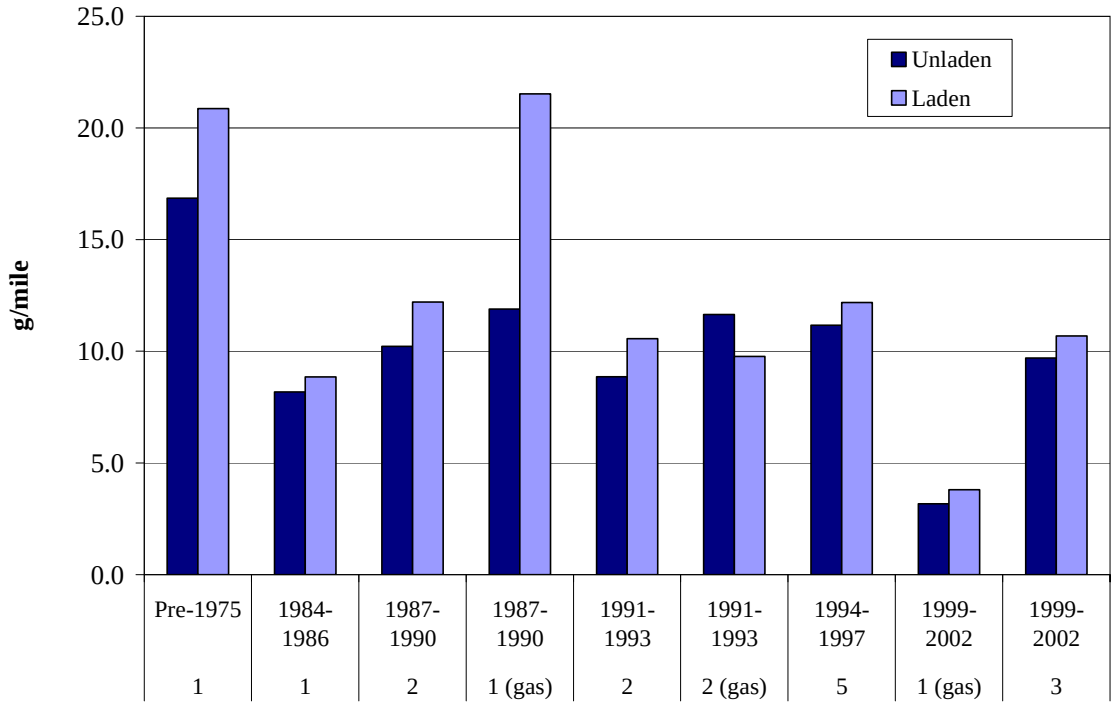

Figure 34: NO_x emissions for the Higher Speed Transient mode (both laden and unladen).

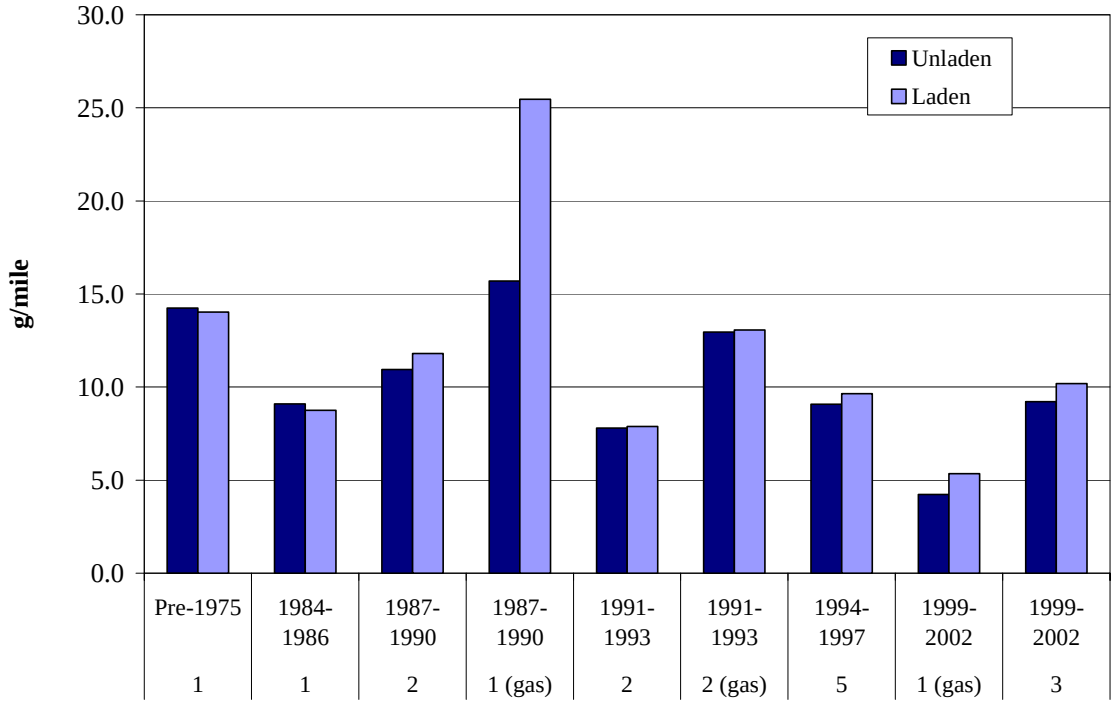

Figure 35: NO_x emissions for the MHDT Cruise mode (both laden and unladen).

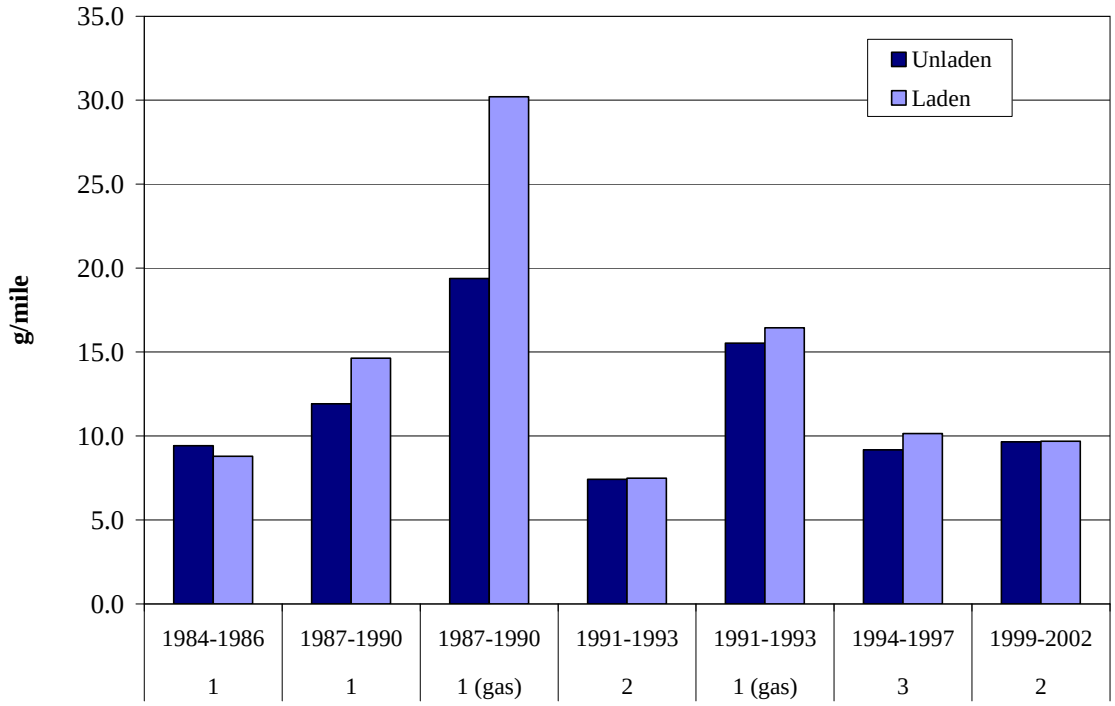

Figure 36: NO_x emissions for the HHDDT_S mode (both laden and unladen).

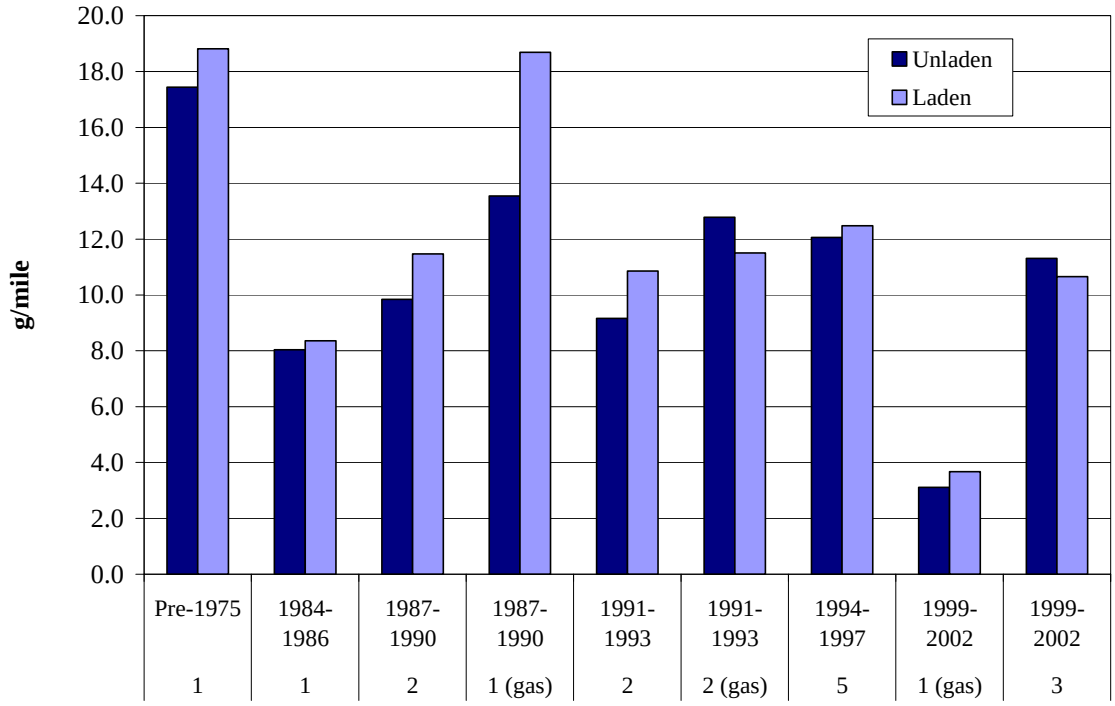

Figure 37: NO_x emissions for the UDDS mode (both laden and unladen).

Figure 38, Figure 39, Figure 40, Figure 41, and Figure 42 show PM emissions for the AC5080, MHDT Lower and Higher Speed transients, the MHDT Cruise mode, and the HHDDT_S mode. As expected, PM values from the gasoline trucks were consistently well below those of the diesel vehicles. The influence of test weight (laden vs. unladen) on PM was noticeably greater than for NO_x. For the limited number of trucks tested, one may conclude that PM levels have not changed from MY 1991 to MY 2002.

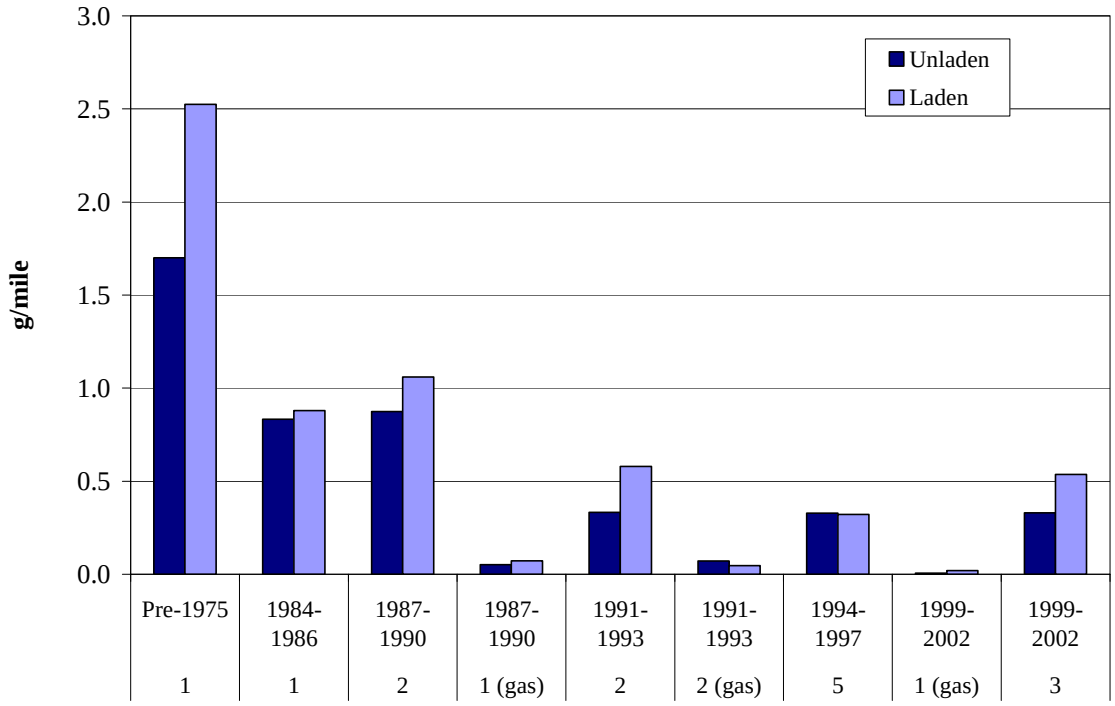

Figure 38: PM emissions for the AC5080 mode (both laden and unladen).

For the HHDDT_S (Figure 42), only selected trucks were used from the MHDT fleet, leading to relatively higher MY 1991-1993 group emissions. E55CRC-76 contributed to the high emissions in the 1991-1993 MY group.

Figure 43 shows emissions of PM for the UDDS. The four gasoline vehicles emitted, on average, an order of magnitude lower PM than the diesel fleet.

Figure 44 and Figure 45 present CO emissions data for the MHDT on the Higher Speed Transient and MHDT Cruise modes. In contrast to their PM contribution, CO from the gasoline vehicles was substantially higher than from the diesel vehicles.

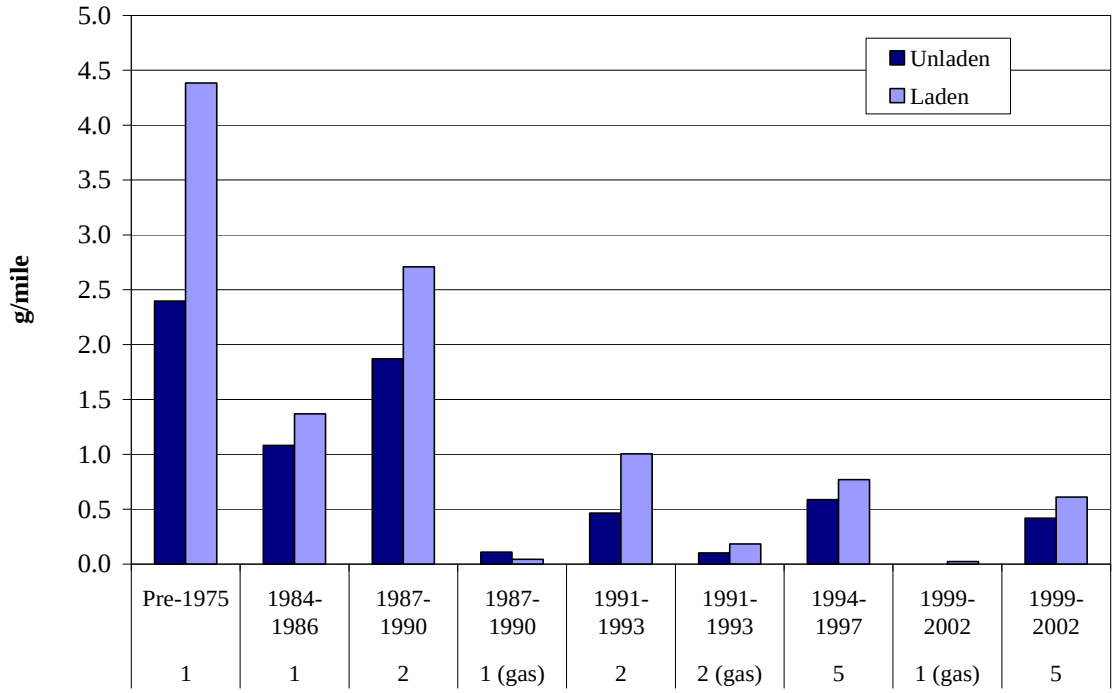

Figure 39: PM emissions for the Lower Speed Transient mode (both laden and unladen).

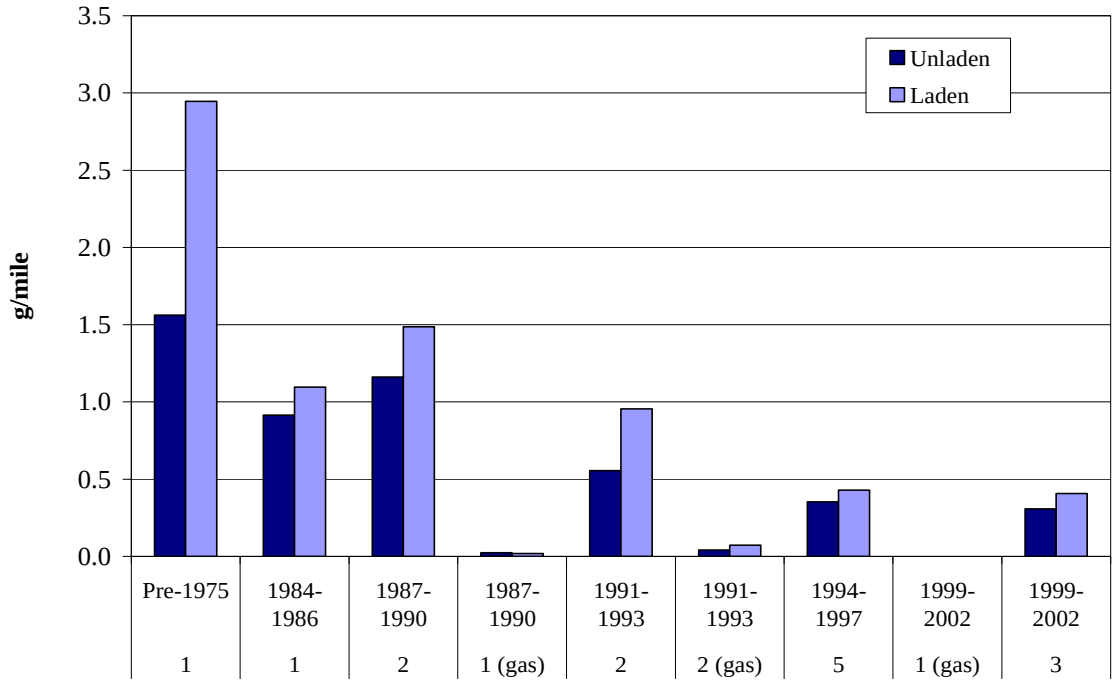

Figure 40: PM emissions for the Higher Speed Transient mode (both laden and unladen).

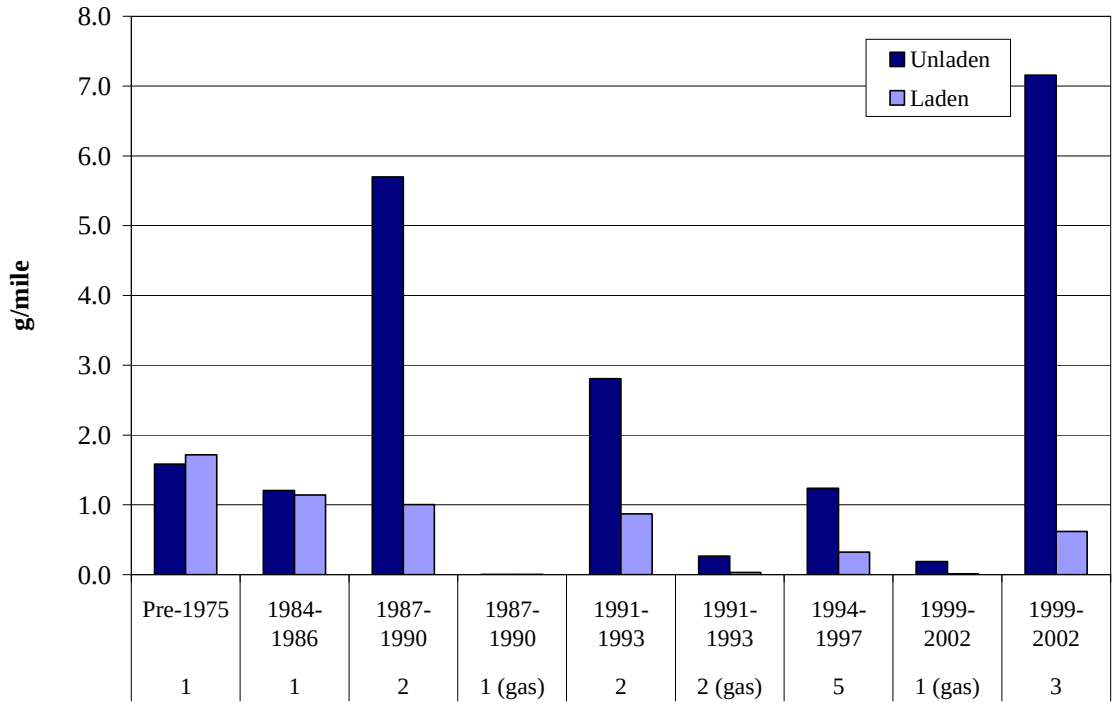

Figure 41: PM emissions for the Cruise mode (both laden and unladen).

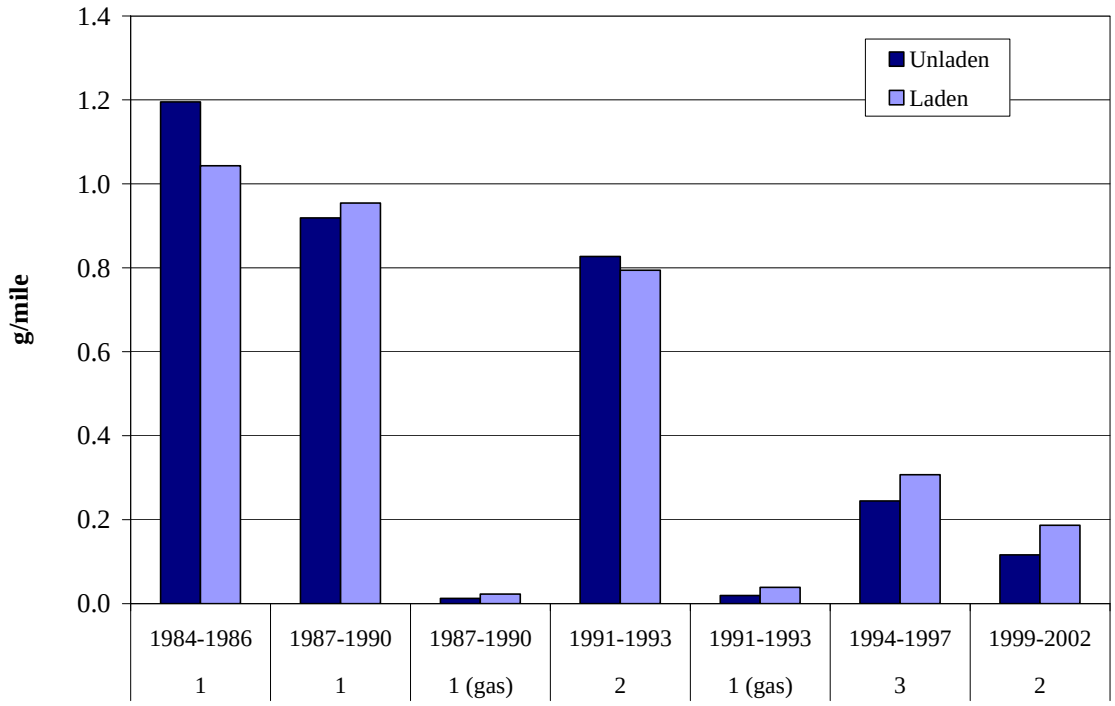

Figure 42: PM emissions for the HHDDT_S mode (both laden and unladen).

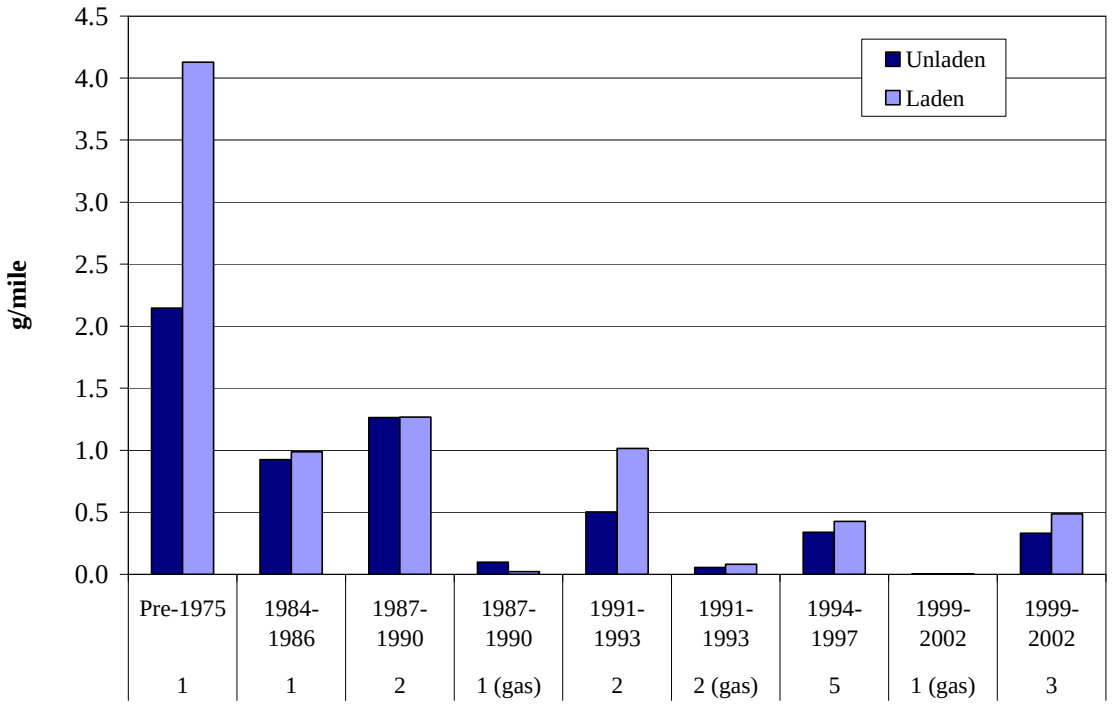

Figure 43: PM emissions for UDDS mode (both laden and unladen).

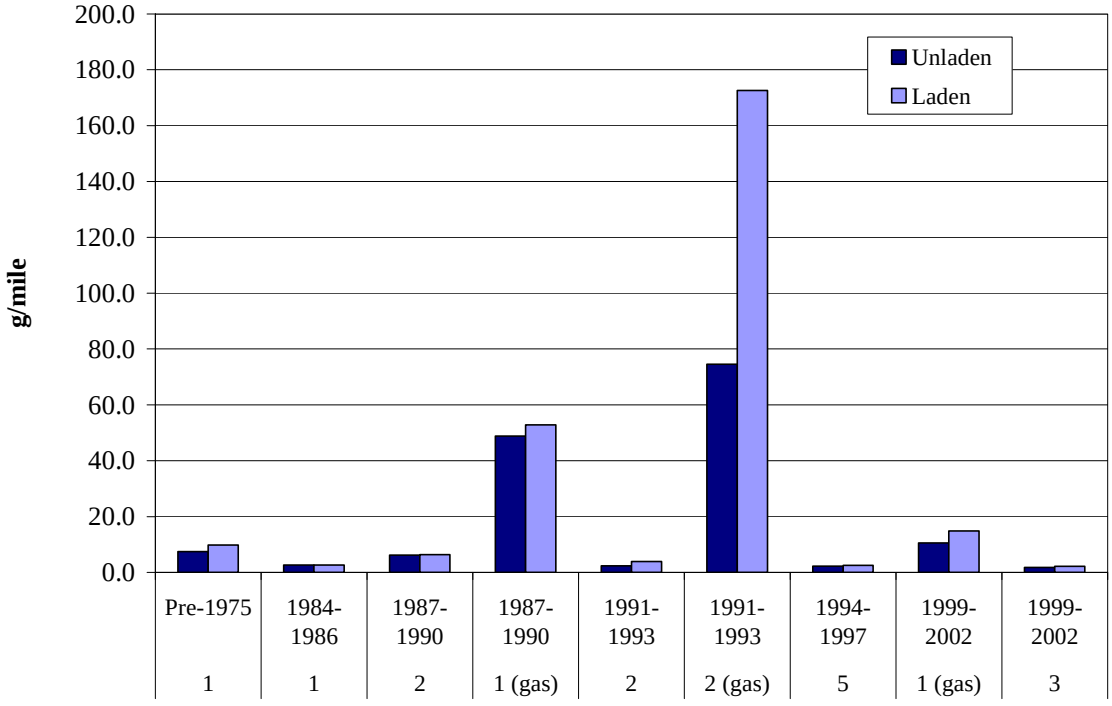

Figure 44: CO emissions for MHDTHI mode (both laden and unladen).

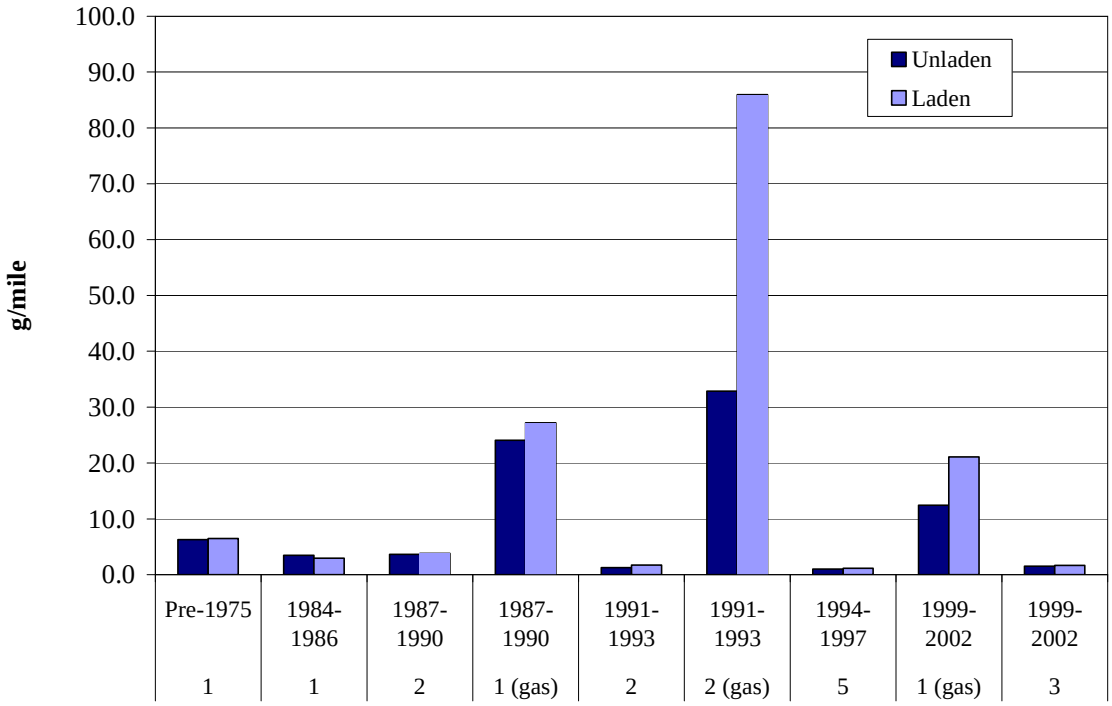

Figure 45: CO emissions for the MHDTCR mode (both laden and unladen).

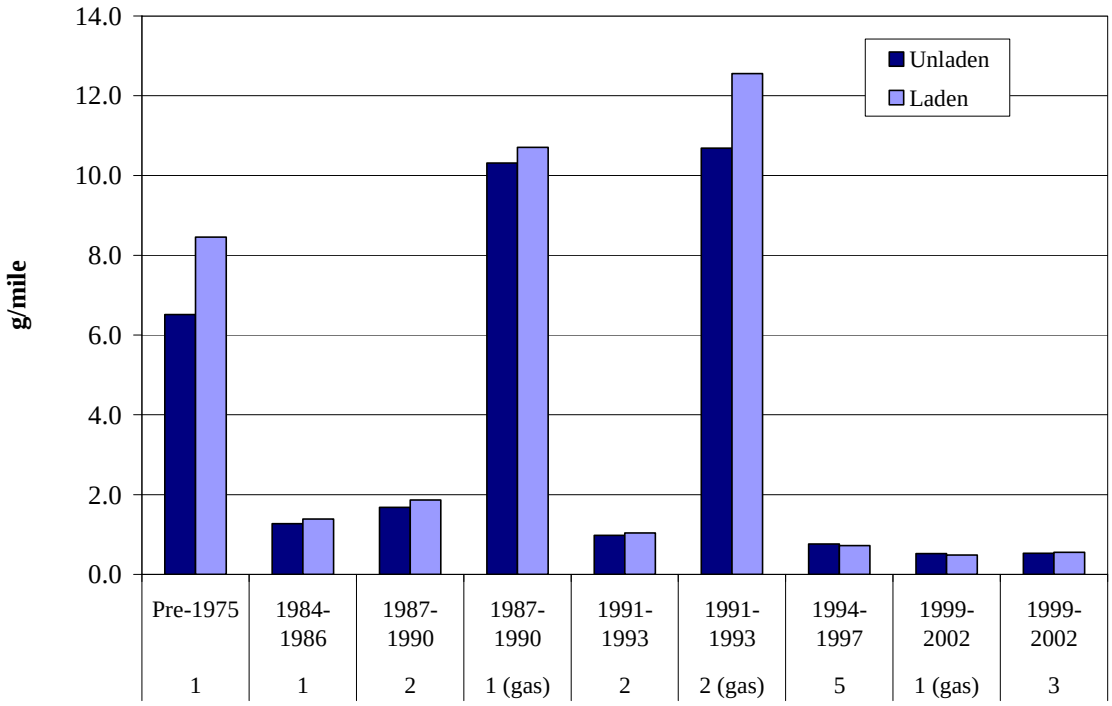

Figure 46: HC emissions for MHDTHI mode (both laden and unladen).

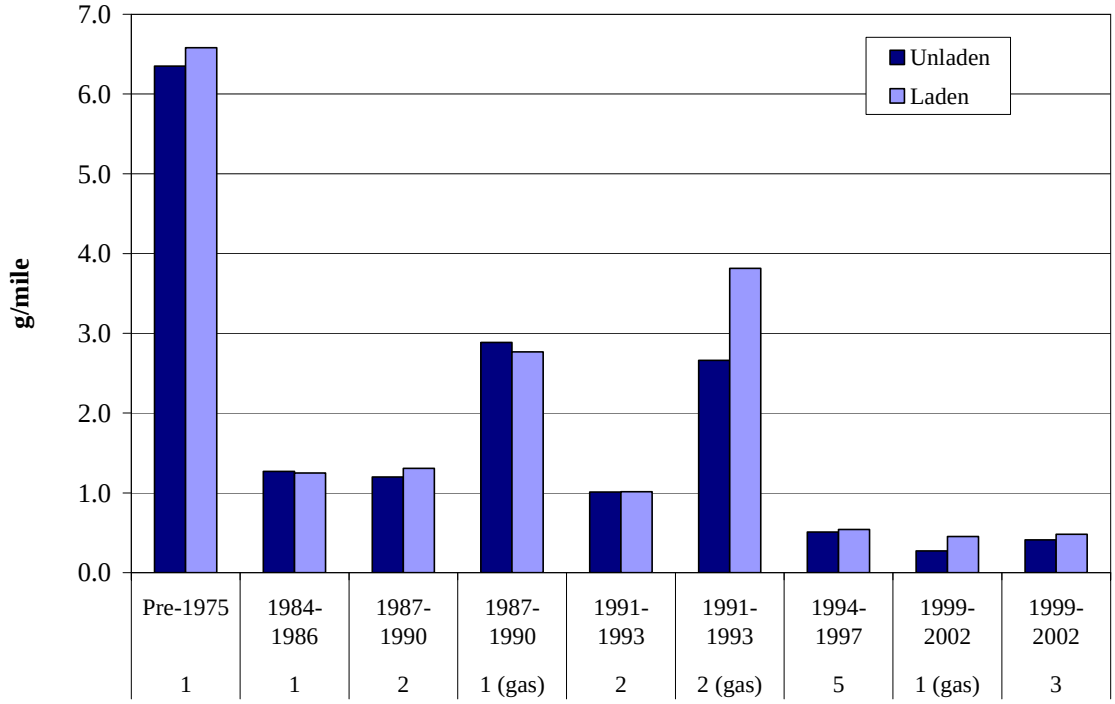

Figure 47: HC emissions for MHDTCR mode (both laden and unladen).

Figure 46 and Figure 47 present HC emissions for the MHDT on the Higher Speed Transient and the MHDT Cruise modes. The oldest MHDDT produced substantially higher emissions of HC than the remaining MHDDT on the MHDT Cruise mode. The newest MHDGT produced no more HC on cruise than the diesel truck of similar MY. Additional plots for MHDT emissions on other modes and cycles are presented in Appendix M.

Continuous Data

All dynamometer speeds and torques, all regulated gaseous emissions, exhaust and tunnel temperatures, and TEOM data are available on a continuous basis. These data are available to the sponsors separately from this report. Figure 48, Figure 49, and Figure 50 present examples of continuous NO_x, HC and CO emissions from E55CRC-42 on the Transient mode at 56,000 lbs. test weight and Figure 51 shows the exhaust temperature of this vehicle.

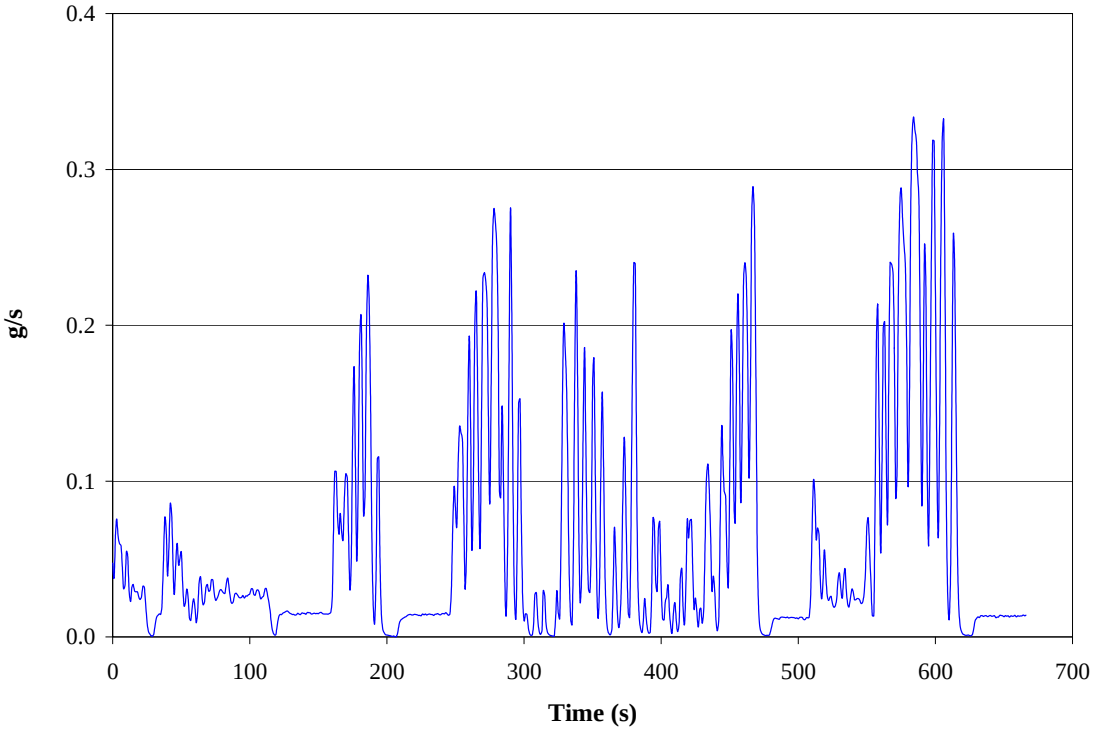

Figure 48: Example of a continuous NO_x emissions plot in g/s for E55CRC-42 (56,000 lbs.) following the HHDDT Transient Mode.

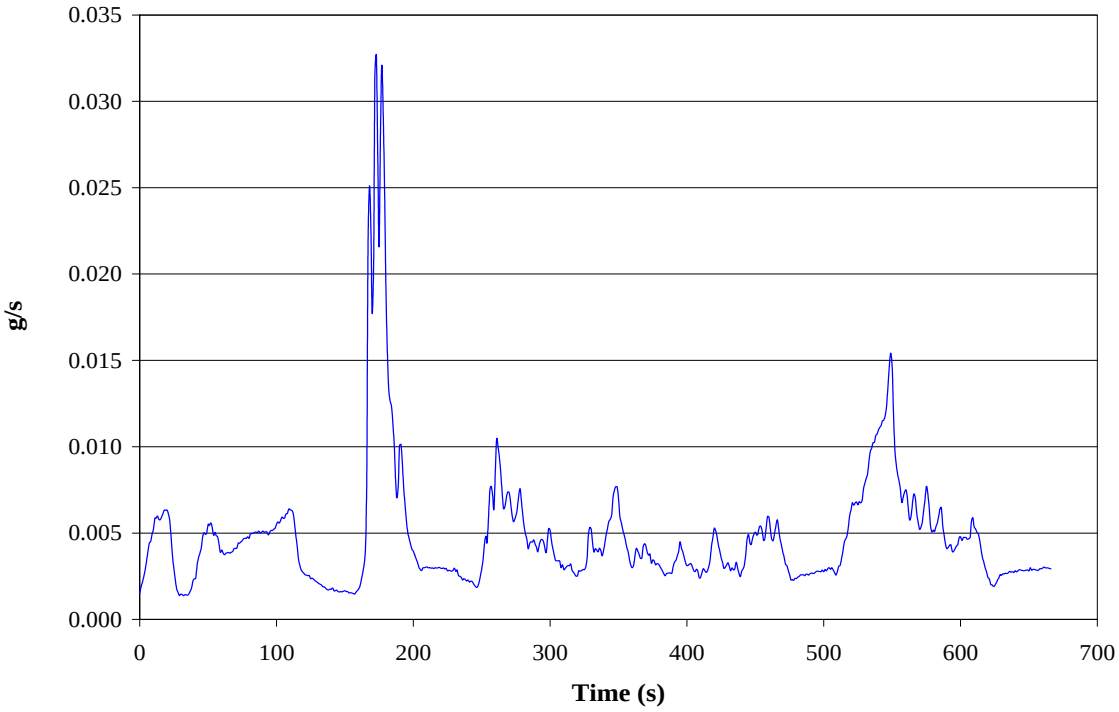

Figure 49: Example of a continuous HC emissions plot in g/s for E55CRC-42 (56,000 lbs.) following the HHDDT Transient Mode.

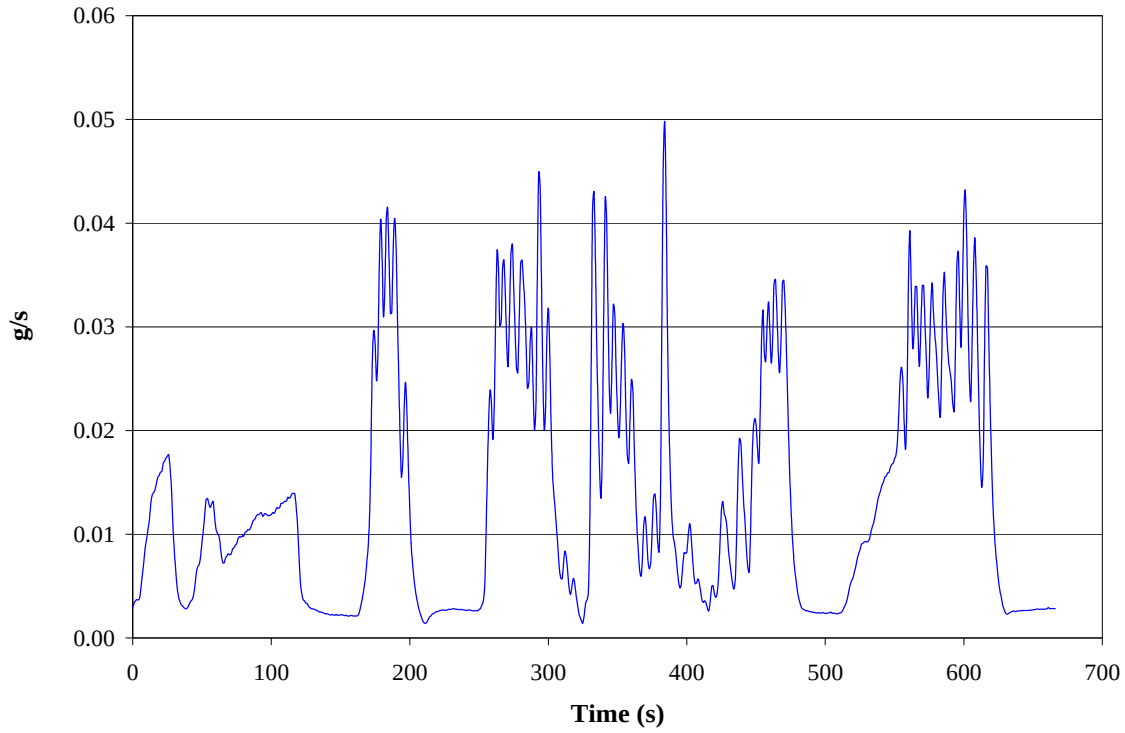

Figure 50: Example of a continuous CO emissions plot in g/s for E55CRC-42 (56,000 lbs.) following the HHDDT Transient Mode.

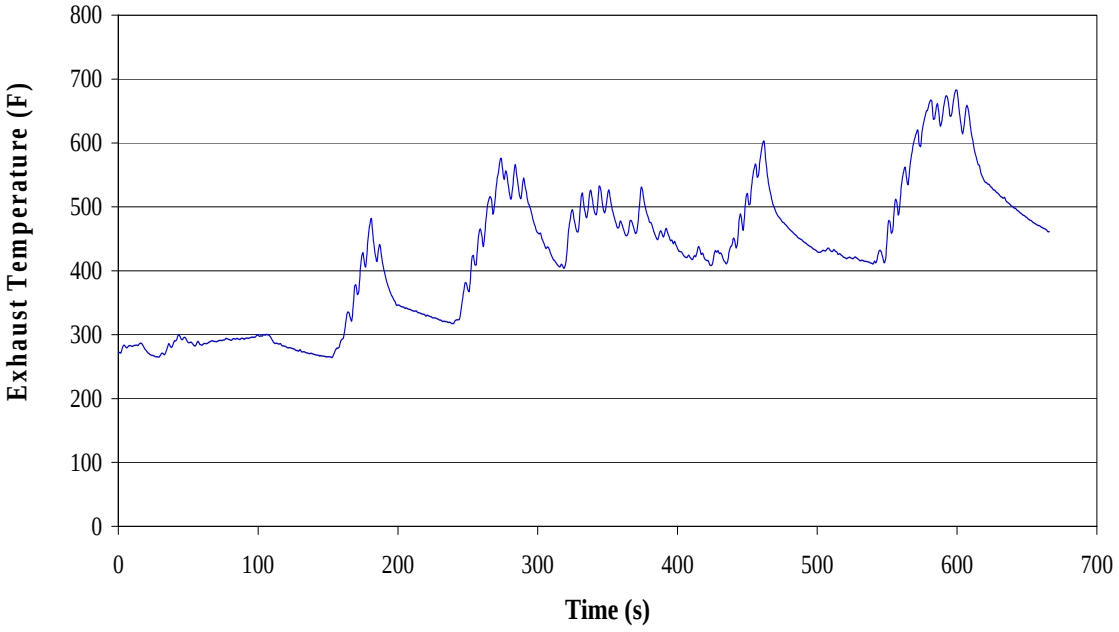

Figure 51: Example of a continuous exhaust temperature reading for E55CRC-42 (56,000 lbs.) following the Transient mode schedule.

HHDDT Effect of Test Weight

HHDDT data have been provided above only for the 56,000 lbs. test weight, which was used for all trucks. Data for fleet subsets tested at 30,000 lbs. and 66,000 lbs. appear in Appendix N. Figure 52, Figure 53, Figure 54 and Figure 55 show the effect of test weight for Transient and Cruise modes, for PM and NO_x, for all trucks that were tested at all three weights. NO_x rose in all cases as the weight rose from 30,000 to 56,000 lbs., but in a few cases, NO_x was lower when the weight was increased to 66,000 lbs. This may be ascribed to variability in injection timing over the engine map, and to different gear selection at the higher weight.

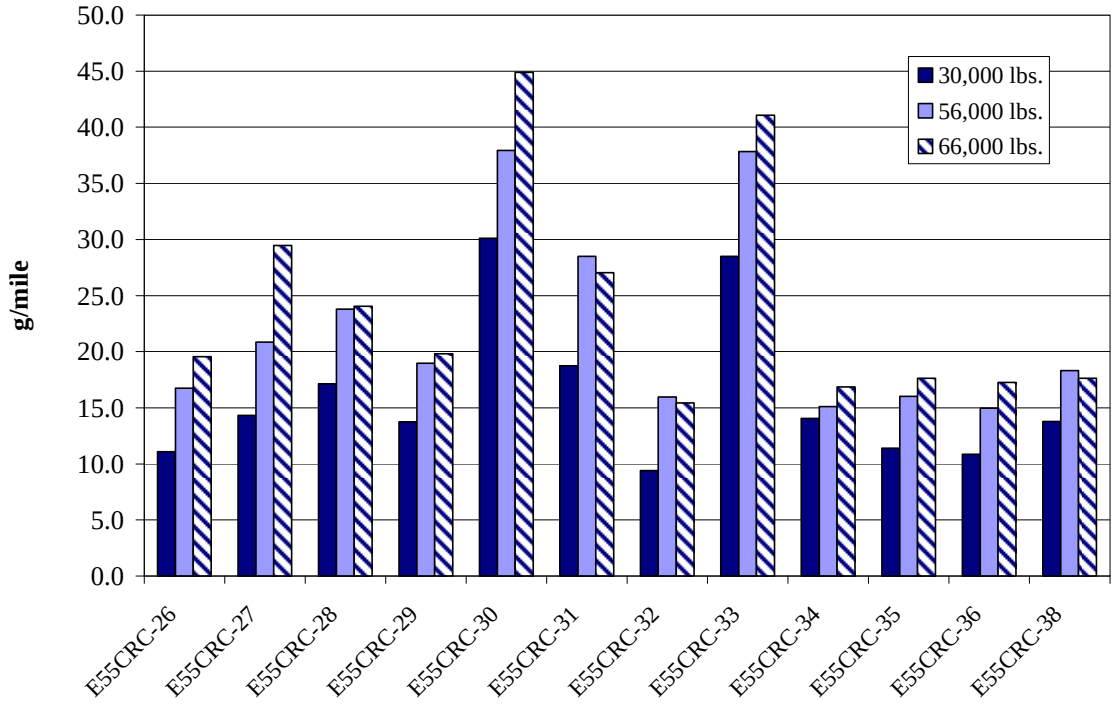

Figure 52: Transient mode NO_x weight effects

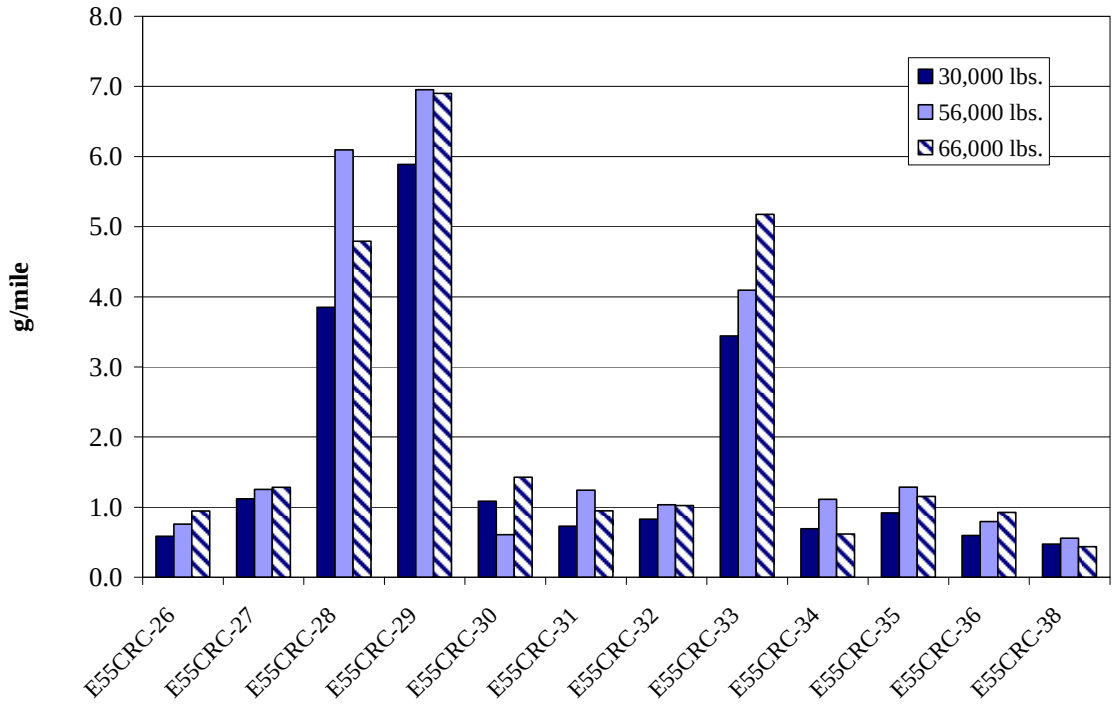

Figure 53: Transient mode PM weight effect

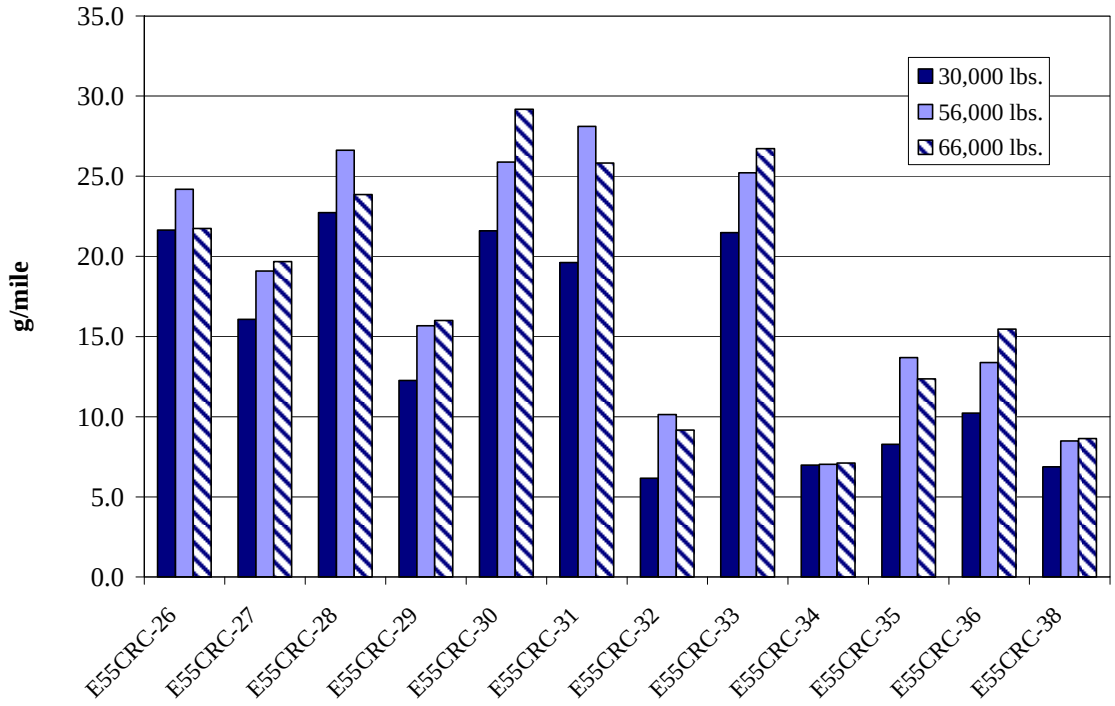

Figure 54: Cruise mode NO_x weight effect

For PM, the weight effect was far less clear. No simple conclusions can be presented except that PM rose as test weight was raised from 30,000 to 56,000 lbs. for almost all cases for the Transient mode.

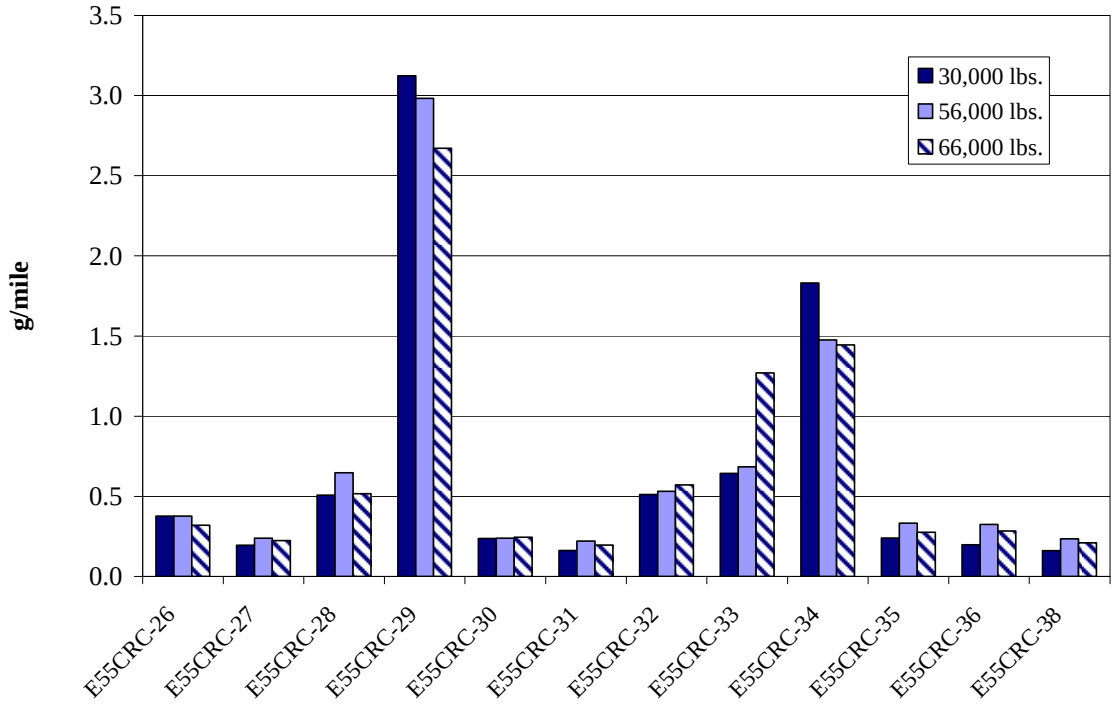

Figure 55: Cruise mode PM weight effect

MHDT Effect of Test Weight

Figure 34 and Figure 35 in the section above provide a partial view of the effect of test weight on NO_x emissions. While there were substantial truck-to-truck variations, the average effect of weight across the MHDT fleet was a rise in NO_x of 9% for the Higher Speed Transient mode and 8% for the cruise mode as the weight increased from 50 percent to 75 percent of the GVWR. The research effort to establish the MHDT schedule[3] found, in agreement with the present study, that effect of weight on NO_x was smaller than previously established for HHDDT. The average effect on PM seen in Figure 40 and Figure 41 indicated an increase of 50% for the Higher Speed Transient mode and 47% for the MHDT Cruise mode as weight was increased from unladen to laden.

COMPARISON OF DATA BETWEEN PHASES

Data for the same MY bins were compared between phases to assess phase to phase repeatability. Figure 56 shows data for CO_2 emissions, in units of g/mile, for all HHDDT operated through the UDDS at 56,000 lbs. test weight.

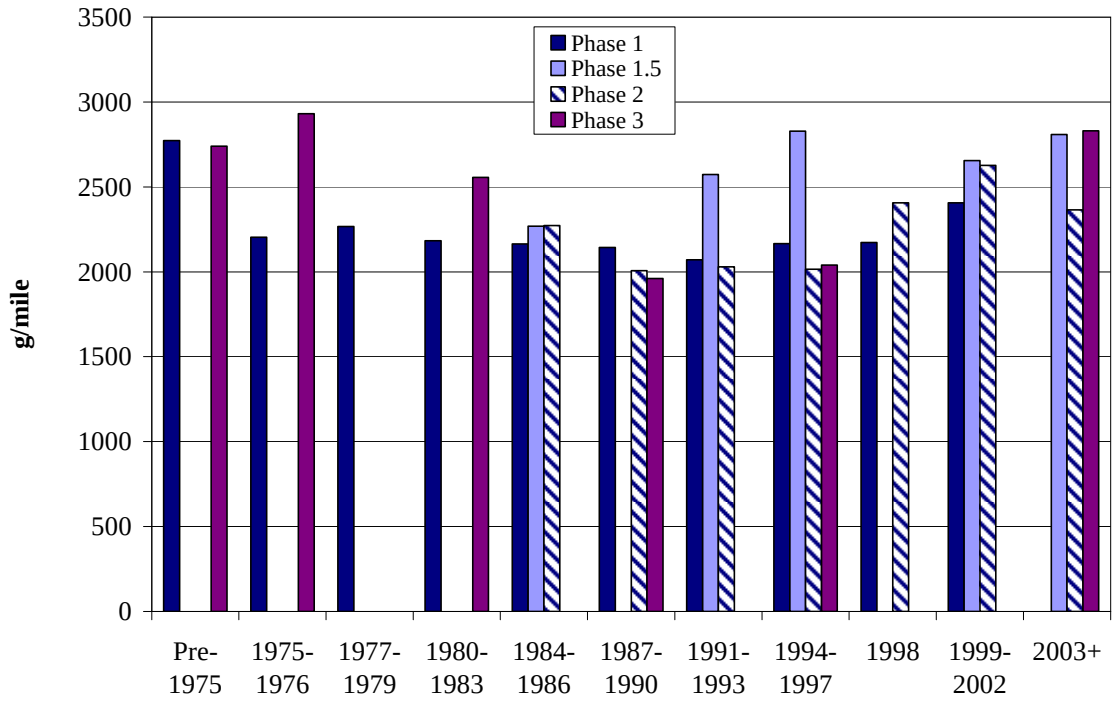

Figure 56: Variation of HHDDT CO_2 emissions by vehicle model year and by phase of the program for the UDDS (56,000 lbs.).

There is little variation in the CO_2 emissions values over MY or by phase, because CO_2 values are governed by the engine efficiency and cycle energy demands. (The standard deviation of the data below is 302 g/mile, approximately 13 percent of the average.) These data build confidence in the repeatability of data between phases, and suggest that both the dilution tunnel flowrate calibration and the CO_2 analyzer response remained consistent between phases. In contrast, Figure 57 shows that CO varied substantially within MY group. (The standard deviation of the data in Figure 57 is 8.7 g/mile, or 84% of the average.) Since CO is known to be a species that varies widely from truck to truck, this suggests that too few vehicles were selected in each phase to form a reliable opinion on average CO emissions for each MY bin. NO_x emissions are less variable over the fleet than CO emissions, as shown in Figure 58. However, Figure 58 still shows variation between phases. The NO_x data were guaranteed to have reasonable accuracy by employing two separate NO_x analyzers for most of the program. PM data also varied between phases, as shown in Figure 59. (The standard deviation of the data in Figure 59

is 9.7 g/mile, or 41% of the average.) A correspondence of Figure 57 and Figure 59 show a correspondence of high CO and PM by phase in sympathy with one another. Examples are the Phase 1.5 data in the 1999-2002 and 2003+ MY bins. One must conclude that the fleets in each individual phase were also too small for use in reaching conclusions on CO, NO_x or PM averages.

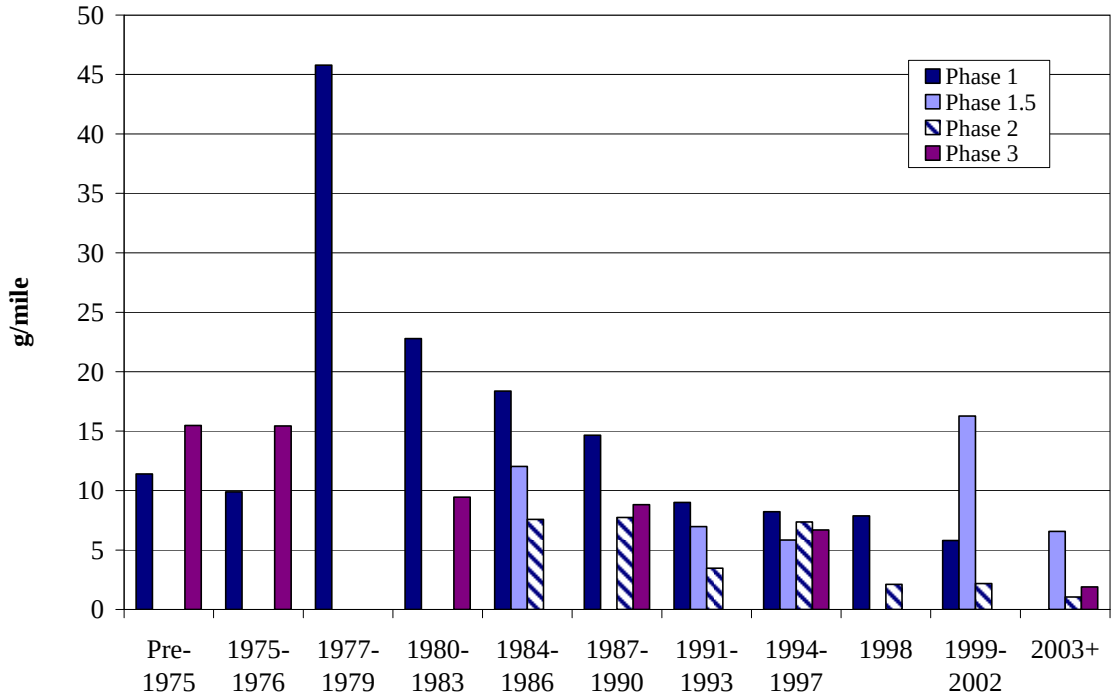

Figure 57: Variation of HHDDT CO emissions by vehicle model year and by phase of the program for the UDDS (56,000 lbs.).

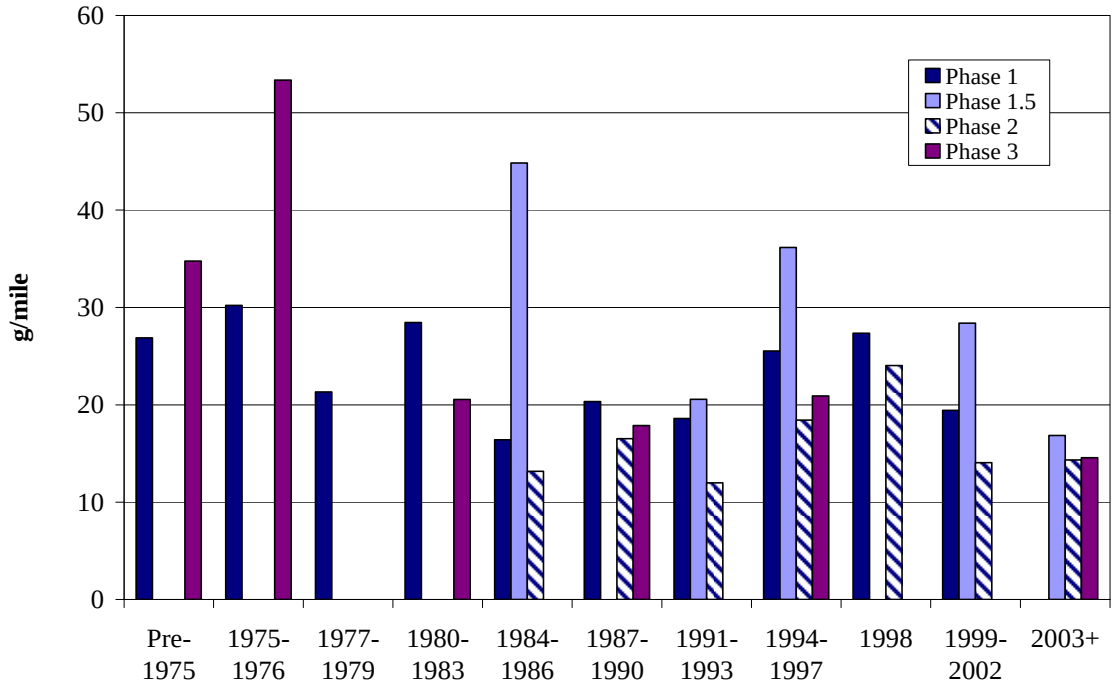

Figure 58: Variation of HHDDT oxides of NO_x by vehicle model year and by phase of the program for the UDDS (56,000 lbs.).

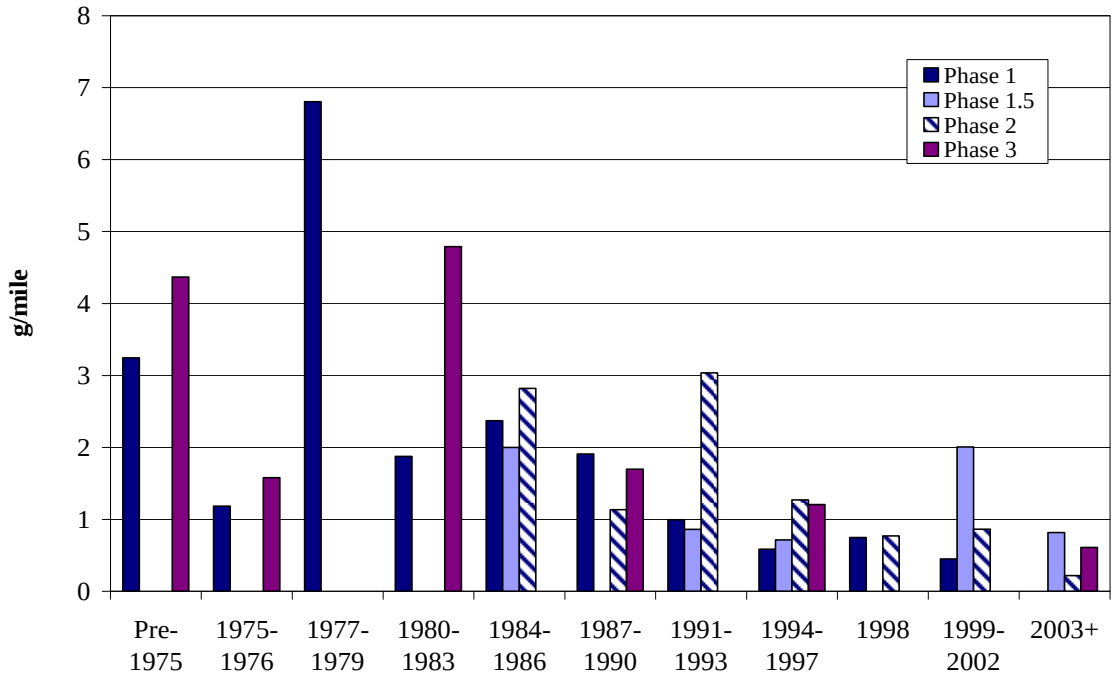

Figure 59: Variation of PM emissions by vehicle model year and by phase of the program for the UDDS (56,000 lbs.).

RESULTS AND DISCUSSION, NONREGULATED SPECIES

Semi-Volatile Organic Compounds

Exhaust Samples

Table 13 lists PAH, oxy-PAH, nitro-PAH, hopanes, steranes, organic acids and other compounds of interest (with their mnemonics) quantified for this study. The minimum detection limit (MDL) for PAH, oxy-PAH and other organic compounds was compound-dependent, and in general, in the range of 20-50 pg/μl. For nitro-PAH analyzed by negative ion CI method, the MDL was in the range of 1pg/μl.

Table 13: List of Target Analytes in the Particulate and Semi-Volatile Fractions.

Mnemonic	Compound	Mnemonic	Compound
Polycyclic Aromatic Hydrocarbons (PAH)and oxy-PAH			
NAPHTH	Naphthalene	ANTHONE	Anthrone
MNAPH2	2-methylnaphthalene	ANRQUONE	Anthraquinone
MNAPH1	1-methylnaphthalene	DM36PH	3,6-dimethylphenanthrene
BIPHEN	Biphenyl	A_DMPH	A-dimethylphenanthrene
ENAP12	1+2ethylnaphthalene	B_DMPH	B-dimethylphenanthrene
DMN267	2,6+2,7-dimethylnaphthalene	C_DMPH	C-dimethylphenanthrene
DM1367	1,3+1,6+1,7dimethylnaphth	DM17PH	1,7-dimethylphenanthrene
D14523	1,4+1,5+2,3-dimethylnaphth	D_DMPH	D-dimethylphenanthrene
DMN12	1,2-dimethylnaphthalene	E_DMPH	E-dimethylphenanthrene
M_2BPH	2-Methylbiphenyl	ANTHRA	Anthracene
M_3BPH	3-Methylbiphenyl	M_9ANT	9-methylanthracene
M_4BPH	4-Methylbiphenyl	FLUORA	Fluoranthene
DBZFUR	Dibenzofuran	PYRENE	Pyrene
ATMNAP	A-trimethylnaphthalene	ANTAL9	9-Anthraaldehyde
BTMNAP	B-trimethylnaphthalene	RETENE	Retene
CTMNAP	C-trimethylnaphthalene	BNTIOP	Benzonaphthothiophene
ETMNAP	E-trimethylnaphthalene	C1MFLPY	1-MeFl+C-MeFl/Py
FTMNAP	F-trimethylnaphthalene	BMPYFL	B-MePy/MeFl
TMI235N	2,3,5+I-trimethylnaphthalene	CMPYFL	C-MePy/MeFl
TM245N	2,4,5-trimethylnaphthalene	DMPYFL	D-MePy/MeFl
JTMNAP	J-trimethylnaphthalene	M_4PYR	4-methylpyrene
TM145N	1,4,5-trimethylnaphthalene	M_1PYR	1-methylpyrene
ACNAPY	Acenaphthylene	BZCPHEN	Benzo(c)phenanthrene
ACNAPE	Acenaphthene	BAANTH	Benz(a)anthracene
FLUORE	Fluorene	M_7BAA	7-methylbenz(a)anthracene
PHENAN	Phenanthrene	CHRYSN	Chrysene
A_MFLU	A-methylfluorene	BZANTHR	Benzanthrone
M_1FLU	1-methylfluorene	BAA7_12	Benz(a)anthracene-7,12-dione
B_MFLU	B-methylfluorene	CHRY56M	5+6-methylchrysene
FL9ONE	9-fluorenone	BBJKFL	Benzo(b+j+k)fluoranthene
XANONE	Xanthone	M_7BPY	7-methylbenzo(a)pyrene
ACQUONE	Acenaphthenequinone	BEPYRN	BeP
PNAPONE	Perinaphthenone	PERYLE	Perylene
A_MPHT	A-methylphenanthrene	BAPYRN	BaP

Mnemonic	Compound	Mnemonic	Compound
M_2PHT	2-methylphenanthrene	INCDPY	Indeno[123-cd]pyrene
B_MPHT	B-methylphenanthrene	BGHIPE	Benzo(ghi)perylene
C_MPHT	C-methylphenanthrene	DBANTH	Dibenzo(ah+ac)anthracene
M_1PHT	1-methylphenanthrene	CORONE	Coronene
Hopanes/Steranes			
STER35	20S-13ß(H),17a(H)-diasterane	STER52	20S5a(H),14ß(H),17ß(H)-stigmastane
STER36	20R-13ß(H),17a(H)-diasterane	HOP13	18a(H),21ß(H)-22,29,30-Trisnorhopane
STER37	20S-13a(H),17ß(H)-diasterane	HOP14	17a(H),18a(H),21ß(H)-25,28,30-Trisnorhopane
STER38	20R-13a(H),17ß(H)-diasterane	STER53	20R5a(H),14a(H),17a(H)-stigmastane
STER39	20S-13ß(H),17a(H)-diasterane	HOP15	17a(H),21ß(H)-22,29,30-Trisnorhopane
STER42	C27-20S5a(H),14a(H)-cholestane	HOP16	17a(H),18a(H),21ß(H)-28,30-Bisnorhopane
STER43	20R5a(H),14ß(H)-cholestane	HOP17	17a(H),21ß(H)-30-Norhopane
STER44	C27-20S5a(H),14ß(H),17ß(H)-cholestane	HOP18	18a(H),21ß(H)-30-Norneohopane
STER45_40	20R5a(H),14a(H),17a(H)-cholestane&C29-20S13ß(H),17a(H)-diasterane	HOP19	17a(H),21ß(H)-Hopane
STER46	20S5a(H),14a(H),17a(H)-ergostane	HOP20	17ß(H),21a(H)-hopane
STER47	20R5a(H),14ß(H),17ß(H)-ergostane	HOP21	22S-17a(H),21ß(H)-30-Homohopane
STER48	20S5a(H),14ß(H),17ß(H)-ergostane	HOP22	22R-17a(H),21ß(H)-30-Homohopane
STER41	20R-13a(H),17ß(H)-diasterane	HOP23	17ß(H),21ß(H)-Hopane
HOP9	C27-tetracyclic terpane	HOP24	22S-17a(H),21ß(H)-30,31-Bishomohopane
STER49	20R5a(H),14a(H),17a(H)-ergostane	HOP25	22R-17a(H),21ß(H)-30,31-Bishomohopane
HOP10	C27-tetracyclic terpane	HOP26	22S-17a(H),21ß(H)-30,31,32-Trisomohopane
HOP11	C28-tetracyclic terpane	HOP27	22R-17a(H),21ß(H)-30,31,32-Trishomohopane
STER50	20S5a(H),14a(H),17a(H)-stigmastane	STER51	20R5a(H),14ß(H),17ß(H)-stigmastane
HOP12	C28-tetracyclic terpane		
Polar Organic Compounds			
HEXAC	hexanoic acid	HEPDAC	heptanedioic (pimelic) acid
HEPTAC	heptanoic acid	ACVAN	acetovanillone
BENAC	benzoic acid	PHTHAC	phthalic acid
OCTANAC	octanoic acid	LEVG	levoglucosan
MALEAC	maleic acid	TDECAC	tridecanoic acid
SUCAC	succinic acid	ISPHAC	isophthalic acid
MEGUA4	4-me-guaiacol	AZEAC	azelaic acid
MESUCAC	me-succinic acid	MYRAC	myristic acid
NONAC	nonanoic acid	PDECAC	pentadecanoic acid
ETGUA4	4-ethyl-guaiacol	PALAC	palmitic acid
GUAC	glutaric acid	HEPTAD	heptadecanoic acid

Mnemonic	Compound	Mnemonic	Compound
SYRI	syringol	OLAC	oleic acid
DIMEB25	2,5-dimethylbenzoic acid	ELAC	elaidic acid
DIMEB24	2,4-dimethylbenzoic acid	STEAC	stearic acid
DIME235	2,3- and 3,5- dimethylbenzoic acid	NDECAC	nonadecanoic acid
DECAC	decanoic acid	DHABAC	dehydroabietic acid
ALGUAI4	4-allyl-guaiacol (eugenol)	ECOSAC	eicosanoic acid
MESYR4	4-methyl-syringol	ABAC	abietic acid
DIMEB34	3,4-dimethylbenzoic acid	HCOSAC	heneicosanoic acid
HEXDAC	hexanedioic (adipic) acid	DOCOSA	docosanoic acid
CPINAC	cis-pinonic acid	TRICOSA	tricosanoic acid
SALCYL	salcylic acid	TETRACO	tetracosanoic acid
FGUAI4	4-formyl-guaiacol (vanillin)	CHOL	cholesterol
UNDEC	undecanoic acid	BSIT	sitosterol
ISEUG	isoeugenol		
Alkanes and Cycloalkanes			
NOYCYHX	Nonylcyclohexane	EICOSA	Eicosane
HPYCYHX	Heptylcyclohexane	HENEIC	Heneicosane
OCYCYHX	Octylcyclohexane	DOCOSA	Docosane
NORFARN	Norfarnesane	TRICOSA	Tricosane
FARNES	Farnesane	DEC5YHX	Pentadecylcyclohexane
TEDRAD	Tetradecane	DEC6YHX	Hexadecylcyclohexane
PENTAD	Pentadecane	DEC7YHX	Heptadecylcyclohexane
HEXAD	Hexadecane_Norpristane	DEC8YHX	Octadecylcyclohexane
HEPTAD	Heptadecane_Pristane	DEC9YHX	Nonadecylcyclohexane
OCTAD	Octadecane	COSAN4	Tetracosane
NONAD	Nonadecane	COSAN5	Pentacosane
PHYTAN	Phytane	COSAN6	Hexacosane
DECYHX	Decylcyclohexane	COSAN7	Heptacosane
DEC1YHX	Undecylcyclohexane	CYHXEIC	Eicosylcyclohexane
DEC2YHX	Dodecylcyclohexane	CYHXHEN	Heneicosylcyclohexane
DEC3YHX	Tridecylcyclohexane	COSAN8	Octacosane
DEC4YHX	Tetradecylcyclohexane		
Nitro-PAH			
NI1NAPTH	1-nitronaphthalene	NI2FLUOR	2-nitrofluoranthene
NI2NAPTH	2-nitronaphthalene	NI3FLUOR	3-nitrofluoranthene
NI2BIPH	2-nitrobiphenyl	NI1PYRE	1-nitropyrene
NI3BIPH	3-nitrobiphenyl	NI27FLUO	2,7-dinitrofluorene
NI4BPH	4-nitrobiphenyl	NI27FL9ON	2,7-dinitrofluoren-9-one
NI13NAP	1,3-dinitronaphthalene	NI7BZANTH	7-nitrobenz(a)anthracene
NI15NAP	1,5-dinitronaphthalene	NI6CHRY	6-nitrochrysene
NI5ACEN	5-nitroacenaphthene	NI13PYR	1,3-dinitropyrene
NI9ANTHR	9-nitroanthracene	NI16PYR	1,6-dinitropyrene
NI4PHEN	4-nitrophenanthrene	NI18PYR	1,8-dinitropyrene
NI9PHEN	9-nitrophenanthrene	NI910ANTH	9,10-dinitroanthracene
NI3PHEN	3-nitrophenanthrene	NI6BAP	6-nitrobenz[a]pyrene
NI18NAP	1,8-dinitronaphthalene		

The data were delivered in electronic format in units of ng/m^3. No unusual events for this group of samples were noticed.

Fuel and Oil Samples

Six fuel and five oil samples were analyzed for PAH and hopanes/steranes. The data were presented in units of ug/ml and ug/g. Figure 60 shows the PAH concentrations in diesel fuel and oil. For simplicity, the methylated isomeric PAH were added together (i.e. dimethylnaphthalenes, trimethylnaphthalenes, etc). As seen from this figure, the lower molecular weight (MW) PAHs were much more abundant in diesel fuel than in the oil. Methylated PAH account for the majority of the PAH.

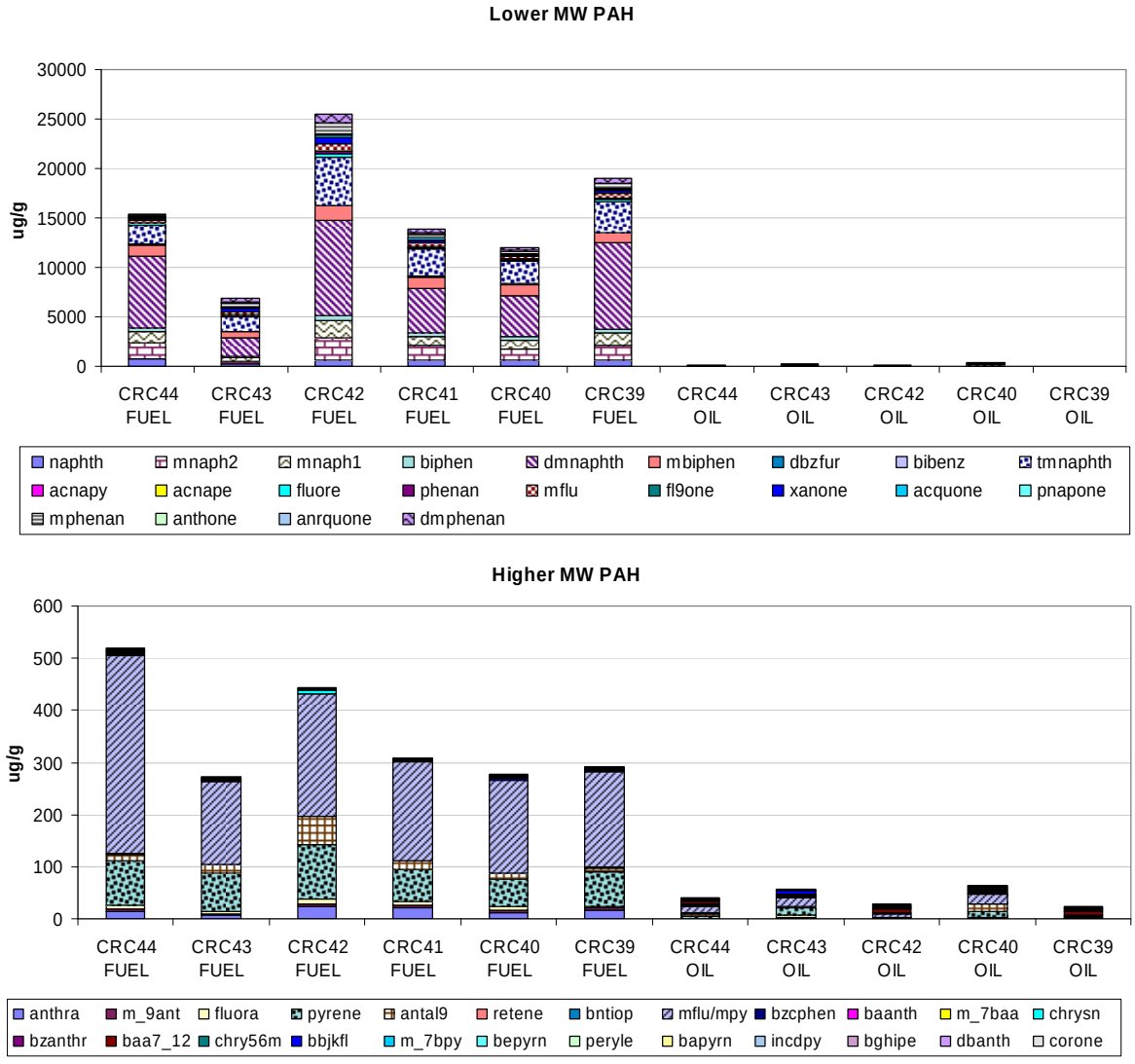

Figure 60: PAH in fuels and oils.

Volatile Organic Compounds

Canister Samples

Table 14 lists the compounds quantified on-site from the canister samples by the GC/MS method. The MDL was 0.1 ppbv for all compounds.

Table 14: List of Gas-phase Compounds Quantified by GC/MS Method from Canisters.

Mnemonic	Compound	Mnemonic	Compound
ethane	ethane	pa224m	2,2,4-trimethylpentane
ethene	ethene	n_hept	n-heptane
acetyl	acetylene	p2e23m	2,3-dimethyl-2-pentene
lpropa	propane	t13dcp	t-1,3-dichloropropene
lprope	propene	mecyhx	methylcyclohexane
lpropy	propyne	pa234m	2,3,4-trimethylpentane
ibuta	iso-butane	tolue	toluene
but1e_ibute	1-butene + isobutene	hx23dm	2,3-dimethylhexane
bud13	1,3-butadiene	hep2me	2-methylheptane
butan	n-butane	hep4me	4-methylheptane
t2but	t-2-butene	hep3me	3-methylheptane
c2but	c-2-butene	hex225	2,2,5-trimethylhexane
bud12	1,2-butadiene	n_oct	n-octane
ipent	iso-pentane	etbz	ethylbenzene
pente1	1-pentene	mp_xyl	m/p-xylene
b1e2m	2-methyl-1-butene	oct3me	3-methyloctane
n_pent	n-pentane	styr	styrene
i_pren	isoprene	o_xyl	o-xylene
t2pene	t-2-pentene	n_non	n-nonane
c2pene	c-2-pentene	iprbz	i-propylbenzene
b2e2m	2-methyl-2-butene	ipcyhex	isopropylcyclohexane
bu22dm	2,2-dimethylbutane	a_pine	alpha-pinene
cpente	cyclopentene	n_prbz	propylbenzene
cpenta	cyclopentane	m_etol	3-ethyltoluene
bu23dm	2,3-dimethylbutane	p_etol	4-ethyltoluene
pena2m	2-methylpentane	bz135m	1,3,5-trimethylbenzene
pena3m	3-methylpentane	o_etol	2-ethyltoluene
p1e2me	2-methyl-1-pentene	b_pine	beta-pinene
n_hex	n-hexane	bz124m_tbutbz	1,2,4-trimethylbenzene+t-butylbenzene
t2hexe	t-2-hexene	n_dec	n-decane
p2e2me	2-methyl-2-pentene	bz123m	1,2,3-trimethylbenzene
p2e3mt	3-methyl-2-pentene	limon	limonene
c2hexe	c-2-hexene	indan	indan
p2e3mc	cis-3-methyl-2-pentene	detbz13	1,3-diethylbenzene
hxdi13	1,3-hexadiene (trans)	detbz14	1,4-diethylbenzene
mcypna	methylcyclopentane	n_bubz	butylbenzene
pen24m	2,4-dimethylpentane	prtol	propyltoluene
cpene1	cyclopentene	iprtol	isopropyltoluene

Mnemonic	Compound	Mnemonic	Compound
benze	benzene	n_unde	n-undecane
cyhexa	cyclohexane	bz1245	1,2,4,5-tetramethylbenzene
hexa2m	2-methylhexane	bz1235	1,2,3,5-tetramethylbenzene
pen23m	2,3-dimethylpentane	ind_2m	2-methylindan
hexa3m	3-methylhexane	ind_1m	1-methylindan
cyhexe	cyclohexene		
cpa13m	1,3-dimethylcyclopentane (cis)		
hep1e	1-heptene		

After the first dynamic system background run, a very high acetone peak that obscured the iso-pentane peak was noticed. This peak persisted for a few subsequent runs but gradually diminished. The system (i.e. dilution tunnel and all sampling lines) was flushed overnight with ambient air on January 13, and the peak was nearly gone. Unfortunately it reappeared again on January 21. In addition, some other peaks identified as n-pentane, n-hexane, and 2-methyl-1-pentene were unusually high for some runs. Clearly, this appears to be a contamination with some solvent, or mixture of solvents, but the origin of the contamination was not determined.

Carbonyl Compounds

Table 15 lists the carbonyl compounds collected on DNPH cartridges and quantified by the HPLC method. The MDL for carbonyl compounds was approximately 0.1 ppbv.

Table 15: List of Target Analytes in the Gas-Phase Carbonyl Compound Fraction

Mnemonic	Compound
FORMAL	Formaldehyde
ACETAL	Acetaldehyde
ACETO	Acetone
ACROLN	Acrolein
PROAL	Propionaldehyde
CROTON	Crotonaldehyde
MEK	Methyl ethyl ketone
MACROL	Methacrolein
BUTAL	Butyraldehyde
BENZAL	Benzaldehyde
GLYOXL	Glyoxal
VALAL	Valeraldehyde
TOLUAL	M-tolualdehyde
HEXAL	Hexanaldehyde

The acetone contamination is clearly visible in these samples as well. Figure 61 shows the concentrations of carbonyl compounds (in ppbv) measured during various runs (shown in chronological sequence).

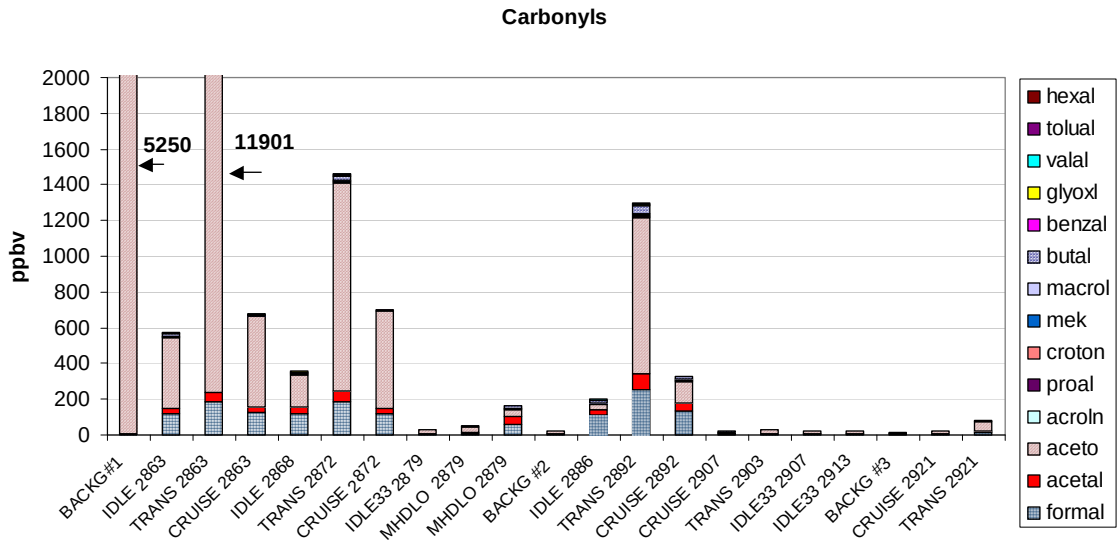

Figure 61: Concentrations of carbonyl compounds (in ppbv) measured during the runs.

For the cycles with sequence numbers 2886 (combining two idle33) and 2892 (six runs including a pair of Transient modes, Cruise modes, and HHDDT_S modes respectively), back-up cartridges were used to check for breakthrough. In general, the breakthrough was negligible.

Nitrosoamines

Table 16 shows the nitrosoamines measured for this program.

Table 16: Nitrosoamines Targeted for Analysis in the Vehicle Exhaust

Compound Name Nitrosoamines	**LQL [a] (µg/sample)**
n-nitrosomorpholine	0.01
n-nitrosodiethylamine	0.01
n-nitrosodimethylamine	0.01
n-nitrosodibutylamine	0.01
n-nitrosopyrolidine	0.01

The concentrations of nitrosoamines in the exhaust were low, close to the MDL. It should be noted that due to the sampling on the same Thermosorb cartridge over all cycles from the individual vehicle, any invalidated run was also sampled on the same cartridge. Three samples out of the six collected have invalidated runs sampled on the cartridge: samples collected on 01/09/04, 01/16/04, and 1/28-1/30/04.

Tenax Samples

Table 17 lists compounds quantified from Tenax cartridges. The MDL for these compounds was in the range of 0.1 ppbv per sample.

Table 17: List of Heavy Hydrocarbons for Tenax Samples

Mnemonic	Compound	Mnemonic	Compound
HEPAL	Heptanal	IPRXYL_5	5-isopropyl-m-xylene
N_NON	Nonane	BZ1245	1,2,4,5-tetramethylbenzene
IPRBZ	Isopropylbenzene	BZ1235	1,2,3,5-tetramethylbenzene
N_PRBZ	Propylbenzene	IAMBZ	Isoamylbenzene
M_ETOL	m-ethyltoluene	IND_2M	2-methylindan
P_ETOL	p-ethyltoluene	IND_1M	1-methylindan
BZ135M	1,3,5-trimethylbenzene	BZ1234	1,2,3,4-tetramethylbenzene
PHENOL	Phenol	DIPRB_13	1,3-diisopropylbenzene
O_ETOL	o-ethyltoluene	C5BZ_3	Pentylbenzene
FURBZ	2,3-benzofuran	THNAPH	1,2,3,4-tetrahydronaphthalene
FURPEN	2-pentylfuran	DHNAPH	1,2-dihydronaphthalene
T_BUBZ	t-butylbenzene	DIPRB_14	1,4-diisopropylbenzene
OCTAL	Octanal	NAPHTH	Naphthalene
BZ124M	1,2,4-trimethylbenzene	INDDMA	A-dimethylindane
MESTYR	4-methylstyrene	INDDMB	B-dimethylindane
MPCBZ	1,3-dichlorobenzene	INDDMC	C-dimethylindane
DEC1E	1-decene	INDDMD	D-dimethylindan
I_BUBZ	Isobutylbenzene	DECONE2	2-decanone
N_DEC	Decane	DECAL	Decanal
S_BUBZ	Sec-butylbenzene	DODE1E	Dodecene
BZ123M	1,2,3-trimethylbenzene	N_DODE	Dodecane
M_IPRTOL	m-isopropyltoluene	PMEBZ	Pentamethylbenzene
P_IPRTOL	p-isopropyltoluene	NAP_2M	2-methylnaphthalene
ODCBZ	1,2-dichlorobenzene	NAP_1M	1-methylnaphthalene
INDAN	Indan	N_TRID	Tridecane
INDENE	Indene	BIPHEN	Biphenyl
O_IPRTOL	o-isopropyltoluene	ENAP12	1+2-ethylnaphthalene
O_MEPHOL	o-methylphenol	DMN267	2,6+2,7-dimethylnaphthalene
DETBZ1	1,3-diethylbenzene	N_TETD	Tetradecane
M_TOLALD	m-tolualdehyde	DM1367	1,6+1,3+1,7-dimethylnaphthalene
TOL4PR	4-n-propyltoluene + 1,4-diethylbenzene	D14523	2,3+1,5+1,4-dimethylnaphthalene
BUTBZ	Butylbenzene	ACENAP	Acenaphthylene
M_XYLET5	5-ethyl-m-xylene	DMN12	1,2-dimethylnaphthalene
DETBZ3	1,2-diethylbenzene	ACENPE	Acenaphthene
MP_MEPHO	m/p-methylphenol	N_PEND	Pentadecane
TOL2PR	2-n-propyltoluene	FLUORE	Fluorene
P_XYLET2	2-ethyl-p-xylene	N_HEXD	Hexadecane
O_XYLET4	4-ethyl-o-xylene	N_HEPD	Heptadecane
TBUTOL_4	4-tert-butyltoluene	PHENA	Phenanthrene
NONAL	Nonanal	N_OCTD	Octadecane
UNDE1E	1-undecene	N_NOND	Nonadecane

Mnemonic	Compound	Mnemonic	Compound
FUBZ2ME	2-methylbenzofuran	N_EICO	Eicosane
N_UNDE	Undecane		

Since Tenax samples cannot be combined for analyses, each replicate run was analyzed separately. Nine samples were invalidated due to problems with the B sampling channel and damage to some of the A cartridges during transport. These samples are shown in Table 18.

Table 18: Damaged Tenax Samples.

Cycle	Test ID	Test Run ID
Cruise3	2863	09
Cruise3	3863	10
MHDTLO	2879	06
MHDTLO	2879	07
MHDTCR	2879	08
MHDTCR	2879	09
Idle33	2907	03
Idle33	2913	01
Idle33	2913	02
Trans3	2921	01
Cruise3	2921	05
Cruise3	2921	06

SPECIATION AND SIZING RESULTS

This section discusses exhaust particle size distributions (SMPS and DMS500) and chemical speciation results for five heavy heavy-duty diesel trucks operating on various modes of the California HHDDT cycle. Particle size distribution results from the SMPS were corrected for dilution ratios. Since dilution ratio on the main tunnel was not accurately known, DMS500 data presented in this report are for dilute flow in the main CVS tunnel. The raw uncorrected results obtained from DRI's analytical laboratory for chemical speciation were presented in ng/m^3. All speciation data were reduced by correcting for flow rates in the sampling system. The mass values for chemical speciation were found using the equation

g/cycle of chemical species= (Vtunnel* Speciated sample in ng/ m^3)/ 1.00E+09.

Vtunnel = Vmix + Total PM volume + PM_{10} volume + DRI volume (m^3).

Vmix was the total integrated volume sampled from the venturi for a particular cycle. Total PM volume was the integrated volume sampled from the secondary dilution tunnel for a particular cycle. PM_{10} volume was the integrated volume sampled from the PM_{10} cyclone for a particular cycle. DRI operated three $PM_{2.5}$ cyclones at 113 lpm each; e.g., 0.34 m^3/min total. To obtain the total DRI sample volume, 0.34 m^3/min was multiplied by the sample time. The PM_{10} and DRI flows were small with respect to tunnel flow.

Chemical speciation results are usually reported in g/mile, but since Idle mode was also considered for comparison purposes, all speciation data are presented in g/hour. Only for chemical speciation, both the Cruise Modes were integrated and results reflect the combination of both the normal and High-speed Cruise Modes.

The data are depicted as "Tunnel Background" and "Test, Uncorrected" to illustrate the magnitude of reductions, while being mindful of the role the tunnel background plays when the primary emissions are so low.

Results presented for chemical speciation were not corrected for background values, which is a departure from regulatory compliance reporting, and is different from the treatment of regulatory emissions presented in this report. Background data are provided separately. There are two barriers to representing data with background correction. First, the exhaust dilution ratio in the main CVS was not known. The background correction for regulated species was performed using a dilution factor, prescribed in the Code of Federal Regulations (CFR), and this factor is not equal to the ratio. Second, background levels of each species are known to vary with time, so that accurate quantitative correction is not possible without parallel sampling trains. Finally, the role played by the tunnel background, and tunnel history effects in speciation results is an unknown.

E55CRC-39

E55CRC-39 was powered with a Cummins ISX 530 MY 2004 engine. Particle sizing and chemical speciation results are presented below for various modes of the HHDDT schedule. Figure 62 and Figure 63 present the SMPS particle size distribution for Idle and steady modes.

A very distinct clear bimodal distribution was noted for the Idle mode with a nuclei mode in the particle size range of 18 nm and an accumulation mode of 157 nm with concentrations in the range of $3.5x10^5$ and $1.5x10^5$, respectively. The nuclei mode formation is attributed to low engine load at Idle conditions. Exhaust temperatures are low under idling conditions, which lead to formation of higher levels of volatile organic compounds.

These volatile compounds are usually in the gas phase in the tailpipe. As the exhaust is diluted and cooled in the atmosphere or the dilution system, these volatile compounds may either adsorb the nucleated sulfuric acid and/or undergo homogenous nucleation to form particles. Some semi-volatile particles adsorb onto existing soot particles and increase their size and these particles are measured as the agglomeration mode particles. Nuclei mode particles do not contribute much towards Idle mass emissions as seen in Figure 64, but their number concentrations are high.

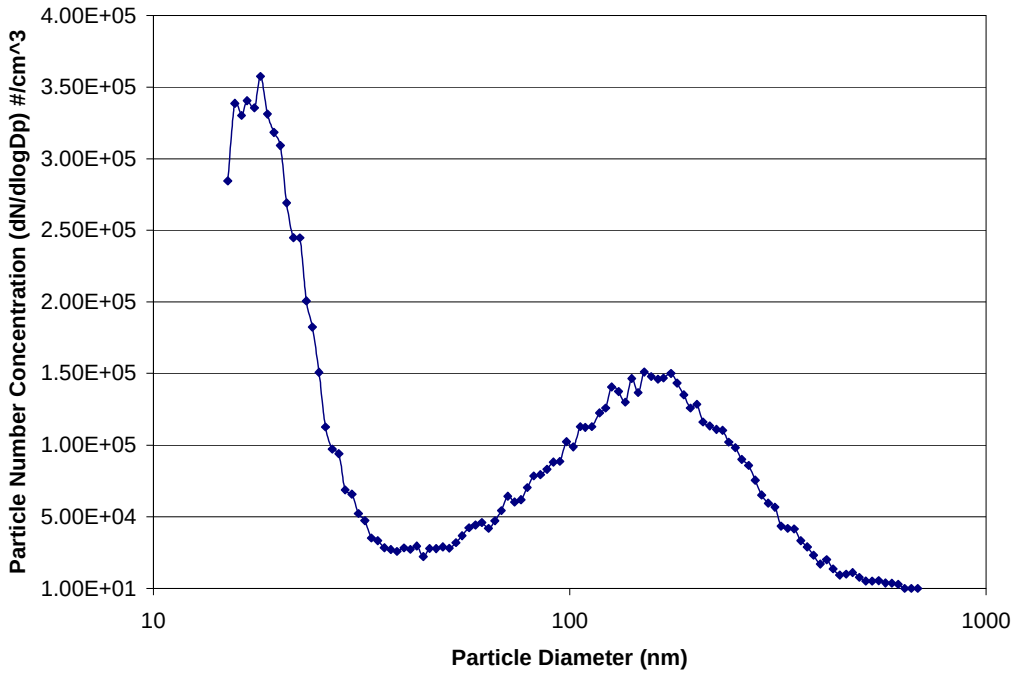

Figure 62: SMPS Particle Size Distribution for E55CRC-39 Operating on an Idle Mode

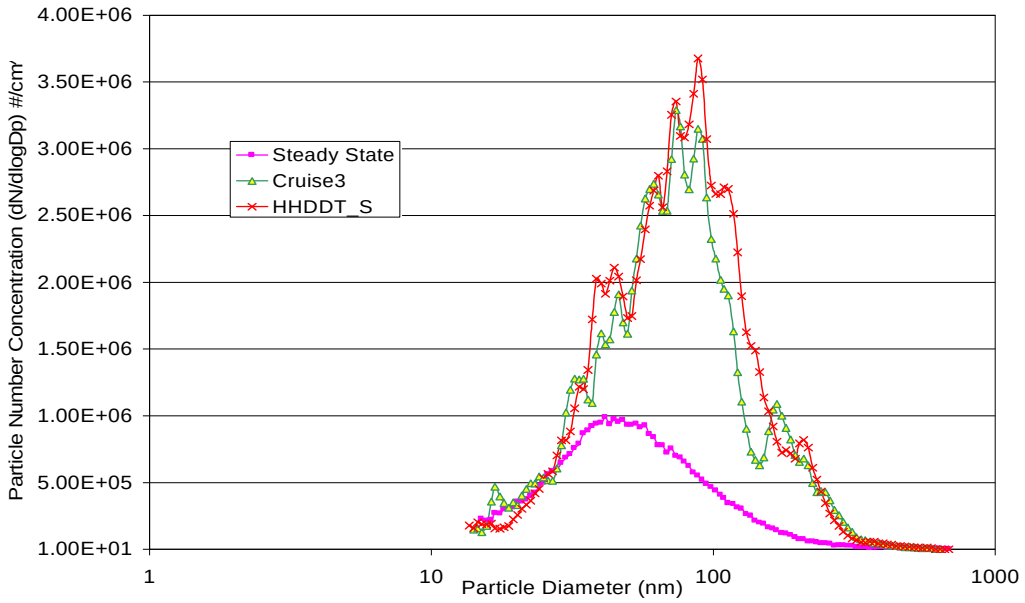

Figure 63: SMPS Particle Size Distribution for E55CRC-39 Operating on Various Steady Cycles

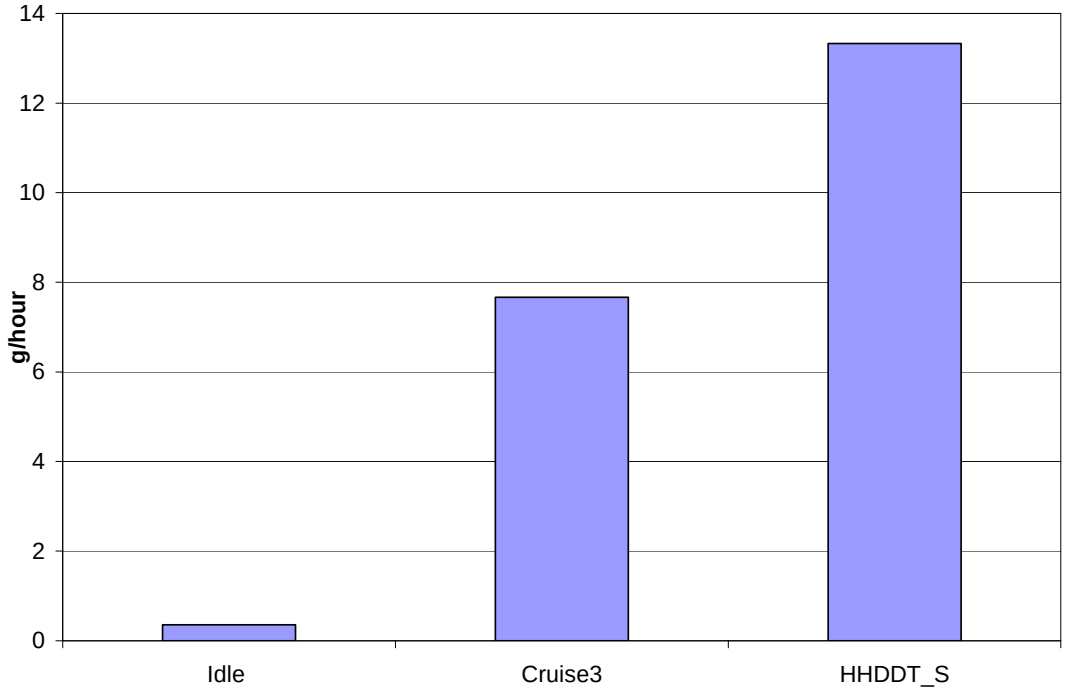

Figure 64: PM Mass Emissions for E55CRC-39

Chemical speciation of exhaust from E55CRC-39 showed that volatile organic compound emissions were very high in the Idle mode at 0.68 g/hour when compared to the Cruise mode at 0.21g/hour (Appendix O: Figure O1 to O5). In the semi-volatile group, polar compound emissions for the Cruise mode were very similar to Idle mode emissions

(Appendix O: Figure O9). The elemental carbon emissions for the Cruise mode were very high at 8.3 g/hour when compared with the Idle mode at 0.21 g/hour (Figure 66). At idle, the volatile compounds experience lower temperatures after being emitted or in the tail pipe. The saturation ratios (partial pressure/saturation pressure) are also higher in light of the fact that elemental carbon is present in very low quantities; hence, idle operation PM emissions are driven by the lower exhaust temperatures and higher saturation ratios. The lower concentration of elemental carbon contributes to nucleation of nano-particle formation. These analyses clearly indicate that, for this vehicle, the nano-particles or nuclei mode particles which are measured during the Idle Mode, are mostly made up of volatile compounds. The heavier organic species undergo condensation onto the hetro-molecular complex of water, sulfuric acid and lubricating oil based nano-sized ash particles. For the steady state mode at 40 kmph (25mph), the Count Median Diameter (CMD) of the particle size distribution was 48.89 nm with a maximum concentration level of $1x10^6$ particles/cm^3. For the High-speed Cruise and normal Cruise Mode, the particle size distribution was very similar with a CMD of 75.91 and 71.84 nm, respectively. The concentration levels for the Cruise Modes were almost twice that of the steady state mode and almost ten times that of the Idle Mode.

The geometric standard deviation (GSD) for the steady state, Cruise and High-speed Cruise Modes were 1.83, 1.84 and 1.79, respectively. The geometric standard deviation represents the distance of shift from the mean of the whole distribution. GSD values close to 1.8 represent a good distribution about the mean for diesel exhaust. For the Idle mode the GSD was 2.9 which indicates that the distribution was skewed and this can also be inferred from Figure 62. The shift towards a higher particle size in the Cruise Modes was likely due to a higher concentration of carbonaceous agglomerates in the exhaust, which also tend to suppress nano-particle formation (see Figure 63). Sulfate emissions were almost 20 times higher in the Cruise mode than in the Idle mode (Figure 66). Acetone emissions were unusually high for the Transient mode at 212.4 g/hour (Appendix O: Figure O11).

On a mass basis, the contribution of nitro-PAH and hopanes & steranes compounds (Appendix O: Figure O8 and O10) were not significant. Sulfates along with semi-volatile and carbonyl compounds usually adsorb onto carbon particles and form a cluster-like structure which increases the size of the particles, and the size spectrum is shifted towards the larger accumulation mode which is evident from Figure 63. These analyses show that accumulation mode particles formed during the Cruise mode are mostly made up of semi-volatile compounds with a solid carbonaceous core.

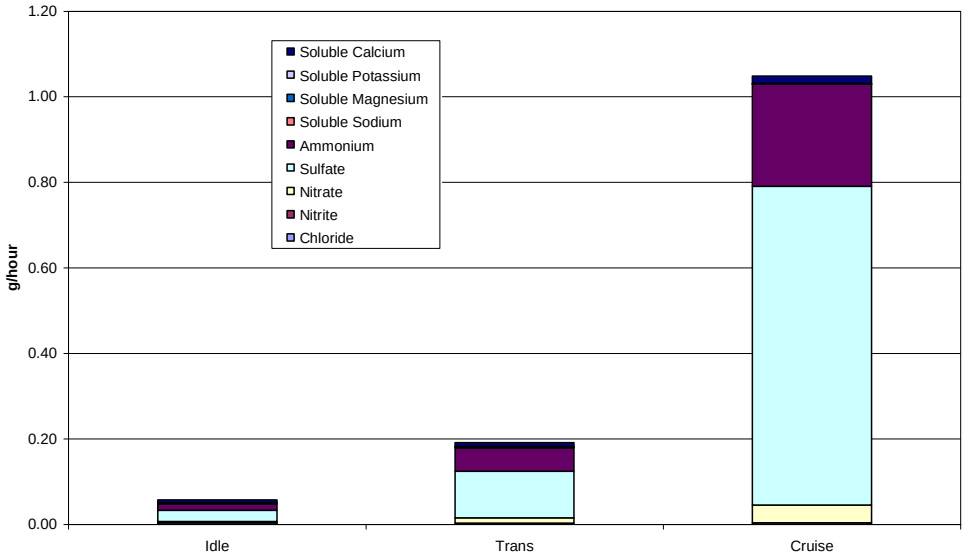

Figure 65: Ion Composite Results for E55CRC- 39

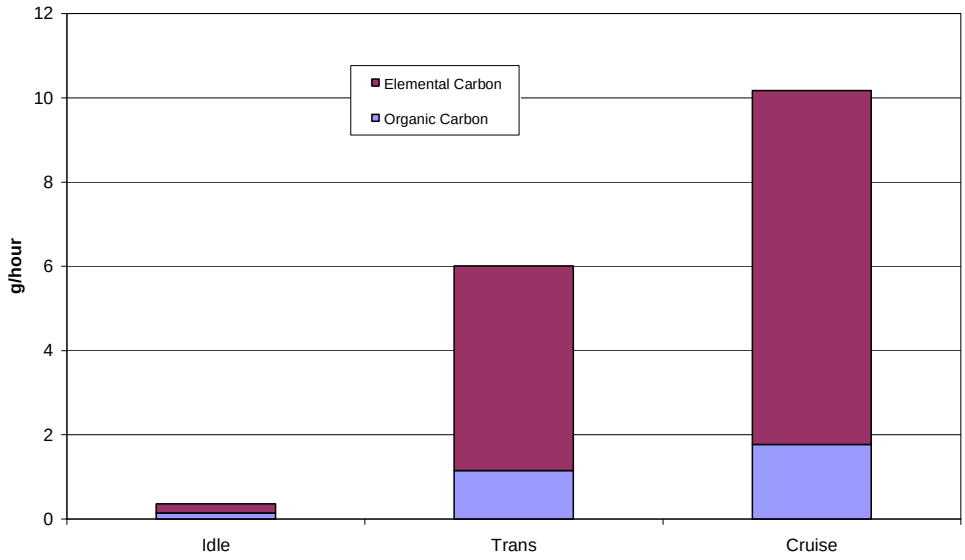

Figure 66: Elemental Carbon and Organic Carbon PM Analysis for E55CRC-39

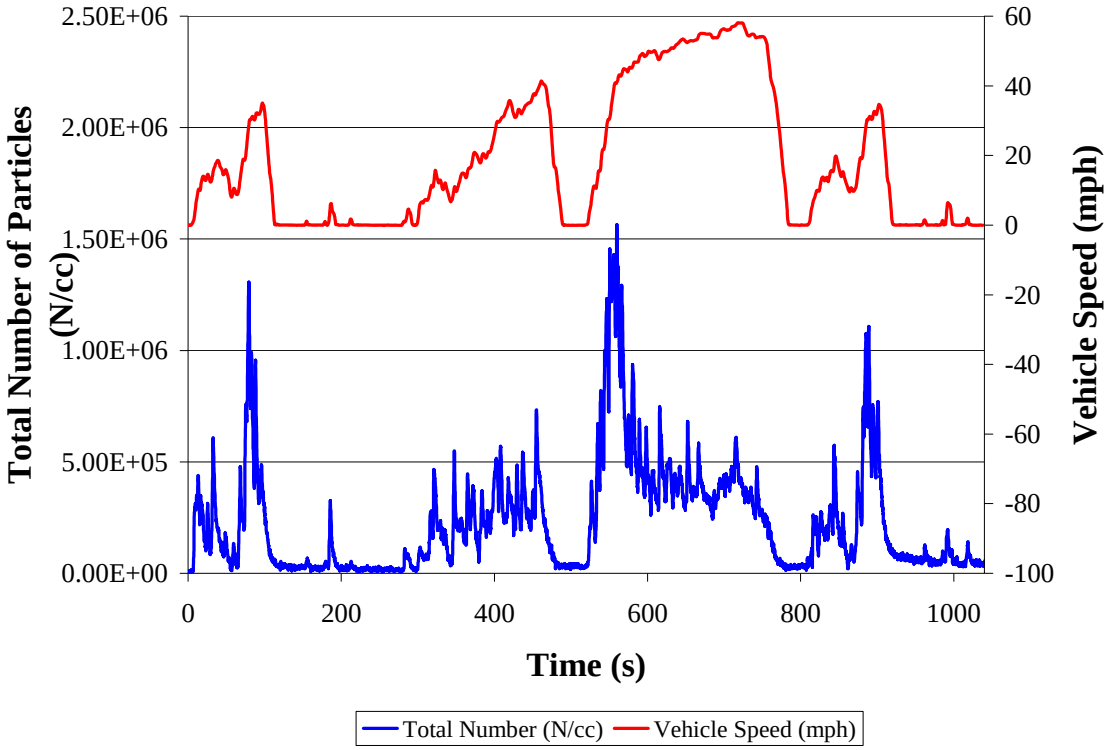

Figure 67: DMS500 Total Number of Particles and Vehicle Speed vs. Time during the UDDS for E55CRC-39 tested at 56,000 lbs.

Comprehensive DMS500 data are available for E55CRC-39. Figure 67 shows the total number of particles and vehicle speed versus time during the UDDS for E55CRC-39. The total number goes as high as $1.5x10^6$ particles/cm^3 during steep accelerations and goes down to $1.5x10^4$ during idle conditions. There is no strong correlation between the total number and engine speed, but as can be observed from Figure 67, during accelerations, the total number was high and when the high speed was continued for a period, the total number started to drop, e.g., between t = 600 and 700s. During decelerations, the total number dropped to a minimum and continued that way during the idle period.

Figure 68 shows the total number of particles and engine power versus time. Figure 69 shows the distribution of the total number concentration of particles in the 60 and 20 nm bins versus time. The 60 nm bin contains particles of diameters between approximately 55 and 65 nm, and the diameters for the 20 nm bin range between 17.5 and 22.5 nm. As can be observed from the plot, the overall number of 60 nm particles, which represent the accumulation mode particles, are almost an order of magnitude higher than the total number of particles in the 20 nm bin. Figure 70 shows the total number of particles in the 60 nm bin versus the total number of particles in the 20 nm bin. There is a much sharper increase in the total number of particles in the 20 nm bin during decelerations and a sharper increase in the total number of particles in the 60 nm bin during accelerations. As can be seen, there is no clear correlation between the two size bins.

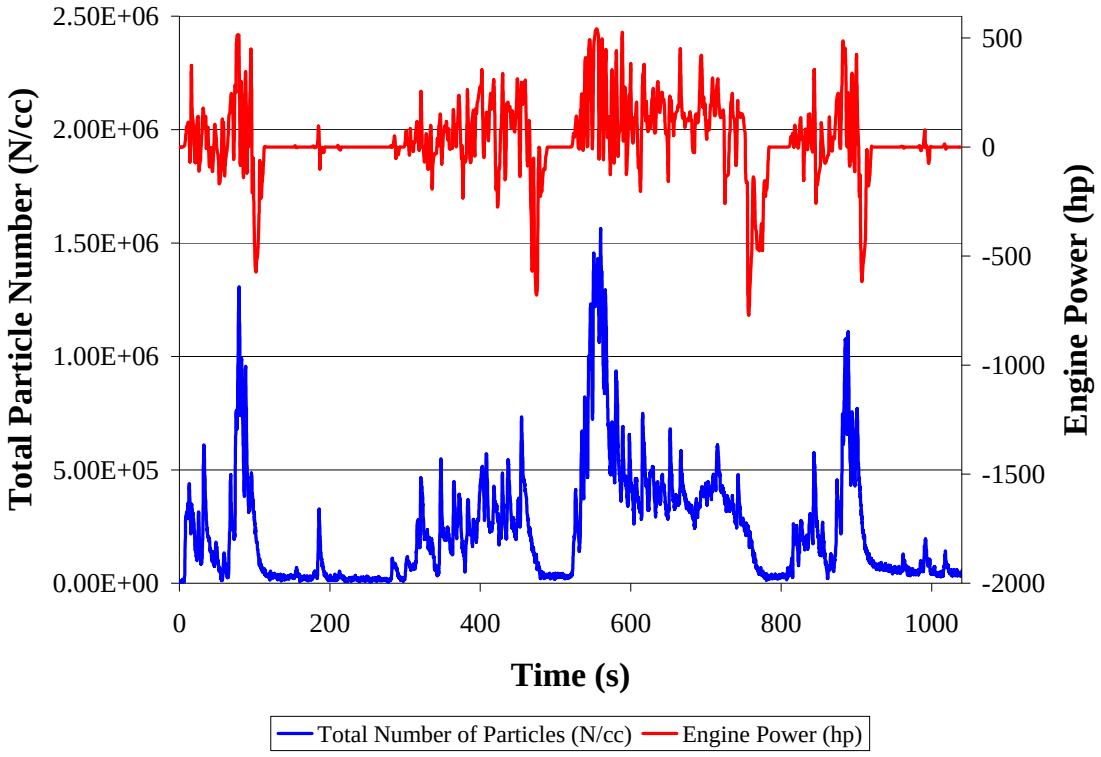

Figure 68: DMS500 Total Number of Particles and Engine Power vs. Time during the UDDS for E55CRC-39 tested at 56,000 lbs.

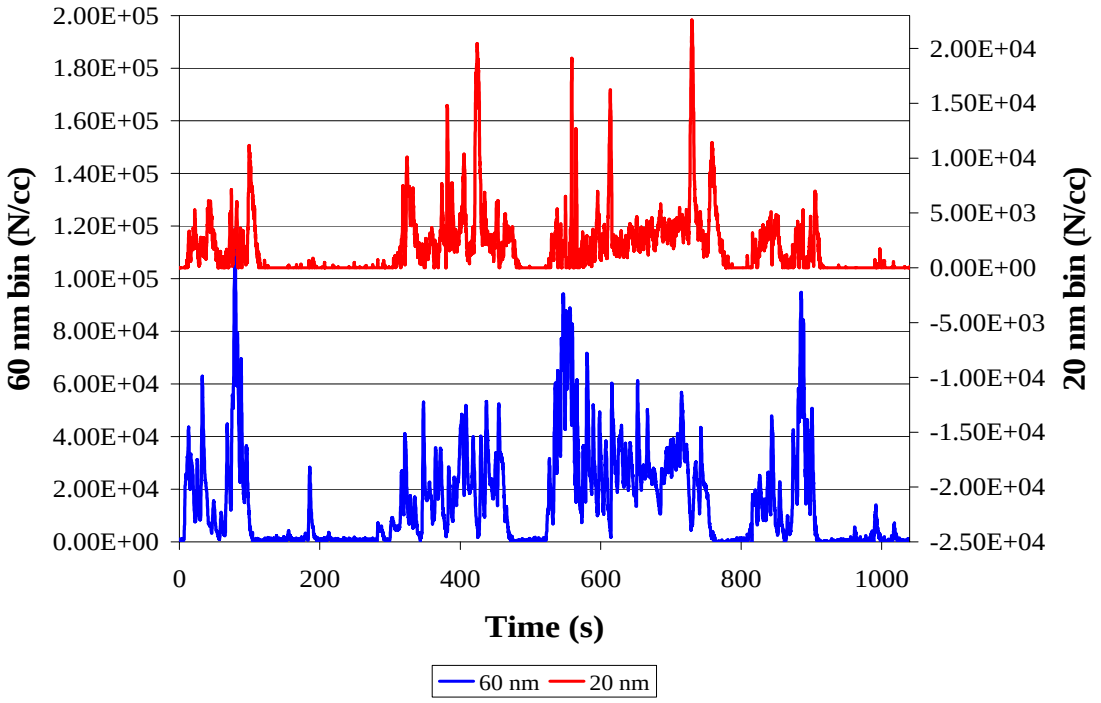

Figure 69: DMS500 60 nm and 20 nm Particle Number vs. Time during the UDDS for E55CRC-39 tested at 56,000 lbs.

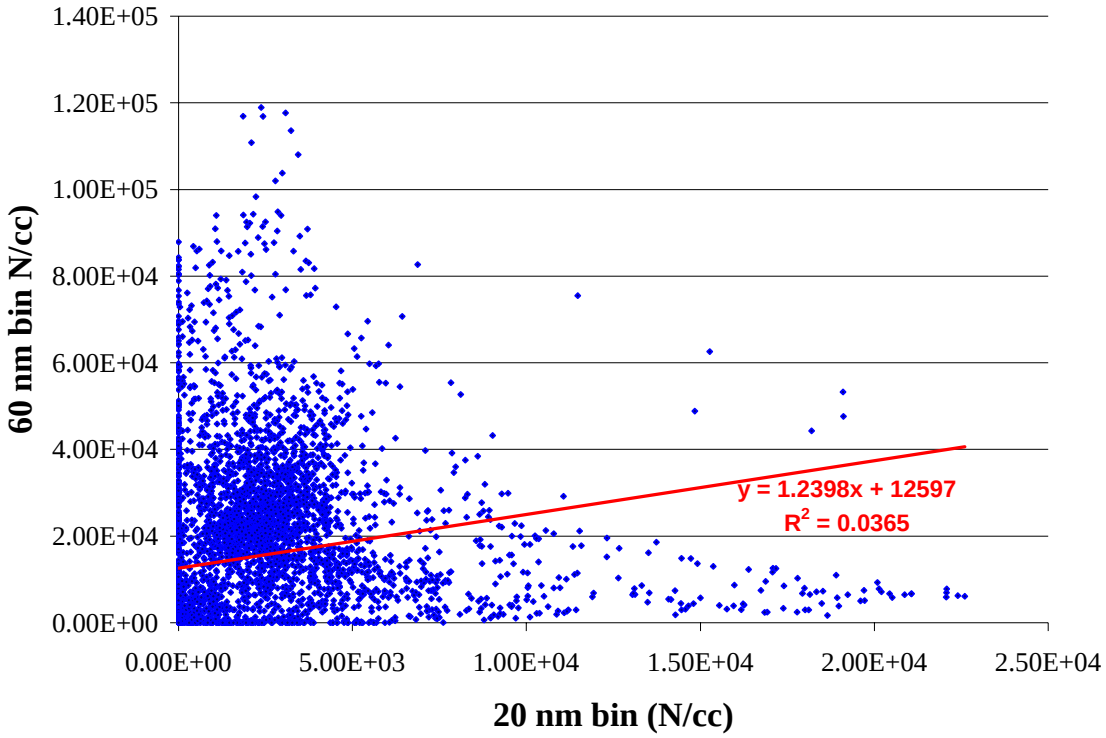

Figure 70: DMS500 60 nm Particle Number vs. 20 nm Particle Number during the UDDS for E55CRC-39 tested at 56,000 lbs.

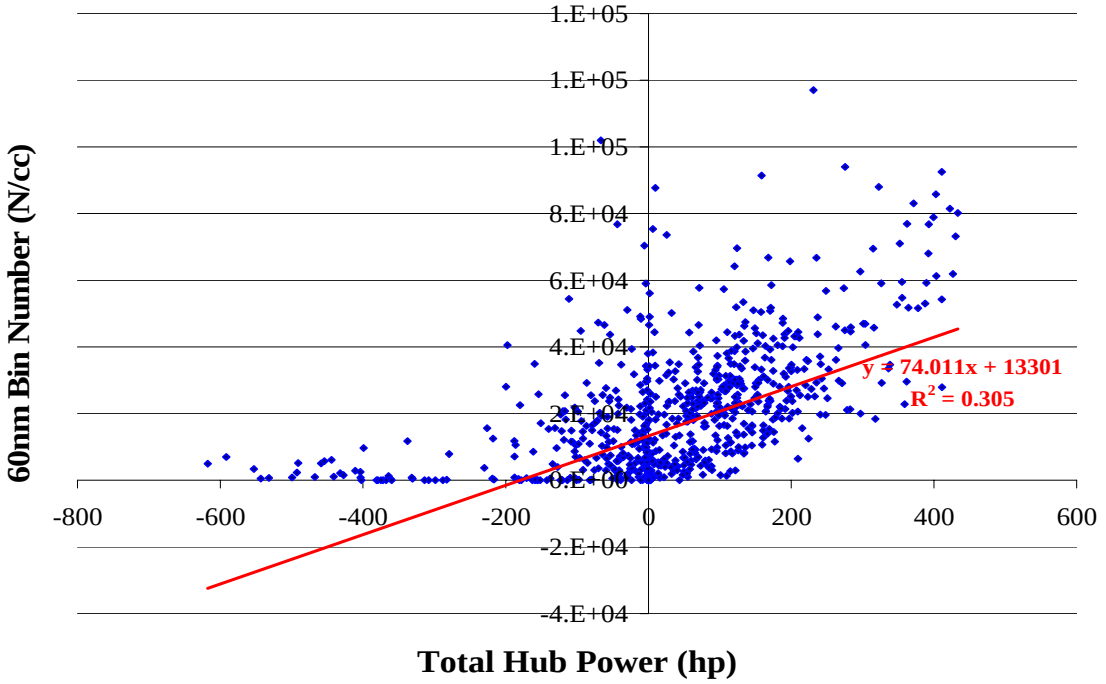

Figure 71: DMS500 60 nm Particle Number vs. Total Hub Power during the UDDS for E55CRC-39 tested at 56,000 lbs.

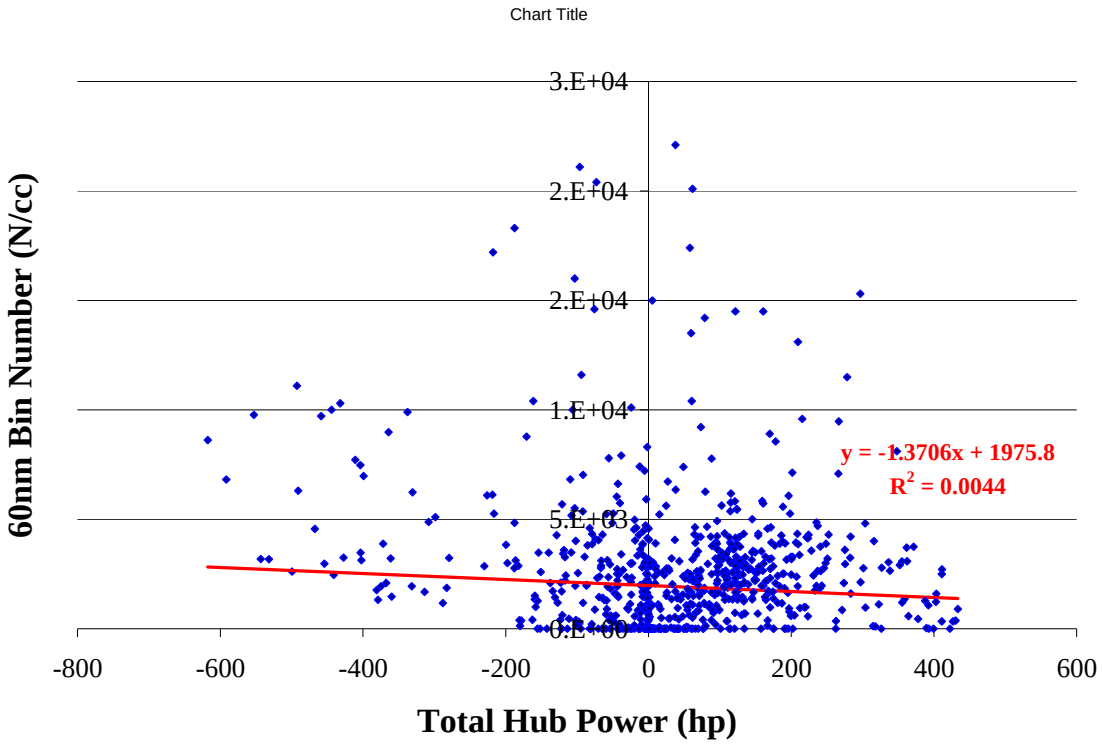

Figure 72: DMS500 20 nm Particle Number vs. Total Hub Power during the UDDS for E55CRC-39 tested at 56,000 lbs.

Figure 71 shows the total number concentration of particles in the 60 nm bin versus the total hub power. There is no strong correlation, but the total number shows an upward trend with the positive hub power range. Since 60 nm particles are in the accumulation mode, one would expect their count to rise when higher power operation demands lower air to fuel ratio. Figure 72 shows the total number concentration of particles in the 20 nm bin versus the total hub power. Again, there is no strong correlation between the two series but in this case as one can observe from the plot, there are more particles in the negative hub power periods, that is during decelerations. This is something to be expected since nuclei mode particles are dominant during the deceleration phases.

The following plots show the size distribution of particles during idle, acceleration and deceleration, respectively for E55CRC-39. As can be observed from Figure 73, particles of around 150 nm are mostly observed. This peak size agrees well with the 157 nm peak for the SMPS data, shown in Figure 62, but the nuclei mode peak evident in the SMPS plot is absent. One must note that the dilution system used for the two devices differed. During acceleration, as shown in Figure 74, a bimodal distribution is observed where there are two peaks centered at around 58 and 135 nm, respectively. This plot shows the transition from the Idle Mode, where particles of diameter 150 nm are dominant, to the acceleration mode, where particles of diameter around 60 nm are observed, which are the accumulation mode particles. Strong modes in the 50 to 100 nm range were observed for the SMPS data shown in Figure 63. Figure 75 shows the distribution during the deceleration region of the UDDS. Again, a bimodal distribution is seen. This time, the

transition is from deceleration to Idle Mode. The first peak is centered around 15 nm, which are mostly nuclei mode particles, and the second peak is centered around 175 nm, which is the Idle region distribution.

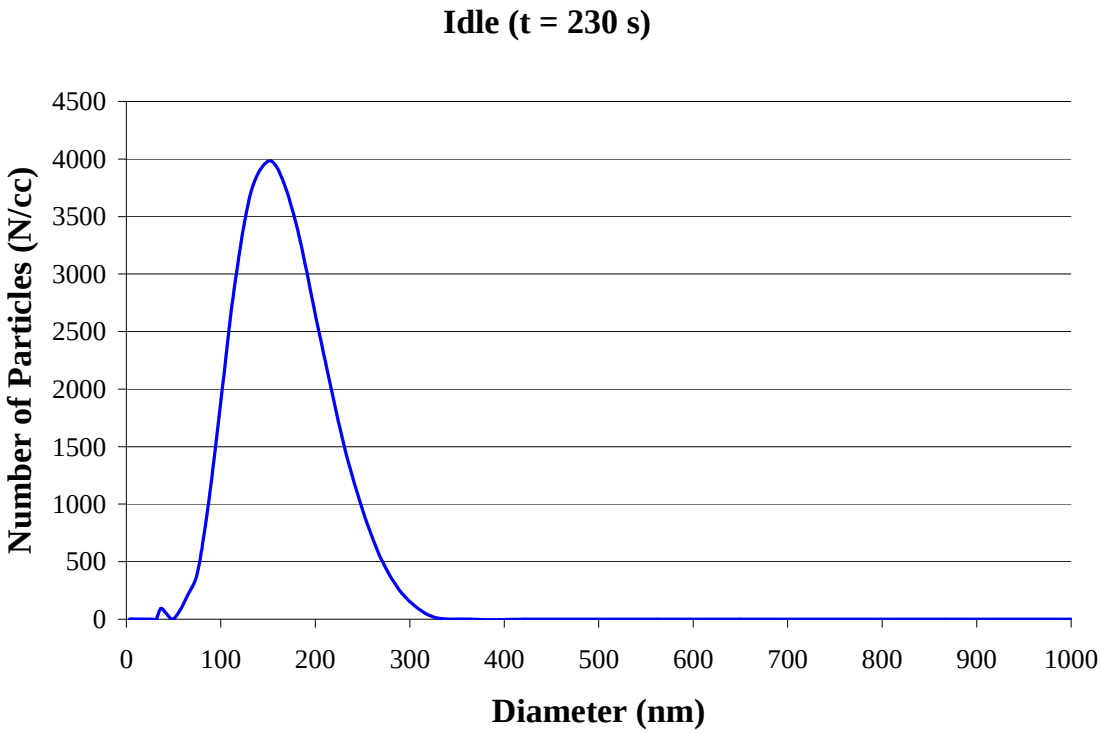

Figure 73: DMS500 size distribution of particles during Idle (t = 230 s) of the UDDS for E55CRC-39 tested at 56,000 lbs.

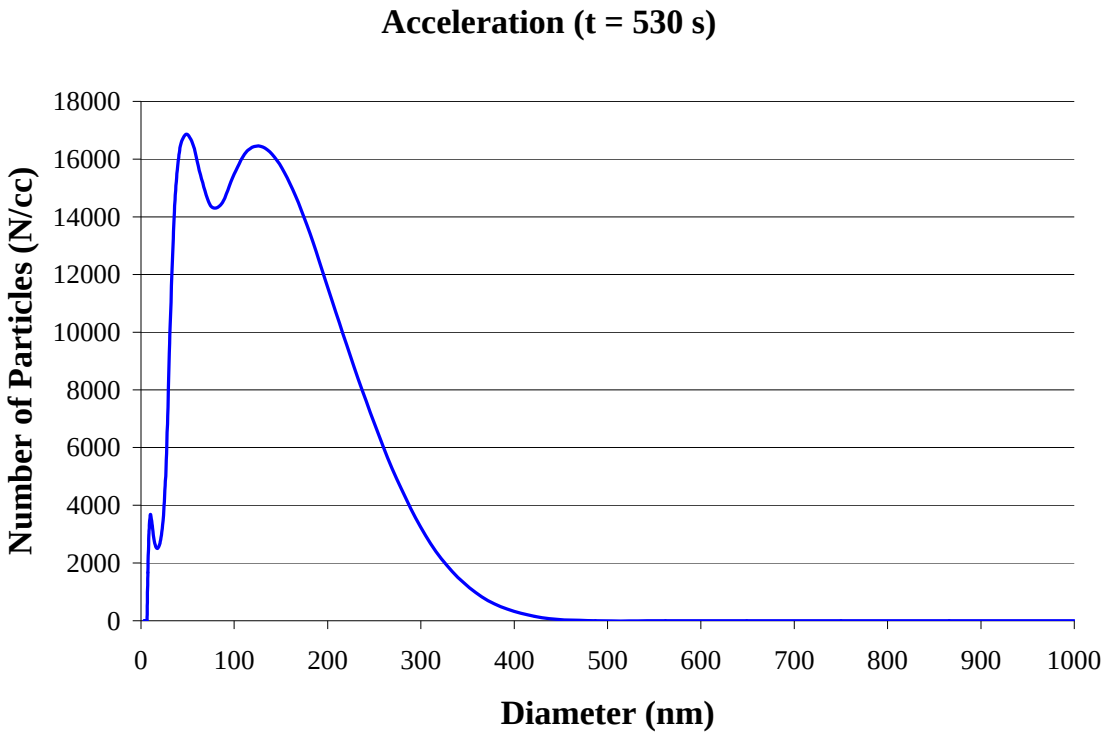

Figure 74: DMS500 size distribution of particles during acceleration (t = 530 s) of the UDDS for E55CRC-39 tested at 56,000 lbs.

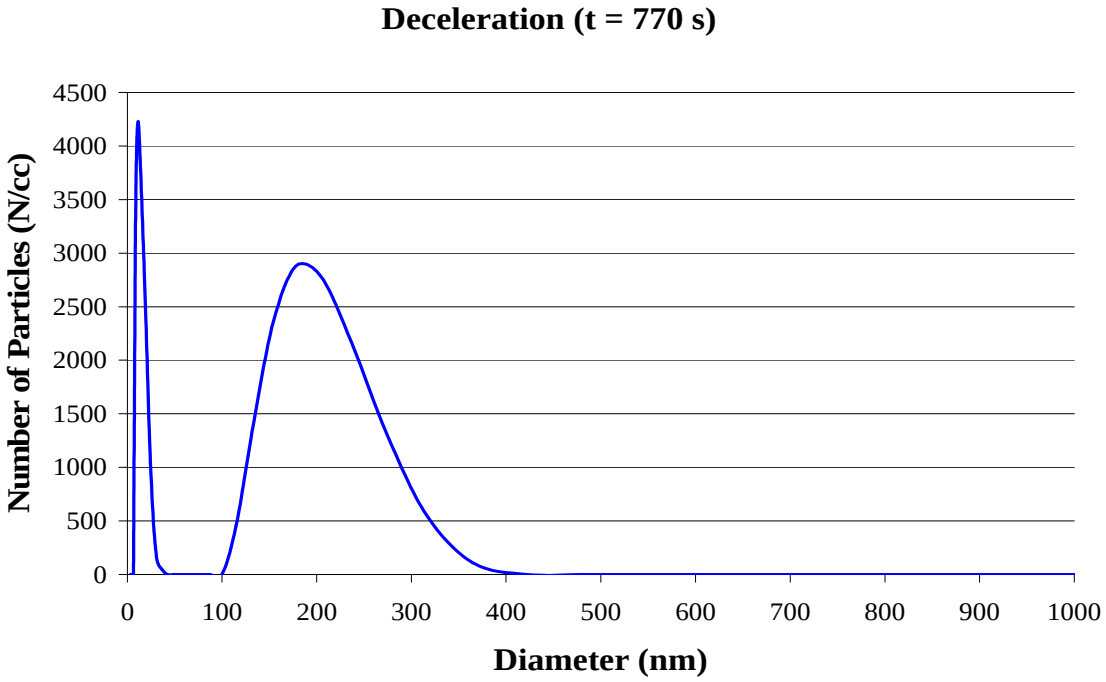

Figure 75: DMS500 size distribution of particles during deceleration (t = 770 s) of the UDDS for E55CRC-39 tested at 56,000 lbs.

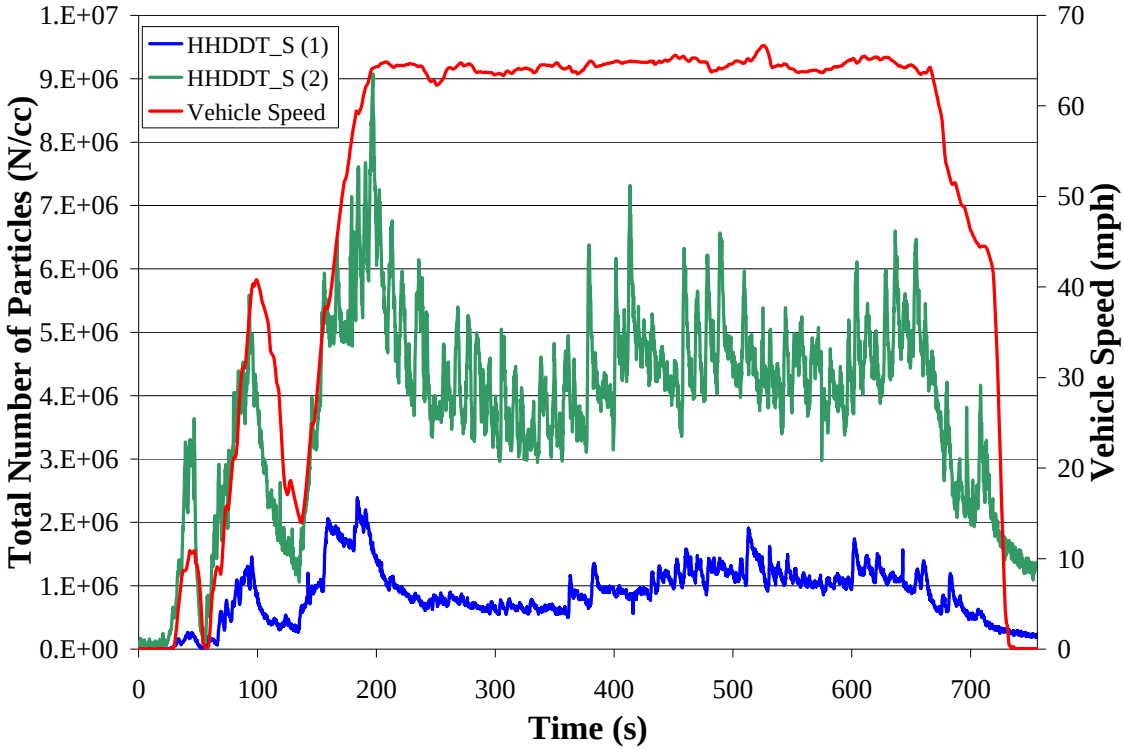

Figure 76: DMS500 size distribution of particles during HHDDT_S and Vehicle Speed vs. Time for E55CRC-39 tested at 56,000 lbs.

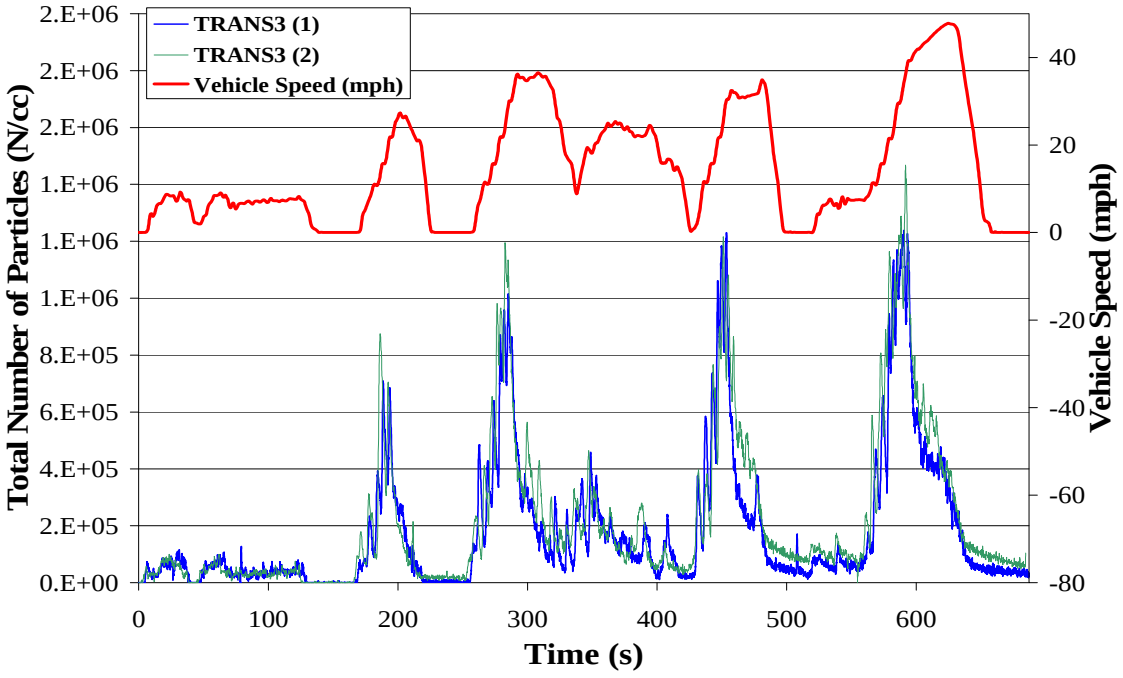

Figure 77: DMS500 size distribution of particles during Transient and Vehicle Speed vs. Time for E55CRC-39 tested at 56,000 lbs.

Figure 76 shows the total number of particles, determined using the DMS500 and vehicle speed versus time during HHDDT_S for E55CRC-39. As can be observed, the total number of particles is as high as $9x10^6$ during steep accelerations, and drops to $9x10^4$ particles/cm^3 during idle regions. Looking at the data profiles for the two tests, the problem may be that the DMS500 inlet probe was not properly mounted on the second HHDDT_S test, thus sucking in air from the ambient and causing a decrease in the particle number concentration readings."

Figure 77 shows the total number of particles, measured by the DMS500, and vehicle speed versus time for two different Transient runs. Again, as it is observed from previous plots, the total number of particles increases during accelerations and decreases during decelerations. During the High-speed Cruise section, the total number starts to decrease due to the decrease in the total number of accumulation mode particles. Repeatability is good for the two traces in Figure 77.

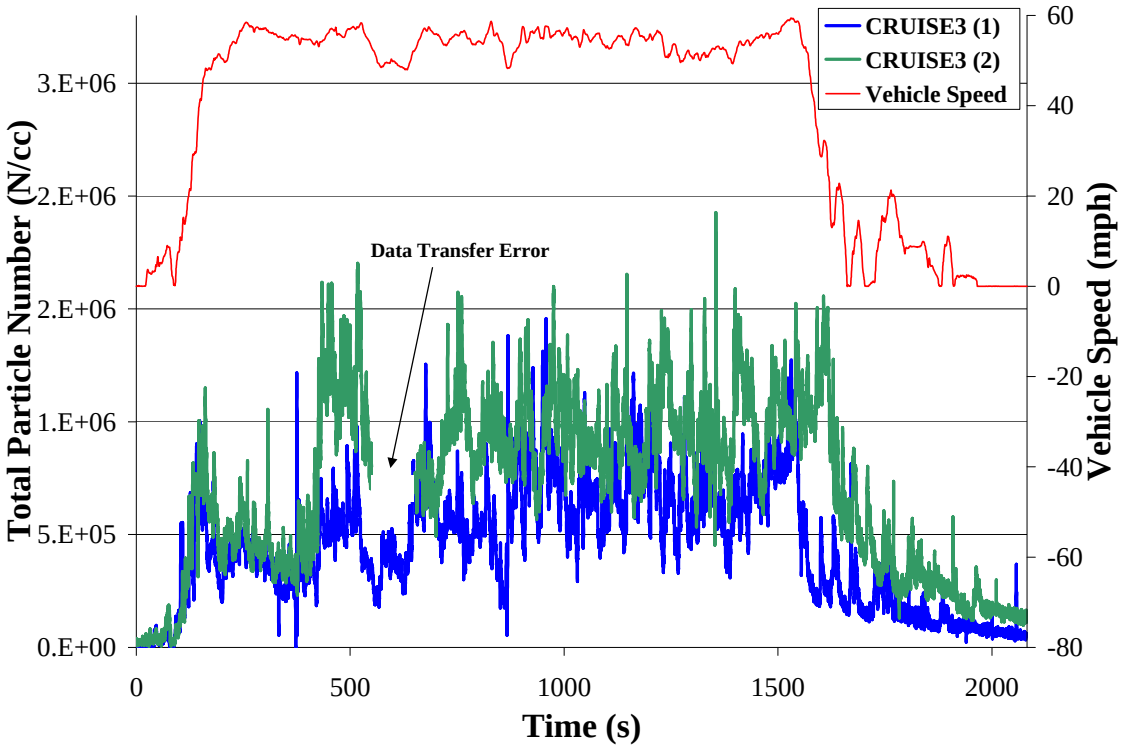

Figure 78: DMS500 size distribution of particles during Cruise3 and Vehicle Speed vs. Time for E55CRC-39 tested at 56,000 lbs.

Figure 78 shows the total number of particles and vehicle speed versus time for two different Cruise runs. During acceleration, the total number of particles increases and during decelerations, the total number decreases. Repeatability is not as good as illustrated in Figure 77, and the researchers speculate that this may have been due to the accumulation of PM in the instrument. This was the first operation of the instrument in the field by the researchers, and protocols for cleaning the instrument were not well established at time of testing.

E55CRC-40

E55CRC-40 was a powered by a Detroit Diesel Series 60, MY 2003 engine. Particle sizing and chemical speciation results are presented below for various modes of the HHDDT schedule. Figure 79 and Figure 80 present the SMPS particle size distributions for Idle and steady modes.

A nuclei mode dominated distribution was seen for the Idle mode with a count median diameter (CMD) of 25.88 nm with a concentration of $8x10^4$ particles/cc and a geometric standard deviation of 1.64. These concentration levels were almost four times lower than those observed for E55CRC-39. This drop in concentration could be attributed to difference in the emissions of volatile organic compounds. The total VOC's emitted for E55CRC-40 at 2.01 g/hour during the Idle mode was almost eight times lower in magnitude as compared to E55CRC-39 at 15.51 g/hour. The VOC mass emission rates reported here include contributions from unburnt fuel and oil. It should be noted that a recent study by Sakurai et al.[13] indicated that the volatile component of diesel particles was comprised primarily of unburnt lubricating oil, and that contributions from unburnt fuel, oxidized organic combustion products, and sulfuric acid were small. Sakurai et al.[13] also reported that the organic component of diesel nanoparticles was comprised of compounds with carbon numbers in the C24 – C32 range, which are almost entirely derived from unburnt oil.

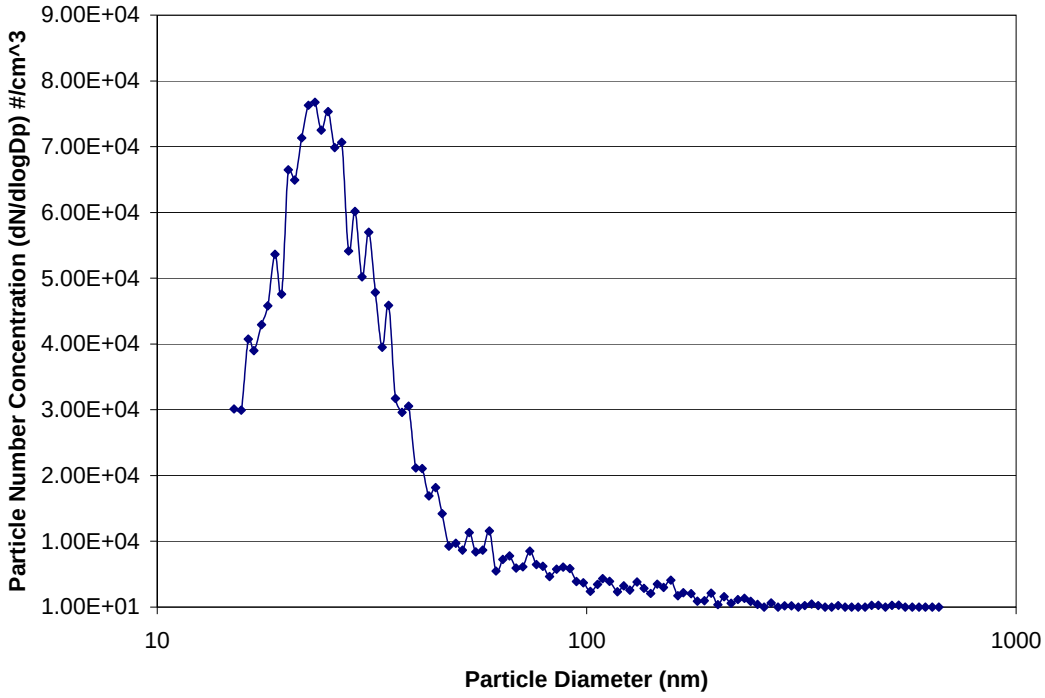

Figure 79: SMPS Particle Size Distribution for E55CRC-40 Operating on an Idle Mode

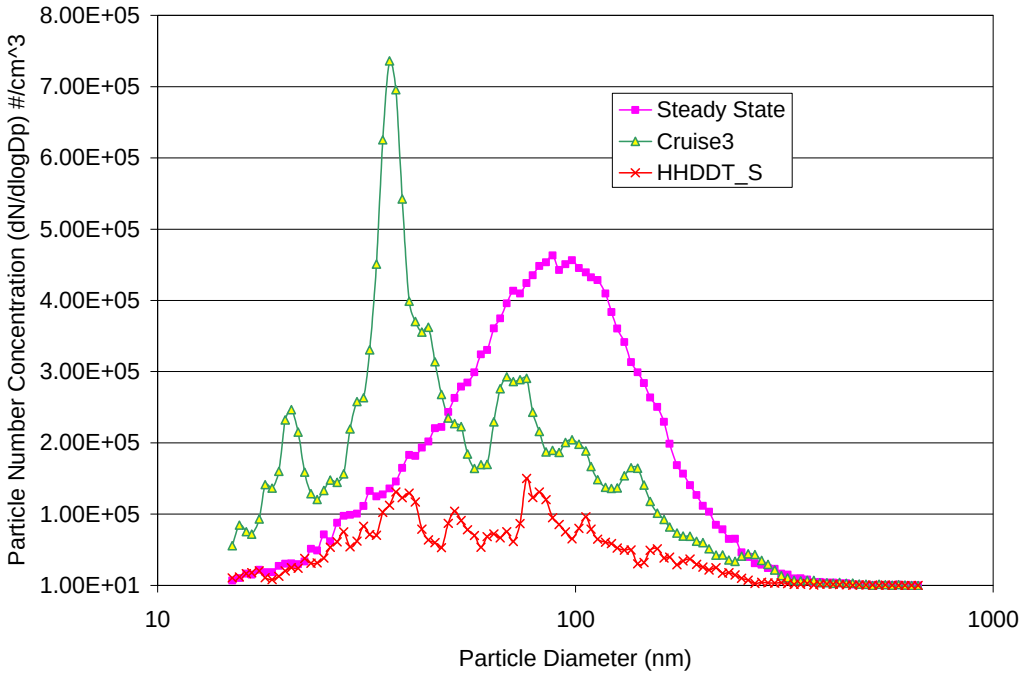

Figure 80: SMPS Particle Size Distribution for E55CRC-40 Operating on Various Steady Cycles

VOC results were very similar for E55CRC-40 when Idle and Cruise mode were compared (Appendix O: Figure O13 to O17). Emissions of n-hexane and 2-methyl-1-pentene were high during the Transient mode when compared with the Idle and Cruise Modes (Appendix O: Figure O15 and O16). For the steady state mode, the CMD for the particle size distribution was 84.96 nm with a concentration of $4.5x10^5$ particles/cm^3 and a GSD of 1.75. Particle size distributions were markedly different for the two Cruise Modes with a CMD of 45.1 nm for the normal Cruise mode and 62.24 nm for the High-speed Cruise Mode. SMPS size distributions observed in the Cruise Modes were characterized by the accumulation mode particles.

The shift of the size spectrum towards a higher accumulation range during the Cruise Modes when compared to the Idle mode could be attributed to higher concentrations of carbonaceous agglomerates (EC emissions) and higher sulfate emissions during the Cruise Mode. Sulfate emissions were very high during the Cruise Mode at 0.27 g/hour when compared with the Idle mode at 0.015g/hour (Figure 83). Sulfate emissions serve as the precursors of particle formation seen in the nuclei mode. Sulfates would undergo a hetero-molecular nucleation with water molecules to form complex clusters. Subsequent adsorption of volatile organics and agglomeration with the elemental carbon results in the distribution seen in Figure 80. Elemental carbon emissions for the Cruise Mode were high at 5.5 g/hour when compared to the Idle mode at 0.07 g/hour (Figure 83), which also contributed to most of the mass emissions (Figure 82). Semi volatile emissions were similar for Idle and Cruise Modes except for alkanes and hopanes & steranes which were higher during the Cruise Mode (Appendix O: Figure O18 to O22).

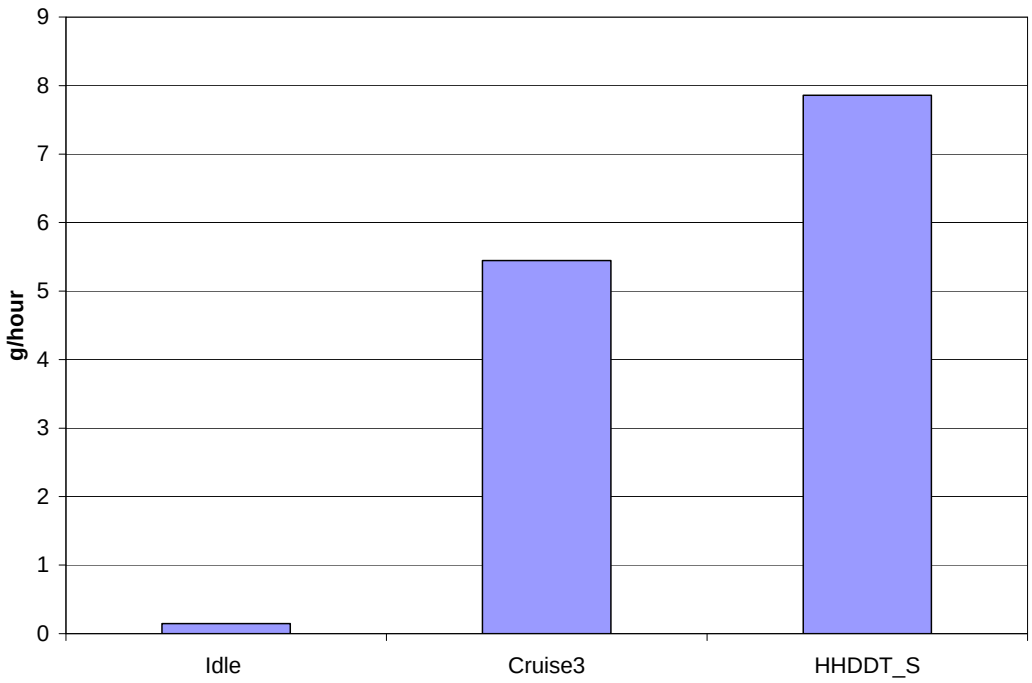

Figure 81: PM Mass Emissions for E55CRC-40

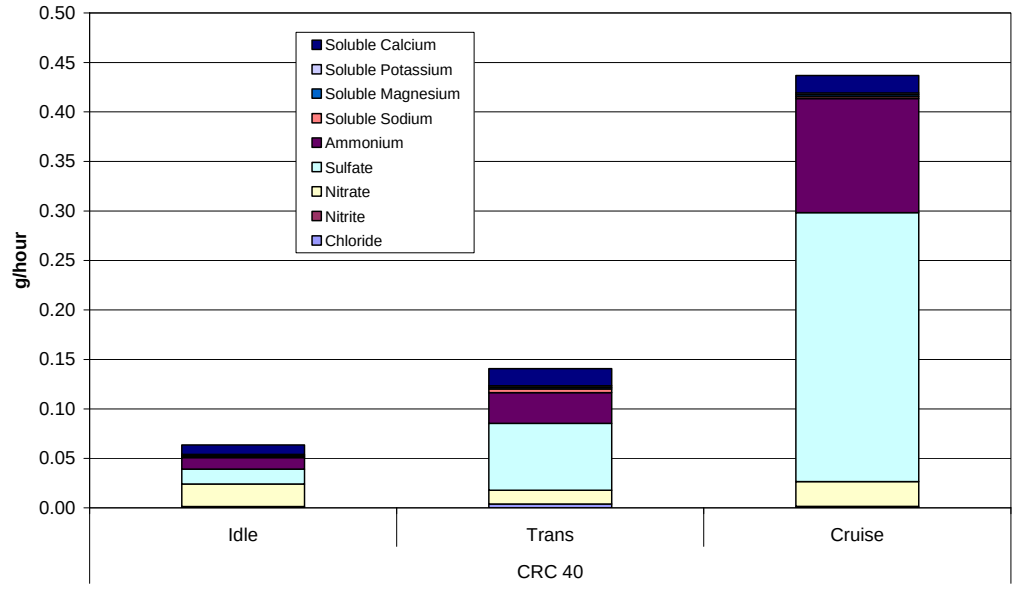

Figure 82: Ion Composite Results for E55CRC-40

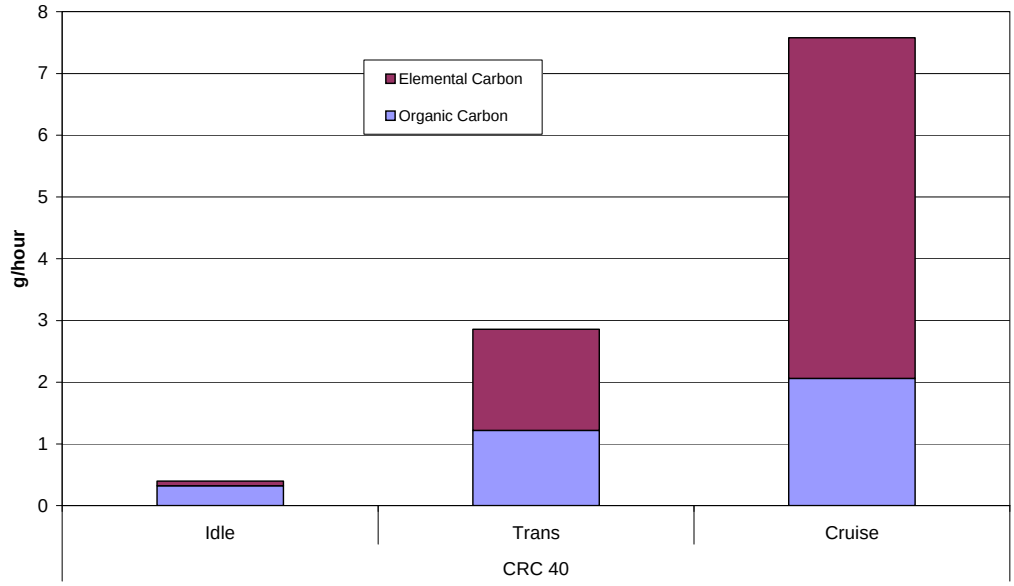

Figure 83: Elemental Carbon and Organic Carbon PM Analysis for E55CRC-40

For E55CRC-40, DMS500 data proved unreliable, and were characterized by spikes in the output data that did not represent credible particle counts.

E55CRC-41

E55CRC-41 was the only MHDT subjected to speciation.

CRC41 was a Medium Heavy-duty Vehicle (MHDT) powered by a MY 1997 Cummins B5.9, 210 hp engine. The vehicle was tested over a lower speed transient, a higher speed Transient, and the Cruise Mode. Additionally, PM concentration and size distribution data was collected over the MHDT schedule that comprised of driving modes mentioned above. Figure 84 shows the PM size distribution over the idle mode.

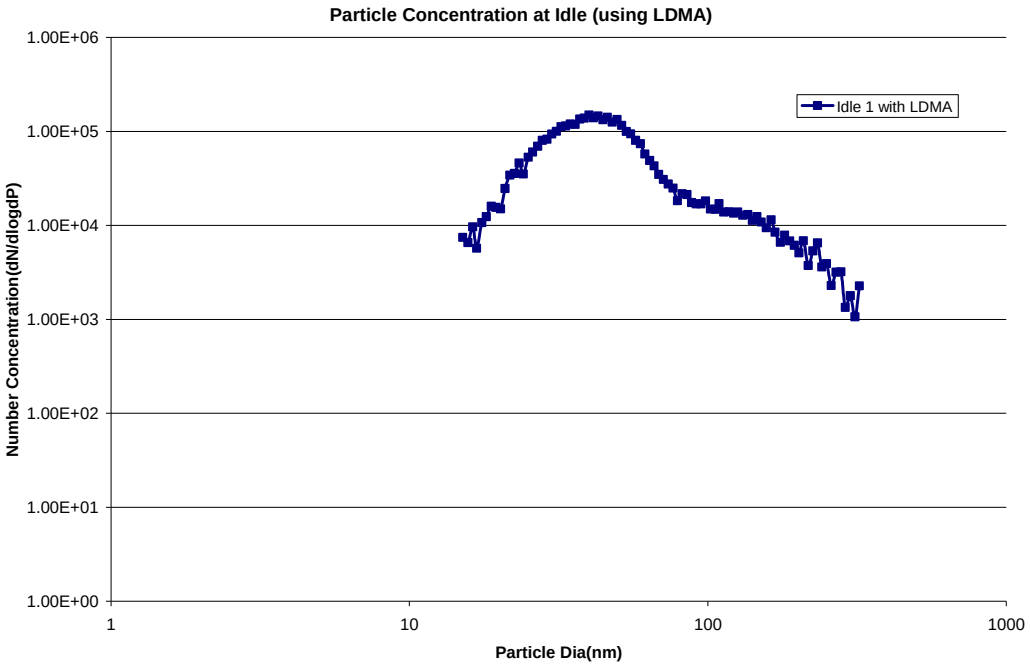

Figure 84: SMPS Particle Size Distribution for E55CRC-41 Operating on an Idle Mode

The size distribution during idle operation (Figure 84) showed a nuclei mode centered at 40 nm and an accumulation mode of 136 nm with concentrations in the range of $1.4x10^5$ and $1.3x10^5$, particles/cc, respectively. Again, the lower exhaust temperatures under idling conditions, and the relatively low carbonaceous soot (resulting in higher saturation ratios) leads to formation of higher levels of nuclei mode particles, primarily from the organics compounds originating from the lubricating oil. Recent studies by Gautam et al.[14] on natural gas-fueled heavy-duty vehicles have shown evidence that supports the argument that lubricating oil significantly contributes to nuclei mode particles. When total surface area provided by soot particles is reduced the nucleation process is advanced. Hence, in driving modes where the elemental carbon component of the total PM emissions is lower, the nuclei mode particles are emitted in higher concentrations, provided the exhaust temperatures and relative humidity are conducive to nucleation[15,16]. The binary nucleation theory of water and sulfuric acid has been shown to underestimate the formation of nucleation mode particles by several orders of magnitude[17]. However, organic compounds have been considered as a key species to control the growth of nucleation mode particles[18].

Chemical speciation of exhaust from CRC41 showed that most volatile organic compounds, except for C_2 to C_5 alkanes, were higher in the Transient and Cruise Modes than in the idle mode of operation (Appendix O: Figure O25 to Figure O36). The polar compound emissions for the transients were the highest (Appendix O: Figure O33). The elemental carbon emissions for the Cruise Mode were nearly seven times higher than the Idle emissions (Figure 85). Figure 86 shows that total PM mass emission rates in the

cruise mode are dominated by the elemental carbon emissions. However, the organic carbon emissions are also significantly higher under cruise mode than under idle and transient modes. This breakdown is reflected in the PM concentrations and size distributions, as seen in Figure 84, Figure 87 and Figure 88). Cruise operation at a vehicle inertia of 75% GVWR shows a nuclei mode peak at 26.9 nm with a concentration of 3.9 x 10^5 particles/cc when measured with a nano-DMA. The accumulation mode, with a CMD of 76.4 nm is similar for the cruise and steady state (25 mph) operation. Particle concentrations at 50% GVWR at cruising conditions did not produce any significant concentrations of nano-particles. This may be attributed to lower emissions of volatile species. Compared to the Idle and Transient Modes, emissions of sulfate emissions were significantly higher in the Cruise Mode (Figure 89). As noted earlier, binary nucleation of sulfuric acid and water do contribute to formation of nucleation mode particles, which may or may not survive in the exhaust depending upon levels of carbonaceous soot present in the exhaust stream.

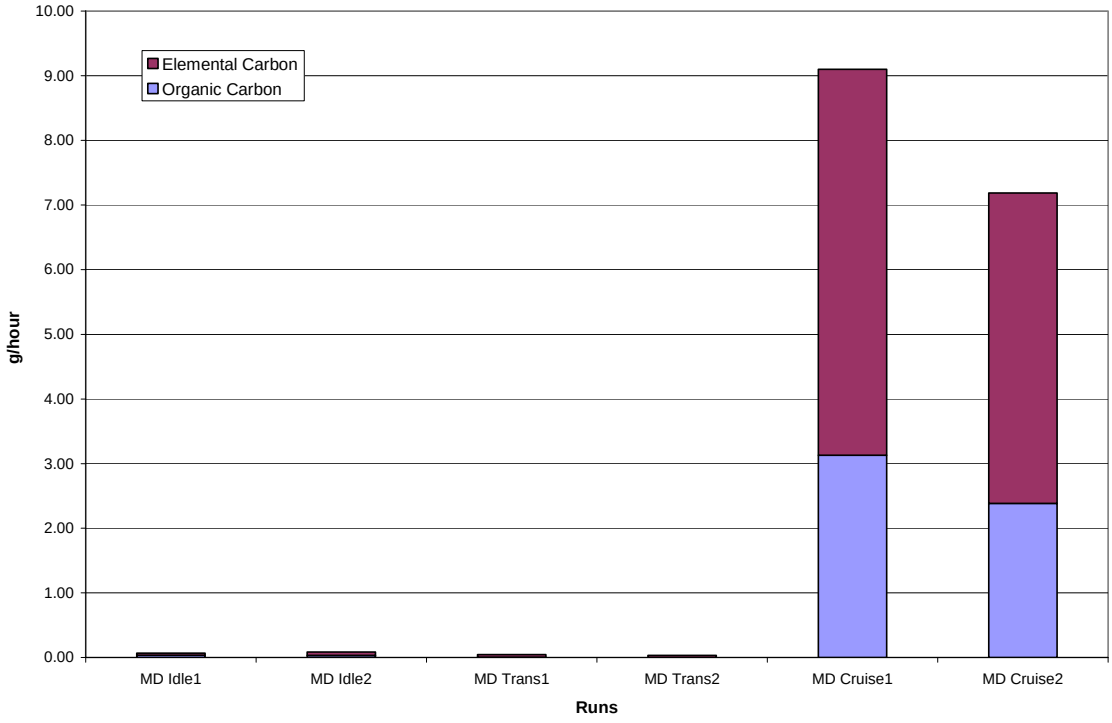

Figure 85: Elemental Carbon and Organic Carbon PM Analysis for E55CRC-41

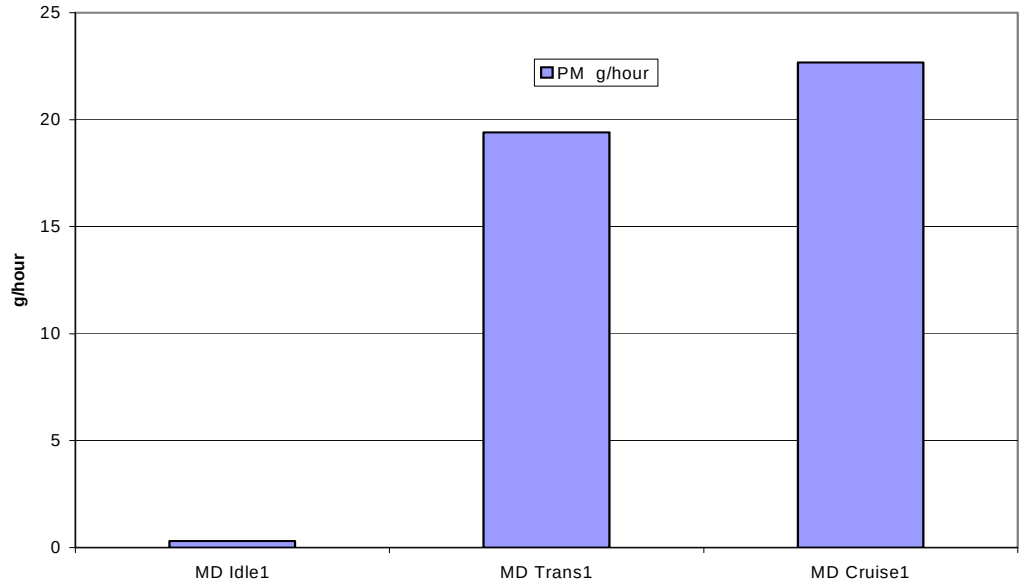

Figure 86: Total PM Mass Emissions Rate (g/hour) for E55CRC-41

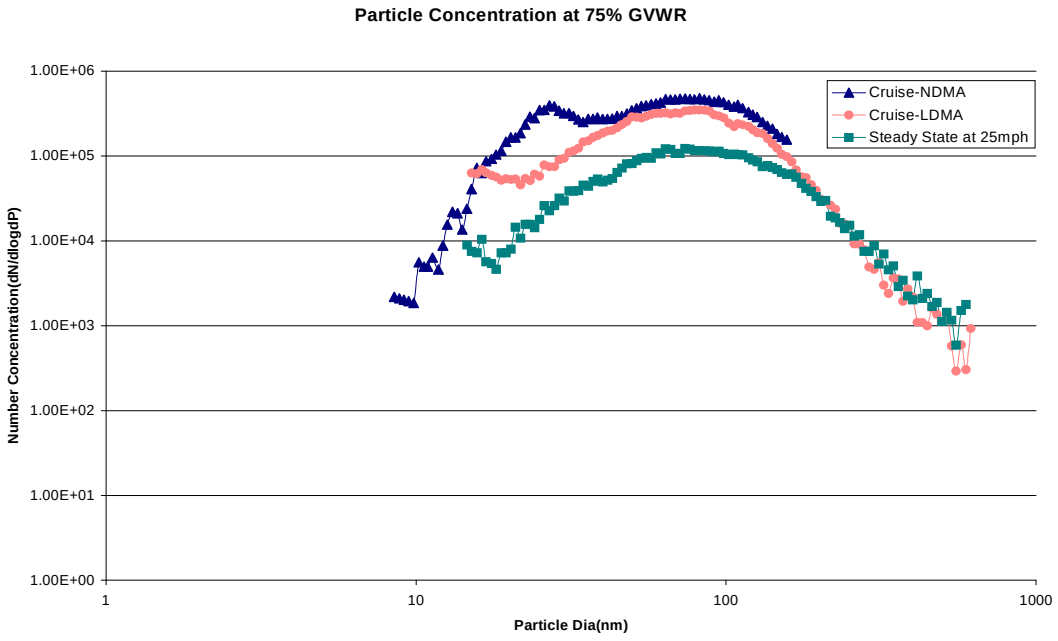

Figure 87: SMPS Particle Size Distribution for E55CRC-41 Operating under Cruise and Steady Conditions

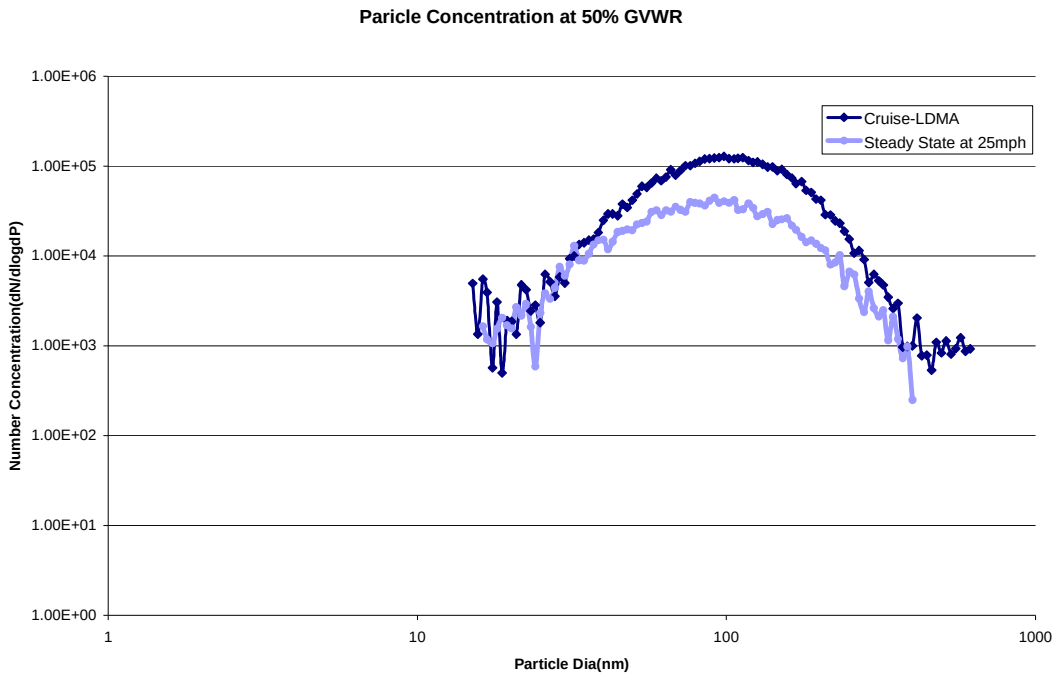

Figure 88: SMPS Particle Size Distribution for E55CRC-41 Operating on Cruise and Steady Conditions (50% GVWR)

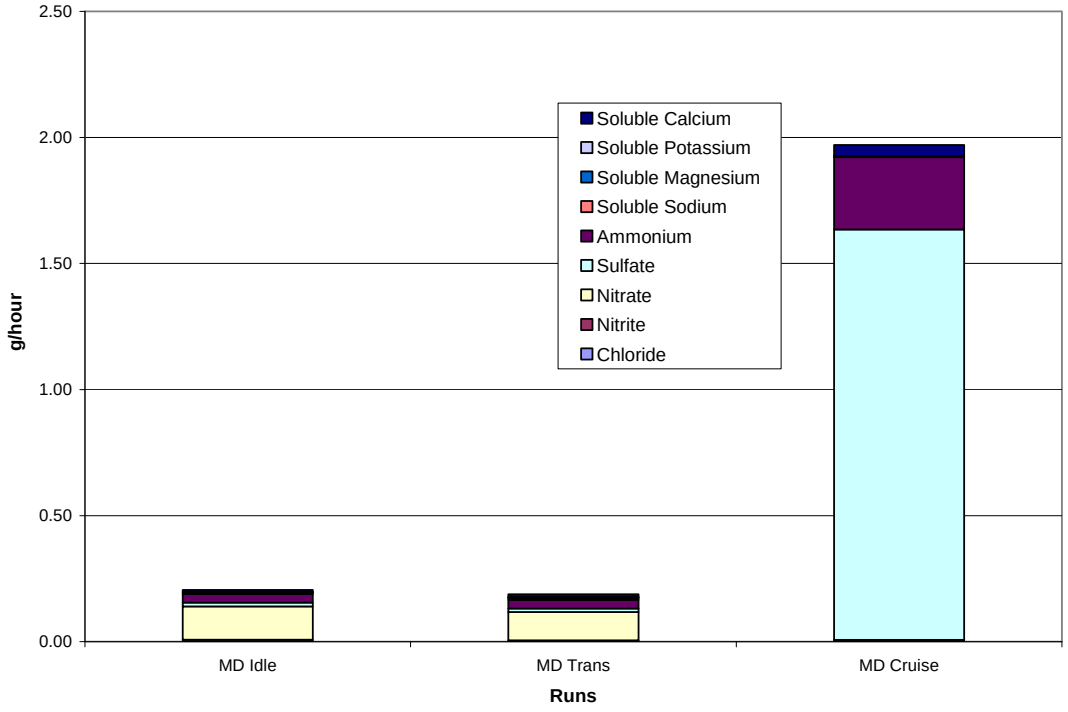

Figure 89: Ion Composite Results for E55CRC-41

Figure 90 to Figure 92 show traces of single particle tracking (82 nm and 24 nm) under transient operations. At 75% GVWR, the 82 nm particles are emitted at higher concentrations than the 24 nm particles. The concentration of 82 nm particles decreases by an order or magnitude at lower inertia weight (50% GVWR).

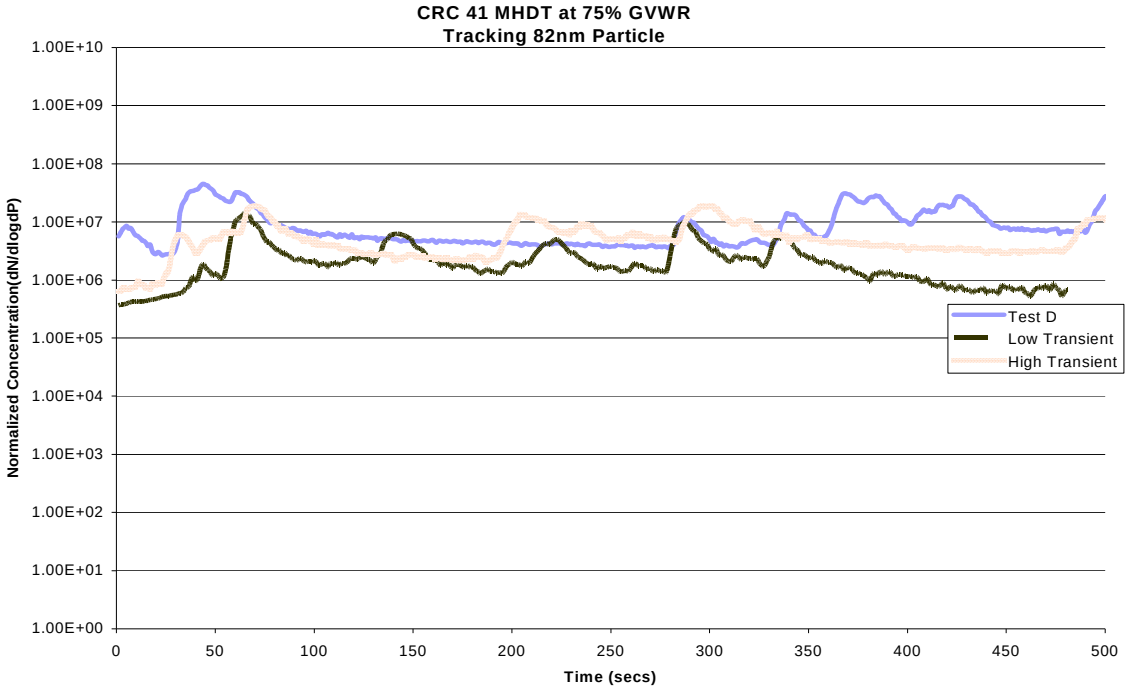

Figure 90: SMPS Single Particle Trace (82 nm) for E55CRC-41 Operating on UDDS, Low Transient and High Transient Cycles (75%GVWR)

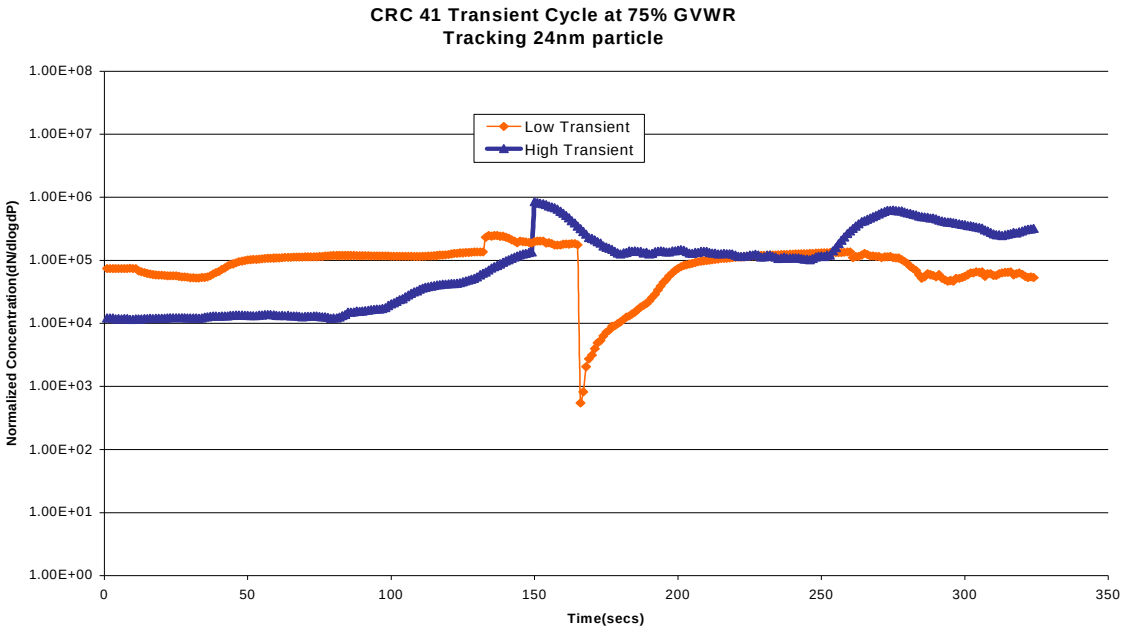

Figure 91: SMPS Single Particle Trace (24 nm) for E55CRC-41 Operating on Low Transient and High Transient Cycles (75% GVWR)

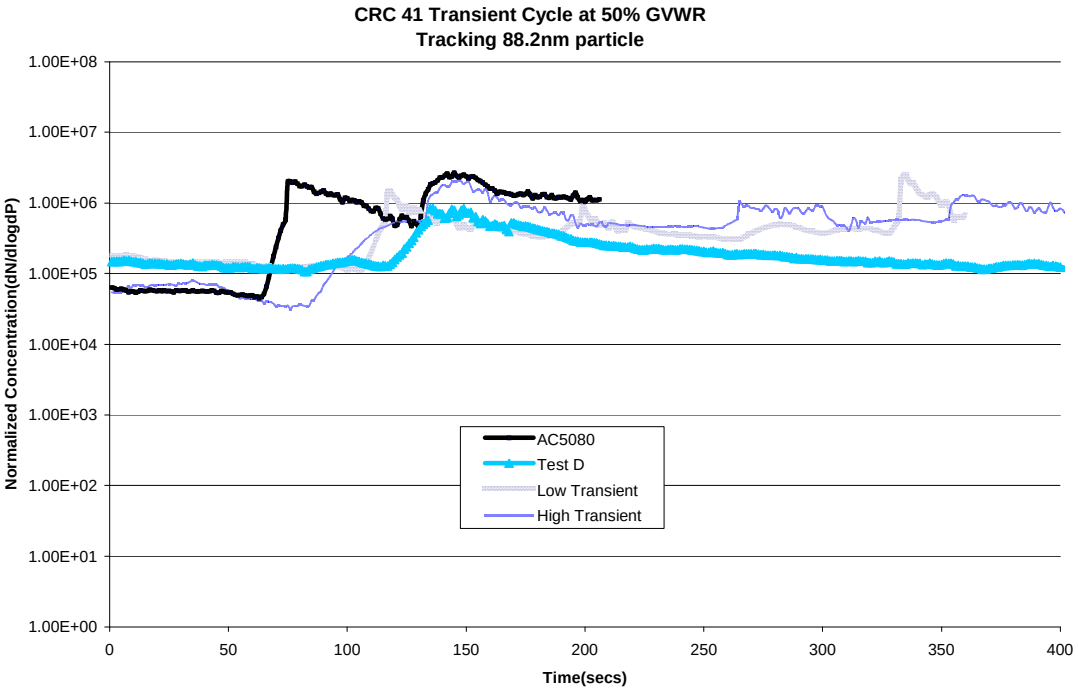

Figure 92: SMPS Single Particle Trace (88 nm) for E55CRC-41 Operating on Low Transient and High Transient Cycles (50% GVWR)

Figure 93 shows the DMS500 total number concentration of particles and vehicle speed versus time during the UDDS for E55CRC-41. The total number is as high as $1.7x10^6$ during steep accelerations and drops to $1.5x10^4$ during Idle conditions. (There was an error on the readings of the instrument until t = 370s in Figure 93) In Figure 93 the high count between 620 and 750 seconds is due to a high count of 20 nm particles over that time. The overall count versus time differs in behavior between this vehicle and heavy-duty vehicles, such as E55CRC-39 (see Figure 67 for UDDS data) and E55CRC-42 and E55CRC-43 (Figure 105 and Figure 111 for transient behavior). E55CRC-41 did not show a high count associated with acceleration, while the HHDDT showed this behavior clearly. E55CRC-41 had a smaller displacement than the HHDDT, higher engine speed, lower boost, two valves per cylinder (versus four for the HHDDT) and an in-line injection system. However, it should be speculative to associate any of these factors directly with the differing behavior.

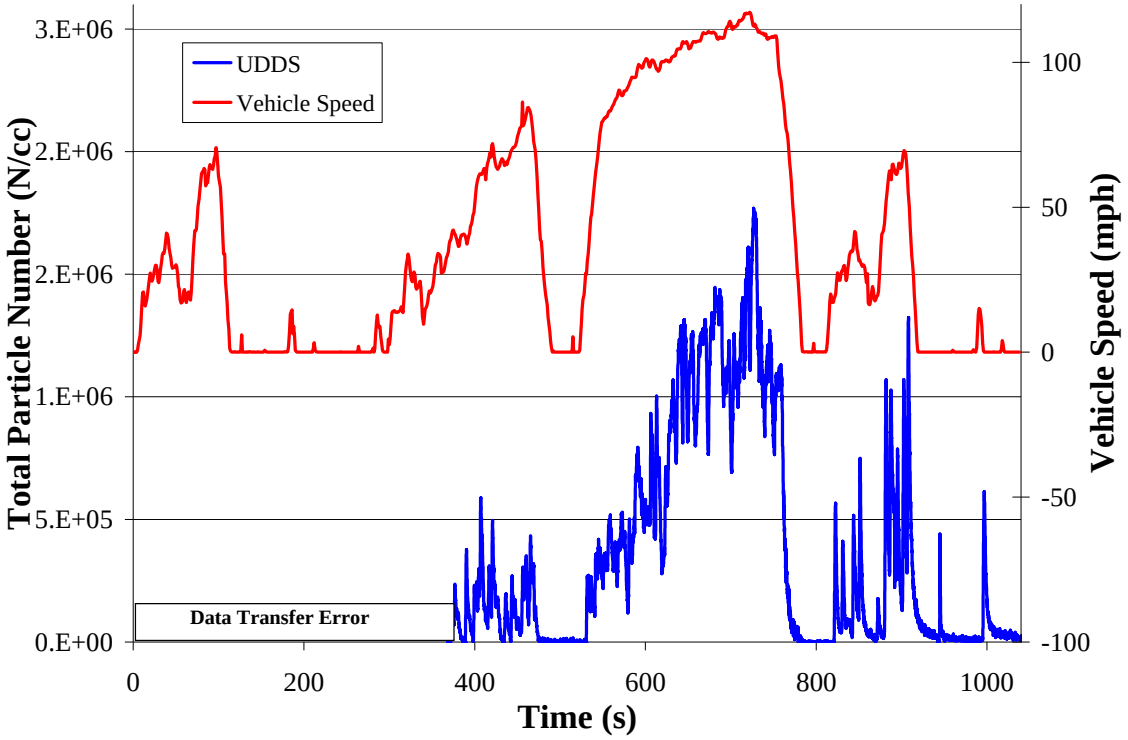

Figure 93: DMS500 Total Number of Particles and Vehicle Speed vs. Time during UDDS for E55CRC-41 tested at 56,000 lbs.

Figure 94 shows the distribution of the total number of particles in the 60 and 20 nm bins versus time. The 60 nm bin contains particles of diameters between approximately 55 and 65 nm, and the diameters for the 20 nm bin range between 17.5 and 22.5 nm. There is a sharp increase in the total number of particles in the 20 nm bin during decelerations and a sharp increase in the total number of particles in the 60 nm bin during accelerations, sharp meaning a greater percentage of decrease/increase.

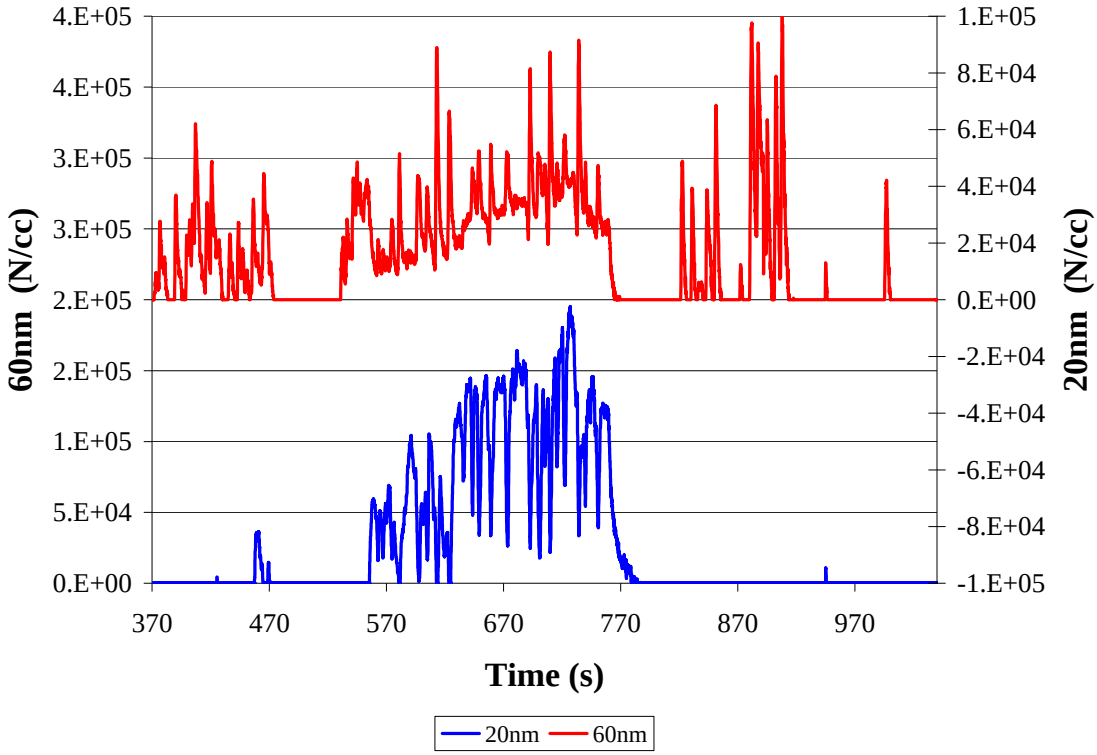

Figure 94: DMS500 60 nm and 20 nm Particle Number vs. Time for E55CRC-41 tested at 56,000 lbs.

Figure 95 shows the total number of particles and CO versus time. This plot shows the correlation between the two series. This kind of a relation is actually expected due to the fact that a large portion of particulate matter is elemental carbon (EC).

Figure 96 shows the total number of particles in the 60 nm bin versus the total number of particles in the 20 nm bin. As can be seen, there is no clear correlation between the two size bins, although the envelope of the points is well defined.

Figure 97 shows the total number of particles in the 20 nm bin versus the total hub power. There is no strong correlation between the two series. Figure 98 shows the total number of particles in the 60 nm bin versus the total hub power. Again, there is no strong correlation, suggesting that the particle formation cannot be attributed to engine load alone.

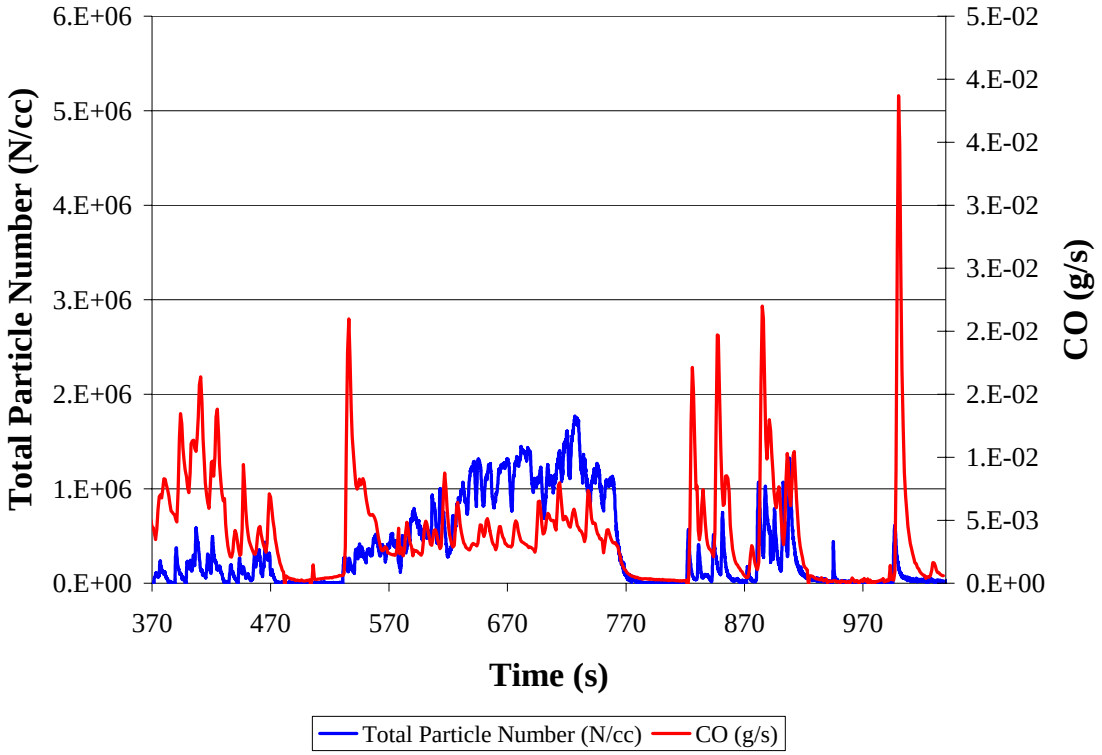

Figure 95: DMS500 Total Number of Particles and CO vs. Time for E55CRC-41 tested at 56,000 lbs.

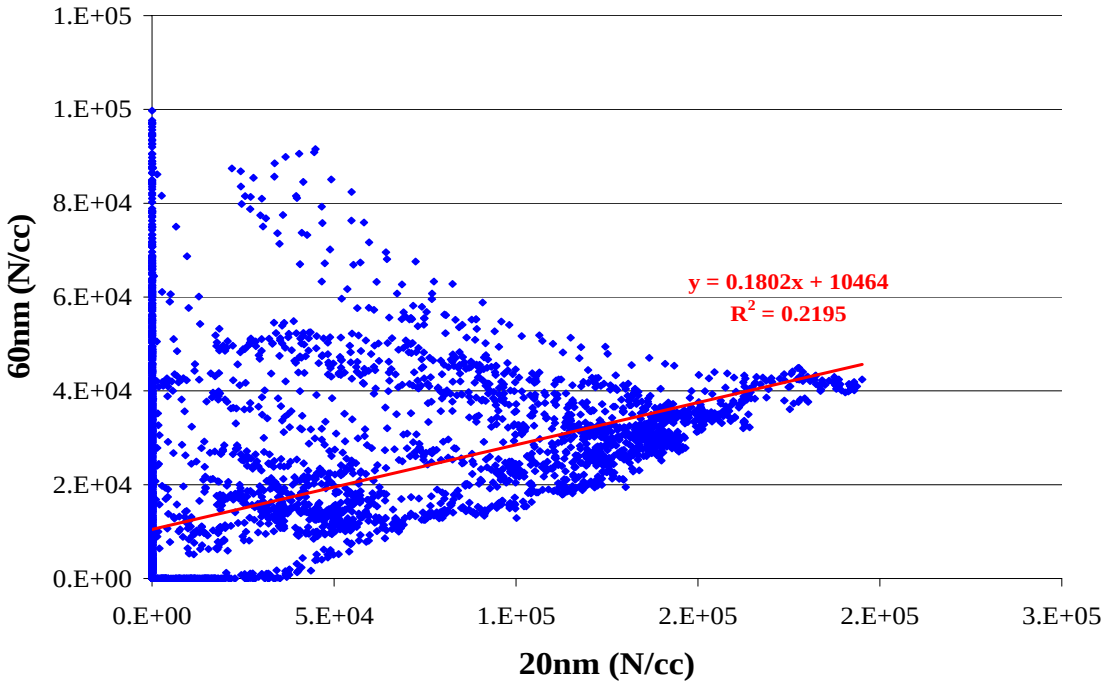

Figure 96: DMS500 60 nm Particle Number vs. 20 nm Particle Number for E55CRC-41 tested at 56,000 lbs.

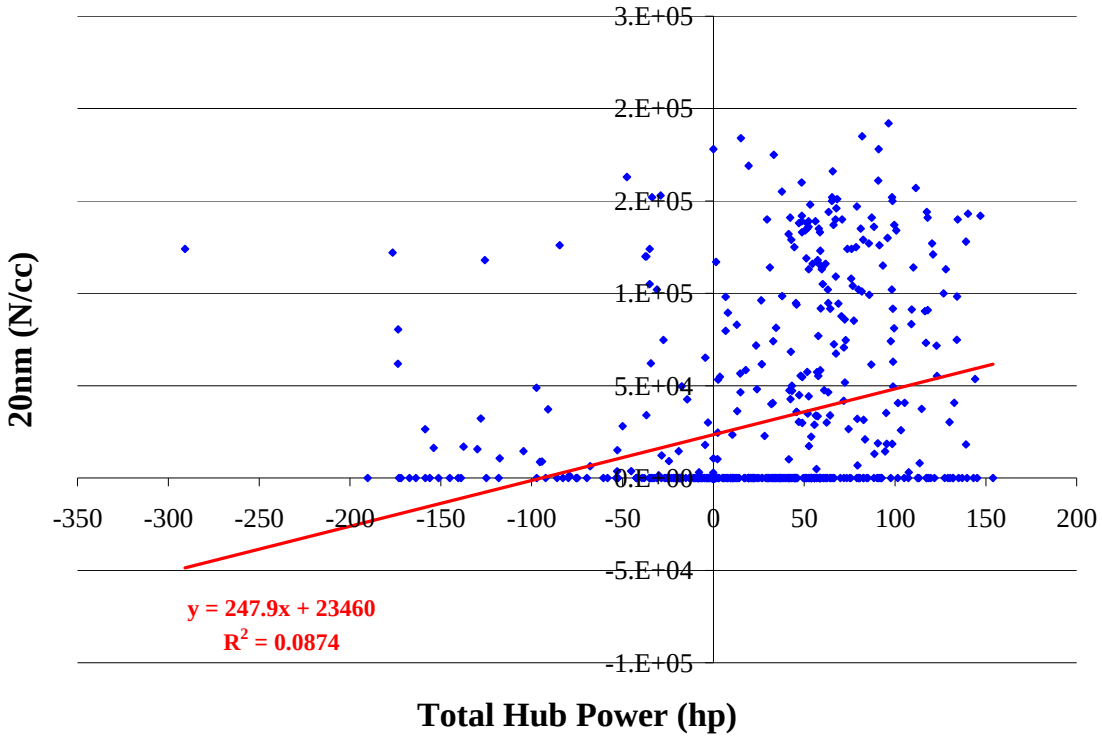

Figure 97: DMS500 20 nm Particle Number vs. Total Hub Power for E55CRC-41 tested at 56,000 lbs.

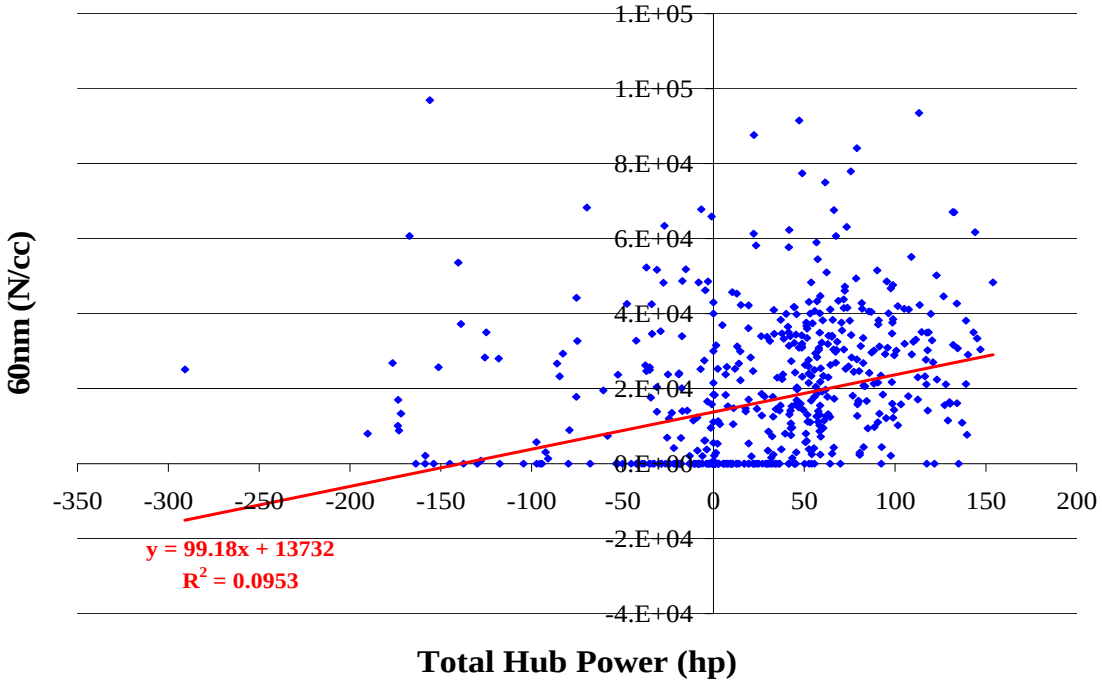

Figure 98: DMS500 60 nm Particle Number vs. Total Hub Power for E55CRC-41 tested at 56,000 lbs.

Figure 99 shows the size distribution of particles during acceleration and deceleration periods. During acceleration, a single mode distribution is observed where the peak is centered at around 100 nm. This is expected since during accelerations, accumulation mode particles are formed. For the deceleration region, a single mode distribution is seen. The peak is centered around 20 nm, and these are the nuclei mode particles. This mode is observed during deceleration periods, as the plot also shows.

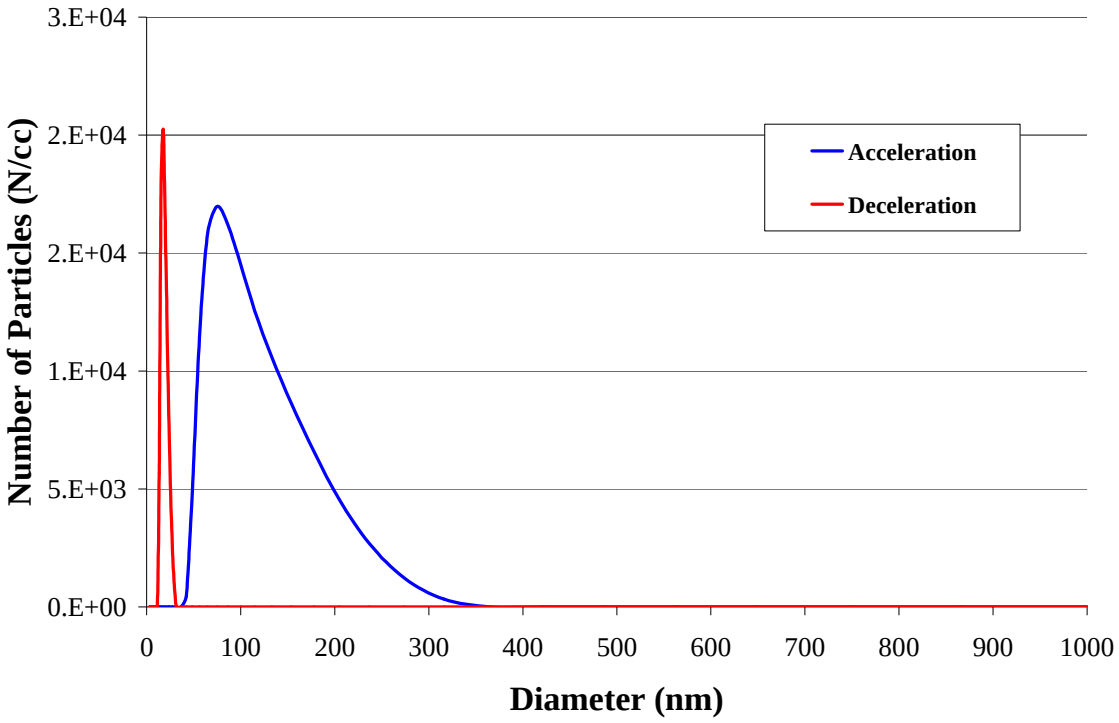

Figure 99: DMS500 size distribution of particles during acceleration and deceleration for E55CRC-41 tested at 56,000 lbs.

E55CRC-42

E55CRC-42 was a powered by a Caterpillar 3406, MY 1999 engine. Particle sizing and chemical speciation results are presented below for various modes of the HHDDT schedule. Figure 100 and Figure 101 present the particle size distribution for Idle and steady modes.

A typical uni-modal size distribution was noted for the Idle mode for E55CRC-42 (Figure 101) with a CMD of 40 nm and concentration of $1.3x10^5$ particles/cc. In comparison to E55CRC-39 and E55CRC-40, the size distribution shifted towards a larger particle size for E55CRC-42 during the Idle Mode. In addition to the nuclei mode, the size distribution is also characterized by a mode with a CMD of 100 nm.

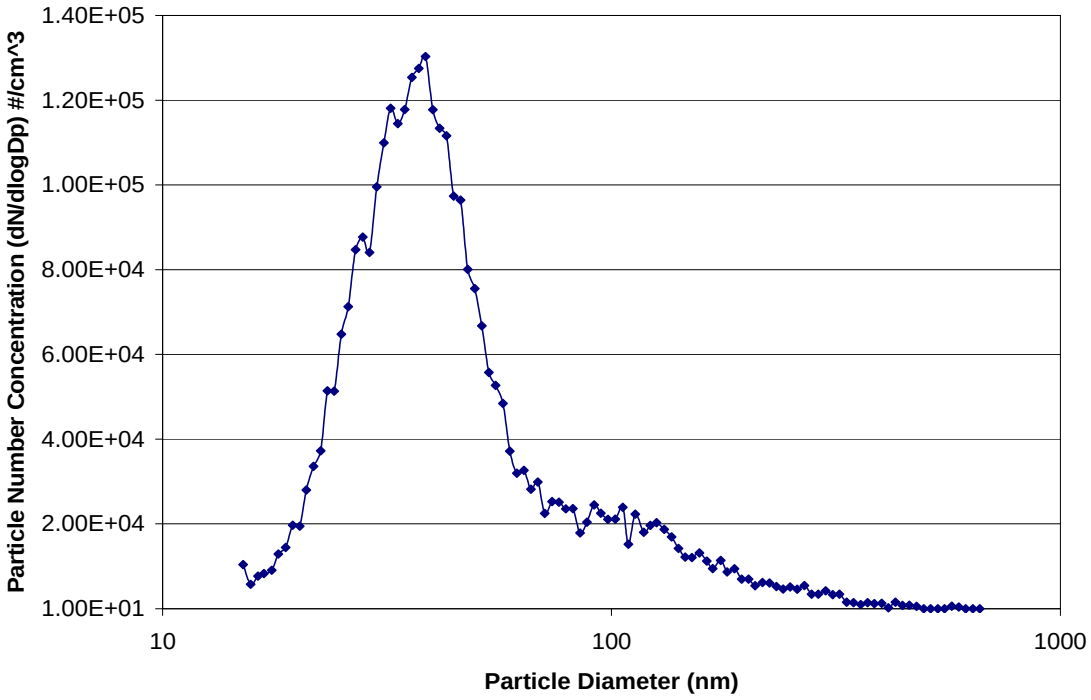

Figure 100: SMPS Particle Size Distribution for E55CRC-42 Operating on an Idle Mode

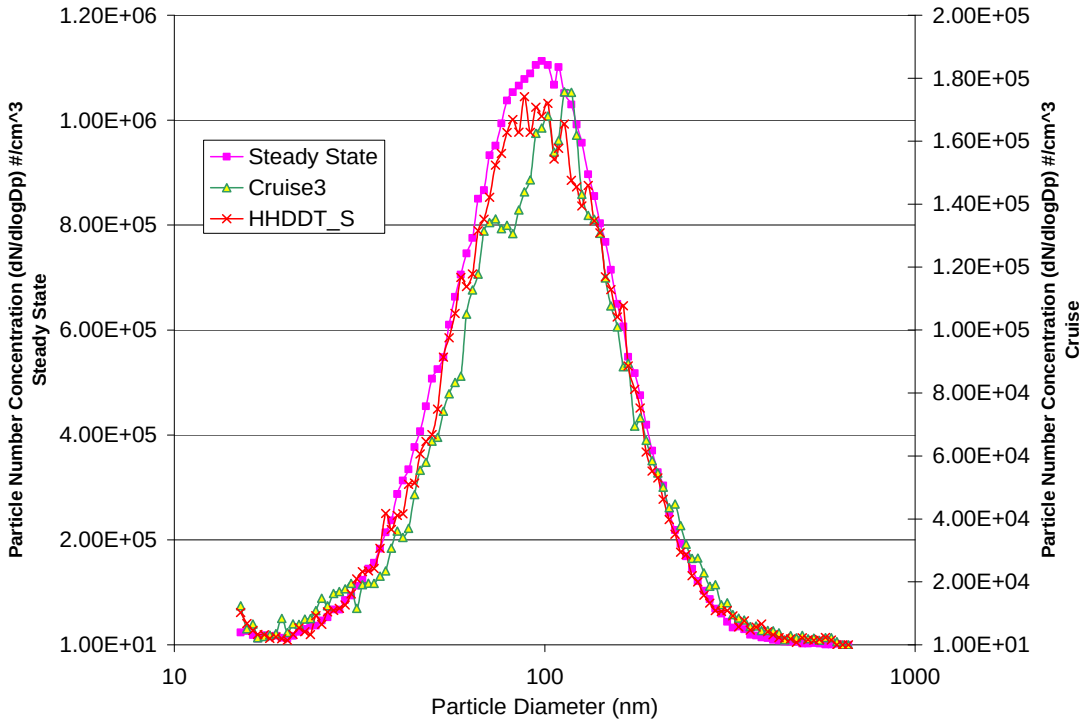

Figure 101: SMPS Particle Size distribution for E55CRC-42 operating on various steady cycles

The accumulation mode observed during the Idle could be due to an increase in elemental carbon emission when compared to the previous vehicles tested. During the Idle Mode, the elemental carbon emitted by E55CRC-39 and E55CRC-40 were 0.21 g/hour and 0.07 g/hour, respectively and for E55CRC-42, the values were higher at 0.55 g/hour (Figure 104). This increase in elemental carbon also increased the mass emission for the Idle mode at 1.34 g/hour (Figure 102). Mass emissions during Idle for E55CRC-39 and 40 were 0.35 g/hour and 0.14 g/hour, respectively. Total volatile organic compounds emitted by E55CRC-42 during the Idle mode at 2.99 g/hour were much lower when compared with the Cruise mode at 6.04 g/hour (Appendix O: Figure O25 to O29).

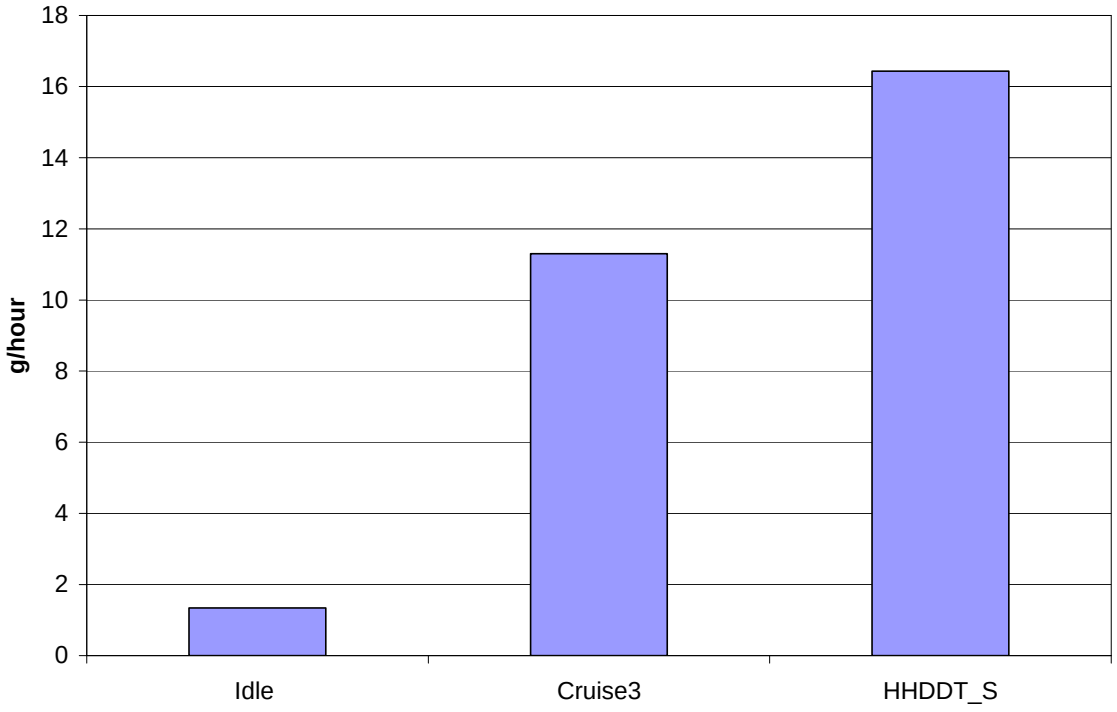

Figure 102: PM Mass Emissions for E55CRC-42

Particle sizes measured during the steady state and Cruise mode were similar with a CMD of 93.6 nm, 98.39 nm and 93.71 nm for the steady state, normal Cruise and High-speed Cruise Modes, respectively. Concentrations for the steady state mode were 6 times higher in magnitude as compared with both the Cruise Modes. Concentration drop for the Cruise mode could be due to a higher exhaust temperature. Sulfate emissions were higher during the Cruise mode at 0.54 g/hour when compared to Idle mode at 0.06 g/hour (Figure 104). Carbonaceous particles along with sulfates, and adsorbed of volatile and semi-volatile particles mostly constitute the nature of the particles emitted during the steady cycles. The total carbon in the idle mode PM is approximately evenly split between organic and elemental carbon. While the Idle Mode emissions are characterized by a distinct nuclei mode, the contribution of this fraction to the total PM mass emission rate is very small.

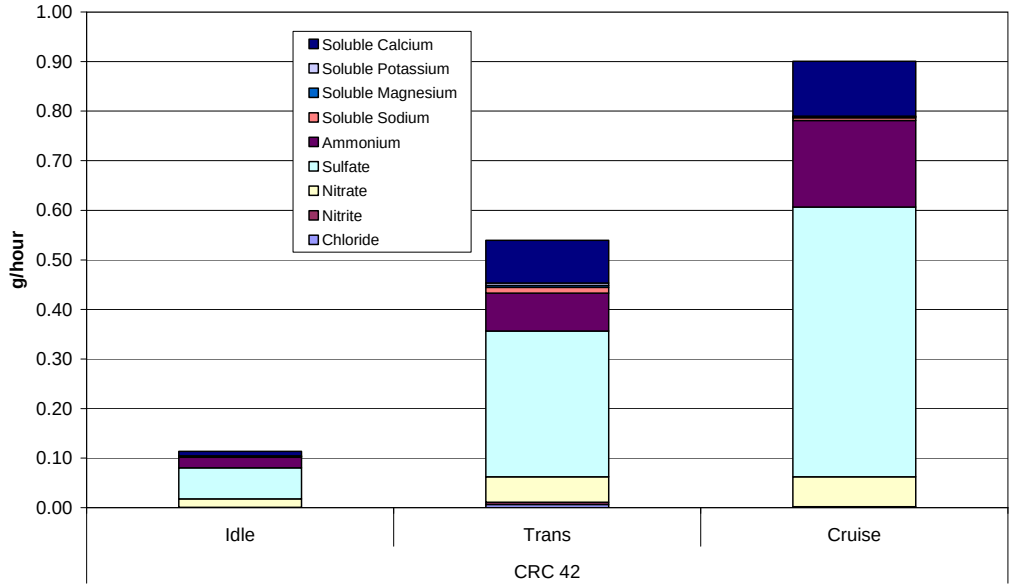

Figure 103: Ion Composite Results for E55CRC-42

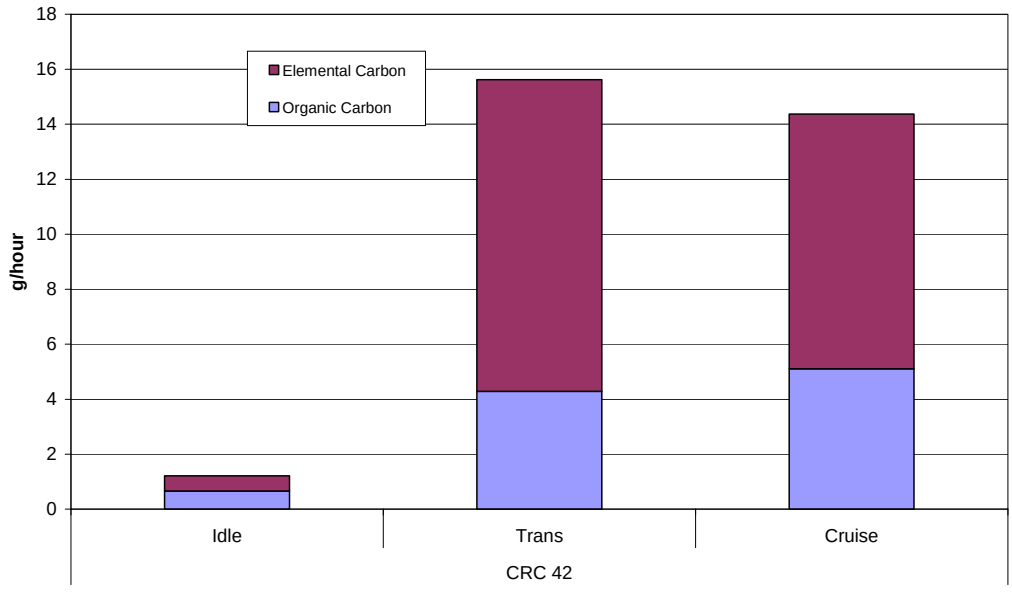

Figure 104: Elemental Carbon and Organic Carbon PM Analysis for E55CRC-42

For E55CRC-42, DMS500 data on the UDDS, Cruise mode and HHDDT_S showed anomalous behavior (output spikes) but two repeat runs on the Transient mode agreed acceptably well, as shown in Figure 105.

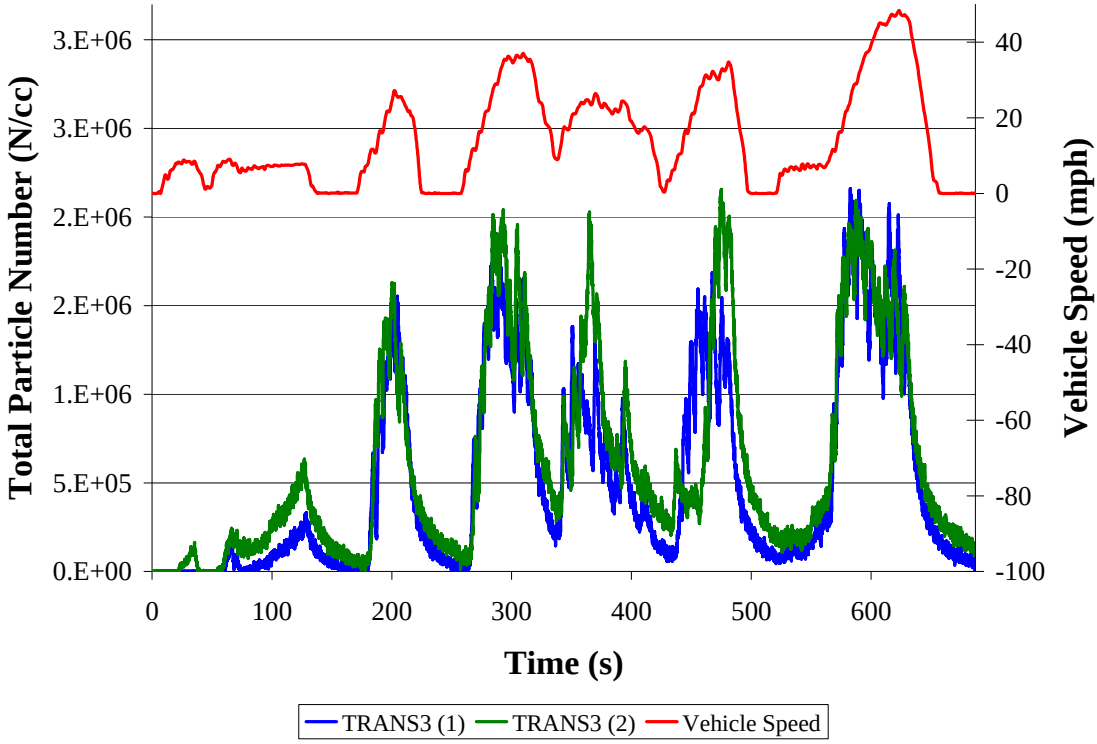

Figure 105: DMS500 Total Number of Particles and Vehicle Speed vs. Time on Transient mode for E55CRC-42 tested at 56,000 lbs.

E55CRC-43

E55CRC-43 was a powered by a Detroit Diesel Series 60, MY 1994 engine. Particle sizing and chemical speciation results are presented below for various modes of the HHDDT schedule. Figure 106 and Figure 107 present the particle size distribution for Idle and steady modes.

Particle size distribution for Idle Mode was unimodal with a CMD of 51.43 nm and a GSD of 1.44 which indicates a good distribution about the mean. Maximum concentration level was around 2.25×10^5 particles/cm^3. These particles are mostly accumulation mode particles as observed for E55CRC-42. Reasons for this accumulation mode are similar to those presented above for E55CRC-42.

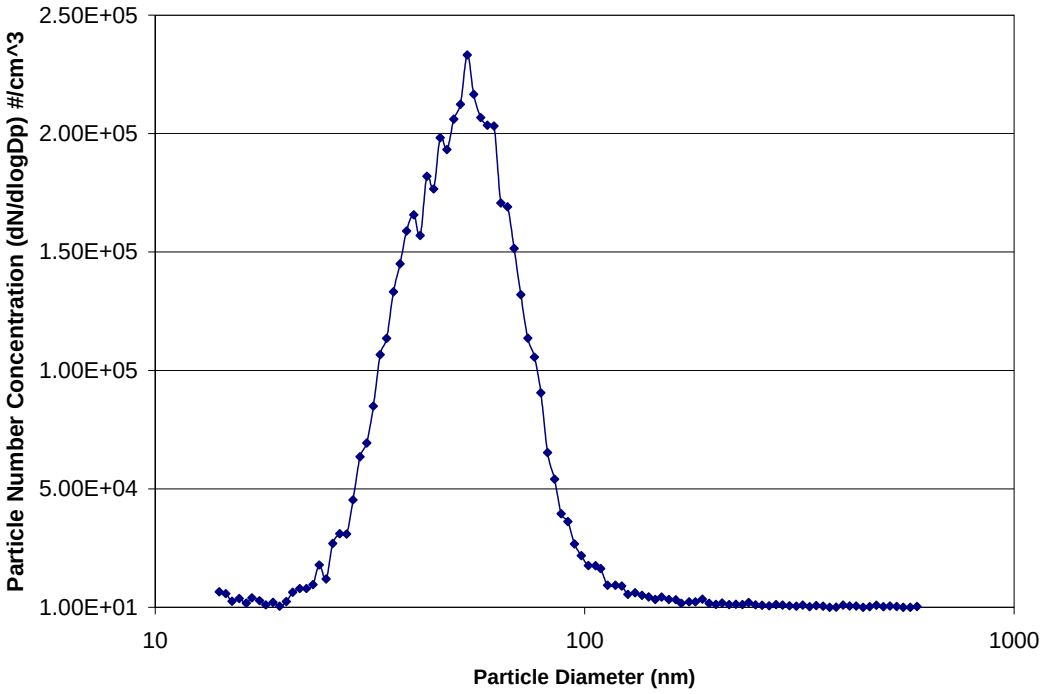

Figure 106: SMPS Particle Size Distribution for E55CRC-43 Operating on an Idle Mode

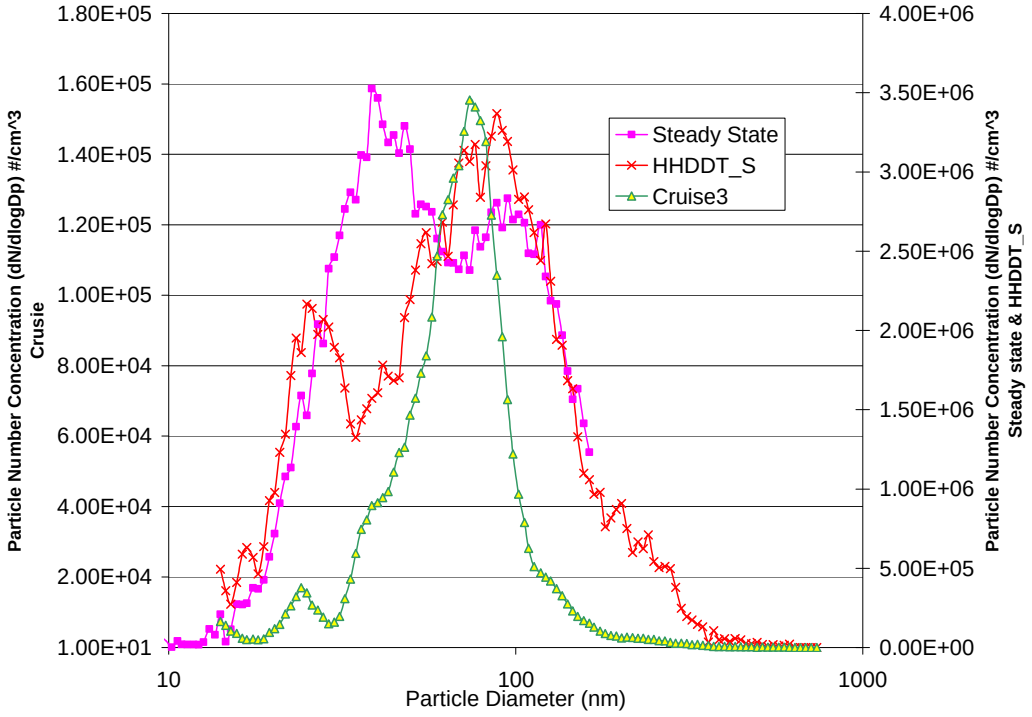

Figure 107: SMPS Particle Size Distribution for E55CRC-43 Operating on Various Steady Cycles

The total volatile organic compounds emitted by this particular vehicle were 2.28 g/hour for Idle and 3.39 g/hour for Cruise. Volatile compound emissions at Idle were 20% lower than E55CRC-42. A shift in the particle size was noted for the steady cycles. For the steady state and High-speed Cruise Modes, the GSD were 1.88 and 2.6, respectively, which is higher than the normal GSD which denotes a random distribution about the mean which can be clearly observed from Figure 107. The CMD noted for the steady state, normal Cruise and High-speed Cruise Modes were 54.32, 68.5 and 69.56 nm, respectively. It should be noted that in the case of a HHDDT_S or Cruise Mode scan, there is no assurance that the driver might not move the pedal and disturb the steady operation during SMPS scan. Elemental carbon emissions were very high during the Cruise Mode at 3.17 g/hour when compared to Idle Mode emissions at 0.25 g/hour. Organic carbon emissions were also higher during the Cruise mode at 6.15 g/hour when compared to Idle Mode emissions at 1.03 g/hour.

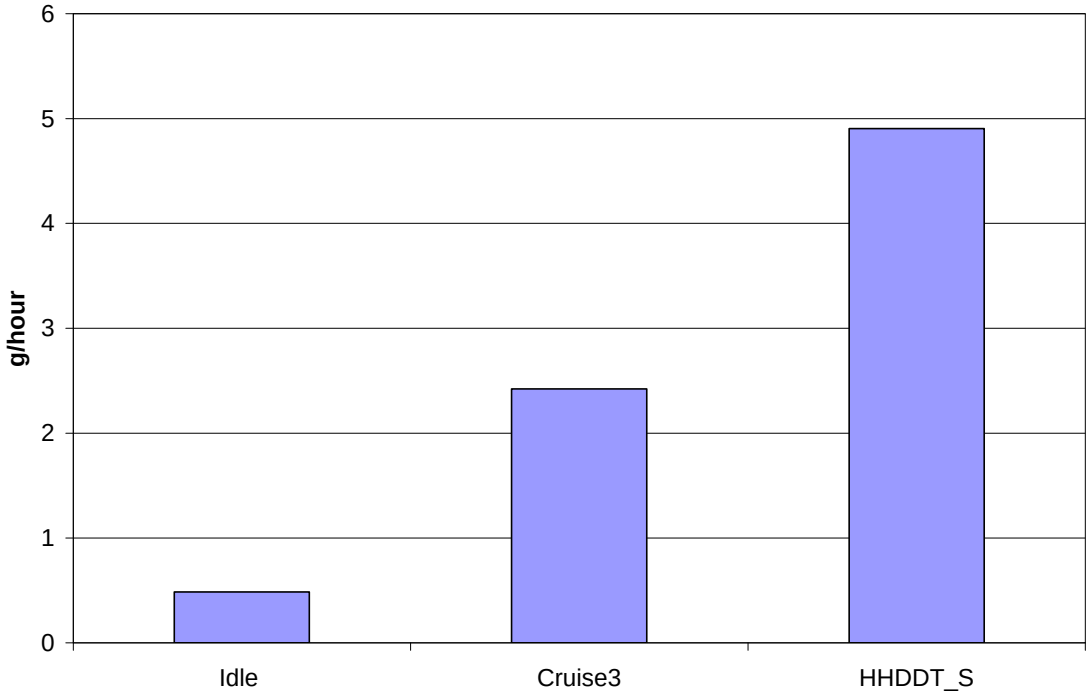

Figure 108: PM Mass Emissions for E55CRC-43

The increase in the particle size and concentration in the Cruise Modes is attributed to the very high increase in the elemental carbon emissions. A slight increase by 12% in the VOC emission was noted for the Cruise mode (Appendix O: Figure O37 to O41). An 85% increase in the sulfate emission was noted for the Cruise mode (Figure 109). Calcium was also a major contributor to the inorganic species with an increase of 91% for the Cruise Mode. Calcium emissions are attributed to lubrication oil, since calcium is a major constituent in lube oil. Particles measured during the Cruise mode of this particular vehicle were primarily carbonaceous soot with heavy hydrocarbons adsorbed onto the surface.

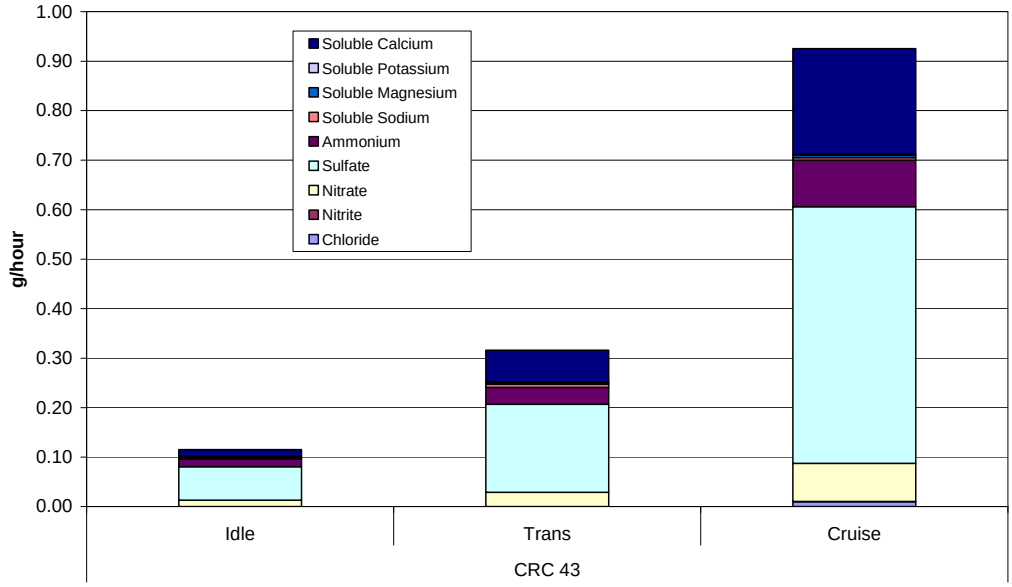

Figure 109: Ion Composite Results for E55CRC-43

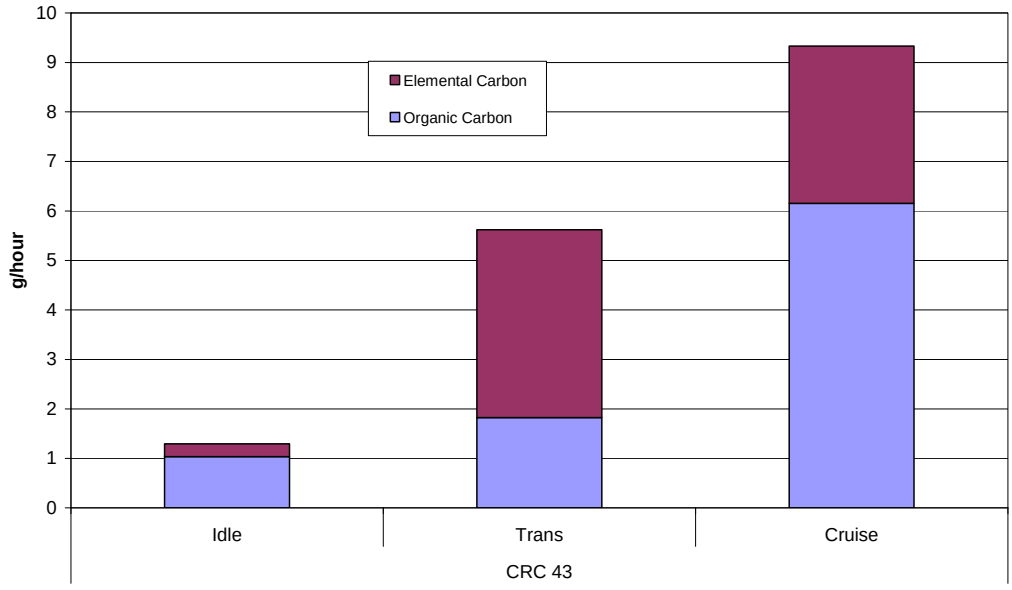

Figure 110: Elemental Carbon and Organic Carbon PM Analysis for E55CRC-43

DMS500 data were acquired for the Transient Mode, and are shown in Figure 111.

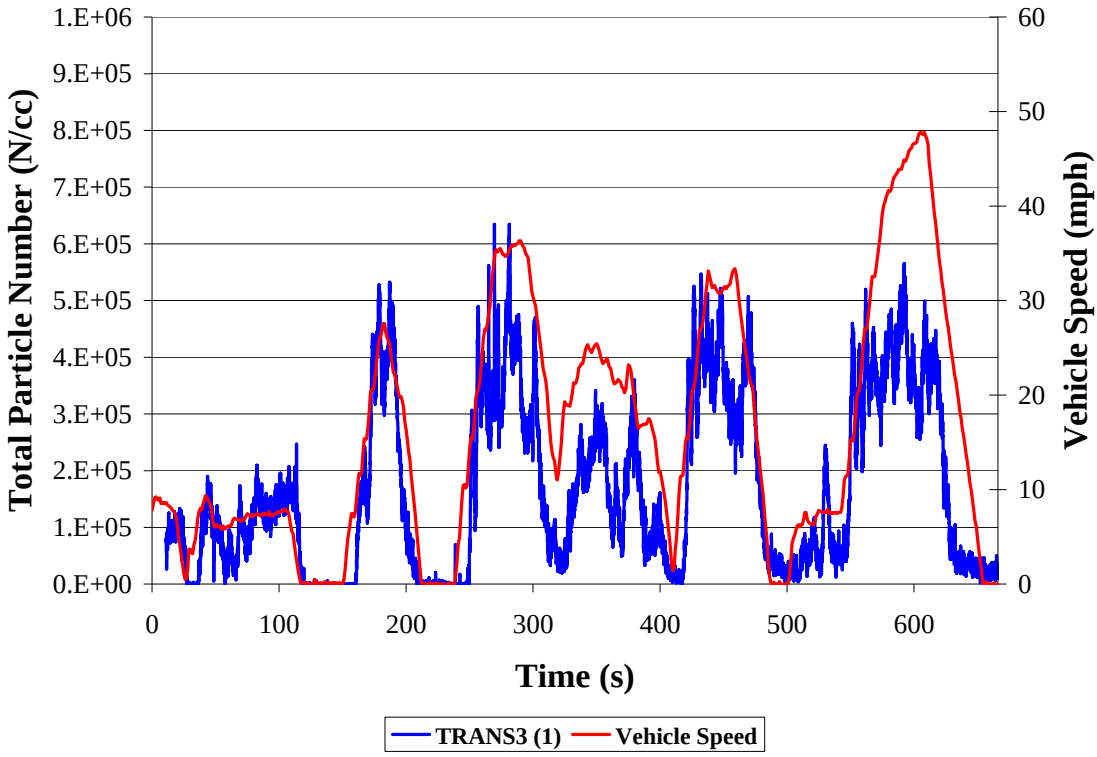

Figure 111: **DMS500 Total Number concentration of Particles and Vehicle Speed vs. Time for E55CRC-43 tested at 56,000 lbs.**

E55CRC-44

E55CRC-44 was a powered by a Caterpillar 3406, MY 1989 engine. Particle sizing and chemical speciation results are presented below for various modes of the HHDDT schedule. Figure 112 and Figure 113 present the particle size distribution for Idle and steady modes.

A bimodal distribution was noted for this particular vehicle during the Idle Mode, with one nano-particle peak at 26.9 nm and another accumulation mode peak at 122 nm. It should be noted that the Idle Mode is characterized by relatively lower PM number concentrations. The only other vehicle where a bimodal distribution was observed was E55CRC-39 which was a 2004 year model engine. The reason for the bimodal distribution for E55CRC-39 was due to high levels of volatile compounds and elemental carbon during the Idle Mode. The elemental carbon contributed to the accumulation mode.

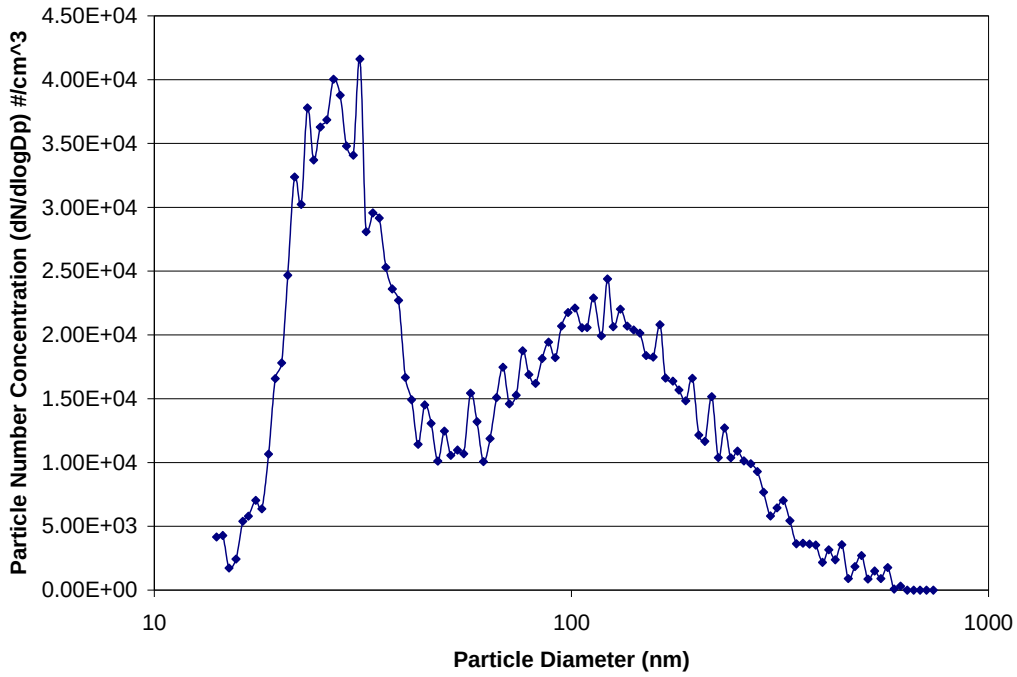

Figure 112: SMPS Particle Size Distribution for E55CRC-44 Operating on an Idle Mode

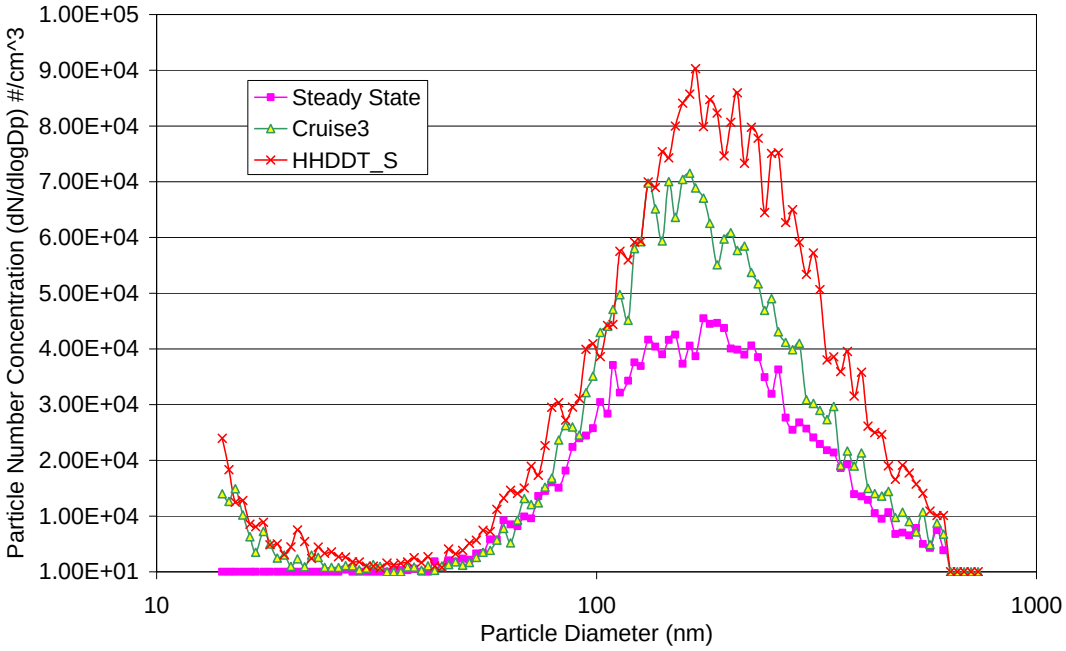

Figure 113: SMPS Particle Size Distribution for E55CRC-44 Operating on Various Steady Cycles

The precursors of the nano-particle emissions could be traced back to lube oil based volatile hydro-carbons, and the lower exhaust temperature during exhaust mode. Again, nano-particle peak could be due to high emissions of semi-volatile compounds (Appendix O: Figure O54 and O55). The total volatile compound emissions for this vehicle were 25% higher than E55CRC-43 and 35% higher than E55CRC-40. Further analysis yields that aromatic emissions during the Idle Mode, especially benzene were prominent for E55CRC-39 and E55CRC-44 when compared with the rest of the vehicles in the study (Appendix O: Figure O53). The accumulation mode in the Idle was attributed to the presence of carbonaceous agglomerates, with elemental carbon emission during the Idle mode being the highest among all the vehicles at 1.22 g/hour.

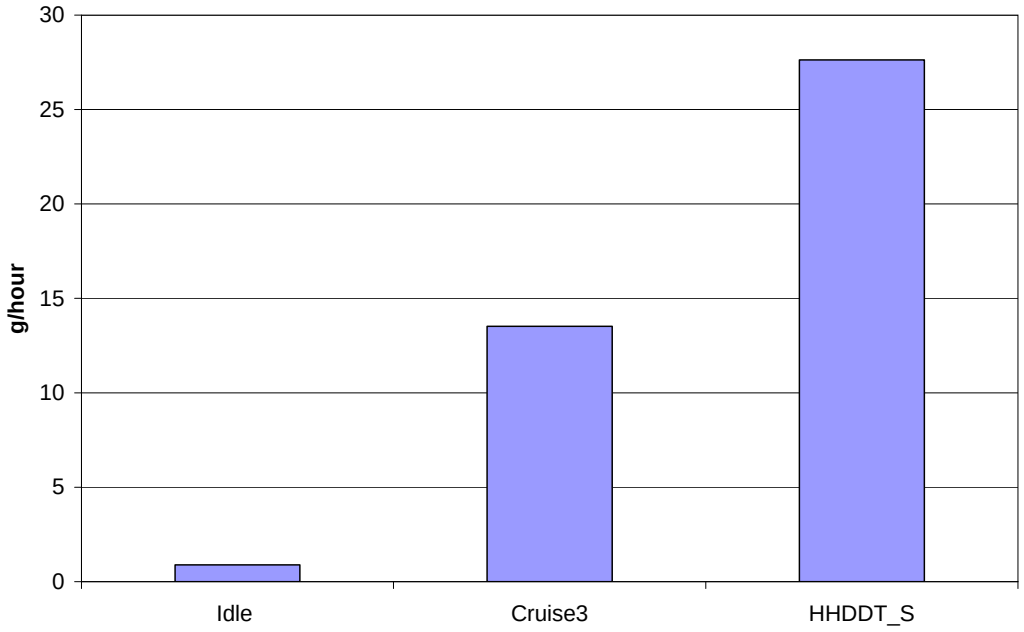

Figure 114: PM Mass Emissions for E55CRC-44

The steady state particle size distributions were compatible with vehicle speed. Particle concentrations were increasing, though minimally, with increasing speed without much variation in the particle size. The count median diameter for the steady state, normal Cruise and High-speed Cruise were 173, 166 and 178 nm, respectively. Mass emissions were highest during the Cruise and High-speed Cruise Modes when compared to other vehicles (Figure 114). Elemental carbon which is basically soot was noted to be the highest among all the vehicles during the Cruise mode (Figure 116) was also a major contributor to the mass emission. This would also contribute to low saturation ratios; hence, the absence of nano-particles. Sulfate emissions were among the lowest when compared with all other vehicles (Figure 115). Results from these data suggest that the fine particles measured during the Cruise mode were mostly solid carbonaceous particles.

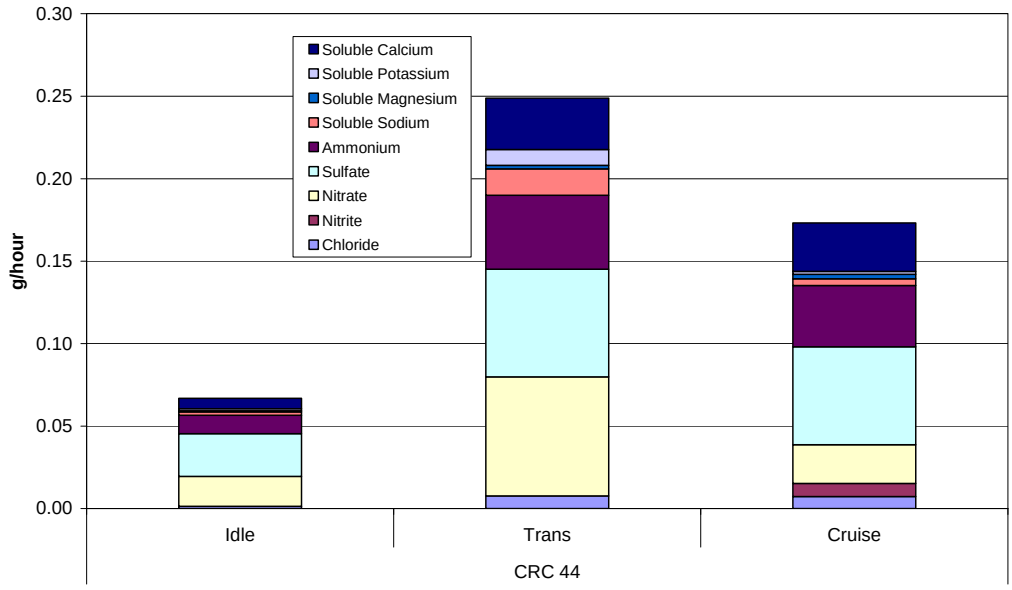

Figure 115: Ion Composite Results for E55CRC-44

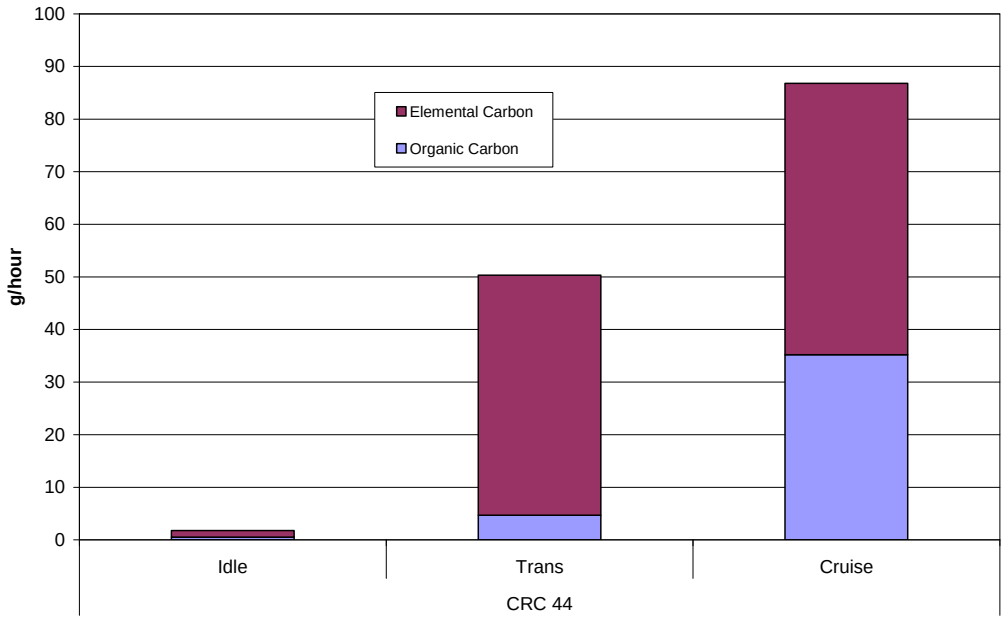

Figure 116: Elemental Carbon and Organic Carbon PM Analysis for E55CRC-44

No DMS500 data are available for E55CRC-44.

CONCLUSIONS, NONREGULATED SPECIES

Size distributions of PM from the six trucks were selected for non-regulated emissions measurement. These were acquired using a Scanning Mobility Particle Sizer (SMPS), as well as a Differential Mobility Spectrometer, Model 500 (DMS500), which was a newly released instrument. The SMPS was fed dilute exhaust from a mini-dilution tunnel, using a dilution ratio of thirty, while the DMS used the main dilution tunnel of the TransLab. The SMPS detected a bimodal distribution with a nuclei mode for Idle operation of one 2004 MY truck (E55CRC-40), and the DMS 500 detected both the nuclei mode and accumulation mode during deceleration on this truck. The nuclei mode was not evident under load for E55CRC-40. The other 2004 MY truck had only one mode, with a very low particle count on Idle. A 1989 MY truck had a bimodal Idle distribution, but the remaining HHDDT were unimodal. Comprehensive data were acquired for steady operation using the SMPS on all trucks, and the DMS500 acquired transient distributions for four of the trucks.

Chemical speciation was performed on the six trucks, with exhaust from the TransLab tunnel fed to a residence time chamber of the DRI. Data were acquired for methane and volatile organic compounds using a canister and a field gas chromatograph. Semi-volatile organic compounds were captured in PUF/XAD media and PM soluble fraction was captured on TIGF filters, and these were extracted and analyzed at the DRI laboratory. Carbonyls were captured using DNPH cartridges, nitrosamines in Thermosorb cartridges. Ions and Elemental/Organic carbon (EC/OC) split were determined from quartz filters. Results from the speciation data are legion, and examples include the fact that the EC/OC split differed substantially on Idle between the two 2004 MY trucks equipped with EGR, and that the ion and metal analyses varied widely between trucks.

Summarized below in a graphical form are the emissions of elemental carbon (as a percentage of total), inorganic ionic species, lubrication oil-based elemental emissions, and engine wear emissions in Figure 117 through Figure 120, respectively. Figure 117 shows that except for idle operation, the elemental carbon constitutes a significant portion of total carbon emissions. Transient operation, in particular, yields in excess of 60% of total carbon as elemental carbon. Total PM mass emissions, as discussed in the text, are the highest for the Transient mode, followed by Cruise, and then Idle. Total PM mass emissions under Idle are significantly lower than the Transient and Cruise modes. However, in terms of total carbon mass emission rates, the Cruise mode emits the highest levels, followed by the Transient mode of operation. The Idle mode is characterized by significantly lower rates of total carbon mass emissions.

The mass emissions rates of sulfates dominate the ionic species in the cruise and transient modes. The only other species of significance were nitrates and ammonium.

Total particulate matter comprises of elemental carbons, organic carbon, engine wear elements, lube oil based ash components, water, and ionic species. Most of these emissions are a result of un-burnt fuel and lubricating oil. Apart from severe engine wear (abrasive wear) on boundary lubricated surfaces (cam lobe wear, tappet polishing,

rocker/crosshead wear, ring wear at top and bottom reversal locations, etc.), oil control is extremely critical from an emissions point of view. Based upon prior studies by Lapin et al.[19] and Gautam et al.[14], it may be hypothesized that products of lubricating oil combustion (partial) result in higher potential mutagenicity of exhaust emissions, and that lubricating oil contributes to high concentrations of nanoparticles in exhaust emissions[1]. Lubricating oil enters the combustion chamber through the following routes: as blow-by gas, leakage past valve stem seals, piston rings and vaporisation from the cylinder liner walls and combustion space[20].

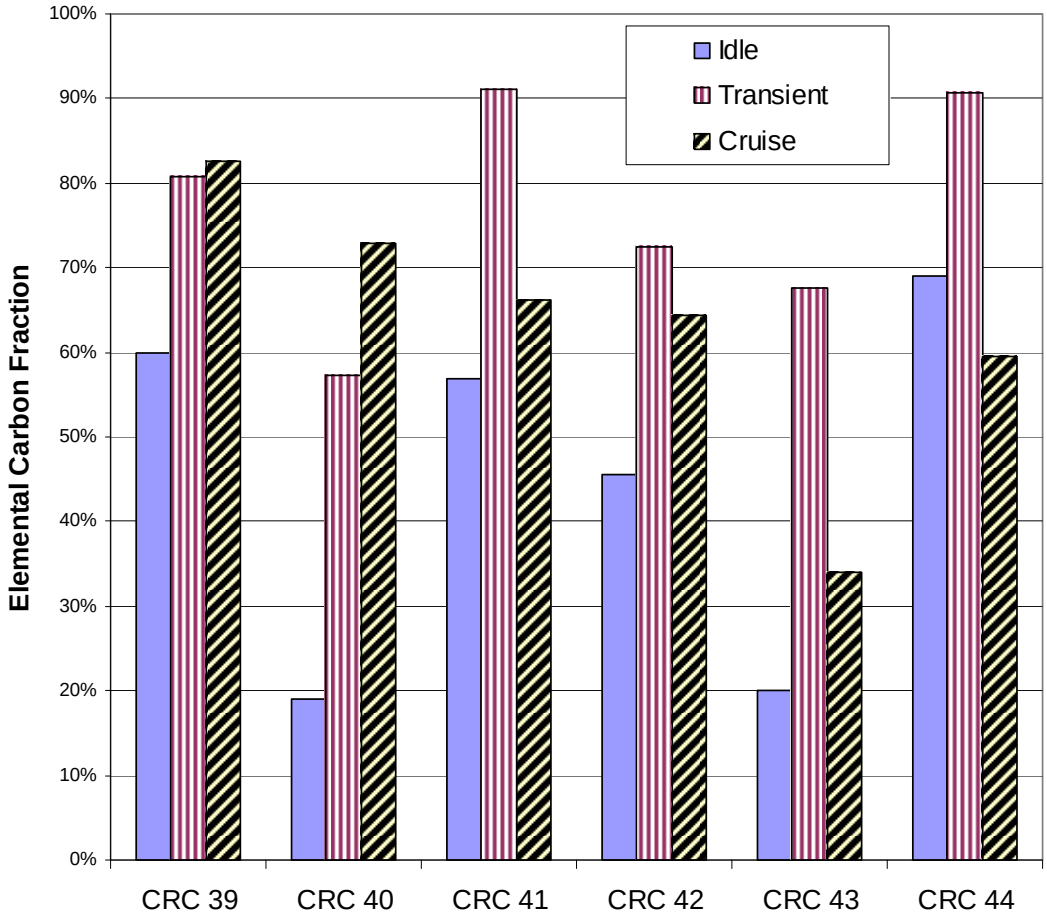

Figure 117: Elemental Carbon Emissions (Percentage of Total Carbon)

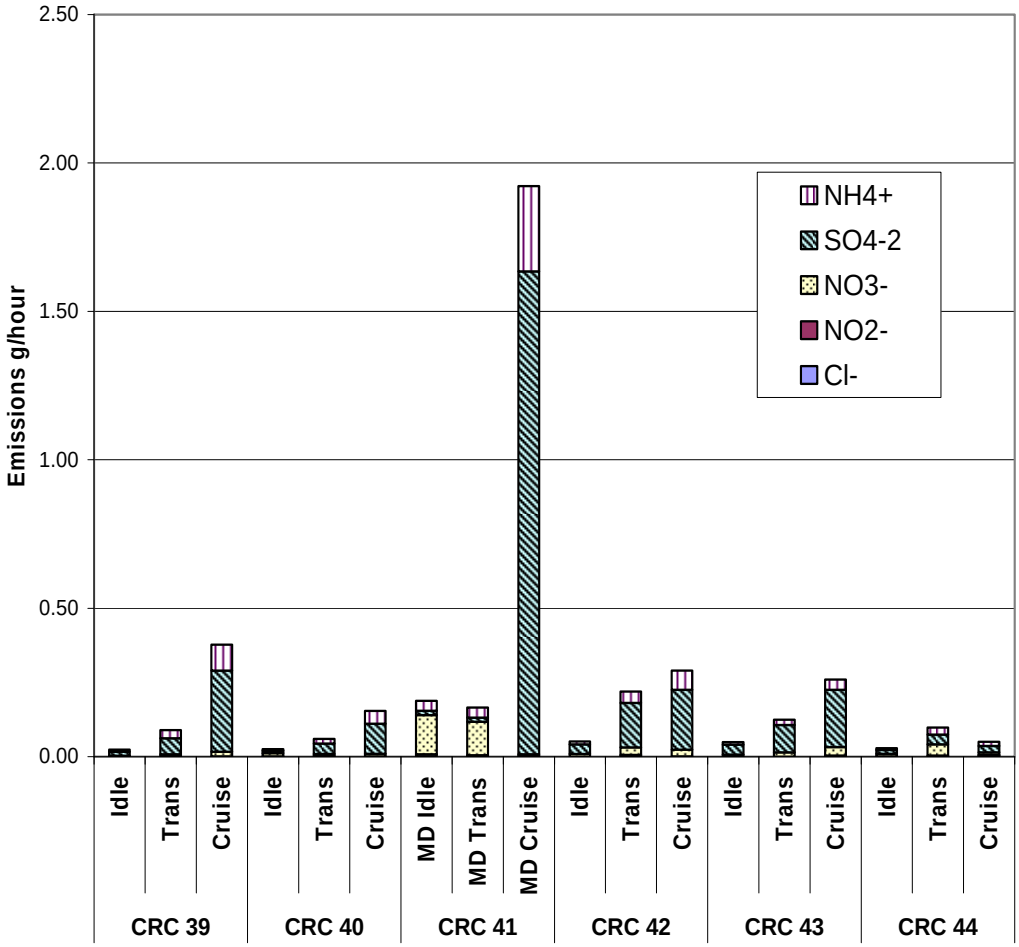

Figure 118: Inorganic Ionic Species Emissions

Figure 119 shows the mass emission rates of lubricating oil based elements from the test engines. These elements contribute to the total PM mass. Again, sulfur and calcium are the principal pollutants that can be traced back to the lubricating oil. In the older engines (CRC-42 and CRC-43) phosphorus emissions were significantly higher than those from other newer engines.

Figure 120 shows a summary of mass emissions rates of engine wear elements. Among these elements, iron contributed the most to the total PM emissions under all modes of operation. Of course, in terms of mass emission rates, iron emissions were the higher in the Transient and Cruise Modes of operation.

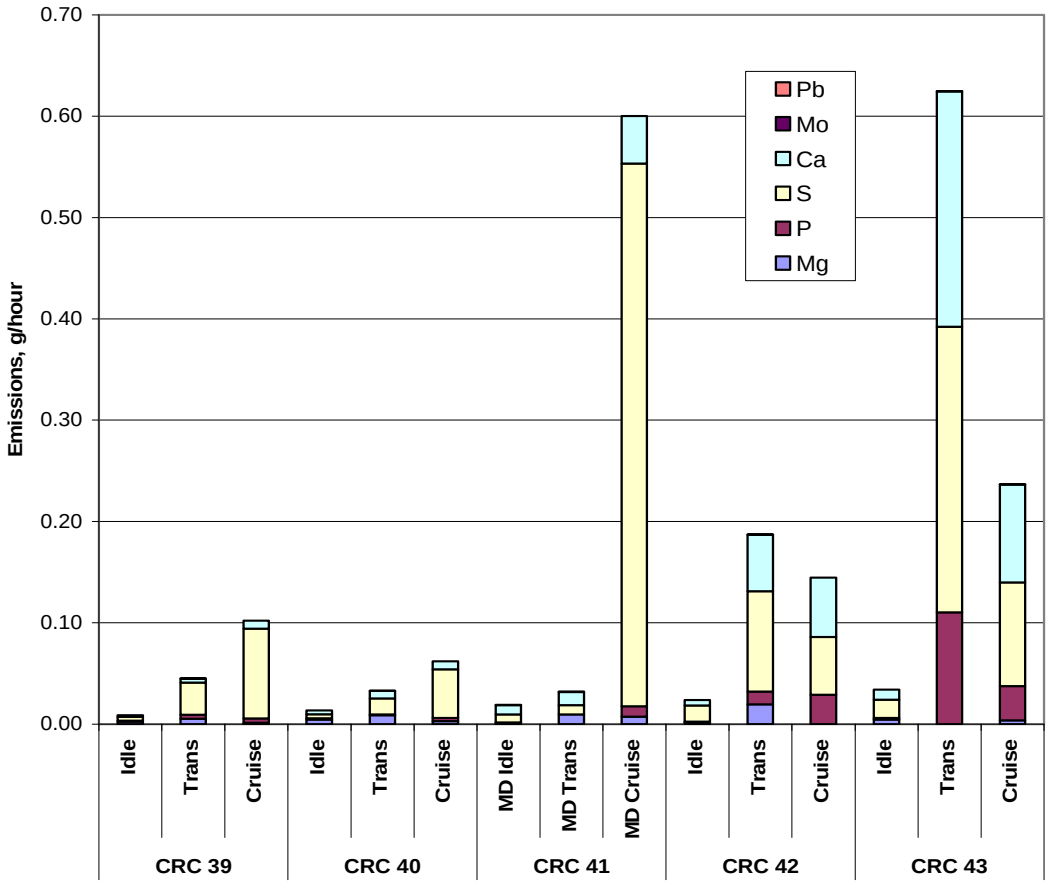

Figure 119: Lubrication Oil Emissions

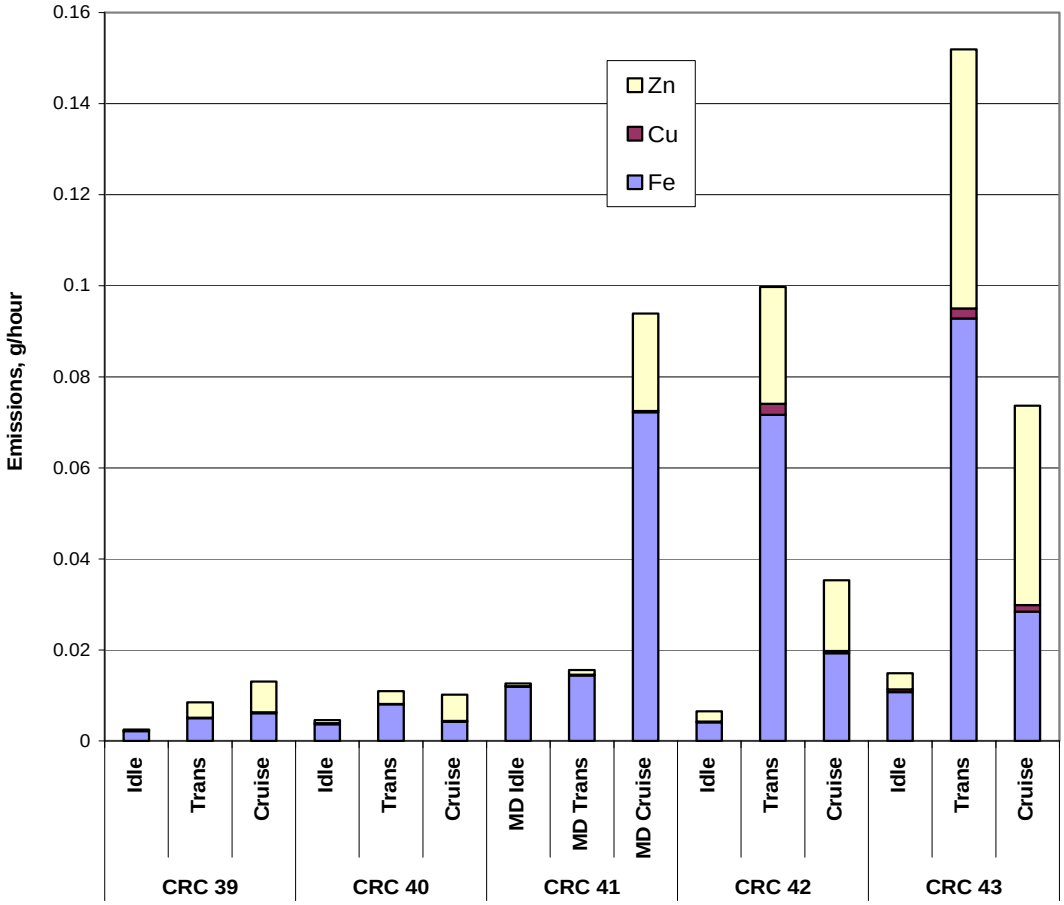

Figure 120: Engine Wear Emissions

TAMPERING, MALMAINTENANCE AND REFLASH VEHICLES

The E-55/59 program sought to identify high emitters, or vehicles that showed evidence of T&M. Vehicles were identified as T&M candidates either from a pretest inspection or from measurement of emissions that were high relative to developed threshold criteria. The criteria for declaring NO_x to be high were developed using NO_x/CO_2 ratios from certification data, and the PM criteria were developed as PM/CO_2 ratios considering Phase 1 fleet data statistically. The program plan provided that high emitters could be subjected to repair, followed by re-testing of emissions. In addition, during Phase 1.5 of the program, three truck engine controllers were reflashed. These trucks had MY that suggested that they may have off-cycle control strategies in the controller, and the effect of reflashing to a lower NO_x strategy was assessed.

Diesel vehicle deterioration and inspection and maintenance have been discussed previously by Weaver and Klausmeier[21] and Weaver et al.[22], but few data exist either on the incidence of high emitters or the effect of repair on truck emissions. The website http://www.driveclean.com/downloads/2003_HDV_Report.pdf provides modeling information as part of the Ontario, Canada, Drive Clean program. Yanowitz and co-workers1'[23] have presented the change of emissions with truck MY, but this cannot be uniquely ascribed to deterioration of emissions.

T&M Criteria

An objective of the E55/59 program was to quantify the influence of T&M on heavy-duty vehicle emissions. This was achieved by identifying test vehicles that qualified as candidates for the study, using two separate pathways:

1. *Vehicle Inspection:* Vehicles were considered candidates if they showed evidence of T&M that may affect emissions. The evidence might be found at the time of vehicle inspection, or revealed during the test procedure. A vehicle might qualify for repair and retest as a result of inspection, but might prove to yield emissions at a level below that considered high or gross.
2. *High Emissions Levels:* Vehicles were considered as candidates if they showed emissions levels that were high, or gross, relative to expected levels for those vehicles. It was not required that visual T&M was evident for these high emitting vehicles.

Determination of Candidates from Vehicle Inspection

The vehicles from the program in Phase 1 of E-55/59 were recruited either directly by WVU or with the aid of the California Trucking Association. In subsequent phases the vehicles were recruited by WVU alone. Vehicles were transported to the test site in Riverside, CA. Each vehicle was inspected to identify any of the following tampering or malmaintenance items.

1. Cleanliness of air filter.
2. Integrity of lines between turbocharger an intercooler.
3. Integrity of lines between intercooler and engine intake.
4. Presence of manifold air pressure sensor (MAP) and integrity of wiring connection to MAP (This applies to most electronic engines).
5. Presence of manifold air temperature sensor (MAT) and integrity of wiring connection to MAT (This applies to most electronic engines).
6. Integrity of wiring harness and connections to engine controller (This applies to all electronic engines where the controller is visible).
7. Integrity of wastegate/boost control on turbocharger (This applies to many newer electronic engines).
8. Condition of intercooler, though in many cases the core will not be visible because it is sandwiched between the air conditioner and radiator.
9. Integrity of linkages and fuel lines surrounding fuel injection pump, or breakage of seal on fuel injection pump (This applies to older mechanical engines).
10. Correctness of fuel (not dyed off-road fuel) in tank, where practical.

If inspection identified a technical or maintenance concern that might affect emissions, the vehicle immediately became a "T&M candidate," which could potentially be subjected to repair and retest.

Determination of T&M Candidate from Emissions

In the study, vehicles were potential candidates for repair and retest if they were identified as high emitters. The term "high emitters" was intended to represent vehicles emitting PM or NO_x at gross levels; that is, levels, which are substantially higher than would be expected from a statistical sample of similar, correctly operating vehicles. In E-55/59 the criteria for high emissions were developed during Phase 1, and were applied in this form to all phases of the program.

High HHDDT emitters of NO_x were identified in the following fashion. NO_x emissions were known to be dependent on engine power (and hence fuel consumed), but relatively insensitive to the transient nature of tests unless the engine control included off-cycle strategies. In many cases NO_x varies in a linear fashion with brake power and in direct proportion to fuel consumed[24,25]. It is therefore reasonable to compare NO_x/CO_2 ratios for different tests, although the investigators were aware of the way in which off-cycle engine timing could elevate NO_x levels. Cycle effects on NO_x emissions have recently been discussed by Clark et al.[26] and are addressed in a paper by Yanowitz et al.[1.]

Table 6 provides the U.S. certification levels for engines. The "2003+" value for NO_x recognizes that the 2004 regulations were brought forward from 2004 for the manufacturer according to the Consent Decree, and approximates the NO_x level at 2.0 g/bhp-hr. Ratios by mass of NO_x/CO_2 implied by the certification can be determined if a

typical Federal Test Procedure certification level of 550 g/bhp-hr (738 g/kw-hr) of CO_2 is assumed. When a normally operating engine is exercised through cycles other than the certification cycle as in the case of the E-55/59 program, NO_x/CO_2 ratios may deviate from the certification NO_x/CO_2 ratios for two reasons. Firstly, the engine timing is not uniform over the whole operating envelope, and may differ slightly between the certification envelope and remainder of the operation envelope. This may cause modest increases (or decreases) in the NO_x/CO_2 ratio. This is likely to have a greater effect in electronic engines or in mechanical engines without variable injection timing. Secondly, many electronic engines have off-cycle NO_x missions as a result of employing a separate timing map during some instances of real-world operation. This is known to raise NO_x by a factor of up to 2.5[27], corresponding to 10 to 12 g/bhp-hr (13 to 16 g/kw-hr) NO_x for engines certified to 5 g/bhp-hr (6.7 g/kw-hr), even at high load conditions. Engines operating off-cycle are not considered to fit the T&M criteria because they are in original condition and need not be reconfigured except at the time of rebuild, under rules prevailing during the time of the E-55/59 program. Off-cycle emissions of this kind occur solely with electronic engines.

In the E-55/59 program, emissions values used to determine whether a vehicle was a high NO_x or PM emitter were taken from the transient and cruise modes of the HHDDT schedule. This schedule was created and evaluated by the California Air Resources Board and WVU in a previous cooperative effort[28,29]. There were at least two repeat runs of the transient and cruise modes for each vehicle. Data were acquired at a test weight of 56,000 lbs. (25,402 kg). A vehicle (1) had to show high NO_x in two transient runs to be considered a high NO_x emitter on the transient mode, or (2) had to show high NO_x in two cruise runs to be considered a high NO_x emitter on the cruise mode. Similarly, the vehicle (3) had to emit high PM in two transient runs conducted to be considered a high PM emitter on the Transient or (4) produce high PM in two cruise runs conducted to be considered a high PM emitter on the transient mode. The vehicle was considered a high emitter and as a candidate for repair and retest under any one of these four circumstances. In order to avoid capturing "off-cycle" emissions vehicles as T&M vehicles, the NO_x/CO_2 ratio for identifying a candidate vehicle was set at three times the certification NO_x/CO_2 ratio for electronic engines. For mechanically injected engines, the criterion NO_x/CO_2 ratio was set at twice the certification NO_x/CO_2 ratio.

Table 19 shows the resulting emissions level criteria used to declare a truck to be a high NO_x emitter. Table 19 uses California certification values and vehicle MY as a basis.

In cases where vehicles pre-dated the advent of brake-specific emissions standards for values of NO_x emissions, a value of 10g/bhp-hr (13.4 g/kw-hr) was used as if it were a certification standard in identifying high NO_x emitters. Early vehicles all have mechanically controlled engines, so that the failure criteria shown below were based on a NO_x/CO_2 ratio for these early vehicles using twice this assumed level; i.e., 20 g/bhp-hr (26.8 g/kw-hr).

Table 19: Emissions level criteria used to declare a truck to be a high NO_x emitter.

California	NO_x g/bhp-hr (g/kw-hr)	CO_2 g/bhp-hr (g/kw-hr)	NO_x / CO_2 Certification Ratio	Mechanical High Emitter Criterion (Cert x 2) NO_x/CO_2	Electronic High Emitter Criterion (Cert x 3) NOx/CO_2
1987-90	6 (8)	550 (738)	0.0109	0.0218	0.0327
1991-93	5 (6.7)	550 (738)	0.0091	0.0182	0.0273
1994+	5 (6.7)	550 (738)	0.0091	0.0182	0.0273
1994-95	5 (6.7)	550 (738)	0.0091	0.0182	0.0273
1996+	4 (5.4)	550 (738)	0.0073	0.0145	0.0218

No detailed criteria were developed in Phases 2 and 3 for the MHDT: the researchers used their own judgment in reviewing the NO_x emissions data to determine if a truck should be considered as an MHDT T&M candidate. One MHDT, CRC-57, revealed a cooling malfunction on the dynamometer and was the only MHDT that was identified as a T&M candidate. CRC-57 was not repaired, and is discussed in a separate section below. Determining high HHDDT PM emitters was more difficult than determining high NO_x emitters because PM is highly sensitive to the transient content of a cycle and therefore cannot be projected for different cycles using certification data[26,30,31]. PM emissions drop only very slightly as a result of off-cycle operation, so off-cycle operation need not be considered with regard to PM. To determine PM high emitters, the data for each of the 25 trucks (all HHDDT) in Phase 1 of the program in the transient and cruise modes were expressed as ratios of PM/CO_2. This ratio was then divided by the PM/CO_2 ratio for the certification standards for that engine MY, assuming a level of 550g/bhp-hr (738 g/kw-hr) of CO_2 for certification. This "criterion ratio" calculation is shown below. The criterion ratio for vehicles that pre-date the PM transient test (FTP) standards in their MY was based on a PM pseudo-standard of 1g/bhp-hr (1.3 g/kw-hr) PM.

Consider an example using actual data from a vehicle with an engine manufactured in 1999 or 2000 during the Transient mode of the HHDDT schedule:

Actual data for Transient Mode

PM = 0.4435 g/mile (0.2756 g/km)

CO_2 = 2599 g/mile (1615 g/km)

$(PM/CO_2)_{Trans}$ = 0.000171

1999 – 2000 Certification

PM = 0.1 g/bhp-hr (0.134 g/kw-hr)

CO_2 = 550 g/bhp-hr (738 g/kw-hr)

$(PM/CO_2)_{Cert}$ = 0.000182

$$\text{Criterion\_Ratio} = \frac{(PM/CO_2)_{Trans}}{(PM/CO_2)_{Cert}} = 0.939$$

For a vehicle to be identified as a high PM emitter, this criterion ratio described above had to be significantly higher than the criterion ratios for typical vehicles in the fleet. In this case the term "typical vehicles" refers to both normal and high emitters. Note that the inclusion of certification levels in the criterion ratio does allow for influence of changing technology in identifying high PM emitters. To achieve this identification goal, it was necessary to build a database of PM criterion ratios from the initial vehicles that were tested, and determine the average and standard deviation of those criterion ratios. Any truck that was two standard deviations above the average on two runs of the Transient mode was deemed a high PM emitter for the transient mode. Any truck that was two standard deviations above the average on two runs of the Cruise mode was deemed a high PM emitter for the cruise mode. Since the database of vehicles tested evolved over the duration of the program, it was possible that the statistics would change over time, but no remedy for this change was possible. It was noted that in this methodology vehicles with high emissions on the Transient mode but not on the Cruise mode would most likely be "puffers," caused by turbocharger damage or fuelling limit tampering, while those that were found to be high using the cruise criterion (whether they are high on the transient or not) were likely to be continuous smokers at high load. The statistical criteria for high PM emitters were finalized in Phase 1 and used to identify for high emitters of PM in subsequent phases.

No detailed PM high emitter criteria were developed in Phases 2 and 3 for the MHDT: the researchers used their own judgment in reviewing the PM emissions data to determine if a truck should be considered as an MHDT T&M candidate.

Once a vehicle was identified as a high NO_x or PM emitter, it was treated in the same way as a vehicle that was found to have evidence of T&M upon inspection.

Results: T&M by Inspection

All vehicles were subjected to both inspection and emissions characterization. One vehicle, E55CRC-21, was found to have a dirty air filter by inspection, and became a T&M candidate. The repair and retest data of E55CRC-21 are presented in a separate section below. Two other vehicles, E55CRC-16 and E55CRC-45, were visually identified as prodigious smokers. E55CRC-16 subsequently was found to have emissions management components removed, but it was treated in the program as having high PM emissions by measurement. No other vehicles were considered as T&M vehicles by inspection. However, in Phase 3 one HHDDT brought to the site was visibly in poor repair, ceased running after arrival, and was not tested.

Verifying the Criteria in Phase 1: NO_x Analysis

Figure 121 shows the NO_x/CO_2 ratios for each run on the twenty-five Phase 1 vehicles, for both Transient and Cruise Modes. Vehicle E55CRC-10 was the only vehicle to be identified as a "high" NO_x emitter according to the T&M plan.

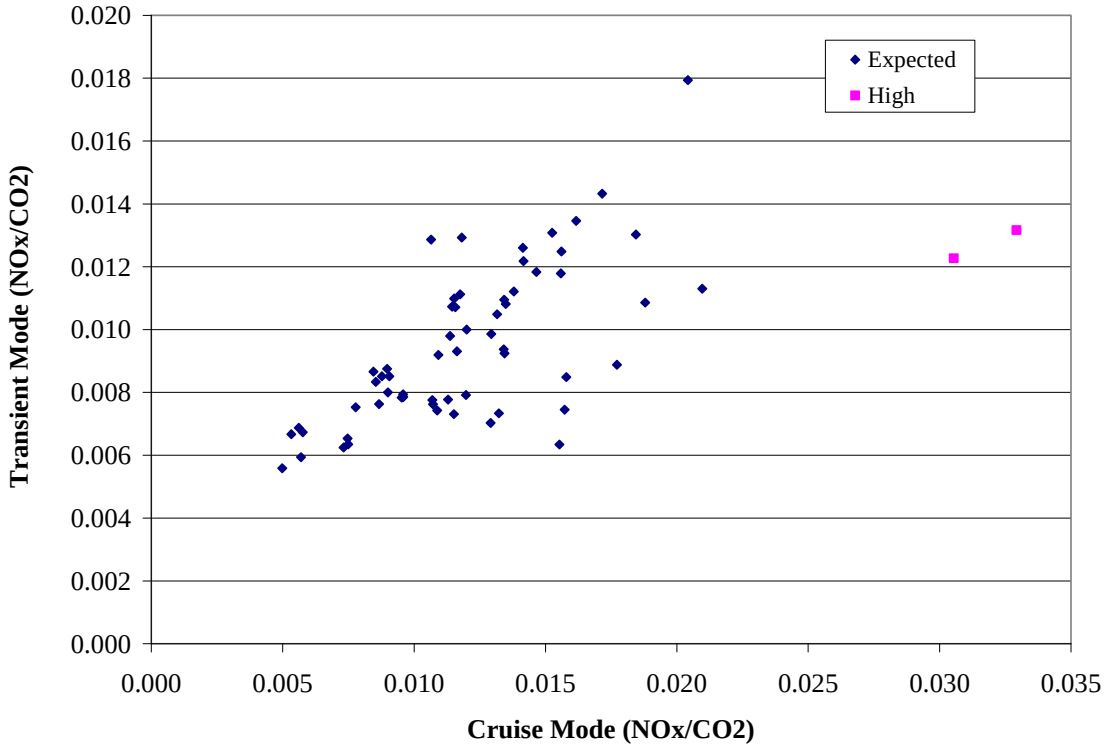

Figure 121: NO_x/CO_2 ratios for each run on the 25 vehicles, both transient and cruise. One vehicle was found to have high NO_x emissions on two runs of the cruise mode

The high criterion for vehicle E55CRC-10 was 0.0218 (See Table 2). Since the vehicle greatly exceeded the criterion, the data were more closely investigated. The fact that NO_x emissions were high on cruise but low on transient operation was an indicator that off-cycle emissions were the cause. To investigate these further, NO_x emissions were plotted continuously against the power. Figure 122 shows the NO_x emissions versus dispersed power plot for both the cruise and transient modes of the new ARB HHDDT schedule for E55CRC-10. Dispersed power is power that has been diffused in time to provide a closer correlation with measured emissions[32]. In preparing plots of this kind it is important to shift the emissions in time to match the power, because of measurement delay: this is achieved using cross correlation, because it is known that power and NO_x vary in sympathy. It is evident that the vehicle exhibited classical "off-cycle" behavior with the bulk of the transient emissions at a low NO_x level, and the bulk of the cruise emissions at a high NO_x level. However, whereas most trucks yield off-cycle values (in brake-specific terms) that are about 2.5 times the "on-cycle" values, this truck had values exceeding three times. A contribution to this high ratio was its low original standard of 4 g/bhp-hr

(5.36 g/kw-hr). The investigators believed that the high NO_x was simply an original off-cycle phenomenon, and would therefore not be remedied by any repair. This vehicle was therefore not selected as a T&M vehicle, but was selected for reflash of its controller and termed a Reflash Vehicle.

The finding that the high NO_x emissions of E55CRC-10 were not due to a T&M cause suggested that it would be difficult to identify high NO_x emitters as T&M candidates if they had electronic engine controllers that caused off-cycle emissions. In Phase 1.5 of the program, rather than seeking high NO_x emitters by the criterion, three trucks with electronic engine control were selected directly for reflash and retest. The results for these three trucks, which coincidentally included a T&M vehicle (E55CRC-28), are treated in a separate section below.

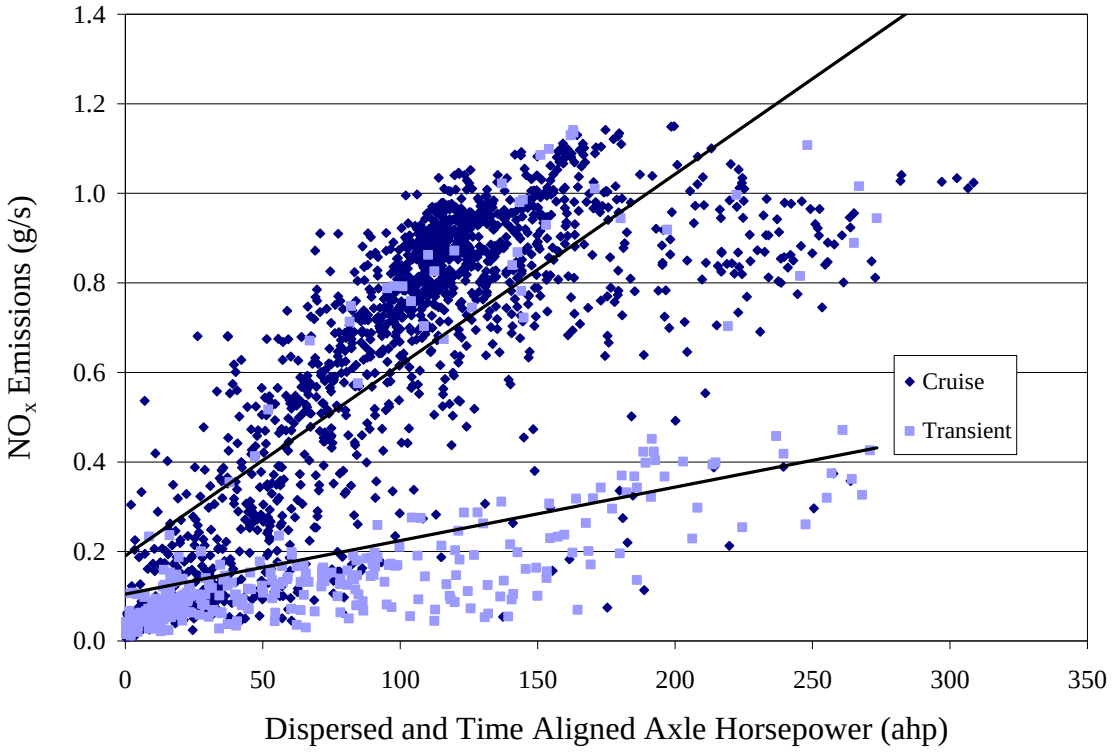

Figure 122: NO_x emissions plotted against the dispersed and time aligned power for vehicle E55CRC-10. Most emissions during the Cruise mode were at an off-cycle level. The vehicle was targeted for Reflash as a result of these data.

Verifying the Criteria in Phase 1: PM Analysis

Figure 123 presents the average value of PM/CO_2 ratios for Cruise mode operation of each Phase 1 HHDDT, and Figure 124 presents the average value of PM/CO_2 ratios for the Transient Mode operation of each vehicle. These values were then converted to criterion ratios according to the T&M methodology described above. It was found that the average criterion ratio for the Transient Mode was 1.2736 with a standard deviation of 1.1486. It was found that the average criterion ratio for the cruise cycle was 0.5207 with a standard deviation of 0.3567. These data suggest that if trucks were as "clean" as

when they were certified using the FTP, the Transient Cycle elicited higher brake-specific PM than the FTP, while the cruise cycle exhibited lower PM than the FTP. This is to be expected noting the relative transient content of the Transient and Cruise Modes[29,33] and the fact that transient behavior usually elicits higher PM production.

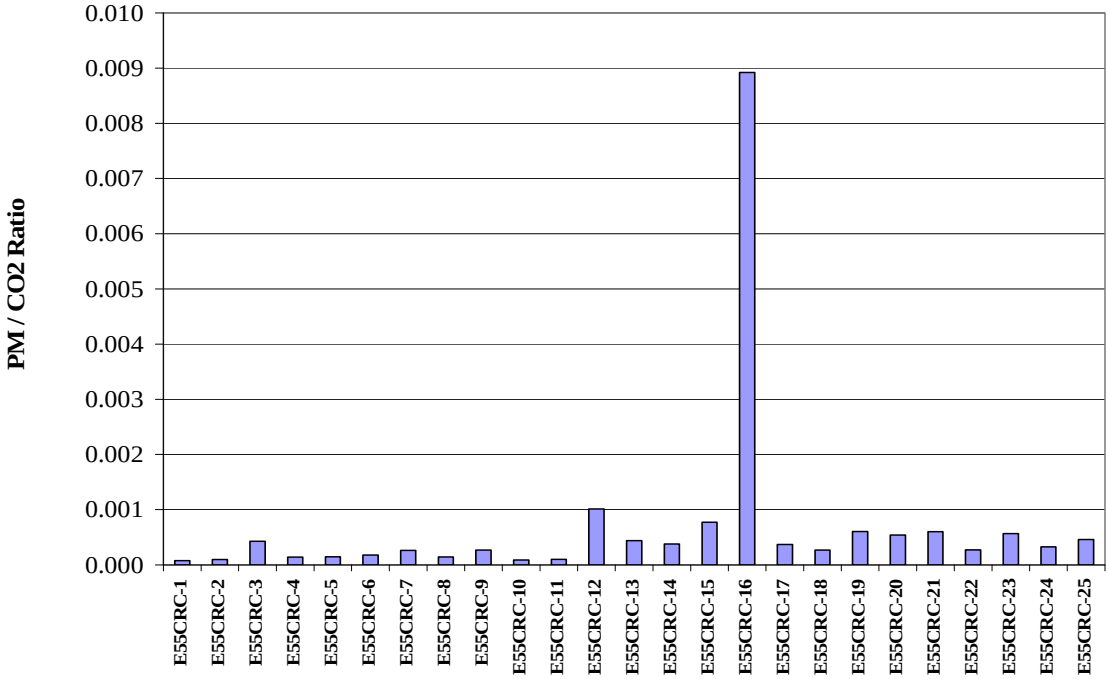

Figure 123: PM/CO_2 ratios for Cruise Mode operation of average value for each vehicle. There are two runs each for E55CRC-1 to -13, and three runs each for E55CRC-14 to -25.

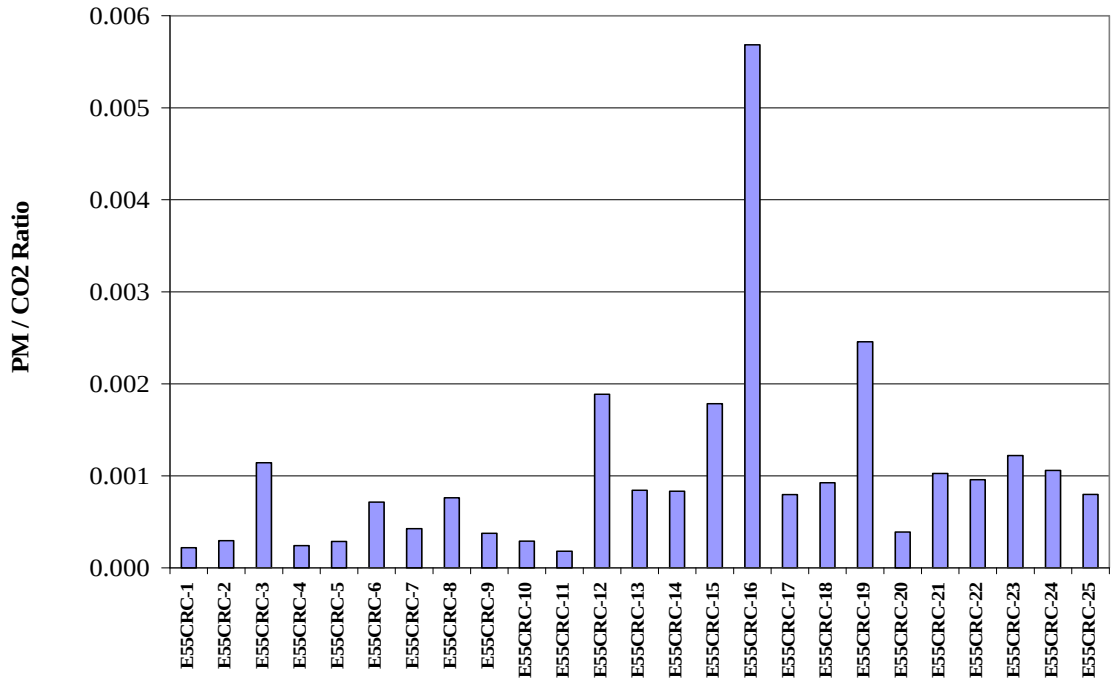

Figure 124: PM/CO_2 ratios for the Transient Mode operation of average value for each vehicle. There are 2 runs each for E55CRC-1 to -13, 3 runs each for E55CRC-14 to -25. One run for E55CRC-20 was anomalous low, but no cause was evident.

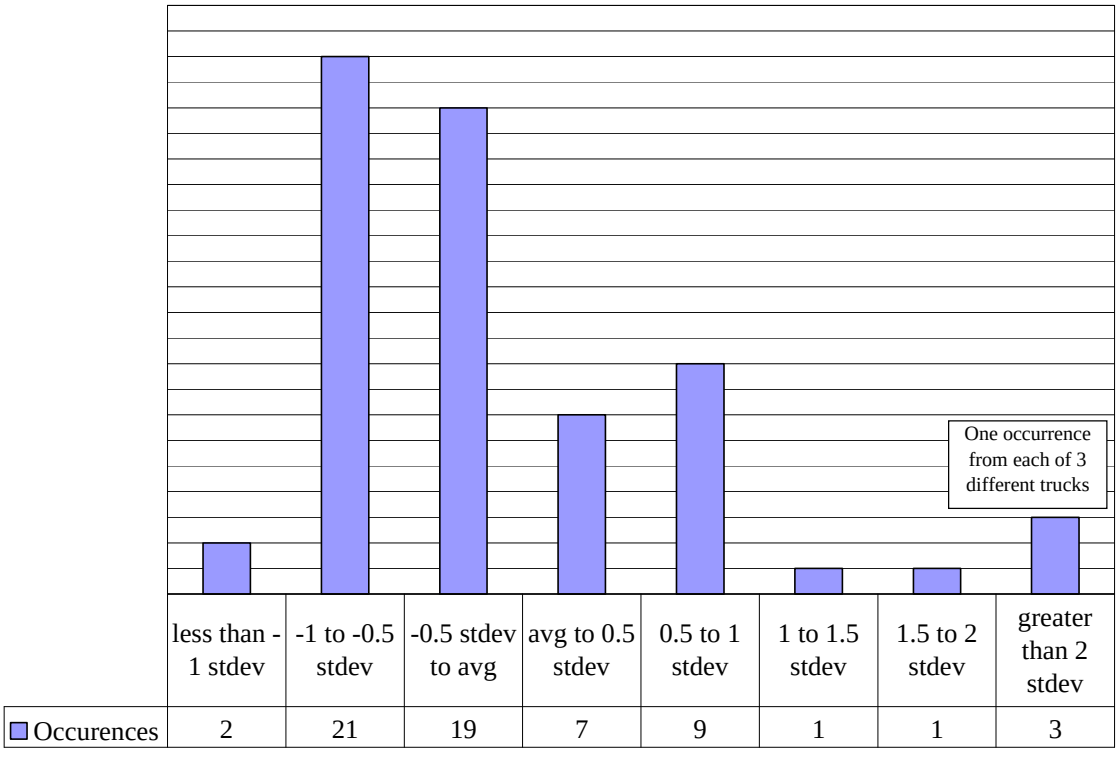

Figure 125 shows the occurrence of criterion ratios by bin for the Transient Mode, where the bins are described in

Table 20. The resulting PM/CO_2 ratios for each transient run identify E55CRC-6 with high emissions on one run of the transient test.

Figure 126 shows the occurrence of criterion ratios by bin for the Cruise Mode, where the bins are described in Table 21. Only one run for vehicle E55CRC-6, for the transient case, fell outside of the two standard deviation limits so that this run represented high emissions. The other run for the Transient Mode case for E55CRC-6 lay between 1.5 and 2 standard deviations above the average and so was not statistically high at the 95% level. Therefore, since both runs did not indicate high emissions, E55CRC-6 was not designated as a high emitter based on population statistics. E55CRC-8 and E55CRC-15 were similarly behaved.

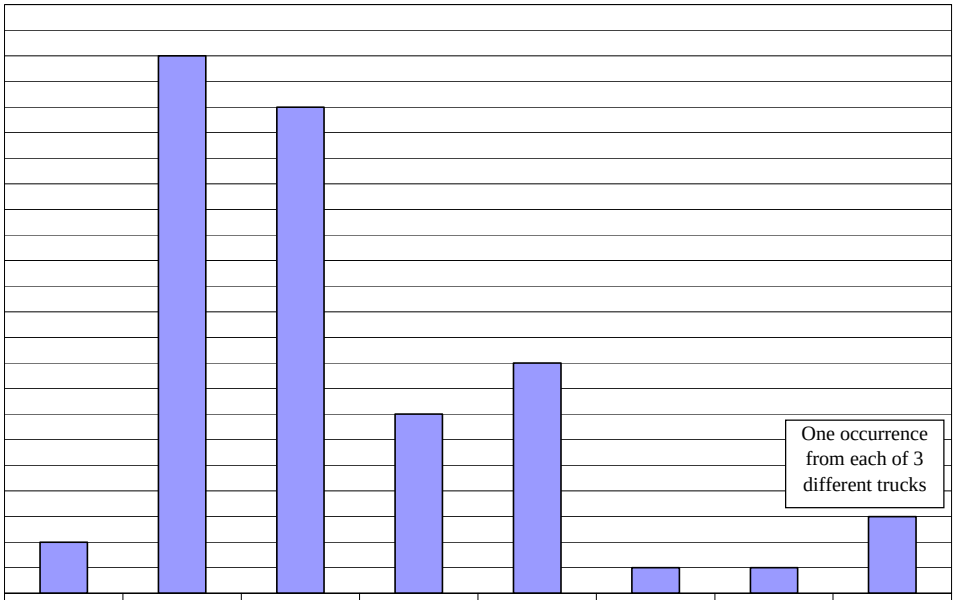

	less than -1 stdev	-1 to -0.5 stdev	-0.5 stdev to avg	avg to 0.5 stdev	0.5 to 1 stdev	1 to 1.5 stdev	1.5 to 2 stdev	greater than 2 stdev
Occurences	2	21	19	7	9	1	1	3

Figure 125: Occurrence of criterion ratios by bin for the Laden Transient Mode (PM/CO_2). E55CRC-16 was not included in this analysis, because it was an extreme outlier.

Table 20: Definition of criterion ratios by bin for the Laden Transient Mode: see Figure 125.

Bin description	Bin Range
less than -1 stdev	less than 0.125
-0.5 to -1 stdev	0.125 to 0.699
-0.5 stdev to avg	0.699 to 1.274
avg to 0.5 stdev	1.274 to 1.848
0.5 to 1 stdev	1.848 to 2.422
1 to 1.5 stdev	2.422 to 2.997
1.5 to 2 stdev	2.997 to 3.571
greater than 2 stdev	greater than 3.571

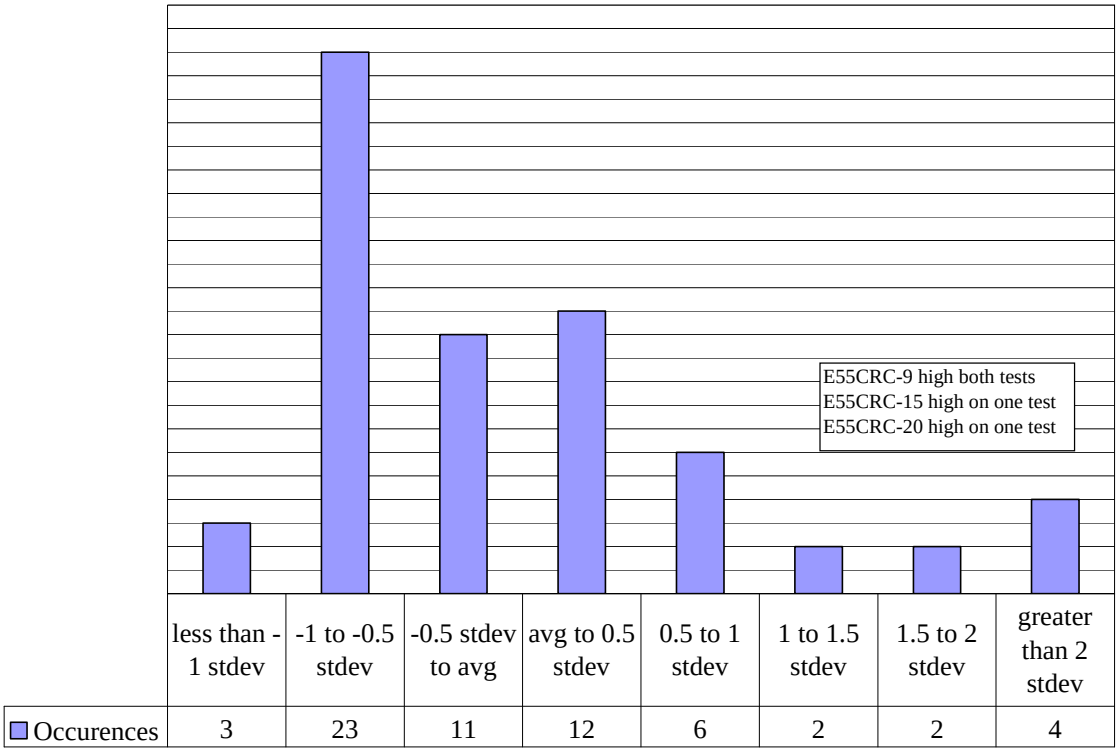

	less than -1 stdev	-1 to -0.5 stdev	-0.5 stdev to avg	avg to 0.5 stdev	0.5 to 1 stdev	1 to 1.5 stdev	1.5 to 2 stdev	greater than 2 stdev
Occurences	3	23	11	12	6	2	2	4

Figure 126: Occurrence of criterion ratios by bin for the Laden Cruise mode (PM/CO_2). E55CRC-16 was not included in this analysis because it was an extreme outliner.

Table 21: Definition of criterion by bin for the Laden Cruise Mode: See Figure 126.

Bin Description	Bin Range
less than -1 stdev	less than 0.164
-0.5 to -1 stdev	0.164 to 0.342
-0.5 stdev to avg	0.343 to 0.521
avg to 0.5 stdev	0.521 to 0.699
0.5 to 1 stdev	0.699 to 0.878
1 to 1.5 stdev	0.878 to 1.056
1.5 to 2 stdev	1.056 to 1.234
greater than 2 stdev	greater than 1.234

The resulting PM/CO_2 ratios for each cruise run identified E55CRC-9 as having high emissions on two cruise runs. E55CRC-9 was therefore designated as a high emitter and was a potential T&M candidate. The cause of the high PM emissions was not obvious, but may have been due to engine wear. Repairs in this case would be costly. There were several potential candidate T&M vehicles that had arisen at the time the E55CRC-9 was discussed by the researchers, and insufficient support to address them all. A sponsor decision was not to pursue E55CRC-9 for T&M repair and retest. E55CRC-20 showed high PM emissions on only one Cruise mode run and was therefore not designated as a high emitter.

The PM emissions of E55CRC-16 were prodigious and it exhibited high PM emissions by all criteria on both Transient and Cruise Modes. It was selected as a T&M vehicle, and is discussed in a separate subsection below. Because the values were so high that they would skew the results, the E55CRC-16 results were not considered when calculating the "expected"/"high" statistical criteria.

It is of interest to note that E55CRC-16 was most likely puffing because its Transient Mode PM emissions were high but Cruise Mode PM emissions were modest in contrast to E55CRC-9, which showed the opposite trend. Data also confirmed the visual observation of high PM output from vehicle E55CRC-16. E55CRC-16 was designated as a T&M candidate and is discussed in a separate subsection below. E55CRC-21 became a T&M vehicle by inspection of its dirty air filter, but was not a high PM emitter by test data criteria.

The criteria for PM high emitters was finalized in Phase 1, and applied to HHDDT in subsequent phases. After Phase 1, some HHDDT in the program were only subjected to one run of each mode: the criterion that the vehicle must have two high values in the Transient mode or two high values in the Cruise mode could not be applied to those vehicles. It revealed in Phase 1.5 that E55CRC-28 was a high PM emitter in Phase 1.5 and that E55CRC-45 was a high PM emitter in Phase 2.

Criteria ratios for all phases

Show the T&M criteria for all of the HHDDT vehicles examined in this study where "high" NO_x and PM emitters, as identified by the previously discussed methodology, are highlighted in these tables. Only initial test data, not including any re-test data, were used

in determining the average and standard deviations in the particulate matter calculations. CRC-16, a gross PM emitter, was not included in the statistical calculations either.

Table 22: T&M Determination Data for the HHDDT Vehicles over the Cruise Mode

Vehicle	Model Year	(NO_X / CO_2) Actual	(NO_X/CO_2) Certification	Multiplier	Actual / (Cert * Multiplier)	(PM/CO_2) Actual	(PM/CO_2) Certification	Actual / Certification	(Actual / Cert) / Average (Actual/Cert + 2 Sigma)
E55CRC-1	1994	0.0184	0.0091	3	0.68	0.000075	0.00018	0.4128	0.13
E55CRC-1	1994	0.0204	0.0091	3	0.75	0.000081	0.00018	0.4441	0.14
E55CRC-2	1995	0.0129	0.0091	3	0.47	0.000099	0.00018	0.5470	0.17
E55CRC-2	1995	0.0132	0.0091	3	0.48	0.000093	0.00018	0.5124	0.16
E55CRC-3	1985	0.0057	0.0093	2	0.31	0.000434	0.00182	0.2389	0.07
E55CRC-3	1985	0.0050	0.0093	2	0.27	0.000419	0.00182	0.2302	0.07
E55CRC-4	1999	0.0107	0.0073	3	0.49	0.000131	0.00018	0.7191	0.22
E55CRC-4	1999	0.0114	0.0073	3	0.52	0.000150	0.00018	0.8250	0.25
E55CRC-5	2000	0.0120	0.0073	3	0.55	0.000149	0.00018	0.8213	0.25
E55CRC-5	2000	0.0147	0.0073	3	0.67	0.000146	0.00018	0.8048	0.25
E55CRC-6	1995	0.0188	0.0091	3	0.69	0.000172	0.00018	0.9452	0.29
E55CRC-6	1995	0.0158	0.0091	3	0.58	0.000181	0.00018	0.9951	0.31
E55CRC-7	1990	0.0107	0.0109	3	0.33	0.000272	0.00109	0.2497	0.08
E55CRC-7	1990	0.0118	0.0109	3	0.36	0.000254	0.00109	0.2332	0.07
E55CRC-8	1996	0.0177	0.0091	3	0.65	0.000144	0.00018	0.7916	0.24
E55CRC-8	1996	0.0210	0.0091	3	0.77	0.000148	0.00018	0.8128	0.25
E55CRC-9	1998	0.0155	0.0073	3	0.71	0.000278	0.00018	1.5302	0.47
E55CRC-9	1998	0.0157	0.0073	3	0.72	0.000262	0.00018	1.4402	0.44
E55CRC-10	1998	0.0329	0.0073	3	1.51	0.000081	0.00018	0.4476	0.14
E55CRC-10	1998	0.0305	0.0073	3	1.40	0.000096	0.00018	0.5306	0.16
E55CRC-11	2000	0.0107	0.0073	3	0.49	0.000111	0.00018	0.6101	0.19
E55CRC-11	2000	0.0109	0.0093	2	0.59	0.000092	0.00182	0.0504	0.02
E55CRC-12	1986	0.0087	0.0093	2	0.47	0.001187	0.00182	0.6527	0.20
E55CRC-12	1986	0.0078	0.0093	2	0.42	0.000843	0.00182	0.4638	0.14
E55CRC-13	1978	0.0134	0.0093	2	0.72	0.000455	0.00182	0.2501	0.08
E55CRC-13	1978	0.0132	0.0093	2	0.71	0.000426	0.00182	0.2345	0.07
E55CRC-14	1985	0.0095	0.0093	2	0.51	0.000390	0.00182	0.2144	0.07

Vehicle	Model Year	(NO_X / CO_2) Actual	(NO_X/CO_2) Certification	Multiplier	Actual / (Cert * Multiplier)	(PM/CO_2) Actual	(PM/CO_2) Certification	Actual / Certification	(Actual / Cert) / Average (Actual/Cert + 2 Sigma)
E55CRC-14	1985	0.0096	0.0093	2	0.52	0.000376	0.00182	0.2068	0.06
E55CRC-14	1985	0.0096	0.0093	2	0.52	0.000368	0.00182	0.2022	0.06
E55CRC-15	1986	0.0091	0.0093	2	0.49	0.000810	0.00182	0.4455	0.14
E55CRC-15	1986	0.0090	0.0093	2	0.48	0.000728	0.00182	0.4002	0.12
E55CRC-15	1986	0.0090	0.0091	2	0.50	0.000778	0.00045	1.7109	0.52
E55CRC-16	1979	0.0056	0.0091	2	0.31	0.009448	0.00045	20.7851	6.38
E55CRC-16	1979	0.0053	0.0091	2	0.29	0.008619	0.00045	18.9624	5.82
E55CRC-16	1979	0.0058	0.0091	2	0.32	0.008698	0.00045	19.1364	5.87
E55CRC-17	1993	0.0120	0.0109	3	0.37	0.000365	0.00109	0.3349	0.10
E55CRC-17	1993	0.0113	0.0109	3	0.35	0.000429	0.00109	0.3930	0.12
E55CRC-17	1993	0.0115	0.0109	3	0.35	0.000310	0.00109	0.2841	0.09
E55CRC-18	1991	0.0085	0.0109	2	0.39	0.000276	0.00109	0.2529	0.08
E55CRC-18	1991	0.0085	0.0109	3	0.26	0.000263	0.00109	0.2408	0.07
E55CRC-18	1991	0.0088	0.0109	3	0.27	0.000267	0.00109	0.2449	0.08
E55CRC-19	1987	0.0073	0.0109	2	0.34	0.000603	0.00109	0.5529	0.17
E55CRC-19	1987	0.0075	0.0109	2	0.34	0.000633	0.00109	0.5801	0.18
E55CRC-19	1987	0.0075	0.0109	2	0.34	0.000577	0.00109	0.5290	0.16
E55CRC-20	1992	0.0141	0.0091	3	0.52	0.000520	0.00045	1.1443	0.35
E55CRC-20	1992	0.0142	0.0091	3	0.52	0.000534	0.00045	1.1751	0.36
E55CRC-20	1992	0.0135	0.0091	3	0.49	0.000567	0.00045	1.2475	0.38
E55CRC-21	1990	0.0116	0.0109	2	0.53	0.000643	0.00109	0.5891	0.18
E55CRC-21	1990	0.0115	0.0109	3	0.35	0.000623	0.00109	0.5714	0.18
E55CRC-21	1990	0.0118	0.0109	3	0.36	0.000540	0.00109	0.4951	0.15
E55CRC-22	1993	0.0109	0.0091	3	0.40	0.000285	0.00045	0.6262	0.19
E55CRC-22	1993	0.0116	0.0091	3	0.43	0.000268	0.00045	0.5891	0.18
E55CRC-22	1993	0.0114	0.0091	3	0.42	0.000259	0.00045	0.5697	0.17
E55CRC-23	1983	0.0129	0.0109	2	0.59	0.000545	0.00182	0.2997	0.09
E55CRC-23	1983	0.0134	0.0109	2	0.62	0.000577	0.00182	0.3171	0.10
E55CRC-23	1983	0.0134	0.0109	2	0.61	0.000581	0.00182	0.3194	0.10

Vehicle	Model Year	(NO_X / CO_2) Actual	(NO_X/CO_2) Certification	Multiplier	Actual / (Cert * Multiplier)	(PM/CO_2) Actual	(PM/CO_2) Certification	Actual / Certification	(Actual / Cert) / Average (Actual/Cert + 2 Sigma)
E55CRC-24	1975	0.0153	0.0182	2	0.42	0.000360	0.00182	0.1977	0.06
E55CRC-24	1975	0.0172	0.0182	2	0.47	0.000324	0.00182	0.1784	0.05
E55CRC-24	1975	0.0162	0.0182	2	0.44	0.000295	0.00182	0.1625	0.05
E55CRC-25	1983	0.0138	0.0109	2	0.63	0.000492	0.00182	0.2704	0.08
E55CRC-25	1983	0.0156	0.0109	2	0.71	0.000464	0.00182	0.2553	0.08
E55CRC-25	1983	0.0156	0.0109	2	0.72	0.000428	0.00182	0.2355	0.07
E55CRC-26	1998	0.0140	0.0073	3	0.64	0.000219	0.00018	1.2024	0.37
E55CRC-27	1999	0.0118	0.0073	3	0.54	0.000148	0.00018	0.8125	0.25
E55CRC-28	1998	0.0155	0.0073	3	0.71	0.000377	0.00018	2.0711	0.64
E55CRC-29	1999	0.0097	0.0073	3	0.44	0.001838	0.00018	10.1100	3.10
E55CRC-30	1998	0.0160	0.0073	3	0.73	0.000148	0.00018	0.8114	0.25
E55CRC-31	1997	0.0178	0.0091	3	0.65	0.000140	0.00018	0.7707	0.24
E55CRC-32	1991	0.0068	0.0091	2	0.37	0.000355	0.00045	0.7809	0.24
E55CRC-33	1984	0.0174	0.0093	2	0.94	0.000471	0.00182	0.2593	0.08
E55CRC-34	2003	0.0040	0.0036	3	0.36	0.000829	0.00018	4.5598	1.40
E55CRC-35	2000	0.0099	0.0073	3	0.45	0.000240	0.00018	1.3176	0.40
E55CRC-36	2001	0.0087	0.0073	3	0.40	0.000211	0.00018	1.1610	0.36
E55CRC-38	2004	0.0049	0.0036	3	0.45	0.000114	0.00018	0.63	0.19
E55CRC-38	2004	0.0045	0.0036	3	0.41	0.000108	0.00018	0.60	0.18
E55CRC-38	2004	0.0049	0.0036	3	0.45	0.000134	0.00018	0.75	0.23
E55CRC-39	2004	0.0047	0.0036	3	0.43	0.000104	0.00018	0.58	0.18
E55CRC-39	2004	0.0044	0.0036	3	0.41	0.000113	0.00018	0.63	0.19
E55CRC-40	2004	0.0074	0.0036	3	0.68	0.000107	0.00018	0.60	0.18
E55CRC-40	2004	0.0082	0.0036	3	0.76	0.000086	0.00018	0.48	0.15
E55CRC-42	2000	0.0075	0.0073	3	0.34	0.000173	0.00018	0.96	0.30
E55CRC-42	2000	0.0077	0.0073	3	0.35	0.000178	0.00018	0.99	0.30
E55CRC-43	1995	0.0138	0.0091	3	0.51	0.000044	0.00018	0.24	0.07
E55CRC-43	1995	0.0123	0.0091	3	0.45	0.000040	0.00018	0.22	0.07
E55CRC-44	1989	0.0090	0.0109	2	0.41	0.000227	0.00109	0.21	0.06

Vehicle	Model Year	(NO_X / CO_2) Actual	(NO_X/CO_2) Certification	Multiplier	Actual / (Cert * Multiplier)	(PM/CO_2) Actual	(PM/CO_2) Certification	Actual / Certification	(Actual / Cert) / Average (Actual/Cert + 2 Sigma)
E55CRC-44	1989	0.0088	0.0109	2	0.40	0.000224	0.00109	0.21	0.06
E55CRC-45	1993	0.0060	0.0091	3	0.22	0.000762	0.00045	1.69	0.52
E55CRC-46	1989	0.0104	0.0109	2	0.48	0.000506	0.00109	0.46	0.14
E55CRC-47	1986	0.0056	0.0093	2	0.30	0.000674	0.00182	0.37	0.11
E55CRC-48	1998	0.0162	0.0073	3	0.74	0.000261	0.00018	1.45	0.44
E55CRC-49	1994	0.0080	0.0091	3	0.29	0.000605	0.00018	3.36	1.03
E55CRC-60	1995	0.0098	0.0091	3	0.36	0.000789	0.00018	4.38	1.34
E55CRC-62	1983	0.0090	0.0109	2	0.41	0.001317	0.00182	0.72	0.22
E55CRC-63	2005	0.0074	0.0036	3	0.69	0.000214	0.00018	1.19	0.36
E55CRC-64	1994	0.0154	0.0091	3	0.57	0.000000	0.00018	0.00	0.00
E55CRC-65	1994	0.0132	0.0091	3	0.48	0.000420	0.00018	2.33	0.72
E55CRC-66	1989	0.0109	0.0109	2	0.50	0.000417	0.00109	0.38	0.12
E55CRC-69	1989	0.0083	0.0109	2	0.38	0.000895	0.00109	0.82	0.25
E55CRC-74	1969	0.0135	0.0182	2	0.37	0.001053	0.00182	0.58	0.18
E55CRC-78	1975	0.0249	0.0182	2	0.68	0.001652	0.00182	0.91	0.28

Table 23: T&M Determination Data for the HHDDT Vehicles over the Transient Mode

Vehicle	Model Year	(NO_X / CO_2) Actual	(NO_X/CO_2) Certification	Multiplier	Actual / (Cert * Multiplier)	(PM/CO_2) Actual	(PM/CO_2) Certification	Actual / Certification	(Actual / Cert) / Average (Actual/Cert + 2 Sigma)
E55CRC-1	1994	0.0130	0.0091	3	0.48	0.00019	0.00018	1.07	0.12
E55CRC-1	1994	0.0179	0.0091	3	0.66	0.00025	0.00018	1.36	0.15
E55CRC-2	1995	0.0070	0.0091	3	0.26	0.00026	0.00018	1.41	0.15
E55CRC-2	1995	0.0073	0.0091	3	0.27	0.00034	0.00018	1.85	0.20
E55CRC-3	1985	0.0059	0.0093	2	0.32	0.00105	0.00182	0.58	0.06
E55CRC-3	1985	0.0056	0.0093	2	0.30	0.00124	0.00182	0.68	0.07
E55CRC-4	1999	0.0078	0.0073	3	0.36	0.00017	0.00018	0.94	0.10
E55CRC-4	1999	0.0107	0.0073	3	0.49	0.00032	0.00018	1.74	0.19
E55CRC-5	2000	0.0100	0.0073	3	0.46	0.00029	0.00018	1.57	0.17
E55CRC-5	2000	0.0118	0.0073	3	0.54	0.00029	0.00018	1.57	0.17
E55CRC-6	1995	0.0109	0.0091	3	0.40	0.00081	0.00018	4.46	0.48
E55CRC-6	1995	0.0085	0.0091	3	0.31	0.00062	0.00018	3.40	0.37
E55CRC-7	1990	0.0129	0.0109	3	0.39	0.00045	0.00109	0.41	0.04
E55CRC-7	1990	0.0129	0.0109	3	0.40	0.00041	0.00109	0.37	0.04
E55CRC-8	1996	0.0089	0.0091	3	0.33	0.00037	0.00018	2.03	0.22
E55CRC-8	1996	0.0113	0.0091	3	0.41	0.00116	0.00018	6.36	0.69
E55CRC-9	1998	0.0063	0.0073	3	0.29	0.00039	0.00018	2.13	0.23
E55CRC-9	1998	0.0074	0.0073	3	0.34	0.00036	0.00018	2.00	0.22
E55CRC-10	1998	0.0132	0.0073	3	0.60	0.00031	0.00018	1.71	0.18
E55CRC-10	1998	0.0123	0.0073	3	0.56	0.00027	0.00018	1.49	0.16
E55CRC-11	2000	0.0076	0.0073	3	0.35	0.00017	0.00018	0.92	0.10
E55CRC-11	2000	0.0074	0.0093	2	0.40	0.00020	0.00182	0.11	0.01
E55CRC-12	1986	0.0076	0.0093	2	0.41	0.00189	0.00182	1.04	0.11
E55CRC-12	1986	0.0075	0.0093	2	0.41	0.00188	0.00182	1.03	0.11
E55CRC-13	1978	0.0109	0.0093	2	0.59	0.00087	0.00182	0.48	0.05
E55CRC-13	1978	0.0105	0.0093	2	0.57	0.00082	0.00182	0.45	0.05

Vehicle	Model Year	(NO_X / CO_2) Actual	(NO_X/CO_2) Certification	Multiplier	Actual / (Cert * Multiplier)	(PM/CO_2) Actual	(PM/CO_2) Certification	Actual / Certification	(Actual / Cert) / Average (Actual/Cert + 2 Sigma)
E55CRC-14	1985	0.0078	0.0093	2	0.42	0.00080	0.00182	0.44	0.05
E55CRC-14	1985	0.0079	0.0093	2	0.43	0.00089	0.00182	0.49	0.05
E55CRC-14	1985	0.0079	0.0093	2	0.42	0.00081	0.00182	0.45	0.05
E55CRC-15	1986	0.0085	0.0093	2	0.46	0.00152	0.00182	0.84	0.09
E55CRC-15	1986	0.0088	0.0093	2	0.47	0.00148	0.00182	0.82	0.09
E55CRC-15	1986	0.0080	0.0091	2	0.44	0.00235	0.00045	5.17	0.56
E55CRC-16	1979	0.0069	0.0091	2	0.38	0.00529	0.00045	11.63	1.26
E55CRC-16	1979	0.0067	0.0091	2	0.37	0.00607	0.00045	13.35	1.44
E55CRC-16	1979	0.0067	0.0091	2	0.37	0.00570	0.00045	12.53	1.35
E55CRC-17	1993	0.0079	0.0109	3	0.24	0.00075	0.00109	0.69	0.07
E55CRC-17	1993	0.0078	0.0109	3	0.24	0.00084	0.00109	0.77	0.08
E55CRC-17	1993	0.0073	0.0109	3	0.22	0.00080	0.00109	0.73	0.08
E55CRC-18	1991	0.0083	0.0109	2	0.38	0.00066	0.00109	0.60	0.06
E55CRC-18	1991	0.0087	0.0109	3	0.26	0.00106	0.00109	0.97	0.10
E55CRC-18	1991	0.0085	0.0109	3	0.26	0.00106	0.00109	0.97	0.11
E55CRC-19	1987	0.0062	0.0109	2	0.29	0.00256	0.00109	2.34	0.25
E55CRC-19	1987	0.0065	0.0109	2	0.30	0.00210	0.00109	1.93	0.21
E55CRC-19	1987	0.0063	0.0109	2	0.29	0.00271	0.00109	2.48	0.27
E55CRC-20	1992	0.0126	0.0091	3	0.46	0.00004	0.00045	0.09	0.01
E55CRC-20	1992	0.0122	0.0091	3	0.45	0.00056	0.00045	1.23	0.13
E55CRC-20	1992	0.0108	0.0091	3	0.40	0.00057	0.00045	1.26	0.14
E55CRC-21	1990	0.0107	0.0109	2	0.49	0.00101	0.00109	0.92	0.10
E55CRC-21	1990	0.0110	0.0109	3	0.34	0.00106	0.00109	0.97	0.10
E55CRC-21	1990	0.0111	0.0109	3	0.34	0.00102	0.00109	0.93	0.10
E55CRC-22	1993	0.0092	0.0091	3	0.34	0.00099	0.00045	2.17	0.23
E55CRC-22	1993	0.0093	0.0091	3	0.34	0.00090	0.00045	1.97	0.21
E55CRC-22	1993	0.0098	0.0091	3	0.36	0.00099	0.00045	2.17	0.23
E55CRC-23	1983	0.0099	0.0109	2	0.45	0.00120	0.00182	0.66	0.07
E55CRC-23	1983	0.0092	0.0109	2	0.42	0.00125	0.00182	0.69	0.07

Vehicle	Model Year	(NO_X / CO_2) Actual	(NO_X/CO_2) Certification	Multiplier	Actual / (Cert * Multiplier)	(PM/CO_2) Actual	(PM/CO_2) Certification	Actual / Certification	(Actual / Cert) / Average (Actual/Cert + 2 Sigma)
E55CRC-23	1983	0.0094	0.0109	2	0.43	0.00122	0.00182	0.67	0.07
E55CRC-24	1975	0.0131	0.0182	2	0.36	0.00078	0.00182	0.43	0.05
E55CRC-24	1975	0.0143	0.0182	2	0.39	0.00169	0.00182	0.93	0.10
E55CRC-24	1975	0.0135	0.0182	2	0.37	0.00071	0.00182	0.39	0.04
E55CRC-25	1983	0.0112	0.0109	2	0.51	0.00087	0.00182	0.48	0.05
E55CRC-25	1983	0.0118	0.0109	2	0.54	0.00081	0.00182	0.45	0.05
E55CRC-25	1983	0.0125	0.0109	2	0.57	0.00071	0.00182	0.39	0.04
E55CRC-26	1998	0.0064	0.0073	3	0.30	0.00029	0.00018	1.60	0.17
E55CRC-27	1999	0.0072	0.0073	3	0.33	0.00044	0.00018	2.39	0.26
E55CRC-28	1998	0.0087	0.0073	3	0.40	0.00222	0.00018	12.23	1.32
E55CRC-29	1999	0.0060	0.0073	3	0.28	0.00220	0.00018	12.12	1.31
E55CRC-30	1998	0.0157	0.0073	3	0.72	0.00025	0.00018	1.39	0.15
E55CRC-31	1997	0.0093	0.0091	3	0.34	0.00040	0.00018	2.22	0.24
E55CRC-32	1991	0.0068	0.0091	2	0.37	0.00044	0.00045	0.97	0.10
E55CRC-33	1984	0.0139	0.0093	2	0.75	0.00150	0.00182	0.83	0.09
E55CRC-34	2003	0.0055	0.0036	3	0.51	0.00041	0.00018	2.23	0.24
E55CRC-35	2000	0.0066	0.0073	3	0.30	0.00053	0.00018	2.90	0.31
E55CRC-36	2001	0.0059	0.0073	3	0.27	0.00031	0.00018	1.72	0.19
E55CRC-38	2004	0.0060	0.0036	3	0.55	0.00021	0.00018	1.14	0.12
E55CRC-38	2004	0.0052	0.0036	3	0.49	0.00013	0.00018	0.72	0.08
E55CRC-38	2004	0.0059	0.0036	3	0.54	0.00018	0.00018	1.00	0.11
E55CRC-39	2004	0.0058	0.0036	3	0.53	0.00014	0.00018	0.78	0.08
E55CRC-39	2004	0.0056	0.0036	3	0.52	0.00014	0.00018	0.80	0.09
E55CRC-40	2004	0.0063	0.0036	3	0.59	0.00010	0.00018	0.53	0.06
E55CRC-40	2004	0.0061	0.0036	3	0.57	0.00010	0.00018	0.54	0.06
E55CRC-42	2000	0.0054	0.0073	3	0.25	0.00038	0.00018	2.09	0.23
E55CRC-42	2000	0.0052	0.0073	3	0.24	0.00035	0.00018	1.94	0.21
E55CRC-43	1995	0.0105	0.0091	3	0.38	0.00038	0.00018	2.09	0.23
E55CRC-43	1995	0.0086	0.0091	3	0.31	0.00011	0.00018	0.62	0.07

Vehicle	Model Year	(NO_X / CO_2) Actual	(NO_X/CO_2) Certification	Multiplier	Actual / (Cert * Multiplier)	(PM/CO_2) Actual	(PM/CO_2) Certification	Actual / Certification	(Actual / Cert) / Average (Actual/Cert + 2 Sigma)
E55CRC-44	1989	0.0081	0.0109	2	0.37	0.00044	0.00109	0.41	0.04
E55CRC-44	1989	0.0081	0.0109	2	0.37	0.00037	0.00109	0.34	0.04
E55CRC-45	1993	0.0058	0.0091	3	0.21	0.00723	0.00045	16.08	1.73
E55CRC-46	1989	0.0080	0.0109	2	0.37	0.00076	0.00109	0.70	0.08
E55CRC-47	1986	0.0062	0.0093	2	0.33	0.00131	0.00182	0.72	0.08
E55CRC-48	1998	0.0113	0.0073	3	0.52	0.00050	0.00018	2.79	0.30
E55CRC-49	1994	0.0069	0.0091	3	0.25	0.00125	0.00018	6.97	0.75
E55CRC-60	1995	0.0098	0.0091	3	0.36	0.00503	0.00018	27.93	3.01
E55CRC-62	1983	0.0082	0.0109	2	0.38	0.00204	0.00182	1.12	0.12
E55CRC-63	2005	0.0053	0.0036	3	0.49	0.00022	0.00018	1.24	0.13
E55CRC-64	1994	0.0090	0.0091	3	0.33	0.00000	0.00018	0.00	0.00
E55CRC-65	1994	0.0105	0.0091	3	0.38	0.00092	0.00018	5.12	0.55
E55CRC-66	1989	0.0084	0.0109	2	0.38	0.00095	0.00109	0.87	0.09
E55CRC-69	1989	0.0087	0.0109	2	0.40	0.00117	0.00109	1.07	0.12
E55CRC-74	1969	0.0113	0.0182	2	0.31	0.00159	0.00182	0.87	0.09
E55CRC-78	1975	0.0190	0.0182	2	0.52	0.00062	0.00182	0.34	0.04

"Before and After" Emissions

Each vehicle that was identified as a T&M vehicle, repaired and retested, or reflashed and retested, is presented below in order of occurrence in the program.

E55CRC-3: Injection Timing Change, Phase 1.

E55CRC-3, a single axle full size road tractor with a 1985 Cummins 14 liter engine, became a T&M subject fortuitously. It was tested twice, because it was mistakenly believed that data from the first set of tests were in error and that retest was necessary, and the vehicle owner happened to effect repairs between the two test periods. E55CRC-3 did not meet the high PM emissions criteria but it was observed during a later data analysis that PM was higher than would be expected for a vehicle of its MY and NO_x was lower. Data from the first round of testing suggested that the engine might be operating at NO_x levels as low as 3g/bhp-hr (4 g/kw-hr) and the NO_x data for the retest corresponded to about 4.5g/bhp-hr (6 g/kw-hr) on a certified engine test (FTP), based on NO_x/CO_2 ratio. The certification level for that engine was 5.1g/bhp-hr (6.8 g/kw-hr) so 4.5g/bhp-hr (6 g/kw-hr) would correspond to certification level less a 10% "safety margin". Fuel specifications in CA. had also changed since 1985 and recent CA fuel is argued to cause lower NO_x. It was evident from the retest data that the PM, CO and HC were lower in the retest than in the original test. Table 24 and Table 25 summarize the data taken from the test and retest for laden UDDS.
Table 26 to Table 29 summarize the data taken from the test and retest for laden HHDDT.

Table 24: E55CRC-3: UDDS (g/mile)

Run Seq. No.	CO	NO_x[1]	NO_x[2]	HC	PM	CO_2	mile/gal	BTU/mile	Miles
1826-3	14	12.5	12.2	2.7	1.76	2155	4.6	28238	5.52
1826-4	12.4	12.3	12.6	2.78	1.76	2255	4.41	29450	5.51

Table 25: E55CRC-3 retest UDDS (g/mile)

Run Seq. No.	CO	NO_x[1]	NO_x[2]	HC	PM	CO_2	mile/gal	BTU/mile	Miles
1936-2	8.22	17.9	18.8	1.76	1.15	2413	4.13	31421	5.2
1936-3	8.53	17.1	16.9	1.66	1.57	2408	4.14	31359	5.26

Table 26: E55CRC-3: 1828-1 Idle, 1828-2 Creep, 1828-3 Transient, 1828-4 Cruise. (g/mile, except idle in g/cycle)

Run Seq. No.	CO	NO_x[1]	NO_x[2]	HC	PM	CO_2	mile/gal	BTU/mile	Miles
1828-1	10.4	8.7	8.8	7.2	1.84	1088	0.02	9052	0.01
1828-2	26.48	14.42	13.24	12.49	5.10	2740	0.94	36451	0.13
1828-3	8.58	9.07	8.89	2.98	1.60	965	2.69	12768	2.73
1828-4	2.30	5.53	5.47	1.12	0.42	549	4.77	7188	23.02

Table 27: E55CRC-3: 1829-1 Idle, 1829-2 Creep, 1829-3 Transient, 1829-4 Cruise. (g/mile, except idle in g/cycle)

Run Seq. No.	CO	NO_x[1]	NO_x[2]	HC	PM	CO_2	mile/gal	BTU/mile	Miles
1829-1	29.6	1.8	2	2.4	2.37	1167	<0	15780	-0.01
1829-2	48	25.6	25	23.4	6.05	5896	1.66	78121	0.13
1829-3	12.6	13.7	14.4	5.6	3.02	1884	5.23	24826	2.78
1829-4	3.3	7.8	8.1	1.7	0.65	851	11.66	11137	23

Table 28: E55CRC-3 retest: 1939-1 Idle, 1939-5 Creep, 1939-3 Transient, 1939-4 Cruise (g/mile, except idle in g/cycle)

Run Seq. No.	CO	NO_x[1]	NO_x[2]	HC	PM	CO_2	mile/gal	BTU/mile	Miles
1939-1	5.87	9.2	9.2	4.19	0.75	1406	<0	18462	-0.01
1939-5	20.7	44.3	45.5	10.19	2.53	4878	2.03	63862	0.12
1939-3	9.47	20.4	20	2.38	1.56	2743	3.63	35731	2.65
1939-4	2.65	12.4	12.5	0.99	0.45	1579	6.34	20492	22.04

Table 29: E55CRC-3 retest: 1942-1 Idle, 1942-5 Creep, 1942-3 Transient, 1942-4 Cruise. (g/mile, except idle in g/cycle)

Run Seq. No.	CO	NO_x[1]	NO_x[2]	HC	PM	CO_2	mile/gal	BTU/mile	Miles
1942-1	6.8	12.5	12.3	4.28	0.75	1480	<0	80732	0
1942-5	25.4	31.5	25.7	9.01	3.55	5593	1.77	73153	0.11
1942-3	11.1	18.6	19	2.95	1.66	3313	3.01	43158	2.63
1942-4	3.1	10.7	10.8	1.03	0.49	1603	6.24	20812	22.02

The low NO_x in the first round was due to substantially retarded timing on the truck. This engine employed a mechanical variable injection timing system, which included an air-operated cylinder that varied the position of the cam followers. It is likely that this unit was worn, because during preventive maintenance between the original test and retest, the vehicle owner effected repairs to the truck that included a rebuild of this air cylinder with new seals. In other words, the timing was corrected between the original testing and retesting, resulting in raised NO_x, and lower PM, CO and HC, according to the well-known NO_x-PM tradeoff.

E55CRC-10: Reflash Vehicle in Phase 1

E55CRC-10, a 1998 MY Sterling tractor with a DDC Series 60 engine, exhibited high NO_x emissions. The emissions, as tested on the Heavy-Duty UDDS and the HHDDT Schedule at 56,000 lbs. (25,402 kg), are shown in Table 22. It was evident that the major cause of the elevated emissions was “off-cycle” operation, as shown in Figure 122 above.

After the vehicle was reflashed, the Transient mode NO_x emissions for E55CRC-10 did not change, but the UDDS NO_x emissions dropped by about 20% as shown in

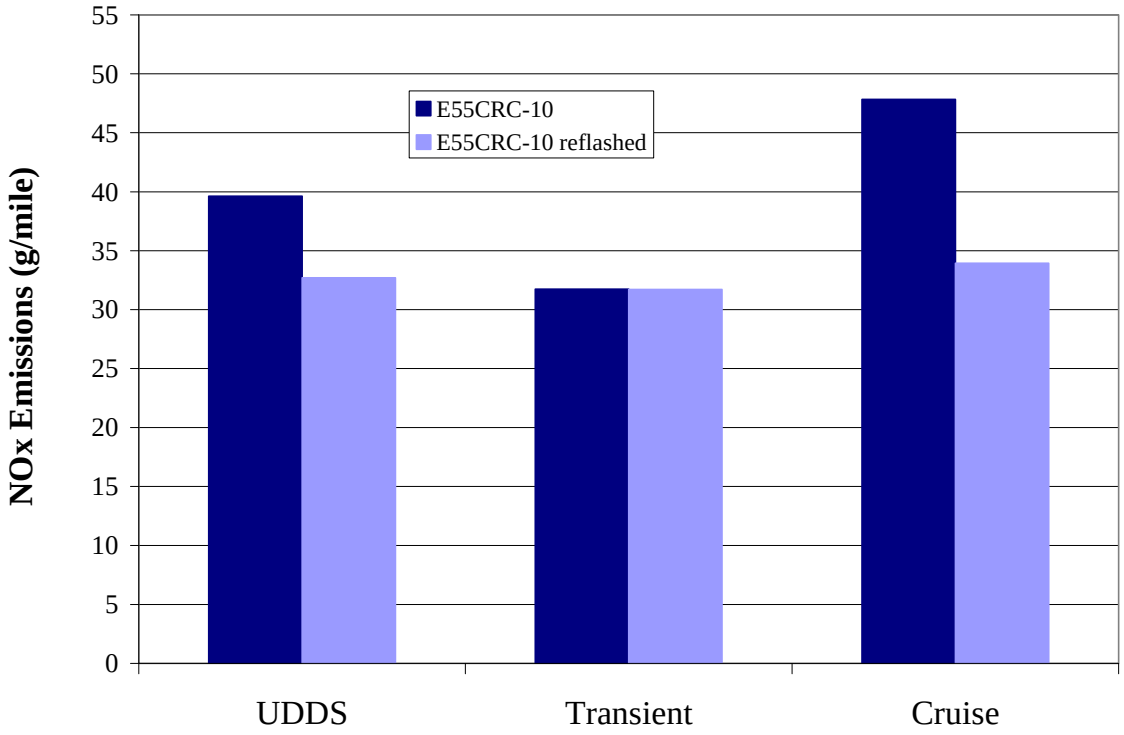

Figure 127 and the reduction on cruise was over 30%. This is to be expected keeping in mind the relative amounts of steady operation in each of these test modes and the fact that steady operation encourages "off-cycle" behavior. Figure 128 shows the NO_x emissions versus power for E55CRC-10 after reflash, and this figure may be compared with Figure 122. The investigators concede that Idle and Creep data were too variable for "before and after" comparisons because auxiliary engine loads affect idle and creep modes.

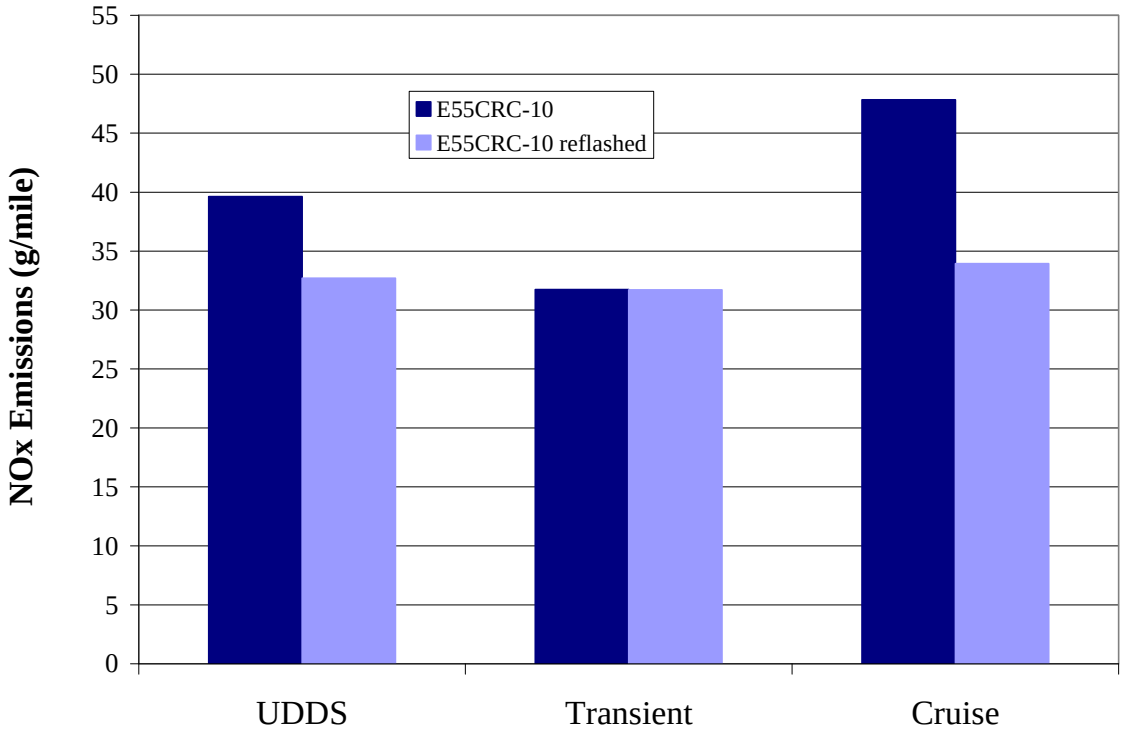

Figure 127: Transient Mode NO_x emissions before and after reflashing E55CRC-10.

Table 30: E55CRC-10 baseline emissions and "reflash" emissions. T&M runs are denoted in bold. NO_x^1 and NO_x^2 show values from two similar analyzers in parallel. It should be noted that Idle and Creep Modes often return highly variable emissions due to changing auxiliary loads on the vehicle.

Test ID	Test Run ID	Driving Schedule	CO	NO_X^1	NO_X^2	HC	PM	CO_2
			(g/mile)	(g/mile)	(g/mile)	(g/mile)	(g/mile)	(g/mile)
1963 Before	2	UDDS	8.37	38.68	38.58	0.22	0.53	2190
1963 Before	3	UDDS	9.16	40.57	40.25	0.22	0.53	2088
2195 Reflash	**5**	**UDDS**	**10.02**	**32.71**	**32.79**	**0.27**	**0.41**	**2188**
1966 Before	1	Idle	6.45	21.36	22.71	1.49	0.16	1176
1969 Before	1	Idle	7.65	17.81	17.66	1.15	0.13	923
2197 Reflash	**2**	**Idle**	**4.47**	**27.78**	**29.73**	**0.9**	**0.07**	**1057**
1966 Before	2	Creep	30.07	54.9	50.52	4.43	1.07	3834
1969 Before	2	Creep	40.23	60.71	62.35	5.26	1.49	4415
2197 Reflash	**3**	**Creep**	**33.31**	**75.66**	**75.1**	**5.4**	**1.09**	**4697**
1966 Before	3	Transient	11.77	32.99	33.13	0.46	0.78	2506
1969 Before	3	Transient	10.91	30.48	31.09	0.49	0.67	2485
2197 Reflash	**4**	**Transient**	**9.53**	**31.71**	**31.54**	**0.66**	**0.59**	**2666**
1966 Before	4	Cruise	2.78	49.43	49.11	0.13	0.12	1501
1969 Before	4	Cruise	3.05	46.24	46.42	0.14	0.15	1514
2197 Reflash	**5**	**Cruise**	**2.42**	**33.93**	**33.58**	**0.15**	**0.12**	**1513**

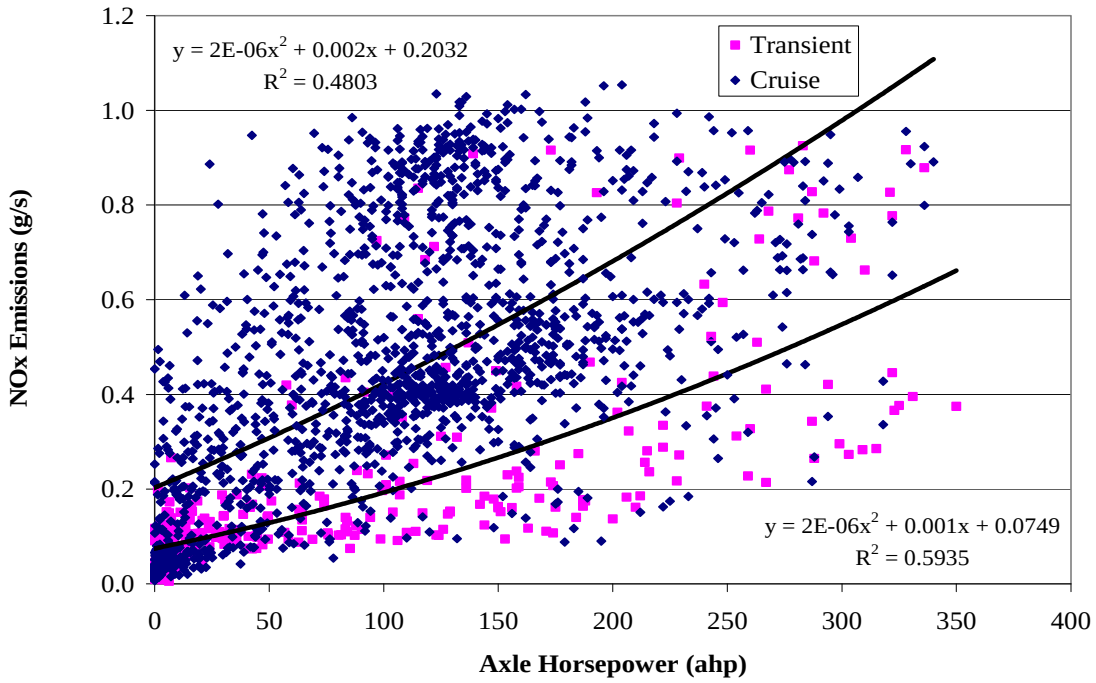

Figure 128: NO_x emissions versus power for E55CRC-10 after reflashing. The mass rate of NO_x emissions was reduced in many parts of the Cruise mode (compared to Figure 122). The highest mass rate emissions were also slightly lower than before the reflash.

E55CRC-16: High PM T&M Vehicle in Phase 1

E55CRC-16 was a 1979 White tractor with a 3208 Caterpillar engine. It was identified visually as a prodigious smoker and returned data as a high emitter. It was chosen as a T&M candidate. Emissions data for this vehicle are presented in Table 31. The vehicle was naturally aspirated, so the investigators believed that the high PM was due to over fueling or substantially retarded timing. It was suggested[34] that cam wear also might be an issue. The vehicle was sent to a Caterpillar dealership with directions to inspect the engine. They found no substantial wear or indication of poor injection timing. The dealership determined that the engine had originally been equipped with exhaust gas recirculation (EGR) for NO_x reduction, but that EGR components had been removed and that the system was not functioning.

The WVU investigators and the program sponsors determined that the fuel pump flow should be measured, and corrected if necessary, or the fuel pump should be replaced with a rebuilt unit. The dealership determined that they were unable to quantify the flow and so the pump was replaced.

Table 31: E55CRC-16 Emissions before and after T&M procedures. T&M 1 in bold represents testing with a new fuel injection pump; T&M 2 in bold italics represents testing with a new pump and EGR totally disabled.

Test ID	Test Run ID	Driving Schedule	CO	NO_X[1]	NO_X[2]	HC	PM	CO_2
			(g/mile)	(g/mile)	(g/mile)	(g/mile)	(g/mile)	(g/mile)
2088 Before	3	UDDS	20.54	14.69	14.83	1.61	10.89	2181
2088 Before	4	UDDS	20.62	15.29	15.35	2.08	12.99	2316
2088 Before	5	UDDS	20.44	14.55	14.19	1.52	12.5	2192
2180 T&M 1	**3**	UDDS	**109.16**	**13.78**	**13.87**	**4.4**	**24.23**	**2065**
2182 T&M 2	***2***	***UDDS***	***60.59***	***14.79***	***15.39***	***1.31***	***16.31***	***1821***
2181 Before	1	Idle	9.53	10.23	12.5	1.05	0.54	992
2183 Before	1	Idle	8.28	6.58	6.24	0.19	0.04	889
2093 Before	2	Creep	33.1	60.74	59.82	8.59	6.05	3867
2094 Before	2	Creep	37.92	52.56	50.75	7.25	8.66	3410
2095 Before	2	Creep	34.52	56.75	56.86	7.46	6.23	3736
2181 T&M 1	**2**	**Creep**	**26.89**	**51.21**	**53.17**	**2.64**	**6.23**	**3644**
2183 T&M 2	***2***	***Creep***	***28.67***	***53.17***	***54.25***	***3.29***	***4.23***	***3419***
2093 Before	3	Transient	27.13	17.97	17.67	4.08	13.82	2615
2094 Before	3	Transient	26.97	16.95	16.95	4.08	15.42	2541
2095 Before	3	Transient	27.22	17.01	16.82	3.74	14.39	2526
2181 T&M 1	**3**	**Transient**	**181.23**	**16.09**	**15.89**	**5.48**	**25.97**	**2321**
2183 T&M 2	***3***	***Transient***	***119.05***	***20.88***	***21.03***	***6.7***	***17.48***	***2538***
2093 Before	4	Cruise	9.07	10.17	10.25	0.34	17.14	1814
2094 Before	4	Cruise	8.99	9.5	9.99	0.3	15.37	1784
2095 Before	4	Cruise	8.99	10.26	10.04	0.33	15.48	1779
2181 T&M 1	**4**	**Cruise**	**51.26**	**10.07**	**10.23**	**1.01**	**9.31**	**1476**
2183 T&M 2	***4***	***Cruise***	***19.95***	***13.2***	***13.1***	***1.56***	***4.6***	***1504***

The vehicle was retested with the new fuel pump, and data are shown in denoted as T&M 1. There was virtually no change in the NO_x emissions with the new pump on the UDDS, the Cruise mode and the Transient mode. PM rose with the new pump for the Transient cycle and UDDS, but was lowered for the Cruise mode.

A final inspection of the vehicle found soot in the intake manifold, which suggested that the EGR system was still adding some EGR into the intake. The EGR feed was then blocked and this eliminated EGR entirely, and the vehicle was tested again. This was not a repair, but a diagnostic move. The elimination of the EGR (with the new fuel injection pump) raised the NO_x on the Transient and Cruise modes and on the UDDS as shown in Table 31 denoted as T&M 2. PM was reduced relative to the PM with the new fuel pump prior to disabling the EGR (i.e. PM for T&M 2 was lower than PM for T&M 1), for the UDDS, and the Transient and Cruise modes. The Cruise mode reduction was substantial. However, it was not clear that the cause of the high PM emissions was completely resolved. The final PM levels for E55CRC-16 after both pump replacement and disabling of EGR were higher for the UDDS and Transient modes than for the vehicle as received. The T&M exercise with E55CRC-16 was therefore not fully successful and emphasized the difficulty in attacking an old, potentially worn engine with no single, clear malfunction.

E55CRC-21: T&M Vehicle by Inspection in Phase 1

E55CRC-21, a 1990 Caterpillar powered tractor, became a T&M vehicle by inspection. The air filter was visibly dirty. Table 32 presents the emissions from E55CRC-21. It was found using a manometer that the pressure drop across the filter at high air flow (during full power acceleration) into the engine was 39 inches of water (9,714 Pa). This exceeded the typical recommended intake depression limit of 18 inches of water (4,483 Pa). Intake restriction reduces engine air intake flow, increases internal exhaust gas retained in the cylinder, lowers the air to fuel ratio, and promotes formation of products of incomplete combustion. The filter was replaced with a new filter. The intake depression dropped to 5.5 inches of water. The vehicle was retested and data are shown in Table 32. PM for the vehicle on the UDDS dropped by 27%, while it dropped 18% for the transient mode and 25% for the Cruise mode. The CO dropped by over 20% for the UDDS and Cruise modes, while the Transient mode showed a CO decrease of only 2 percent. The data suggest that CO and PM may be reduced by replacing air filters regularly.

Table 32: E55CRC-21 emissions T&M results in bold.

Test ID	Run ID	Driving Schedule	CO (g/mile)	NO_{X1} (g/mile)	NO_{X2} (g/mile)	HC (g/mile)	PM (g/mile)	CO_2 (g/mile)
2156	3	UDDS	19.79	23.79	24.37	0.41	2.89	2389
2156	4	UDDS	19.16	24.27	24.94	0.49	2.93	2364
2156	5	UDDS	22.45	23.64	24.22	0.4	3.09	2400
2168 T&M	**3**	**UDDS**	**16.19**	**25.39**	**25.95**	**0.43**	**2.18**	**2430**
2157	1	CARB - idle3.cyc	9.58	25.49	26.49	1.02	0.27	971
2158	1	CARB - idle3.cyc	9.81	25.84	26.4	1.85	0.36	1055
2159	1	CARB - idle3.cyc	13.09	12.5	14.18	1.63	0.38	967
2169 T&M	**1**	**CARB - idle3.cyc**	**16.93**	**24.16**	**23.62**	**2.13**	**0.49**	**1102**
2157	2	CARB - creep3.cyc	42.37	82.16	82.7	5.76	2.29	4067
2158	2	CARB - creep3.cyc	47.09	84.99	87.7	6.92	2.68	4220
2159	2	CARB - creep3.cyc	56.18	87.99	86.1	9.11	3.48	4537
2169 T&M	**2**	**CARB - creep3.cyc**	**56.73**	**79.73**	**77.26**	**7.75**	**3.59**	**4417**
2157	3	CARB - trans3.cyc	18.62	28.53	28.97	0.96	2.68	2664
2158	3	CARB - trans3.cyc	20.01	30.03	30.01	1.38	2.89	2733
2159	3	CARB - trans3.cyc	19.08	29.67	28.69	1.13	2.72	2668
2169 T&M	**3**	**CARB - trans3.cyc**	**18.92**	**28.64**	**29.33**	**1.1**	**2.25**	**2621**
2157	4	CARB - cruise3.cyc	7.81	18.81	18.26	0.24	1.05	1627
2158	4	CARB - cruise3.cyc	9.42	18.8	18.56	0.26	1.02	1632
2159	4	CARB - cruise3.cyc	8.05	19.27	18.94	0.26	0.89	1640
2169 T&M	**4**	**CARB - cruise3.cyc**	**6.58**	**19.76**	**19.45**	**0.21**	**0.74**	**1618**
2160	1	AC5080	8.36	19.49	19.16	0.31	1.41	1863
2160	2	AC5080	8.14	19.33	20.87	0.32	1.33	1852

CRC-26, CRC-28 and CRC-31, Reflash Vehicles in Phase 1.5

CRC26 was a 1999 Freightliner tractor with a 1998 Caterpillar C-10 Engine. CRC28 was a 1999 Freightliner with a 1998 Series 60 Detroit Diesel Engine. CRC31 was a 1998 Kenworth with a 1997 N14 Cummins engine. E55CRC-26, E55CRC-28 and E55CRC-31 were tested using the full baseline test program in Phase 1.5. At the end of the baseline test program, all three vehicles were reflashed to a "low-NO_x" ECU map by their respective dealerships, and re-tested. After the reflash, the vehicle was retested using a limited set of schedules, as follows. After warming the vehicle and dynamometer, the researchers conducted a coastdown, a UDDS at 56,000 lbs., a HHDDT Idle, a HHDDT 56,000 lbs. Creep Mode, a HHDDT 56,000 lbs. Transient Mode and a HHDDT 56,000 lbs. Cruise Mode.

E55CRC-28 was also identified as a high PM emitter, and was tested (i) as received, (ii) without repair but with reflash, (iii) with repair and reflash, and (iv) without repair but with reflash. E55CRC-31 was a vehicle that required mechanical attention during testing, as discussed in a section below.

Each of the three reflash vehicles is discussed separately below. Figure 129 (as received) and Figure 130 (after reflash) show the NO_x versus hub power plots for all three reflash

vehicles on the Cruise Mode. Reduction of NO_x due to reflash is evident. E55CRC-31 still shows a bifurcation in its emissions rate versus power output, but values over 0.8 g/sec have been eliminated after reflash.

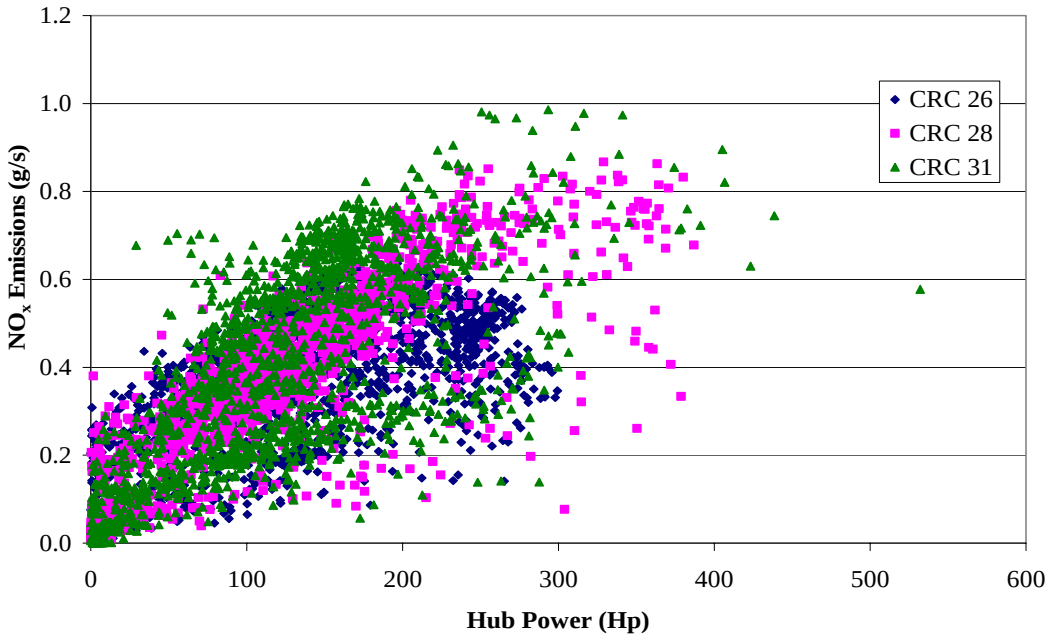

Figure 129: NO_x emissions on Cruise mode (56,000 lbs.) for three vehicles before reflash. NO_x emissions and hub power were time-aligned before plotting.

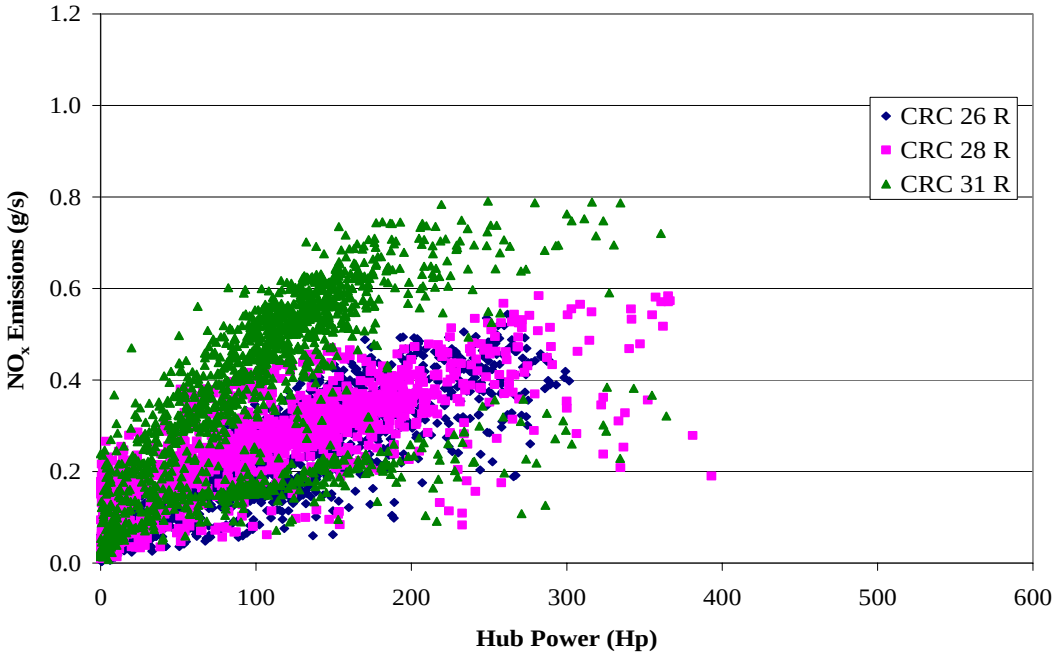

Figure 130: NO_x emissions on the three reflash vehicles were reduced in Cruise mode after reflash. Test weight was 56,000 lbs.

As-received and reflash data for NO_x for E55CRC-26 are presented in Figure 131. As might be expected, transient operation was not affected by the reflash, and the NO_x data for the UDDS, Creep mode and Transient mode did not change appreciably due to reflash.

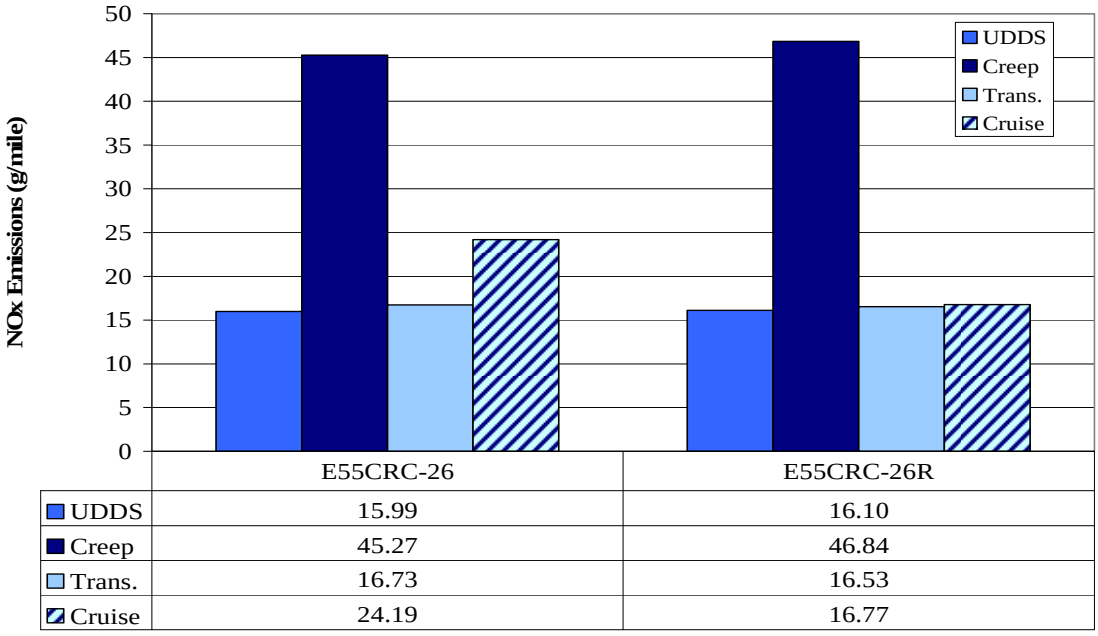

	E55CRC-26	E55CRC-26R
UDDS	15.99	16.10
Creep	45.27	46.84
Trans.	16.73	16.53
Cruise	24.19	16.77

Figure 131: As-received and retest after reflash NO_x data for E55CRC-26 (56,000 lbs.).

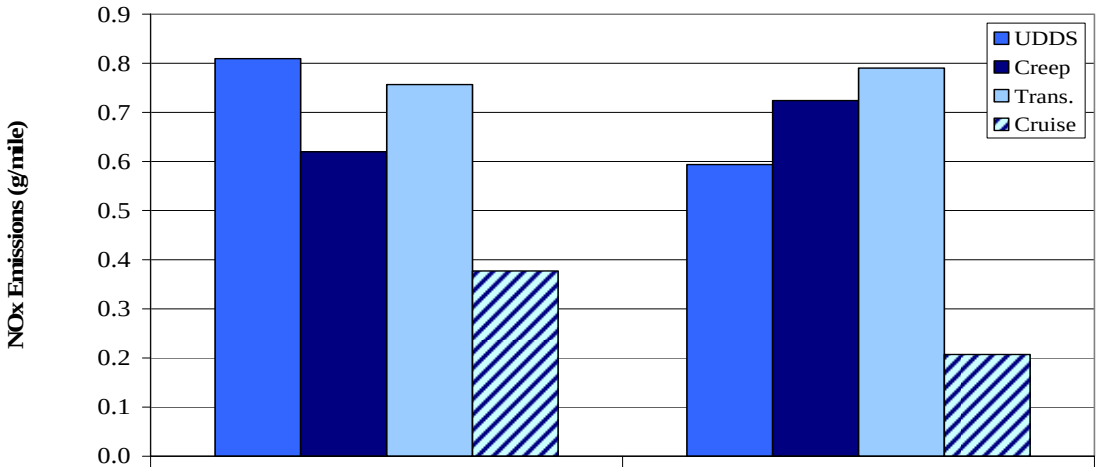

	E55CRC-26	E55CRC-26R
UDDS	0.81	0.59
Creep	0.62	0.72
Trans.	0.76	0.79
Cruise	0.38	0.21

Figure 132: As-received and retest after reflash PM data for E55CRC-26 (56,000 lbs.).

The Cruise Mode, however, exhibited a reduction in NO_x from 24.19 to 16.77 g/mile due to the reflash. PM data for the Creep Mode, and Transient mode were not changed appreciably by the reflash, but the PM for the UDDS was 27% lower and the PM for the Cruise mode dropped from 0.38 to 0.21 g/mile after the reflash. One might expect PM values to rise slightly after a reflash as part of the NO_x -PM tradeoff, but TEOM data (0.37 g/mile as-received, 0.20 g/mile after reflash) were consulted and found to support the substantial reduction in PM filter mass on the Cruise mode after reflash.

E55CRC-28, selected as a reflash vehicle, was also identified as a high PM emitter. The researchers suggested that the cause might be a failed manifold air pressure (MAP) sensor. The MAP sensor is used in the engine control strategy to limit fueling in sympathy with rising turbocharger boost during transients that demand rise in torque. Without fueling limitation, the combustion becomes insufficiently lean and elemental carbon is produced in rich zones during combustion. High CO is also produced by failure to limit fueling during transients, and E55CRC-28 was also observed to have high CO emissions. Valley Detroit Diesel, a dealership in Fontana, CA, confirmed that the MAP sensor had failed, and were able to provide a new sensor. These sensors are readily changed.

PM was the species of interest for the repair. Figure 133 and Figure 134 show the PM levels produced by E55CRC-28 on the UDDS and HHDDT (four modes) at 56,000 lbs. test weight with and without reflash and with and without MAP sensor replacement (repair).

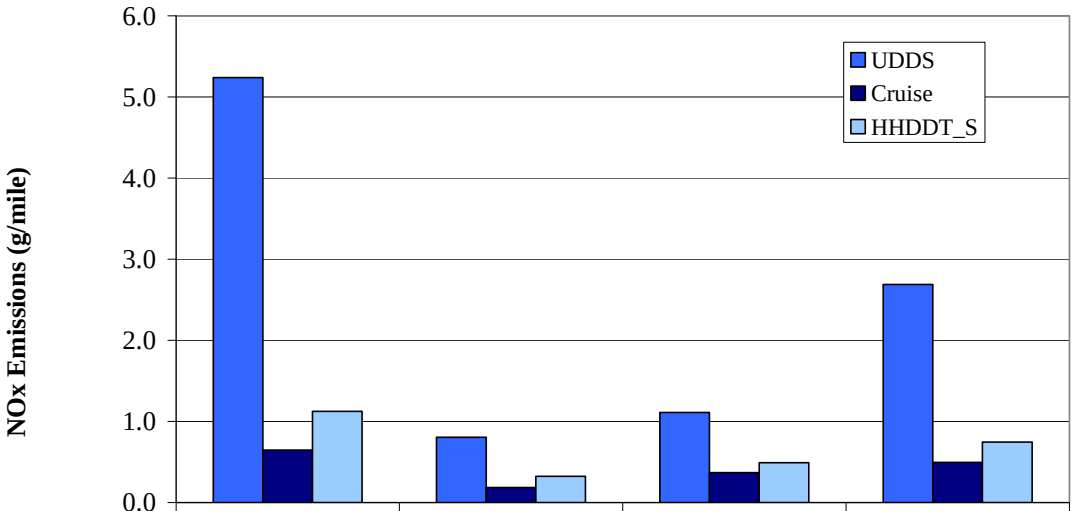

	E55CRC-28	E55CRC-28 Repair without reflash	E55CRC-28 Repair & reflash	E55CRC-28 Reflash without repair
UDDS	5.24	0.81	1.11	2.69
Cruise	0.65	0.19	0.37	0.50
HHDDT_S	1.13	0.32	0.49	0.75

Figure 133: PM emission for E55CRC-28 for the UDDS, Cruise and HHDDT_S Modes.

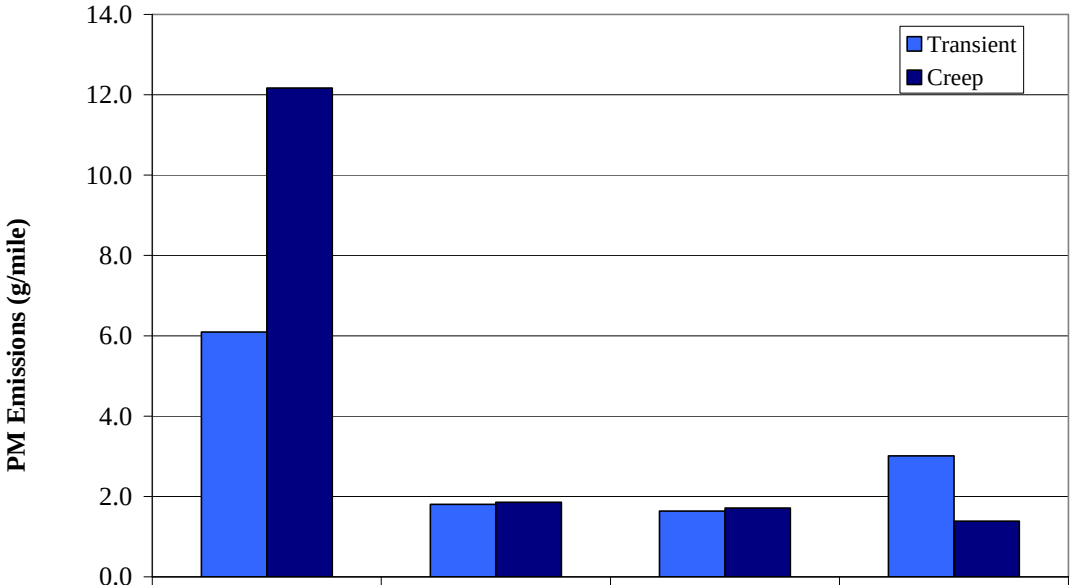

	E55CRC-28	E55CRC-28 Repair without reflash	E55CRC-28 Repair & reflash	E55CRC-28 Reflash without repair
Transient	6.10	1.80	1.64	3.01
Creep	12.17	1.86	1.71	1.39

Figure 134: PM emissions for the Transient and Creep Modes for E55CRC-28.

In all cases, repair lowered PM substantially, whether with or without reflash of the ECU. However, PM was also lowered in general for the reflash without repair. In the case of the Creep Mode, the PM from reflash without repair was below even the values for PM with repair. However, PM is known to be variable on the Creep Mode. It is possible to curb PM production even if the MAP sensor fails by adding a time-based fueling limitation to the ECU strategy. However, the authors have no direct information as to whether the reflash code may have contained this added strategy.

The reflash would be expected to influence NO_x more than other species. Figure 135 and Figure 136 show the NO_x levels before and after reflash. The repair without the reflash raised NO_x values by about 30% for the UDDS and the four HHDDT modes. The reflash did little to abate NO_x for the Transient and Creep Modes, but offered modest reductions for the Cruise and HHDDT_S Modes and the UDDS for the repaired condition. NO_x on the UDDS was actually found to rise slightly on the UDDS for the case without repair.

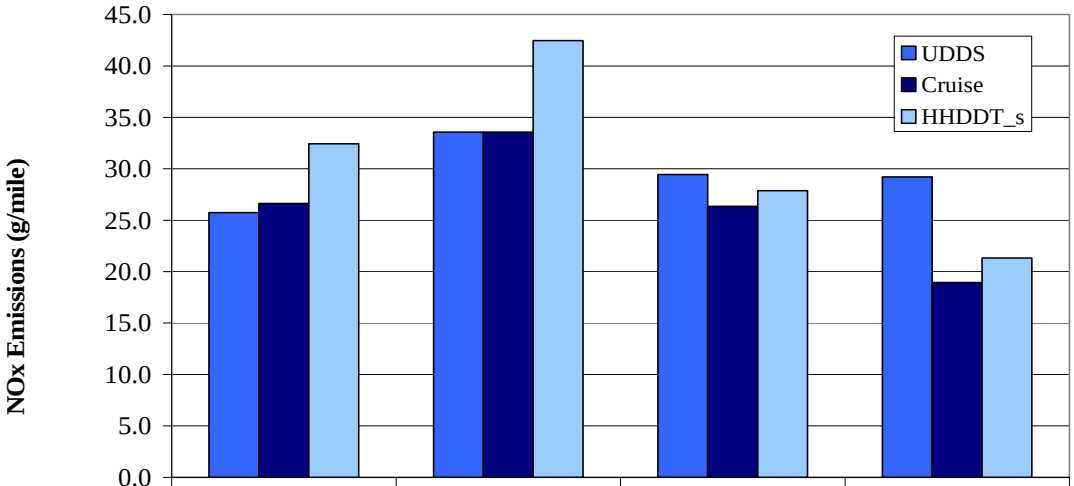

	E55CRC-28	E55CRC-28 Repair without reflash	E55CRC-28 Repair & reflash	E55CRC-28 Reflash without repair
UDDS	25.73	33.57	29.43	29.22
Cruise	26.63	33.57	26.36	18.95
HHDDT_s	32.45	42.46	27.88	21.33

Figure 135: NO_x emissions for E55CRC-28 at 56,000 lbs. on the UDDS and the Cruise and HHDDT_S Modes.

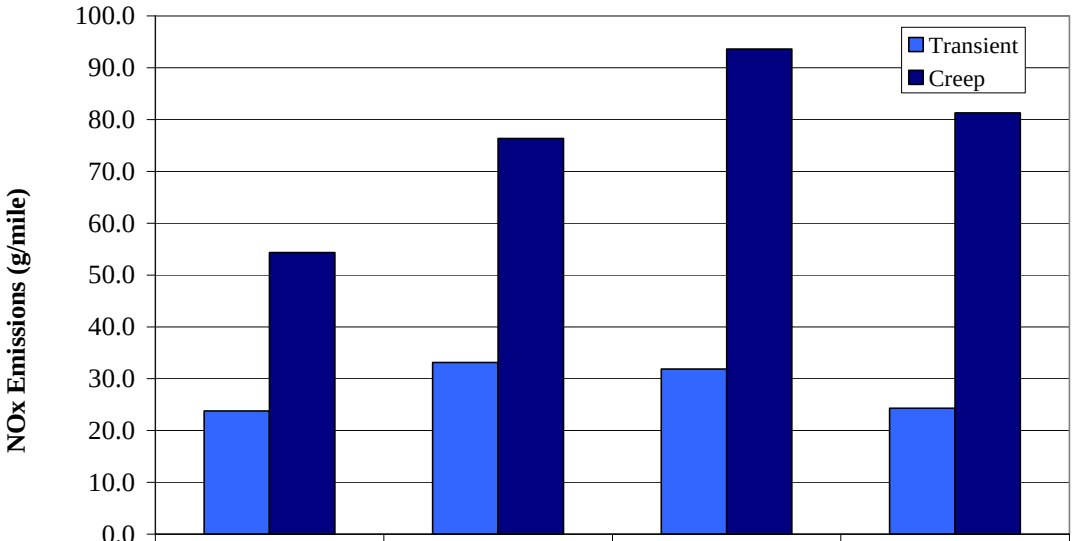

	E55CRC-28	E55CRC-28 Repair without reflash	E55CRC-28 Repair & reflash	E55CRC-28 Reflash without repair
Transient	23.79	33.11	31.89	24.31
Creep	54.34	76.36	93.63	81.28

Figure 136: NO_x emissions for E55CRC-28 at 56,000 lbs. on the Transient and Creep Modes.

E55CRC-31 was subjected to as-received testing and testing after reflash. The vehicle suffered from a clutch failure, an exhaust leak, and a fuel injector failure during testing. The initial testing of vehicle E55CRC-31 was conducted on 7/2/03 during the time of the speciation sampling. HHDDT and UDDS tests were performed at 56,000 lbs. and an HHDDT at 66,000 lbs. The vehicle was re-procured on 7/15/03 for the HHDDT 30,000 lbs. test to complete the as-received testing.

The vehicle was then sent to a local dealership to be "reflashed" for a low NO_x calibration. On 7/16/03, the vehicle was retested with the reflash. One HHDDT at 56,000 lbs. was completed but the required UDDS was not performed.

The vehicle was brought back on 7/28/03 to complete the reflash testing. While conducting the retest with the low NO_x reflash of vehicle E55CRC-31, a significant exhaust leak developed. The vehicle was removed from the test bed to repair the exhaust leak and testing continued with other vehicles. When vehicle E55CRC-31 was procured again, a problem with the clutch prevented testing. WVU staff adjusted the clutch but this did not solve the problem. A technician from the rental company was called to service the vehicle. Both the clutch-brake and the clutch were found to need replacement. While testing the vehicle after changing the clutch, an engine mis-fire was detected that was not present during prior testing. The technician determined the problem to be a faulty injector. The fuel injector was replaced. Testing was completed. Table 33 shows the sequences of repairs and retests. These repairs were not treated as T & M repairs.

Table 33: Sequence of testing for E55CRC-31

Date	Tests performed	Seq. No.	Action
7/2/03	56,000 HHDDT 56,000 UDDS 66,000 HHDDT	2532 2534 2535	Tests reported
7/15/03	30,000 HHDDT	2573	Tests reported
7/16/03	56,000 HHDDT reflash did not do the 56,000 UDDS	2577/78	Tests not reported
7/28/03	56,000 HHDDT reflash (Trans3, Cruise3) to verify data from 7/16/03 56,000 UDDS reflash (significant exhaust leak developed) Found problems with the clutch, clutch brake, and fuel injector	2625 2626	Tests not reported Truck repaired
8/19/03	56,000 HHDDT reflash 56,000 UDDS reflash	2685 2684	Tests reported

As-received and reflash emissions are shown in Figure 137 and Figure 138. The reflash reduced NO_x emissions (in g/mile) for the UDDS and the Creep, Transient and Cruise modes of the HHDDT. PM emissions (in g/mile) rose slightly on the UDDS, and dropped from 1.24 g/mile to 0.76 g/mile on the Transient Mode, but were otherwise changed little. However, it was found that CO_2 emissions were also reduced, (as shown in the short reports in Appendix K) which is not expected, so that g/gallon values are not aligned with the distance specific values.

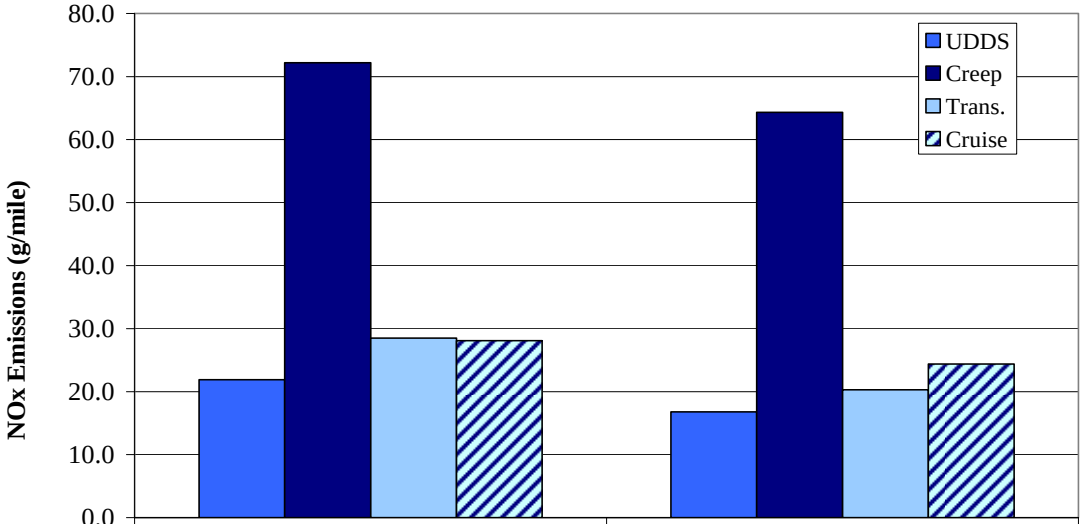

	E55CRC-31	E55CRC-31R
UDDS	21.91	16.79
Creep	72.16	64.34
Trans.	28.50	20.31
Cruise	28.11	24.36

Figure 137: As-received and reflash emissions for NO_x emissions for E55CRC-31 tested at 56,000 lbs.

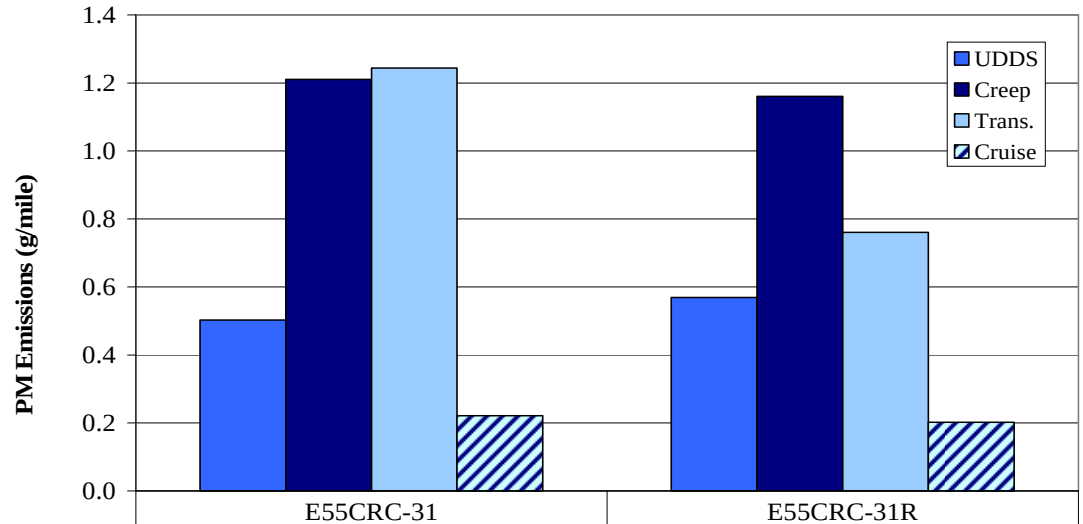

	E55CRC-31	E55CRC-31R
UDDS	0.50	0.57
Creep	1.21	1.16
Trans.	1.24	0.76
Cruise	0.22	0.20

Figure 138: As-received and reflash emissions for PM emissions for E55CRC-31

CRC-45 T&M High PM Vehicle in Phase 2

The Phase 2 E-55/59 program test plan included a provision for repair and retest of one vehicle that was identified during the T&M inspection or determined otherwise to have abnormally high emissions. Vehicle E55CRC-45 was noted visually to be a prodigious smoker. It was not a high emitter on the Cruise mode but was a high emitter (on only one test run) on the Transient mode. This vehicle emitted PM at an impressively high level at low engine load. On the Creep mode, the PM mass (67.8 g/mile) exceeded the NO_x mass substantially, and PM exceeded NO_x also on the Transient mode. The high PM mass was accompanied by exceptionally high HC emissions. In some cases, the HC emissions were of the order of one tenth of the fuel burned to form CO_2, and it was realized that raw fuel was most likely being admitted to the exhaust stream.

The sponsors were notified of the high emissions and they elected to authorize repair and retest. A repair was effected: it was determined at the dealership that the No. 1 injector timing was out of specification, and the injector was replaced. The vehicle was retested as E55CRC-45R. PM remained high after the repair. Both PM and NO_x were reduced on the Creep mode, but NO_x and PM mass were still similar to one another (38.2 and 37.5 g/mile respectively). On Transient mode PM was virtually unchanged. PM rose from 1.1 g/mile on the Cruise mode before repair to 4.5 g/mile on the Cruise mode after repair, and a similar increase was seen on the HHDDT_S. Clearly the emissions from the vehicle had changed, but the cause of the high PM at low load had not been addressed.

The vehicle was returned to the dealer for additional diagnosis and repair, and a reconditioned turbocharger was fitted. Data collected after this second repair were recorded under the vehicle designation E55CRC-45RR. The emissions changed, but the high PM was not cured. Once again, on Creep and Transient modes, the PM mass was similar to the NO_x mass.

Table 34 shows the emissions from E55CRC-45 as received, after the first repair, and after the second repair. It is evident that the PM emissions were associated with high HC emissions and that the fault was not diagnosed. The WVU investigators suspect that a leak from an injector into the cylinder might have been the cause, but no further repairs were authorized by the sponsors.

Table 34: E55CRC-45 as received, after first repair (R), and after second repair (RR).

WVU Ref Num	Test ID	Test Run ID	Cycle	CO g/mile	CO_2 g/mile	NO_x g/mile	NO_x^2 g/mile	HC g/mile	PM g/mile
E55CRC-45	2967	2	TEST_D	3.47	2029	11.98	12.36	15.76	3.04
E55CRC-45 R	2985	1	TEST_D	5.42	2230	11.11	11.20	31.70	4.73
E55CRC-45 RR	20008	1	TEST_D	9.70	2164	11.78	12.04	29.24	4.54
E55CRC-45	2968	3	TRANS3	4.99	2369	13.68	13.63	29.46	17.14
E55CRC-45 R	2986	3	TRANS3	7.14	2502	12.72	12.70	47.03	16.59
E55CRC-45 RR	20009	3	TRANS3	15.56	2513	13.61	13.42	40.96	13.27
E55CRC-45	2968	2	CREEP34	32.95	3806	44.97	44.14	222.73	67.77
E55CRC-45 R	2986	2	CREEP34	27.66	4061	38.38	37.95	158.52	37.51
E55CRC-45 RR	20009	2	CREEP34	47.56	3857	40.80	38.14	134.90	29.59
E55CRC-45	2968	4	CRUISE3	1.53	1468	8.81	8.77	5.43	1.12
E55CRC-45 R	2986	7	CRUISE3	2.69	1447	7.13	7.33	17.40	4.52
E55CRC-45 RR	20009	6	CRUISE3	5.39	1372	10.33	10.33	14.54	2.52
E55CRC-45	2968	5	HHDDT_S	1.18	1612	9.62	9.46	3.09	0.86
E55CRC-45 R	2986	5	HHDDT_S	2.69	1611	8.30	8.41	19.78	2.93
E55CRC-45 RR	20009	7	HHDDT_S	4.39	1580	10.54	10.42	17.09	2.99

E55CRC57: MHDT Temperature Sensor Failure

There were no formal criteria for identifying high MHDT emissions. Vehicle CRC57, a MHDDT powered by a Caterpillar engine, showed unusually high unladen NO_x emissions. This vehicles apparently had an issue with a temperature sensor that indicated an overheated engine to the ECU. The ECU would then command a limp home mode resulting in the vehicle's inability to follow the test target speed (See Figure 139). The clutch actuated cooling fan would only kick in after the engine actually was warm. At that point the driver could return the vehicle speed to one consistent with the target trace. Conversation with Robert Graze, of Caterpillar, confirmed that the WVU diagnosis of a temperature sensor misrepresenting the temperature to the ECU was reasonable.

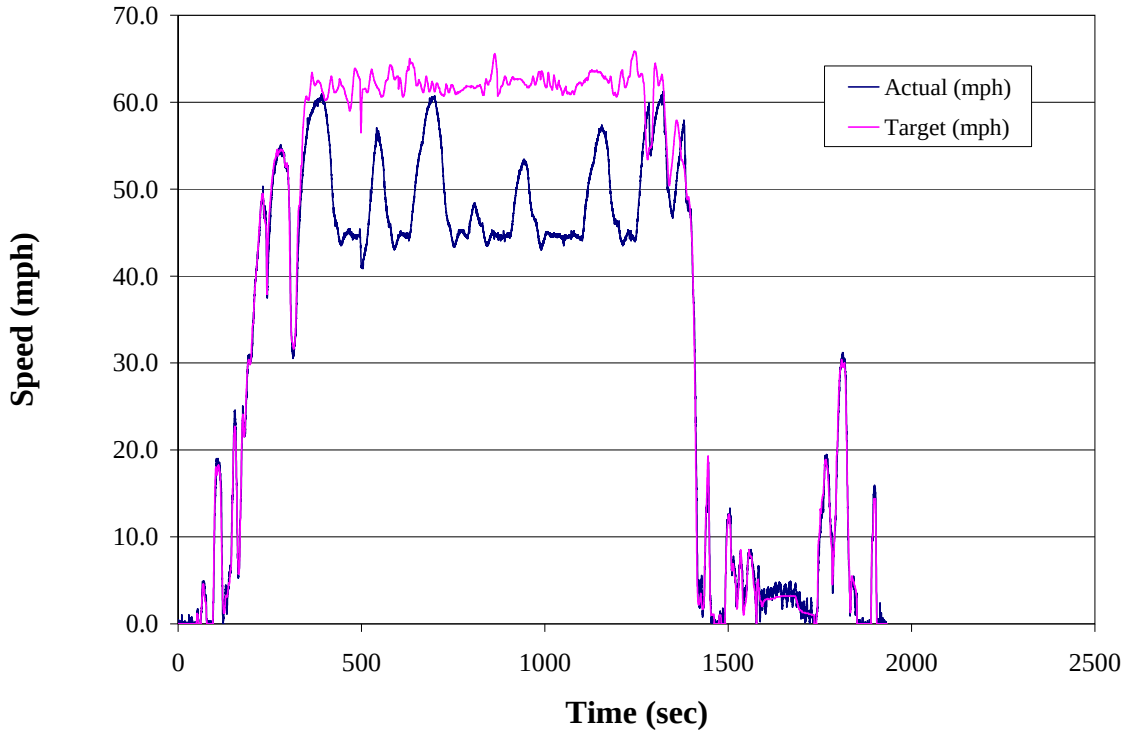

Figure 139: shows the inability of E55CRC-57 to meet the target trace.

T&M and Reflash Discussion

Identification of vehicles for T&M by inspection proved successful insofar as it targeted E55-21, with a dirty air filter. Also, the excessive smoking of E55CRC-16 and E55CRC-45 provided visual indications of T&M vehicles. However, inspections are difficult to perform, and some forms of tampering with sensors may be difficult to identify. In this way, visual inspection is not foolproof, but will detect some emissions-related problems.
The method of identifying high PM emitters also appeared to be sound, and used the best approach that could be employed for rapid processing of field data. Moreover, the identification of high PM emitters using data from two different HHDDT Schedule Modes (Transient and Cruise) allowed the researchers to infer the cause of the smoking.

High PM emissions on the Transient Mode, without high emissions on the Cruise Mode, might indicate poor puff control.

The criterion for identifying high NO_x emitters was based on a multiple of the certification NO_x to CO_2 ratio. NO_x tracks CO_2 closely for a vehicle with a timing map that keeps location of peak in-cylinder pressure at the same crank angle over a broad operating range. In this way, the NO_x to CO_2 ratio should be largely cycle independent, and should rise with advanced timing and fall with retarded timing. Unfortunately this approach is confused by the timing strategy that causes "off-cycle" NO_x emissions in many electronic engines. Off-cycle strategies may be based on two maps, one with advanced timing (high NO_x), and one with retarded timing (low NO_x), and these maps may be invoked during different sections of a cycle. Off-cycle strategies cannot be regarded as a T&M target because the engine is behaving in the way that it was originally sold, and any high NO_x emissions arising during off-cycle use are neither due to tampering nor due to malmaintenance.

Being cognizant of the "off-cycle" phenomenon, the researchers set generous T&M margins to detect high NO_x emitters. The intent was not to snare off-cycle trucks, but to detect only extreme (uncharacteristically high) NO_x emitters. In execution of this strategy, only one high NO_x emitter was detected, and this was determined through further study to be rooted in an off-cycle issue. An important point was that the emissions for this vehicle, E55CRC-10, were extreme for the Cruise Mode: it is known that steady state cruising tends to elicit off-cycle behavior in many cases. The investigators also admit that E55CRC-10 was found to be high because the criterion was developed with 5 g/bhp-hr (6.7 g/kw-hr) NO_x engines in mind, while E55CRC-10 was a 4 g/bhp-hr (5.4 g/kw-hr) engine. The criterion should perhaps have been a NO_x to CO_2 ratio that was fixed in value (say 0.03 by mass) rather than "three times the certification ratio". However, E55CRC-10 would still have just been high on Cruise mode with a 0.03 criterion. It would have had "expected" emissions levels after reflashing if a 0.03 criterion were used. Otherwise, more sophisticated strategies, using plots such as those shown in Figure 122, could be used to distinguish high NO_x T&M trucks from "off-cycle" behavior. The E55CRC-10 findings, in part, led to the reflash research in Phase 1.5 of the program, where reflash NO_x reductions were verified.

As part of an inventory program in southern California, trucks that were identified as high emitters were repaired and retested for emissions. A 1990 Caterpillar-powered tractor was identified as having a dirty air filter, and air filter replacement did reduce CO and PM emissions. A 1979 Caterpillar-powered truck was identified as a prodigious smoker, but the cause of the high emissions was not satisfactorily identified. A 1998 Detroit Diesel-powered tractor was identified as having high NO_x emissions, but they were attributed to "off-cycle" timing strategies rather than T&M issues. The vehicle was "reflashed" with a more retarded timing strategy and lower NO_x emissions were seen under cruise conditions. In the case of a 1985 Cummins-powered tractor, repairs to a failed variable mechanical injection timing system raised NO_x to an expected level and reduced other regulated emissions. For a 1993 Cummins-powered truck, the cause of excessive PM production was not cured, despite two rounds of repair: it was evident that

the high PM was associated with exceptionally high HC emissions. A MHDDT malfunctioned during testing, and was unable to follow the trace due to a false high temperature warning. This was not an emissions fault, but did affect distance-specific emissions by not allowing the vehicle to follow the cycle closely. It is concluded that trucks that are poorly maintained or have failures are contributing additional emissions to the inventory, but that diagnosis and repair is not necessarily straightforward.

ACKNOWLEDGEMENTS

The WVU researchers are grateful to the sponsors listed below, for support of this program.

- Coordinating Research Council, Inc.
- California Air Resources Board
- U.S. Environmental Protection Agency
- U.S. Department of Energy Office of FreedomCAR & Vehicle Technologies through the National Renewable Energy Laboratory
- South Coast Air Quality Management District
- Engine Manufacturers Association

The dedication of the WVU field research team is gratefully acknowledged.

Ralphs Grocery was kind to provide a location for the WVU laboratory during part of this research program.

The contributions of Thomas R. Long, Jr., Sairam Thiagarajan, Shuhong (Susan) Xu, David McKain and Kuntal Vora in preparing and editing sections of this report are acknowledged.

REFERENCES

1. Yanowitz, J., McCormick, R.L., and Graboski, M.S., "Critical Review: In-Use Emissions from Heavy-Duty Diesel Vehicles", Environmental Science & Technology. Vol.334:729-740.

2. Gautam, M., Clark, N.N., Riddle, W., Nine, R., Wayne, W.S., Maldonado, H., Agrawal, A. and Carlock, M., "Development and Initial Use of a Heavy-Duty Diesel Truck Test Schedule for Emissions Characterization," 2002 SAE Transactions: Journal of Fuels & Lubricants Vol. 111, pp. 812-825.

3. Clark, N.N., Gautam, M., Wayne, W.S., Nine, R.D., Thompson, G.J., Lyons, D.W., Maldonado, H., Carlock, M. & Agrawal, A., "Creation and Evaluation of a Medium Heavy-Duty Truck Test Cycle" SAE Powertrain Conf., Pittsburgh, Oct. 2003, SAE Paper 2003-01-3284.

4. Clark, N.N., Gautam, M., Riddle, W., Nine, R.D., and Wayne, W.S., "Examination of a Heavy-Duty Diesel Truck Chassis Dynamometer Schedule," SAE Powertrain Conference, Tampa, Fla., Oct 2004, SAE Paper 2004 -01-2904.

5. Anyon, P., Brown, S., Pattison, D., Beville-Anderson, J., Walls, G., Mowle, M., "Proposed Diesel Vehicle Emissions National Environment Protection Measure Preparatory Work: In-Service Emissions Performance – Phase 2: Vehicle Testing", National Environment Protection Council, November 2000

6. Hildemann, L. M., Cass, G. R., and Markowski, G. R., (1989) "A dilution stack sampler for collection of organic aerosol emissions: design, characterization and field tests," Journal of Aerosol Science and Technology , Vol. 10, pp 193-204

7. TSI model 3936 SMPS Instruction Manual, 1999.

8. Reavell, K.S., Hands, T., Collings, N., "Determination of Real Time Particulate Size Spectra and Emission Parameters with a Differential Mobility Spectrometer," 6th International ETH-Conference on Nanoparticle Measurement, August 2002.

9. Collings, N., Reavell, K., Hands, T., Tate, J., "Roadside Aerosol Measurements with a Fast Particulate Spectrometer," JSAE Paper 20035407, 2003.

10. Clark, N.N., Wayne, W.S., Buffamonte, T., Hall, T., Lyons,D.W. and Lawson, D., "The Gasoline/Diesel PM Split Study: Heavy Duty Vehicle Regulated Emissions" Coordinating Research Council On-Road Emissions Meeting, San Diego, Ca., May 2003

11. Clark, N.N., Wayne, W.S., Nine, R.D., Buffamonte, T. M., Hall, T., Rapp, B.L., Thompson, G., and Lyons, D.W., “Emissions from diesel-fueled heavy-duty vehicles in Southern California,” SAE/JSAE Spring Fuels & Lubricants Meeting , Yokohama, Japan 2003, JSAE Paper 20030232, SAE Paper 2003-01-1901

12. Yanowitz, J., McCormick, R.L. and Graboski, M.S., "In-Use Emissions from Heavy-Duty Vehicles," Environmental Science & Technology, 2000, Vol 34 pp. 729-740.

13. Sakurai, H., Tobias, H.J., Park K., Zarling, D., Docherty, K.S., Kittelson, D.B., McMurry, P.H., and Ziemann, P.J., “On-line Measurements of Diesel Nanoparticle Composition and Volatility,” Atmospheric Environment, Vol. 37, pp. 1199-1210, 2004.

14. Gautam, M, Thiagarajan, S., Burlingame, T., Wayne, W.S., Clark, N., Carder, D., (2004), “Characterization of Exhaust Emissions from a Catalyzed Trap Equipped Natural Gas Fueled Transit Bus”, 14th CRC On-Road Vehicle Emissions Workshop, March 29-31, 2004, San Diego.

15. Kim, D., Gautam, M., and Gera, D., “Parametric Studies on the Formation of Diesel Particulate Matter via Nucleation and Coagulation Modes,” Journal of Aerosol Science, Vol 33, pp. 1609-1621, 2002.

16. Mathis, U., Mohr, M., and Zenobi, R., “Effect of Organic Compounds on Nanoparticle Formation in Diluted Diesel Exhaust,” Atmospheric Chemistry and Physics, 4, pp. 609-620, 2004.

17. Mohr, M., Jaeger, L. W., Boulouchos, K., “The Influence of Engine Parameters on Particulate Emissions,” MTZ Worldwide, 62, pp. 686-692, 2001.

18. Mathis, U., Mohr, M., and Zenobi, R., “Effect of Organic Compounds on Nanoparticle Formation in Diluted Diesel Exhaust,” Atmospheric Chemistry and Physics, 4, pp. 609-620, 2004.

19. Lapin, C.A., Gautam, M., Zielinska, B, Wagner, V.O., McClellan, R.O., (2002), “Mutagenicity of Emissions from a Natural Gas Fueled Truck”, Mutation Research, Vol 519, pp. 205-209.

20. Matz, G.“Massenspektrometrische Bestimmung der Ölemission im Abgas von Otto- und Dieselmotoren,” Technische Universität Hamburg-Harburg, Zwischenbericht über das Vorhaben Nr. 758 (FVV-Nr. 67580).

21. Weaver, C.S. and Klausmeier, R.F., “Heavy-Duty Diesel Vehicle Inspection and Maintenance Study”, California Air Resources Board Contract A4-151-32, Final Report, May 16, 1988.

22. Weaver, C.S., Balam, M., Mrodick, C.J., Tran, C., Heiken, J., and Pollack, A., “Modeling Deterioration in Heavy-Duty Diesel Particulate Emissions”, EPA Contract 8C-S112-NTSX, Report, 1998.

23. Yanowitz, J; Graboski, MS; Ryan, LBA; et al. (1999) Chassis dynamometer study of emissions from 21 in-use HD diesel vehicles. Environ Sci Technol 33:209-216.

24. Ramamurthy, R. and Clark, N.N., “Atmospheric Emissions Inventory Data for Heavy Duty Vehicles”, Environmental Science & Technology, Vol. 33, Pp. 55-62, 1999

25. Clark, N.N, Atkinson, C.M., Lyons, D.W., and Ramamurthy, R., "Models for Predicting Transient Heavy Duty Vehicle Emissions", SAE Fall Fuels & Lubricants Meeting, San Francisco, October, 1998, SAE Paper 982652.

26. Clark, N.N., Tehranian, A., Nine, R.D., and Jarrett, R., “Translation of Distance-Specific Emissions Rates between Different Chassis Test Cycles using Artificial Neural Networks”, SAE Spring 2002 Fuels & Lubricants Meeting, Reno, NV, SAE Paper 2002-01-1754

27. Kern, J., Clark, N.N., Nine, R. and Atkinson, C.M., “Factors Affecting Heavy-Duty Diesel Vehicle Emissions”, Jour. of the Air & Waste Management Assoc., Vol. 52, Pp. 84-94, 2002.

28. Clark, N.N., Lyons, D.W., Rapp, B.L, Gautam, M., Wang, W.G., Norton, P., White, C. and Chandler, C., “Emissions from Trucks and Buses Powered by Cummins L-10 Natural Gas Engines”, SAE Spring Fuels and Lubricants Meeting, Dearborn, MI, May 1998, SAE Paper 981393.

29. Gautam, M., Clark, N.N., Riddle, W., Nine, R., Wayne, W.S., Maldonado, H., Agrawal, A. and Carlock, M, “Development and Initial Use of a Heavy Duty Diesel Truck Test Schedule for Emissions Characterization”, SAE Spring 2002 Fuels & Lubricants Meeting, Reno, NV, SAE Paper 2002-01-1753

30. Clark, N.N., Jarrett, R.P. and Atkinson, C.M., “Field Measurements of Particulate Matter Emissions and Exhaust Opacity from Heavy Duty Vehicles”, Journal of the Air & Waste Management Assoc., Vol. 49, 1999, pp. 76-84.

31. Jarrett, R. P., 2000, “Evaluation of Opacity, Particulate Matter, and Carbon Monoxide from Heavy-Duty Diesel Transient Chassis Tests”, M.S. Thesis, Dept. of Mech. and Aero. Eng., West Virginia University, Morgantown, WV.

32. Ganesan, B., and Clark, N.N., “Relationships between Instantaneous and Measured Emissions in Heavy Duty Applications”, SAE Transactions 2001, Journal of Fuels and Lubricants, Vol. 110, Section 4, pp. 1798-1806

33. Agrawal, A., Carlock, M., and Maldonado, H., “Development of Heavy-Duty Vehicle Chassis Dynamometer Driving Cycles”, 12th Coordinating Research Council On-Road Emissions Conference, San Diego, CA, April 2002.

34. Personal communications on E55CRC-16 vehicle with Robert Graze, of Caterpillar (Peoria, Ill).